Contrails

WADD TECHNICAL REPORT 60-584
PART II

HANDBOOK OF FIBROUS MATERIALS

WALTER S. BAKER

McGRAW-HILL TECHNICAL WRITING SERVICE

ERNEST R. KASWELL

FABRIC RESEARCH LABORATORIES, INC.

OCTOBER 1961

DIRECTORATE OF MATERIALS AND PROCESSES
CONTRACT No. AF 33(616)-7504
PROJECT No. 7381

AERONAUTICAL SYSTEMS DIVISION
AIR FORCE SYSTEMS COMMAND
UNITED STATES AIR FORCE
WRIGHT-PATTERSON AIR FORCE BASE, OHIO

600 - January 1962 - 16-665 & 666

Approved for Public Release

Contrails

FOREWORD

This report was prepared by the Technical Writing Service Division of the McGraw-Hill Book Company, Inc. under USAF Contract No. AF 33(616)-7504. The contract was initiated under Project No. 7381, "Materials Applications" Task No. 73812, "Data Collection and Correlation." The work was administered under the direction of Directorate of Materials & Processes, Aeronautical Systems Division, Air Force Systems Command, with Joyce C. McGrath acting as project engineer.

Mrs. Mary T. Hale of the McGraw-Hill Technical Writing Service did the editing.

This report covers work from August 1960 to August 1961

Approved for Public Release

Contrails

ABSTRACT

This report contains the summarized and consolidated information extracted from ASD Technical Reports covering several phases of fibrous materials research. The information is arranged to make the results of these reports more readily available and useful to decelerator designers and others interested in the fibrous materials phase of Air Force research.

The report is divided into sections covering the pertinent facets of fibrous material information. Fairly complete information is supplied on various phases of ageing properties; basic design data; friction, abrasion and weather resistance; impact loading; porosity and air permeability; sewability; radiation properties; and aerodynamic heating of different yarns, cords, webbings and fabrics.

PUBLICATION REVIEW

This report has been reviewed and is approved.

FOR THE COMMANDER:

C. A. Willis

C. A. Willis, Chief
Fibrous Materials Branch
Nonmetallic Materials Laboratory
Directorate of Materials & Processes

Approved for Public Release

Contrails

TABLE OF CONTENTS

Page

INTRODUCTION 1

I. AGEING PROPERTIES 2

Effect of Fifteen Years of Ageing on the Deterioration of Parachutes 2
A Comparison of the Ageing Properties of Cocoanut vs. Silicone Oils as Finishing Agents for Nylon Parachute Cloth 8

II. DESIGN DATA, BASIC 13

Development and Evaluation of Webbing made from Nylon 6 13
Development and Evaluation of Cords, Ribbons, and Tapes made from Nylon 6 17
Development of Coreless Braids made from Nylon 6 and Nylon 66 . . 20
Development of High Tenacity Heat Stable Dacron Parachute Items 25
Some Principles of Parachute Fabric Construction with Respect to Fabric Strength, Weight, Bulk, and Air Permeability 41

III. FRICTION, ABRASION, AND WEAR 51

Development of Nylon Webbings of Improved Abrasion Resistance . . 51

IV. IMPACT LOADING 73

Comparative Drop Tests of Chemstrand and du Pont Nylon Parachutes 73
Effect of Repeated Deployments on the Properties of B-47 Deceleration Parachutes 78
Effect of Repeated Deployment on the Properties of F-100 Deceleration Parachutes 79

V. POROSITY AND AIR PERMEABILITY 86

Development of Design Data on the Mechanics of Air Flow Through Parachute Fabrics 86
Development of a Design Procedure to Engineer Parachute Fabrics 119
A Study of the Air Permeability Properties of Commercially Produced Parachute Fabrics 145
Air Permeability and Biaxial Stress Properties of Parachute Fabrics 149

Approved for Public Release

Contrails

TABLE OF CONTENTS (Continued)

Page

VI. SEWABILITY 163

Effect of Webbing and Sewing Thread Design, and Seam Types on Seam Efficiencies. 163

VII. SUNLIGHT AND WEATHER RESISTANCE. 166

Effect of Solar Radiation and Weather on the Breaking Strength of Outdoor Exposed Webbings. 166
Effect of Six Months Protected Outdoor Storage on the Breaking Strengths of Parachute Materials 172

VIII. TEMPERATURE PROPERTIES 175

Effect of Dead Loading and Low Temperature on the Elongation Characteristics of Nylon Braid 175

IX. CHEMICAL RESISTANCE. 177

Effect of Duco Lacquer, 3661 Paint Thinner, on the Strength of Nylon Parachute Materials. 177

X. RADIATION PROPERTIES 178

Effect of Thermal Radiation on Nylon Parachute Ribbons 178
Effect of Thermal Radiation on Nylon and Dacron Webbings 180
Effect of Thermal Radiation on Nylon Parachute Webbings, Lines, and Seams 181
Effect of Thermonuclear Radiation on Parachute Textile Components 182

XI. AERODYNAMIC HEATING. 186

Aerodynamic Heating-Rate Calculations for Nylon Parachute Ribbons. 186
Mass Transfer Cooling of Parachute Ribbons 190

XII. BIBLIOGRAPHY 194

Approved for Public Release

Contrails

LIST OF ILLUSTRATIONS

Figure		Page
1.	Standard Butterfly Attachment	24
2.	Typical Load-Elongation Curves of 220-Denier Dacron Singles Yarn	28
3.	Typical Load-Elongation Curves of Dacron Type E Threads Specification MIL-T-4855	31
4.	Effect of Twist on the Diameter of Nylon Yarns	43
5.	Idealized Yarn Configuration	46
6.	Effect of Twist and Calendering on Thickness of Specification MIL-C-7020, Type II Nylon Parachute Cloth	48
7.	Percent Open Area vs. Air Permeability (at 10 in. water pressure drop)	49
8.	Effect of Pick Variation on Webbing Strength	56
9.	Effect of Weave on Webbing Strength	60
10.	Effect of Number of Ends on Strength	62
11.	Effect of Filament Inclination in Singles Yarns on Webbing Strength	64
12.	Effect of Twist on Webbing Strength	67
13.	Snatch Force vs. Launching Speed for Chemstrand and du Pont Nylon Canopies	75
14.	Opening Force vs. Launching Speed for Chemstrand and du Pont Nylon Canopies	76
15.	Diagrammatic Sketch of Distended Fabric Sample and Device for Distention Measurement	90
16.	Fabric Stress vs. Δ p as a Function of the Biaxial Modulus	91
17.	Fabric Strain vs. Δ p as a Function of Biaxial Modulus	92
18.	The Pore Reynolds Numbers and Corresponding Discharge Coefficients for Seven Experimental Fabrics and a Wire Screen	97

Approved for Public Release

Contrails

LIST OF ILLUSTRATIONS (Continued)

Figure | Page

19. Air Permeability vs. Pressure Differential for Experimental Type I Fabrics with 1/2 Turns per Inch in the Warp. 99

20. Air Permeability vs. Pressure Differential for Experimental Type I Fabrics With 5 Turns per Inch in the Warp. 100

21. Light Penetrability vs. Pressure Differential Under Permeability Test for Type I Experimental Fabrics 101

22. Light Penetrability vs. Pressure Differential Under Permeability Test for Type II Experimental Fabrics. 102

23. Light Penetrability vs. Fabric Strain Measured Under Permeability Test 104

24. Planar Photomicrograph of R5N20. 105

25. Average Biaxial Load Elongation Diagram for R5N5 106

26. LP vs. Biaxial Stress Determined From Biaxial Tests for Type I Experimental Fabrics 107

27. LP vs. Biaxial Stress Determined From Biaxial Tests for T5N5 and T20N20 108

28. Light Penetrability vs. Average Strain Determined From Biaxial Tests. 109

29. Load Elongation Diagram for Repeated Biaxial Loading to 20 Pounds per Inch of R1/2N1/2 110

30. Light Penetrability as a Function of Biaxial Stress for Repeated Loading to 20 Pounds per Inch for R1/2N1/2 111

31. Normal and Oblique Views of Plain Weave. 122

32. Normal and Oblique Views of Twill Weave. 123

33. Idealized Filling Cross-Section. 124

34. Area Inclination Factor vs. Pore Angle 125

35. $(C_D)_o$ vs. Reynolds Number 129

36. Correlation of Experimental and Calculated Discharge Coefficient. 130

Approved for Public Release

Contrails

LIST OF ILLUSTRATIONS (Continued)

Figure — Page

37. Fractional Extension vs. Δ p for Fabric 2. 131

38. Percent LP vs. Δ p for Fabric 2. 132

39. Percent LP vs. Fractional Extension for Fabric 2 133

40. Permeability of Fabric FRL- 1, 2 & 3 135

41. C_D vs. Reynolds Number of Twill and Rip-stop Fabrics 136

42. Surface Photograph of Fabric FRL-2 at Δ p = 25.6, inches of H_2O. 137

43. Permeability of Experimental Fabrics 144

44. Volume Flow vs. Static Pressure Samples S1 - S6. 153

45. Volume Flow vs. Static Pressure Samples E1 - E9. 154

46. Ratio of Volume Flows vs. Static Pressure Various Samples. 155

47. Volume Flow vs. Static Pressure Prestressed Sample S3. 161

48. Stitching Patterns 164

49. Stagnation Temperature in Degrees Fahrenheit vs. Mach number at 100,000 ft 187

Approved for Public Release

Contrails

LIST OF TABLES

Table

Page

1. Average Test Results on Nylon Fabrics Compared to Original and Current Specifications. 3

2. Average Test Results on Nylon Suspension Cord Compared to Original and Current Specifications 4

3. Average Test Results of Rayon Faoric Compared to Original and Current Specifications. 4

4. Average Test Results of Cotton Fabric Compared to Original and Current Specifications. 5

5. Average Test Results of Cotton Suspension Tapes Compared to Current Specifications. 5

6. Properties of Silk Parachute Fabric - AN-CCC-S-371 Range of Values for Fifteen Samples 6

7. Test Results on Silk Cord - AN-C-126, Type II 8

8. Physical Properties of Fabric Taken From Deployed Parachutes. . . . 9

9. Results of Tests on Standard G-11A and Silicone Treated G-11A Parachutes. 10

10. Average Physical Properties of Nylon Cloths Finished With Silicone Oil. 11

11. Constructions Specification MIL-W-4088C 14

12. Physical Characteristics of Natural Specification MIL-W-5625. . . . 15

13. Physical Characteristics Specification MIL-W-4088C. 16

14. Breaking Strength and Elongation Data for Nylon 6 Threads and Cords Tested at 65% R. H. and 70°F. 18

15. Breaking Strength and Elongation Data for Nylon 6 Tapes, Specification MIL-T-5038 and MIL-T-5608, Before and After Heat Ageing at Elevated Temperatures for 24 Hours Tested at Standard Conditions 65% R.H. and 70°F. 19

16. Properties of Type II, MIL-C-5040A Core-Sleeve and Optimum Experimental Coreless Type Braids 22

Approved for Public Release

Contrails

LIST OF TABLES (Continued)

Table		Page
17.	Properties of Type III, MIL-C-5040A Core Sleeve and Optimum Experimental Coreless Type Braids	23
18.	Physical Properties of Unprocessed Control and Processed Producer's Type 5100, 220 Nominal Denier Dacron Yarn.	27
19.	Single Load to Rupture and Repeated Stress Properties of HS-HR Type 5100 Dacron Producer's Yarn Before and After Heat Ageing	29
20.	Physical Properties of Dacron Thread Specification MIL-T-4855 Size E (Equivalent to Nylon Specification MIL-T-7807 Size E)	30
21.	Physical Properties of Dacron Thread Specification MIL-T-4855 Size E (Equivalent to Nylon Specification MIL-T-7807 Size E) Before and After Heat Ageing at 350°F for 24 Hours	32
22.	Physical Properties of Dacron Thread Specification MIL-T-4855 Size 3 Cord (Equivalent to Nylon Specification MIL-T-7807 Size 3 Cord)	34
23.	Physical Properties of Dacron Thread Specification MIL-T-4855 Size 3 Cord (Equivalent to Nylon Specification MIL-T-7807) Before and After Heat Ageing at 350°F for 24 Hours	35
24.	Physical Properties of Dacron Webbing (Equivalent Nylon Specification MIL-W-4088B Type X With Weave of Specification MIL-W-5665A).	36
25.	Physical Properties of HS-HR Dacron Webbing (Equivalent to Nylon Specification MIL-W-4088B Type X With Weave of Specification MIL-W-5665A).	36
26.	Physical Properties of Dacron Tubular Webbing (Equivalent to Nylon Specification MIL-W-5625)	37
27.	Physical Properties of Dacron Type V Coreless Braids (Equivalent to Nylon Specification MIL-C-7515).	38
28.	Physical Properties of Dacron Type V Coreless Braid (Equivalent to Nylon Specification MIL-C-7515) Before and After Heat Ageing at 350°F for 24 Hours	38
29.	Physical Properties of Dacron Type IV Tape (Equivalent to Nylon Specification MIL-T-5038)	39
30.	Physical Properties of Dacron Type IV Tapes (Equivalent to Nylon Specification MIL-T-5038) Before and After Heat Ageing at 350°F for 1 Hour.	39

Approved for Public Release

Contrails

LIST OF TABLES (Continued)

Table		Page
31.	Theoretical Maximum and Minimum Widths of Nylon Yarns Compared to Measured Widths	44
32.	Summary of Experimental Webbings	52
33.	Effect of Pick Variation on Webbing Performance	55
34.	Effect of Weave Variation on Webbing Performance	59
35.	Effect of Number of Ends on Webbing Performance	61
36.	Effect of Singles Yarn Twist on Webbing Performance	63
37.	Effect of Yarn Twists on Webbing Performance	66
38.	Effect of Yarn Plies on Webbing Performance	69
39.	Effect of Filament Size on Webbing Performance	70
40.	Effect of Dyeing on Webbing Performance	71
41.	Life Tests of Chemstrand and du Pont Canopies	77
42.	Air Permeabilities of Fabrics Before and After Drop Tests	77
43.	Breaking Strength of Component Parts of B-47 Deceleration Parachutes after Specified Number of Deployments	80
44.	Percent Loss in Strength After Use	81
45.	Ranges of Deployment Data: F-100 Deceleration Parachutes	82
46.	Breaking Strength and Gage Length Change of Component Items of F-100 Brake Parachute	83
47.	Percent Loss in Strength, Component Items of F-100 Brake Parachute	84
48.	Physical Properties of Fabric from F-100 Brake Parachutes	85
49.	Rip-Stop Fabric Parameters	98
50.	Evaluation of Equation (17) as a Means of Determining LP Changes	114

Approved for Public Release

Contrails

LIST OF TABLES (Continued)

Table		Page
51.	Evaluation of Theoretical Method for Determining Fabric Strain Under a Pressure Differential.	117
52.	List of Symbols	118
53.	List of Symbols	120
54.	Experimental Fabric Parameters.	142
55.	Air Permeability and Light Penetrability Values for Commercial Fabrics	146
56.	Fabric Parameters of Selected Commercial Fabrics.	147
57.	Relative Flow of Selected Commercial Fabrics.	148
58.	Description of Test Parachute Fabrics	150
59.	Summary of Permeometer Results.	156
60.	Webbing Properties, Thread Types, and Seam Types.	163
61.	Average Seam Strengths and Efficiencies	165
62.	Exposure in Langleys.	167
63.	Webbings, Average Breaking Strengths and Percent Retention After Exposure.	168
64.	Breaking Strength of Stored Parachute Materials	174
65.	Percent Elongation vs. Time For Nylon Braids Under Selected Dead Loads	176
66.	Effect of Duco Lacquer, 3661 Paint Thinner, on the Strength of Nylon Ribbons	177
67.	Effect of Thermal Radiation on the Strength of Ribbons and Ribbon Assemblies	179
68.	Critical Thermal Energies Required for Initial Melting of Nylon and Dacron Type XIII Webbings	180
69.	Effect of Thermal Radiation on Breaking Strength of Nylon and Dacron Type XIII Webbings	181

Approved for Public Release

Contrails

LIST OF TABLES (Continued)

Table		Page
70.	Properties of Thermally Radiated Samples.	183
71.	Properties of Nylon Fabric Specification MIL-C-7020, Type I After Exposure to Thermonuclear Radiation	184
72.	Breaking Strength of Nylon Ribbon, Specification MIL-T-5608	184
73.	Listing of Compounds Falling in the Allowable Melting Range Which Meet the Vapor Pressure Requirements.	190
74.	Initial Heating Rates vs. Thermocouple Positions Nylon Ribbon . . .	192
75.	Time to Cause Progressive Failure	192
76.	Lifetime Augmentation of Nylon Ribbons Resulting From Use of Coatings.	193

Approved for Public Release

Contrails

Approved for Public Release

Contrails

INTRODUCTION

Various aspects of fibrous material characteristics and properties have been investigated for decelerator application through both contract research and internal effort by the Directorate of Materials & Processes.

The results of these studies have been contained in ASD Technical Reports issued at the completion of the work. The purpose of this report is the summarizing and consolidation of information from these research reports into a single report more readily available and more useful to designers and others interested in materials for decelerator applications.

This report is divided into sections covering several pertinent phases of fibrous material information. The summarizing of the specific list of ASD reports was not intended to furnish information sufficient to completely fill all the gaps in the complete range of desired information. Additional information, as it becomes available will be added as new sections under appropriate headings so that eventually all pertinent data regarding fibrous materials will be gathered together within one framework.

Manuscript released by the author 15 August 1961 for publication as an ASD Technical Report

Approved for Public Release

Contrails

Section I

AGEING PROPERTIES

1.1 Effect of Fifteen Years of Ageing on the Deterioration of Parachutes

The problem of maintaining large supplies of personnel and cargo parachutes for emergency purposes is of course dependent upon the ability of parachutes of all types to be stored for long periods of time without deterioration to a condition where they are no longer safely useful.

To ascertain the effect of ageing on physical properties, samples of nylon, rayon, silk and cotton parachutes at least fifteen years old were selected as representative of large warehouse stocks, and tested in the laboratory. Properties comparisons were made: (1) against the original specifications at the time the parachutes were manufactured; and (2) against present specifications.

The work was conducted by C. O. Little, Jr., WADC Materials Laboratory, and is reported in WADC Technical Note 59-30, February 1959.

1.1.1 Materials Tested

Rayon, silk, nylon and cotton parachutes, originally designated personnel parachutes but redesignated as cargo chutes because of their age. (Note: Records indicate that cotton has not been used in personnel chutes.) The samples selected were representative of 61,000 overage parachutes in storage.

1.1.2 Test Procedures

Standard textile tests as noted in the tables were conducted according to Federal Specification CCC-T-191b. Permanence of finish was tested according to MIL-C-7020C. Five tests were performed on each gore or section of the parachute canopy, and on each suspension line.

1.1.3 Test Results

Nylon Fabric: Table 1 lists properties of three series of nylon fabrics, Specification MIL-C-7020C, Type II.

Nylon Suspension Cord: Table 2 lists properties of three samples of nylon cord, MIL-C-5040, Type III.

Rayon Fabric: Table 3 lists average properties of five samples of rayon fabric, MIL-C-8006, Type II.

Rayon Suspension Tape: The original Specification 16125-A listed a minimum breaking strength of 500 lb. The current Specification MIL-T-5237, Type I lists a minimum breaking strength of 550 lb. Test results of the 15-year old samples showed an average strength of 533.8 lb. Therefore the material meets the original specification, but fails to meet the current specification.

Cotton Fabric: Table 4 lists average properties of cotton fabric, Specification MIL-C-4279, Type II.

Cotton Suspension Tapes: Table 5 lists average properties of cotton

Approved for Public Release

Table 1. Average Test Results on Nylon Fabrics Compared to Original and Current Specifications

Sample No.	Orig. Spec. AN-CCC-C-486 and ANC-127	Type II			
		Current Spec. MIL-C-7020C	F-1 thru F-4	F-5 thru F-8	F-29 thru F-32
Physical requirements					
Weight (oz/yd^2)	1.6 max	1.6 max	1.42	1.45	1.51
Thickness (in.)	0.0042 max	0.0042 max	0.0041	0.0041	0.0042
Breaking strength					
Warp (lb/in.)	50 min	50 min	58.0	57.5	57.0
Fill (lb/in.)	50 min	50 min	57.8	52.6	55.7
Elongation					
Warp (%)	14 min	20 min	22.4	23.7	21.1
Fill (%)	14 min	20 min	25.3	27.7	25.9
Tearing strength					
Warp (lb)	4.0 min	4.0 min	4.5	4.9	5.2
Fill (lb)	4.0 min	4.0 min	5.2	4.5	5.0
Air permeability ($cu\ ft/min/ft^2$)	100-160	130±30	143.6	142.4	157.4
Permanence of finish					
Thickness (%)	10 max	10 max	0.6 gain	0.6 gain	4.2 gain
Shrinkage in boiling water					
Warp (%)	2 max	2 max	0.05	1.43	0.83
Fill (%)	1 max	2 max	0.02	0.03	0.05
Air permeability change after boiling (%)	15 max	15 max	1.4 loss	0.9 loss	3.2 gain

Approved for Public Release

Contrails

Table 2. Average Test Results on Nylon Suspension Cord Compared to Original and Current Specifications

Sample No.	Orig. Spec. ANC-63 Type II	Type III Current Spec. MIL-C-5040	Type III C-1	Type III C-2	Type III C-7
Breaking strength (lb)	550 min	550 min	579	564	532*
Elongation (%)	30 min	30 min	41	42	41
Yards/lb	75 min	75 min	78.6	80.5	79.5
Picks/inch	26-28	----	27	27	27
Twist/in-core yarns					
Initial ply (t.p.i.)	10-12	10-16	10.7	11.0	12.0
Final ply (t.p.i.)	6-7	6-8	7.0	6.5	7.0
Sleeve yarns					
Singles (t.p.i.)	7.5-9.0	7.0-9.5	8.1	7.8	8.5
Ply (t.p.i.)	5.0-6.0	5.0-7.0	6.2	5.6	6.0

*Failed to meet current specification requirements.

Table 3. Average Test Results of Rayon Fabric Compared to Original and Current Specifications

Sample No.	F-38 thru F-42 Type II	Current* Specification MIL-C-8006 Type II
Breaking strength		
Warp (lb/in.)	85.8	80 min*
Fill (lb/in.)	85.4	80 min
Elongation		
Warp (%)	16.6	15 min
Filling (%)	19.4	15 min
Tearing strength		
Warp (lb)	26.8	10 min
Fill (lb)	27.2	10 min
Air permeability (cu ft/min/ft^2)	141.6	150$\pm$30

*When original Specification No. 16126 was superseded by current Specification MIL-C-8006, the minimum breaking strength was reduced from 85 lb to 80 lb minimum.

Approved for Public Release

Contrails

Table 4. Average Test Results of Cotton Fabric Compared to Original and Current Specifications

Sample No.	Orig. Spec. No. 16147	Current Spec. MIL-C-4279	Type II F-24 thru F-28	Type II F-33 thru F-37
Threads/inch				
Warp		54 min	83	84
Filling		56 min	82	84
Weight oz/yd^2	5 max	3.7-4.6	4.3	4.2
Breaking strength				
Warp (lb/in.)	45 min	48 min	102.5	98.2
Fill (lb/in.)	55 min	42 min	102.2	96.9
Elongation				
Warp (%)	None	None	17	17
Fill (%)	None	None	16.5	17
Tearing strength				
Warp (lb)	4 min	4 min	8.1	7.4
Fill (lb)	2-1/2 min	2-1/2 min	7.9	7.4
Air permeability	200±30	200±30	25.6*	22.5

*Failed to meet current specification requirements.

Table 5. Average Test Results of Cotton Suspension Tapes Compared to Current Specifications

Sample No.	Orig. Spec. AN-JJ-W-151 AN-W-21	Current Spec. MIL-W-5665 Type I	C-6	C-8
Width (in.)	9/16 ± 1/32	9/16 ± 1/16	9/16	9/16
Thickness (in.)	.040 - .050	.040 - .050	.0465	.048
Breaking strength (lb)	350 min	350 min	396.6	403.0
Weight/yd (oz)	0.40 min	0.40 max	0.361	0.396
Filling threads/inch	20 min	20 min	20	21.5

suspension tapes, Specification MIL-W-5665, Type I.

Silk Fabric: Table 6 lists average properties of silk fabric original Specification AN-CCC-S-371. Note: There is no current silk fabric specification.

Approved for Public Release

Table 6. Properties of Silk Parachute Fabric - AN-CCC-S-371
Range of Values for Fifteen Samples

Weight oz/yd	Specification	Range	Comments
Weight oz/yd	1.6 max	1.36-1.55	
Breaking strength			
Warp (lb/in.)	40 min	41.0-50.0	2 samples (29.4 and 30.0 lb) failed spec.
Fill (lb/in.)	40 min	40.0-55.8	
Tearing strength			
Warp (lb)	4 min	4.4-5.6	7 samples (from 3.0 to 3.8 lb) failed spec.
Fill (lb)	4 min	4.0-6.0	2 samples (3.6 lb) failed spec.
Air permeability cu ft/min/ft^2	80-140	100-137.5	
Elongation			
Warp (%)	None	16.7-21.7	3 samples (14.0-15.0%) apparently "substandard"
Fill (%)		15.0-18.3	2 samples (6.7%) apparently "substandard"
Thickness (in.)	"	.0045-.0052	
Acidity (pH)	"	5.4-7.8	
Permanence of finish	"		
Shrinkage in boiling water	"		
Warp (%)		(-)2.2-(+)1.8	(-) signifies shrinkage;
Fill (%)		(-)2.2-(+)3.3	(+) signifies growth
Thickness after boiling (% change)		17.3-34.0	
Air permeability after boiling water (% gained)	"	17.9-67.3	

Approved for Public Release

Confidential

Contrails

Silk Cord: Table 7 lists data on silk cord, original Specification AN-C-126, Type II. Note: There is no current silk cord specification.

1.1.4 Conclusions

Nylon Parachute Fabric: There were individual sections scattered throughout the tested canopies that failed to conform to the original specification requirements.

The average results of each canopy were compared with current specification requirement and found to comply with all specification requirements.

This investigation of parachute fabrics, manufactured over fifteen years ago, revealed no evidence of cloth degradation.

Nylon Suspension Cord: One group out of the three groups of suspension lines tested failed to comply with the current, as well as the original specification requirement, under which the material was manufactured.

The breaking strength of the group of suspension lines below minimum specification requirements (550 lb) was 532 lb. The low breaking strength may be attributed to changes in the elongation characteristics of the core or sleeve yarns and/or breakage in the filaments of the yarns.

Rayon Parachute Fabric: When the rayon fabric was tested and compared to the original specification requirement, the breaking strength did not meet these requirements in two of the five gores tested.

Upon averaging these results and comparing them with the current specifications, it was found that the fabric did meet all the current requirements.

Rayon Suspension Tape: The suspension tape does meet the original specification requirements; however, since its manufacture, the breaking strength of the current specification has been increased resulting in the tape not meeting current requirements.

Cotton Parachute Fabric: The thread count of the fabric is approximately 50-55% more than the minimum requirements of the specification.

Upon comparing the fabrics' strength to the original and current specification requirements, it was found to be extremely high. This high strength is due to the thread count being very high with the yarn size remaining the same.

If a fabric is within the weight requirements and it does contain a substantial increase in the thread count, the fabric must be woven extremely tight. Decreasing the amount of space between the ends and picks in a fabric will decrease the amount of air that passes through the cloth at a given ΔP. This could be the explanation for the air permeability being very low for this fabric, and why it fails to meet the original and current specification requirements.

Silk Parachute Fabric: This fabric cannot be compared with any current specification because the Air Force has deleted all specifications on this type of cloth.

There are indications that some deterioration of the material has occurred

Approved for Public Release

Contrails

Table 7. Test Results on Silk Cord - AN-C-126, Type II

Tests applied to cord	Test Samples			Spec.
Breaking strength (lb)	427	413	414	325
Yards/lb	92.0	86.5	86.5	80 min
Sleeve - no carriers - each end of 3 ply	36	32	32	32
Tests performed which have no specification requirements				
Elongation (%)	24	26	28	--
Picks/inch	18	18	20	--
Twist/inch				
Core yarns				
Initial ply	7.3	8.6	7.2	--
Final ply	6.0	6.7	6.0	--
Sleeve yarn				
Singles yarn	9.5	9.8	10.0	--
Ply yarn	8.3	7.1	7.3	--

over a period of 15 years, inasmuch as 30% of the tearing strength results failed to meet the original specification requirements.

Although the permanence of finish tests were not a part of the original specification requirements, it was performed to give additional information about the fabric. The fabric thickness varied 17-34% and the air permeability varied 18-100% from the original test results. This variance is due to fiber swelling which occurs when saturated with moisture.

Silk Suspension Cord: This suspension cord cannot be compared with a current specification because the Air Force has deleted all specifications using this type of cord.

The suspension cord did meet all the original specification requirements.

1.1.5 References

WADD TR 60-584, pp. 2-4.

1.2 A Comparison of the Ageing Properties of Cocoanut vs. Silicone Oils as Finishing Agents for Nylon Parachute Cloth

The testing of overage or near overage parachutes has indicated that the tearing strength of cloth deteriorates with time. The loss in tear strength is probably caused by the volatilization or drying out of the finishing oils originally applied to increase tear strength. Originally a cocoanut type finishing oil called "Coronyl" was used. Object of the present study was to compare the effect of a new silicone type oil with the cocoanut type oil when applied to nylon cloth used in cargo parachutes Type G-11A. The work was conducted by J. C. McGrath, WADC Materials Laboratory and is reported in WADC Technical Note 59-10, January 1959.

1.2.1 Materials Tested

Approved for Public Release

Contrails

I. Type G-11A parachutes containing nylon fabric Specification MIL-C-7020, Type II finished with:
(a) Coronyl cocoanut type oil.
(b) Silicone oil XE-112A (Dow Corning Corp.).

II. Fifty-three selected samples taken from 50,000 yd of nylon cloth, Specification MIL-C-7020, Type II, finished with silicone oil XE-112A (Dow Corning Corp.) by four different mills.

1.2.2 Test Procedures

1.2.2.1 Parachute Drop Tests: Cocoanut vs. Silicone Oil Finished Fabrics.

Nylon cargo parachutes Type G-11A finished with cocoanut oil and silicone oil, respectively, were repeatedly drop tested and then examined for damage. Two such series of drop tests were made. Fabric samples were then cut from the parachutes and tested for breaking strength, elongation, tearing strength, acidity and air permeability.

1.2.2.2 Physical Properties of 53 Samples of Nylon Parachute Cloth, Specification MIL-C-7020, Type II, Finished with XE-112A Silicone Oil.

Samples were tested for breaking and tear strength before and after ageing, air permeability and permanence of finish.

1.2.3 Test Results

1.2.3.1 Parachute Drop Tests.

Table 8 shows properties of fabric taken from the deployed parachutes. Table 9 shows the damage observed on five cocoanut and five silicone oil parachutes which were repeatedly deployed.

Table 8. Physical Properties of Fabric Taken From Deployed Parachutes

	MIL-C-7020, Type II Specification	Cocoanut Oil	Silicone Oil
Breaking strength (lb/in.)(WxF)*	50 x 50 (min)	57.4 x 56.5	55.8 x 54.4
Breaking elongation (%)(WxF)	20 x 20 (min)	27.9 x 32.1	26.2 x 33.0
Tear strength (lb/in.)(WxF)*	4 x 4 (min)	5.2 x 5.7	5.6 x 6.3
Acidity (pH)	5-9	7.1	7.7
Air permeability ($ft^3/min/ft^2$)	130 ± 30	134.2	118.5

*Warp x Filling

1.2.3.2 Physical Properties of Nylon Cloth Finished with Silicone Oil.

Table 10 gives physical properties of nylon cloth finished with silicone oil by four manufacturers.

1.2.4 Conclusions

In the first series of drop tests (by the Airborne Service Test

Approved for Public Release

Table 9. Results of Tests on Standard G-11A and Silicone Treated G-11A Parachutes

Drop No.**	Damage Sustained by Standard Coronyl Treated G-11A Parachutes					Damage Sustained by Silicone Treated G-11A Parachutes				
	No. C1	No. C2	No. C3	No. C4	No. C5	No. S1	No. S2	No. S3	No. S4	No. S5
A		Light		Medium	Medium	Light	None			Light
B	Light	Light				Medium	None			
C			Light	Light	Light			Light	Light	
D	Light	Light			Light	None	Light			Light
E	None				Light			None		None
F		None					None			None
G			None		None			None	None	
H		Medium	Medium					None	Medium	
I	Medium			Medium		None	Medium			Medium
J			Total*	None					Total*	
K	None					Light		Medium		
L				None						

*Parachute destroyed by disconnect which released in mid-air.

**The letters do not necessarily reflect the number of deployments.

Approved for Public Release

Confidential

Contrails

Table 10. Average Physical Properties of Nylon Cloths Finished With Silicone Oil

	Specification MIL-C-7020, Type II	Finishing Mill 1	2	3	4
Breaking strength (lb/in.)					
Original (WxF)*	50 x 50	60 x 60	60 x 59	60 x 59	56 x 58
After ageing** (WxF)	-	60 x 59	59 x 59	59 x 58	55 x 57
% Loss after ageing (WxF)	-	0 x 2	2 x 0	2 x 2	0 x 2
Tear strength (lb/in.)					
Original (WxF)	4 x 4	8.6 x 9.2	7.9 x 10.0	9.1 x 9.7	7.0 x 8.2
After ageing (WxF)	-	9.3 x 10.8	8.4 x 9.9	8.4 x 10.0	7.7 x 8.9
Air permeability $ft^3/min/ft^2$	130 ± 130	106	144	107	155

*Warp and filling.
**Ageing: 16 hr @ 210°F.

Division, CONARC, Ft. Bragg, North Carolina) it was reported that: (1) Comparative data showed no differences in operational characteristics between the parachutes of silicone oil finished or standard finished cloth; (2) in recovery on frozen ground, the parachutes of silicone oil finished cloth appeared to snag more readily and had more snags and tears than parachutes of standard finished cloth.

In the second series of drop tests (by 6511th Test Group (Parachutes) U. S. Naval Auxiliary Air Station, El Centro, California) it was reported that there was no appreciable difference in the handling or operational characteristics and that there were no apparent advantages or disadvantages in the use of either type parachute. Parachutes of the silicone oil finished fabric showed less damage after drop tests than the parachutes of the standard finished cloth.(See Table 9.)

Physical properties of samples of cloth, taken from the parachutes which had been drop tested, have apparently not been affected by either the age of the parachute or by the drop tests. Tearing strength of the silicone oil finished cloth (from parachutes) was slightly higher than for the standard cocoanut oil finished cloth. In a few instances tearing strength was low, however, this is probably due to damage to the cloth itself and not as a result of the finishing oils. (Based on serial numbers, the parachutes of silicone oil finished cloth are probably a year or so older than parachutes of standard finished cloth. The average air permeability of the samples taken from the parachutes checked very closely with results from the original samples of cloth. Breaking strengths are still well above specification requirements.

Laboratory evaluation of cloth finished by four different mills indicates that neither the breaking strength nor the tearing strength was affected by the use of silicone oil. Tearing strength after ageing (16 hr at 210-220°F) was in most instances higher than the original strength. Other physical properties were not affected either before or after ageing and use of a silicone oil had no apparent effect on the appearance or handle of the finished cloth.

Approved for Public Release

Contrails

Based on data obtained from this program, Specification MIL-C-7020 has been revised to incorporate a requirement for the use of silicone oil as a finishing agent.

1.2.5 References

Sections 1.1, 4.1, 4.2, and 4.3.

Approved for Public Release

Contrails

Section II

DESIGN DATA, BASIC

2.1 Development and Evaluation of Webbing made from Nylon 6

Objective of the study was to evaluate webbings manufactured from nylon 6 caprolactam yarns HB (high tenacity-bright) and HBT (high tenacity-bright-thermally resistant) and compare properties with standard webbings prepared from nylon 66 polyamide yarns. The webbings were manufactured and tested by Phoenix Trimming Company and results are reported by R. J. Neff in WADC TR 57-638, March 1958 (Contract AF 33(600)-33484).

2.1.1 Materials Developed and Tested

2.1.1.1 Yarns Used for Manufacturing Webbings. 210-denier, 32-filament, 1-t.p.i., Z-twist HB; 840-denier, 136-filament, 1/2-t.p.i., Z-twist HBT.

2.1.1.2 Webbings. Table 11 lists experimental webbings generally constructed according to Specification MIL-W-4088C, Types VI, VIII, IX, X, XIII, XVIII, and XIX. Table 12 lists webbings generally constructed according to Specification MIL-W-5625.

2.1.2 Test Methods

Linear Weight, Breaking Strength, Abrasion Resistance, Weathering Resistance, and Elongation were all determined exactly as described in WADD TR 60-584, pages 86 to 87.

Dyeing: The webbings were dyed according to Specification MIL-W-4088C.

Resin Treating: All 840-special-denier webbings and the Type X, 210-denier webbings were Merlon resin (polyvinyl butyral) treated and then cured at 340°F. All others were cured at 240°F.

Shrinkage Test: Fifteen-inch-long specimens with ten-inch gage marks were suspended by one end in boiling water for 15 minutes, removed, allowed to drain, and then air-dried. Percent shrinkage was calculated as a percent change from the original ten-inch gage marks.

Heat Conditioning: Samples were hand rolled and suspended in a hot air circulating oven at temperatures of 200°F, 250°F, 300°F, or 340°F for 24 hours, then reconditioned at room temperature for 24 hours.

2.1.3 Test Results

Tables 12 and 13 tabulate webbing properties.

2.1.4 Conclusions

The 210-denier, Type HB nylon 6 yarn suffers severe strength loss when exposed to 340°F; i.e., that temperature commonly used to cure the Merlon resin or nylon 66 webbings. The 840-denier, Type HBT nylon is significantly better in its heat resistance.

The Type 6 yarn shrinks considerably more during the yarn dyeing

Approved for Public Release

Table 11. Constructions Specification MIL-W-4088C

Type and Condition*	Weight (oz/yd)	Thickness (in.)	Width (in.)	Total Ends Face and Back	Face and Back Yarn Denier and Ply	Binder Ends	Binder Yarn Denier and Ply	Filling Picks (per in.)	Filling Yarn Denier and Ply
VI-U	1.165	0.055	1-23/32	120	210/7			22	210/10
VIII-U	1.55	0.065	1-23/32	132	210/10			18	210/10
IX-U	4.13	0.110	3	309	210/10	38	210/7	28	210/3/3
X-U 210-denier	3.37	0.145	1-23/32	305	210/10	39	210/4	22	210/3/3
X-U 840-denier	3.60	0.146	1-23/32	257	840/3	31	840/1	22	840/2
XIII-U	2.85	0.116	1-23/32	281	840/2	34	840/1	26	840/2
XVIII-U	1.92		1	208	210/10			18	210/10
XIX-U	3.20	0.108	1-23/32	280	840/3			18	840/2

*Condition U refers to no resin treatment on the webbing. All webbings listed were also given a Merlon polyvinyl butyral resin treatment (Condition R). The resin treatments resulted in a 3-8% weight increase and a corresponding thickness decrease for each webbing.

Approved for Public Release

Controlled

Table 12. Physical Characteristics of Natural Specification MIL-W-5625

Width (in.) Condition	Weight (oz/yd)	Thickness (in.)	Breaking Strength (lb)	Total Ends Face and Back	Face and Back Yarn Denier and Ply	Filling Picks (per in.)	Filling Yarn Denier and Ply	Shrinkage Percent After Boiling Water	Effect of Heat Ageing for 24 Hours Strength (lb) 200°F	250°F
1/2-U	0.38	0.060	1268	112	210/4	26	210/4	17.5	1080	392
9/16-U	0.44	0.057	1519	128	840/1	26	840/1	14.8	1467*	
U	0.43	0.065	1533	128	210/4	26	210/4	17.5	1303	311
3/4-U	0.84	0.086	2681	110	210/8	26	210/8	17.5	2270	753
5/8-U	0.58	0.071	2175	176	210/4	26	210/4	17.0	1739	524
1-U	1.2	0.089	4234	160	210/8	26	210/8	17.5	3230	895

*At 300°F.

Approved for Public Release

Confidential

Table 13. Physical Characteristics Specification MIL-W-4088C

Type and Condition	Breaking Strength (lb)	Breaking Strength After 5000 Strokes Abrasion (lb)	% Loss Due to Abrasion	Effect of Heat Ageing for 24 hr Strength (lb) 200°F	250°F	300°F	% Merlon	20-hour Fade-O-Meter	Wash Fastness	Accelerated Ageing (Breaking Strength (lb) After 100-hr Weather-O-Meter Exposure)	% Retained Strength of R Compared with U	Shrinkage % After Boiling Water
VI[a]												
-U	2511			2486	1578			G	G	2286		2.5
R	2571	2411	6.20	2314	1103		7.13	G	G	1970	86.2*	7.5
VIII[a]												
-U	3990			3802	2822			G	G	3616		1.8
R	3901	3740	4.10	3584	1760		7.05	G	G	3314	91.6	5.0
IX[a]												
-U	8290			8436	7208			G	G	7044		1.3
R	8320	8030	3.49	7636	5232		8.64*	G	G	6392	90.7	5.0
X[a]												
-U	9178					2700		G	G	8498		1.6
R	8888	8524	4.09			600	6.01	G	G	7516	88.5*	3.1
X[b]												
-U	9564					8550		G	G	6400		0.6
R	9352	9008	3.72			7770	7.12	G	G	6396	99.9	1.9
XIII[b]												
-U	6708					5932		G	G	3680		0.6
R	6788	6144	9.49			5972	8.23	G	G	3664	99.6	1.9
XVIII[a]												
-U	6068			5600				F*	G	4823		2.5
R	6038	5762	4.50	5600			3.09	F*	G	4764	98.8	4.6
XIX[b]												
-U	10588					8800		G	G	6980		3.8
R	10912	10700	1.94			8156	6.43	G	G	6760	97.8	4.4

a. 210-denier, HB yarn.
b. 840-denier, HBT yarn.

Note: At 340°F all webbings were decomposed to a point where they could not be tested.

* Does not meet requirements.
** G = Good
F = Fair

Approved for Public Release

Contrails

process than Type 66 yarn. To obtain good breaking strength efficiency (when compared to the Condition U webbing) the Condition R webbing must be cured at approximately 240°F. In every case of the yarn dyed webbings, the Condition R material exhibited lower elongation and higher shrinkage than the Condition U material. This would indicate that the yarn dyed webbings possess a considerable amount of early elongation and that the tension used in the treating process tended to remove some of the early yarn shrinkage.

It would seem that the 840-denier, HBT yarn could be used in any and all applications where nylon 66 is presently used, provided it were used in either its natural gold shade or piece dyed.

2.1.5 References

Section 3.1, and WADD TR 60-584, pp. 86 to 88; 164 to 176.

2.2 Development and Evaluation of Cords, Ribbons, and Tapes made from Nylon 6

Objective of the study was to determine if materials made from nylon 6 caprolactam yarns are suitable substitutes for materials made from nylon 66. Certain tapes, ribbons, cords and threads were made in accordance with the construction requirements of appropriate specifications **except** that nylon 6 was used in place of nylon 66. They were then tested for physical properties. The work was conducted by C. F. Holmes, Jr., WADC Materials Laboratory, and is reported in WADC TN 59-14, January 1959.

2.2.1 Materials Developed and Tested

Using nylon 6 yarn, the following structures were prepared:

Tapes: MIL-T-5038; Type II-2 in.; Type III-1/2 in.; Type III-1 in.; Type IV-1 in.; Type V-9/16 in.

Tapes: MIL-T-5608: Class B Types II, III, V; Class C Types III, IV, V; Class E Type II.

Threads: MIL-T-7807: Type I, Class I, Sizes E, FF, 3 cord, 5 cord, 6 cord, 10 cord; Type II, Class I, Sizes E, FF, 3 cord, 5 cord, 6 cord, 8 cord, 10 cord.

Cord: MIL-C-7515: Types II, IV, VI, VIII, IX.

Cord: MIL-C-5040: Types IA, II, III.

With minor and insignificant exceptions, all samples complied with their respective construction requirements of the applicable specification.

2.2.2 Test Methods

All samples were tested for breaking strength and elongation under standard conditions of 65% R. H. and 70°F. In addition, the tapes were tested for breaking strengths under standard conditions after exposure to elevated temperatures of 200°F, 300°F, and 340°F for 24 hours.

2.2.3 Test Results

Table 14 lists strength and elongation values for the thread and cords. Table 15 lists strength and elongation values for the tapes

Approved for Public Release

Contrails

Table 14. Breaking Strength and Elongation Data for Nylon 6 Threads and Cords Tested at 65% R. H. and 70°F

Sample No.	Breaking Strength (lb) Spec. (min)	Breaking Strength (lb) Results	Elongation (%) Spec. (max)	Elongation (%) Results
	Thread MIL-T-7807			
Type I, Class I, E	8.5	10	22	24*
Type I, Class I, FF	16	20	22	23*
Type I, Class I, 3 cord	24	30	22	28*
Type I, Class I, 5 cord	40	47	22	23*
Type I, Class I, 6 cord	50	59	22	30*
Type I, Class I, 10 cord	90	93	22	34*
Type II, Class I, Size E	8.5	9	22	20*
Type II, Class I, Size FF	16	19	22	23*
Type II, Class I, 3 cord	24	28	22	26*
Type II, Class I, 5 cord	40	48	22	27*
Type II, Class I, 6 cord	50	55	22	25*
Type II, Class I, 8 cord	68	75	22	27*
Type II, Class I, 10 cord	90	88*	22	31*
	Cord MIL-C-7515		Spec. (min)	Results
Type II	550	574	20	26
Type IV	1000	1174	20	-
Type VI	2000	2419	-	-
Type VIII	3000	3515	-	-
Type IX	4000	4626	-	-
	Cord MIL-C-5040			
Type IA	100	139	30	53
Type II	375	444	30	49
Type III	550	583	30	50

*Does not meet specification requirements.

at standard conditions, and after heat ageing at the designated temperatures.

Six of the seven MIL-T-5608 tapes did not meet the specification requirement for breaking strength. All six were made of 30- and 40-denier yarns. The one sample (E-II) that met the specification requirement was made of 210-denier yarn.

One sample of thread (Type II, Class I, 10 cord) manufactured under Specification MIL-T-7807, had a breaking strength lower than the specification minimum. This particular thread was the Type II or bonded thread. It appears that the bonding agent is in some way detrimental to the strength of the thread. This is evidenced by the fact that the only difference between the Type I and Type II thread is the bonding agent, yet in practically every case the breaking strength of the bonded thread is 5-10% lower than that of the unbonded thread. The reason for this relationship has not been determined.

All but one of the thread samples had ultimate elongations above the specification maximum.

Approved for Public Release

Table 15. Breaking Strength and Elongation Data for Nylon 6 Tapes, Specification MIL-T-5038 and MIL-T-5608, Before and After Heat Ageing at Elevated Temperatures for 24 Hours Tested at Standard Conditions 65% R.H. and 70°F

Sample No.	Breaking Elongation (%)		Breaking Strength (lb)				
	Spec. (min)	Std. Cond.	Spec. (min)	Std. Cond.	After Ageing at Temp. of 200°F	300°F	340°F
MIL-T-5038							
II-2 in.	18	35	1700	2430	2460	530	100
III-1/2 in.	18	38	250	303	290	76	39
III-1 in.	18	42	525	643	617	161	64
IV-1 in.	18	47	1000	1241	1272	353	140
V-9/16 in.	18	42	500	572	568	157	62
MIL-T-5608							
B-II	18	20	33	30*	29	7	3
B-III	18	31	70	63*	60	14	8
B-V	18	31	200	165*	165	35	19
C-III	18	23	90	82*	78	21	12
C-IV	18	28	185	153*	153	37	28
C-V	18	34	300	269*	266	60	34
E-II	18	41	1000	1185	1195	320	167

*Does not meet specification requirements.

Approved for Public Release

Contrails

The tapes had little or no strength loss after being exposed to 200°F. The tapes exposed to 300°F suffered a loss in breaking strength of approximately 75%, and after exposure to 340°F they had a loss of approximately 90% of their original strength.

2.2.4 Conclusions

Materials made from nylon 6 are not suitable for all applications that ordinarily require nylon 66. Some of the materials tested in this evaluation did not meet breaking strength and elongation requirements of their respective specifications, while others did meet them. This leads to the conclusion that if nylon 6 is to be used it should be done with discrimination and by the use of material specifications that require nylon 6 yarn.

Materials made from 30- and 40-denier yarns appear to lose considerable strength during the weaving process.

The temperature versus breaking strength data indicate that the strength of nylon 6 decreases rapidly at temperatures above 200°F and should not be used in applications that would encounter temperatures above 200°F.

2.2.5 References

Section 2.1 and WADD TR 60-584, p. 368; WADC TR 55-264, pp. 105 to 138.

2.3 Development of Coreless Braids made from Nylon 6 and Nylon 66

Nylon braids of Specification MIL-C-5040A, Types II and III consist of a central "core" around which a "sleeve" is braided. Such braids when used as parachute suspension lines are functionally acceptable, but care must be taken in their design and manufacture to insure that the composite structure is "balanced," i.e., that the core and sleeve have equal breaking elongations, otherwise maximum strength and energy absorption will not be available.

In coreless braids, the balance problem does not exist. Therefore, their potential utilization is of interest, providing that strength requirements can be met.

E. M. Landis and F. W. Fraim III, Essex Mills, Inc., developed and evaluated a series of nylon coreless braids designed generally to meet the specifications of MIL-C-5040A, Types II and III. Results were compared with equivalent core-sleeve braids which met the specification. The coreless braids were made from both nylon 66 and nylon 6 polymer types. The work was conducted under Contract AF 33(616)-3993 and is reported in WADC TR 58-410, December 1958.

2.3.1 Materials Developed and Tested

Various core-sleeve and coreless braids composed of either nylon Type 66 or 6 as designated.

2.3.2 Test Methods

The sample braids were tested for general physical properties as

Approved for Public Release

Contrails

noted in Tables 16 and 17.

Abrasion Resistance was determined according to the method given for webbings under Specification MIL-W-4088C (see WADD TR 60-584, pages 86 to 87 and 165 to 168). The braids were flex abraded over a hexagonal steel bar for 1,000 strokes following which their residual strengths were determined.

Snag Resistance. An apparatus was developed to measure snag resistance, i.e., the ability of the filaments and yarns of the braid to be caught, held, or sometimes broken. The test cord was passed over a drum covered with sandpaper of selected roughness. By means of an inclined plane arrangement, (using a modified Ip-4 Scott Inclined Plane Tester) the cord was moved over the sandpaper and the number of snags determined on a recorder chart.

Seam Efficiency was determined as the ratio of a so-called standard butterfly seam attachment tensile test (Figure 1) to a regular braid tensile test. A 30-inch-long line length above the butterfly attachment was fastened in the upper clamp of the tensile testing machine so that the top of the butterfly attachment was approximately tangent to the bottom of the upper clamp. The parachute cloth skirt with sewn tapes was clamped in the fabric jaws. The six-inch overlap of the line was then a part of the free length between jaws, and the pull was against the seams holding the lines to the skirt as part of the butterfly attachment.

Energy Absorption was determined by measuring the area under the load-elongation diagram, and converting to the proper units.

2.3.3 Test Results

Table 16 lists the specifications and properties of Type II standard nylon 66 core-sleeve braid and the nylon 66 and nylon 6 optimum experimental braids. Table 17 lists similar values for Type III braids. Table 7 of the report (not included) gives a list of braid constructions which were developed and rejected for failure to meet specifications or for other reasons. The coreless type braids listed in Tables 16 and 17 far exceed the minimum requirements for breaking strengths, elongation and weight as required under the specification.

The abrasion resistance of both Type II and Type III coreless braid made from nylon 6 is superior to the nylon 66 coreless or the coresleeve braids.

The snag resistance of nylon 6 coreless braids is inferior to those made from nylon 66. However, more research should be conducted before drawing definite conclusions.

The coreless braids with the greatest energy absorption were made from Type 6 nylon. The coreless and core-sleeve Type 66 braids are about equal in energy absorption.

2.3.4 Conclusions

Coreless type cords can be produced to replace the presently used core and sleeve type cords. Within the scope of this project it was not possible to develop coreless cords which were equal or superior to the present core and sleeve cords as to snag resistance. It was found that the snag resistance of several of the coreless braids developed were approximately equal to the Type

Approved for Public Release

Table 16. Properties of Type II, MIL-C-5040A Core-Sleeve and Optimum Experimental Coreless Type Braids

	Specification		Standard		Coreless	Coreless
	Core	Sleeve	Core	Sleeve	Nylon 66	Nylon 6
Denier	210	210	210	210	210	210
Picks per inch	---	26-28	---	27	15	15
Carriers	---	32	---	32	16	16
Ends per carrier	---	1	---	1	3	3
Number of yarns	4-7	---	4	---	---	---
Twist per inch-spin	App.1	7-9.5	0.9	8.5	7-9.5	7-9.5
Twist per inch-1st ply	10-14	5-7	12.2	6.1	---	---
Twist per inch-final ply	6-8	---	7.3	---	5-7	5-7
Yarn ply	5/3	3	5/3	3	3	3
Yarn construction	---	---	---	---	210/1/3	210/1/3
Steam shrinking:						
Temperature °F	200	160	200	160	160	160
Time in minutes	60	30	90	60	60	60
Nylon type	66	66	66	66	66	6
Melting point (°F)	482	482	482	482	482	420
Yards per pound	105(min)		111		118.6	122
Breaking strength av. (lb)	375(min)		464		418	417
Breaking elongation (%)	30(min)		37.8		37	42
Energy absorption (in-lb/in.)			93		90	102
Strength after abrasion (lb)			384		354	378
% Strength loss after abrasion			17.3		15.2	9.3
Seam strength (lb)			402		395	406
Seam efficiency (%)			86		95	97
Snags produced (number)			12		16	24

Approved for Public Release

Confidential

Table 17. Properties of Type III, MIL-C-5040A Core Sleeve and Optimum Experimental Coreless Type Braids

	Specification		Standard		Coreless	Coreless
	Core	Sleeve	Core	Sleeve	Nylon 66	Nylon 6
Denier	210	210	210	210	210	210
Picks per inch	---	26-28	---	27	11.5	12
Carriers	---	32	---	32	16	16
Ends per carrier	---	1	---	1	3	3
Number of yarns	7-9	---	7	---	---	---
Twist per inch-spin	App.1	7-9.5	0.9	7.4	7-9.5	7-9.5
Twist per inch-first ply	10-14	5-7	11.5	5.4	---	---
Twist per inch-final ply	6-8	---	6.4	---	5-7	5-7
Yarn ply	5/3	3/3	5/3	3	4	4
Yarn construction	---	---	---	---	210/1/4	210/1/4
Steam shrinkage						
Temperature (°F)	200	160	200	160	200	200
Time in minutes	60	30	90	60	90	90
Nylon type	66	66	66	66	66	6
Melting point (°F)	482	482	482	482	482	420
Yards per pound	75(min)		87		93	87.5
Breaking strength av. (lb)	550(min)		618		577	581
Breaking elongation (%)	30(min)		38		36	43
Energy absorption (in-lb/in.)			118		125	140
Strength after abrasion (lb)			506		455	502
% Strength loss after abrasion			18.6		21.0	13.8
Seam strength (lb)			491		556	544
Seam efficiency (%)			79		96	94
Snags produced (number)			15		16	29

Approved for Public Release

Contrails

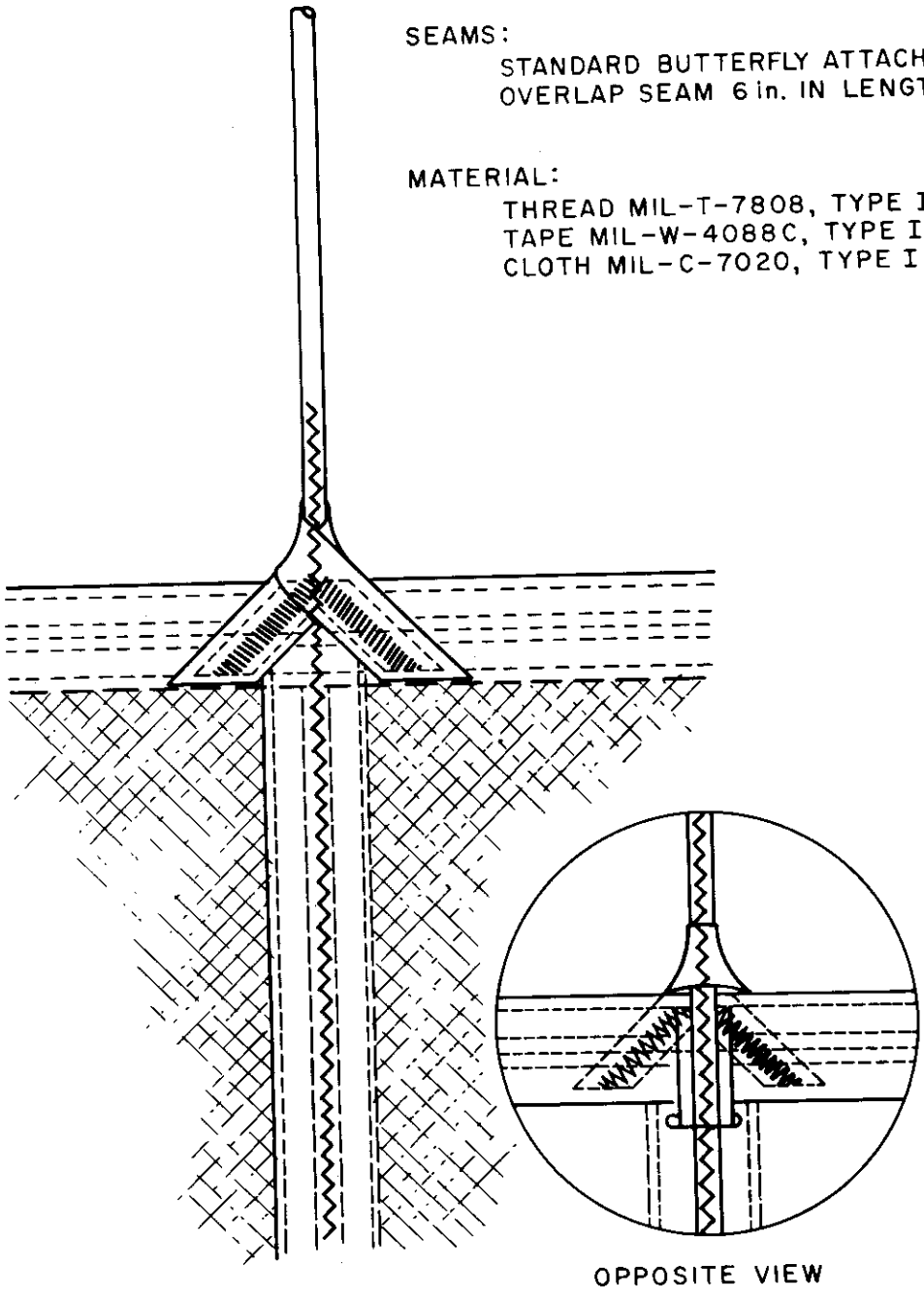

Figure 1 Standard Butterfly Attachment

Approved for Public Release

Contrails

III although higher than the Type II. In all other requirements, which include abrasion resistance, weight per unit length, energy absorption, breaking strength, elongation, and seam efficiency, the new coreless cords are equal or superior.

Nylon type 6 coreless cords compare as follows with nylon 66 coreless cords:

Strength	AE
Elongation	S
Weight (yd/lb)	AE
Abrasion resistance	S
Snag resistance	P
Energy absorption	AE
Seam efficiency	AE

The following compares the coreless cords to the core and sleeve type cords they were developed to replace.

	Compared to Type III		Compared to Type II	
	Coreless		Coreless	
	Type 6	Type 66	Type 6	Type 66
Breaking strength (lb)	S	S	S	S
Elongation (%)	S	S	S	S
Abrasion resistance	S	P	S	S
Snag resistance	P	AE	P	P
Seam efficiency (%)	S	S	S	S
Energy absorption	S	S	S	S
Weight (yd/lb)	S	S	S	S

S-Superior.
P-Poorer.
AE-Approximately equal.

2.3.5 References

Sections 2.1, 2.2, and 6.1 (seams), and WADD TR 60-584, pp. 244 to 246; WADC TR 55-264, pp. 60 to 63.

2.4 Development of High Tenacity Heat Stable Dacron Parachute Items

Reference is made to WADD TR 60-584, pages 13 to 44 which describe the development of heat stabilized Dacron yarns and fabrics.

The purpose of the program was to develop Dacron yarn, thread, webbing, tape and cord fabricated from hot stretched-heat relaxed yarn. Dacron yarn, because of its superior resistance to thermal degradation when exposed to temperatures of 350-400°F for prolonged periods of time, has been suggested as a replacement for nylon in deceleration parachutes. Dacron's strength retention after high temperature exposure is good, but longitudinal shrinkages of the order of 20% take place which present problems of dimensional stability. If the yarn is preshrunk before end item manufacture, in order to eliminate this difficulty, the 20% shrinkage results in heavier deniers and lower strength-to-weight ratios, thus requiring proportionately heavier parachutes. Furthermore, the added elongation resulting from thermal shrinkage at high temperatures is composed primarily of secondary creep or permanent set. Upon deployment

Approved for Public Release

Contrails

of the parachute, the possibility exists that the Dacron components might deform at the time of stress application, but not recover upon stress removal unless and until the parachute or its components were again elevated to the 350° level. Thus, "original" characteristics may not be maintained upon repeated usage.

WADC 55-135 "Development of Dacron Parachute Materials," March 1955 described the properties of selected threads, braids, cloth, webbings, ribbons and tape composed of Dacron which had been heat shrunk and relaxed in order to attain dimensional stability. Because of the potential deficiency due to high non-recoverable elongation, preliminary steps were taken leading to the development of a high tenacity, nominal elongation, heat stable Dacron yarn. Details of this development are given in WADC 55-297 "Development of High Tenacity-Heat Stable Dacron Yarn," July 1955.

At the inception of this phase of the study there was available from the du Pont Company high tenacity (6.1 grams per denier), nominal rupture elongation (9.2%), high thermal shrinkage (20% Dacron yarn, Type 5100). By heat relaxing at an elevated temperature this yarn was convertible to medium tenacity (4.8 grams per denier) high elongation (36%), low shrinkage (< 2%) yarn. Neither of these yarns was completely satisfactory for end use demands. Experimentation showed that cyclical yarn stressing and relaxing sequences at elevated temperatures produced a yarn of the desired high tenacity, normal elongation and low shrinkage, provided that the yarn was allowed to relax completely after the last stressing cycle.

The optimum process consisted of a three-step procedure:
1. 20% hot stretch at yarn temperature of 340-390°F.
2. Fixed length at 430-450°F.
3. Free shrinkage at 350°F.

Yarn produced by the process had a tenacity of 6.7-7.0 grams per denier (g.p.d.), an elongation of 14-16%, and a shrinkage of < 2% at 350°F.

A pilot unit was constructed to process HS-HR (hot stretched-heat relaxed) yarn which was then woven into selected threads, webbings and tapes. Physical properties of these products were compared with similar products made from HR (heat relaxed) yarns as described in WADD TR 60-584, pp. 244-246.

The program was conducted by C. C. Chu, E. R. Kaswell, and D. J. Doull of Fabric Research Laboratories, Inc., under Contract AF 33(616)-3593 and is reported in WADC TR 57-765.

2.4.1 Materials Developed and Tested

All of the following items were produced from HS-HR Dacron yarn:
Yarn: From producers Type 5100, 220-denier.
Thread: Specification MIL-T-4855, Type E, Type 3 cord.
Webbing: Equivalent to Type X, nylon Specification MIL-W-4088B.
Webbing: Equivalent to 9/16-in. tubular webbing, nylon Specification MIL-W-5625.
Coreless braid: Equivalent to Type V, nylon Specification MIL-C-7515.
Tape: Equivalent to Type IV (one inch wide), nylon Specification MIL-T-5038.

2.4.2 Processing and Testing Procedures

The HS-HR yarn was woven into the required end items which were then

Approved for Public Release

Contrails

evaluated for physical properties.

2.4.3 Test Results

2.4.3.1 Producers Yarn. Table 18 compares Type 5100 producers Dacron: (1) unprocessed (U); (2) heat relaxed (HR) as discussed in TR 55-135; and (3) hot stretched-heat relaxed (HS-HR) yarn. Figure 2 shows load-elongation diagrams for the three yarns.

Table 18. Physical Properties of Unprocessed Control and Processed Producer's Type 5100, 220 Nominal Denier Dacron Yarn

	(1) Unprocessed (U)	(2) Heat Relaxed (HR)	(3) Hot Stretched-Heat Relaxed (HS-HR)
Breaking strength (lb)	3.12	2.85	3.15
Rupture elongation (%)	9.10	39.7	19.5
Denier	238	283	222
Tenacity (g.p.d.)	5.9	4.5	6.5
Energy absorption (in-lb/in.)	0.144	0.550	0.258
Energy per denier (in-lb/in./denx10^{-3})	0.60	1.94	1.16
Modulus (g.p.d./unit strain)	77.3	44.3	73.6
Shrinkage (%) after 1 hr @ 350°F	19.0	0	1.2
Diameter (in)	0.0015		0.0020

*From TR 55-135

Comparison will demonstrate the apparent advantage of the hot stretched-heat relaxed process. The original Dacron has a breaking strength of 3.1 lb and a tenacity of 5.9 g.p.d. Its shrinkage, however, is 19%, and this is a potential source of trouble in parachutes because of temperature instability. Examination of Column 2 shows that upon heat relaxation, the rupture of elongation which originally was 9.1% rose to 39.7%. This, in itself, need not be a disadvantage, particularly where the energy absorption rose from 0.144 to 0.55 (lb per in.), and the energy per denier increased from 0.60 x 10^{-3} to 1.94 x 10^{-3}. However, three potential deficiencies exist with the heat relaxed HR yarn: a slight reduction in absolute strength; a considerable reduction in tenacity because of a significant increase in denier resulting from the shrinkage; and development of a considerable amount of permanent set stemming from the high elongation.

Column 3 shows properties of the HS-HR yarn. The absolute breaking strength is maintained at its original value. Rupture elongation at 19.5% falls between the original 9% and the possibly excessive 39.7%, while the denier has been maintained at the original 220-denier level. Tenacity has been increased to 6.5 g.p.d. Note that the heat shrinkage at 350°F has been reduced to the specified less than 2%. Thus, the HS-HR yarn appears to have significantly better elongation and permanent set properties than the heat relaxed HR yarn.

Repeated Stress Properties of Producers Yarn Before and After Heat Ageing.

Approved for Public Release

Contrails

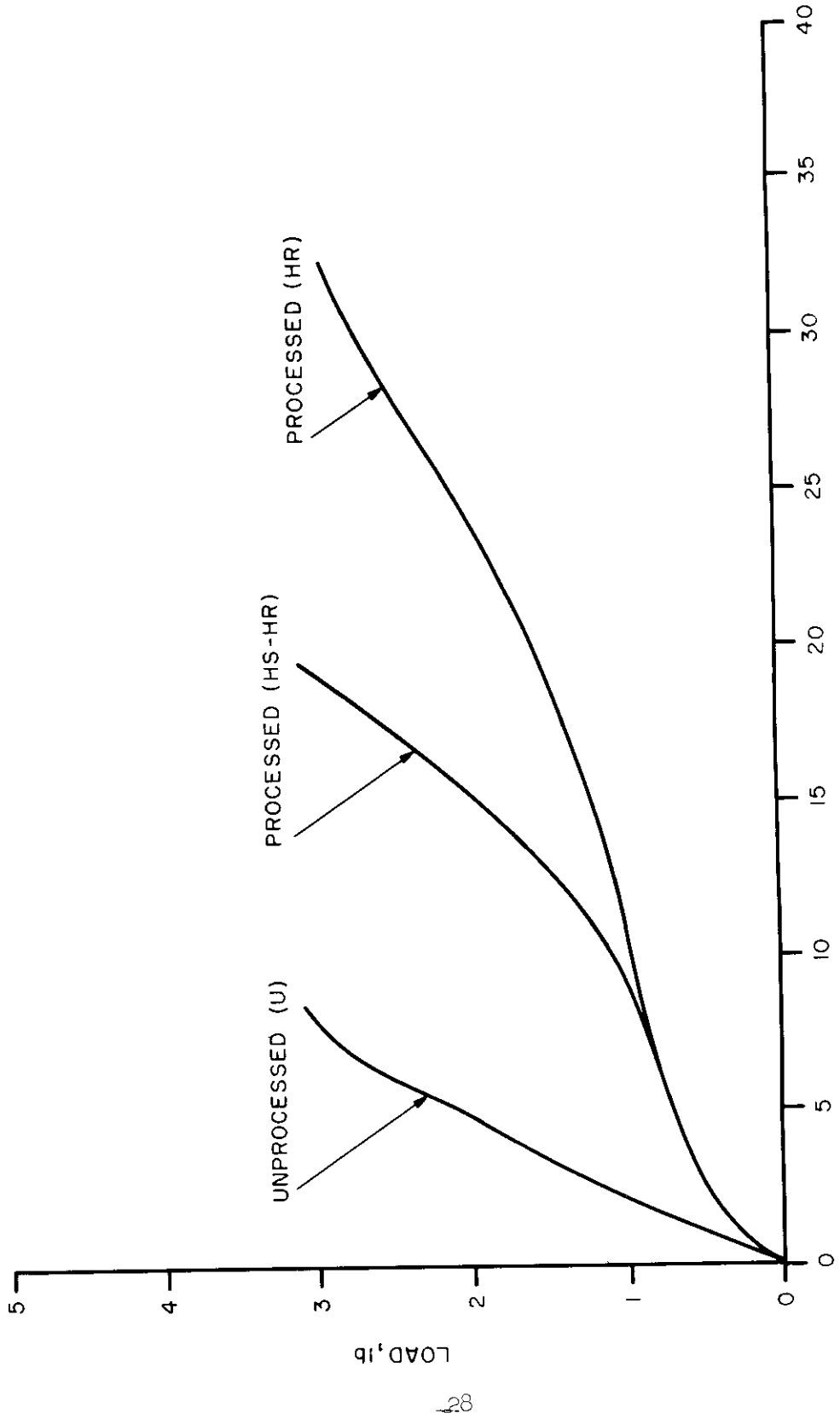

Figure 2 Typical Load-Elongation Curves of 220-Denier Dacron Singles Yarn

Approved for Public Release

Contrails

The HS-HR yarn in single loading to rupture obviously has properties superior to either the unprocessed yarn U or the heat relaxed yarn HR. The question as to whether it can maintain these properties after repeated use may be partially answered in the laboratory by measuring the so-called "repeated stress" characteristics of the yarn. This involves determining the amount of "secondary creep" or "permanent set," as well as the residual rupture elongation after such repeated stressing.

HS-HR yarn samples were cyclically loaded and unloaded in an Instron Tensile Testing machine at 2 in. per min jaw speed for 5 cycles to both a 5% and 15% absolute strain level. The specimens were then ruptured on the sixth cycle, and secondary creep and residual elongation determined.

Table 19 shows repeated stress characteristics of HS-HR yarn both before and after heat ageing at 350°F for 24 hours.

Table 19. Single Load to Rupture and Repeated Stress Properties of HS-HR Type 5100 Dacron Producer's Yarn Before and After Heat Ageing

		Before Ageing	After Ageing @ 350°F for 24 hr	Percent Retained After Ageing (%)
Single Load to Rupture				
Breaking strength (lb)		3.15	2.73	87
Rupture elongation (%)		19.5	17.7	91
Denier		222	213	97
Tenacity (g.p.d.)		6.5	5.8	89
Energy absorption (in-lb/in.)		0.258	0.212	82
Energy per denier (in-lb/in. den x 10^{-3})		1.16	0.99	85
Modulus (g.p.d./unit strain)		73.6	80.5	109
Shrinkage (%) for 1 hr @ 350°F		1.2	0.16	13
Diameter (in.)		0.0020	0.0023	115
Repeated Stress Properties				
Breaking strength (lb)	after 5% strain	3.11	2.80	90
	15% strain	3.12	2.80	90
Tenacity (g.p.d.)	after 5% strain	6.37	5.86	92
	15% strain	6.39	5.88	92
Energy absorption (in-lb/in.)	after 5% strain	0.251	0.228	91
	15% strain	0.167	0.151	91
Energy per denier (in-lb/in.den x 10^{-3})	after 5% strain	1.13	1.05	93
	15% strain	0.75	0.70	93
Modulus (g.p.d.)	after 5% strain	75.3	79.5	106
	15% strain	84.3	84.5	100
Secondary creep (%)	after 5% strain	1.94	1.60	83
	15% strain	8.60	8.48	99
Corrected residual elongation (%)	after 5% strain	17.15	16.79	98
	15% strain	9.54	9.62	100

Before ageing, repeated stressing to both 5% and 15% absolute strain levels shows no significant loss in strength. (The 5% and 15% strain levels are equal to approximately 25% and 70% of the rupture.) Secondary creep at 5% strain is small (1.9%) and so residual elongation is high (17.1%). At the 15% strain level secondary creep increases to 8.6% with an accompanying reduction of

Approved for Public Release

Contrails

rupture elongation to 9.5%.

Unfortunately, no similar data for the HR producers yarn were obtained.

Oven ageing for 24 hours at 350°F causes a reduction in strength, elongation, and tenacity of about 10% (90% retention). The modulus increases due to slight embrittlement of the fiber; this is typical of many polymers. The last vestiges of shrinkage are removed by this prolonged heat relaxation. With respect to repeated stressing after oven ageing, again values are generally about 90% of what they were before oven ageing with the exception of a slight increase in modulus. It can be concluded that no severe loss in either single load-to-rupture or repeated stress properties results from the above heat ageing conditions.

2.4.3.2 Dacron Thread, MIL-T-4855 Type E. Table 20 lists properties of U, HS-HR and HR Type E threads. Dacron and nylon thread specifications are also given. Apparently the Dacron specification was written on the basis of the previously developed high denier-low tenacity HR type, for it is considerably less rigid than the equivalent nylon specification. The HR thread cannot meet the nylon specification, but the HS-HR thread does meet it, thus demonstrating its superior properties--at least in one time loading to rupture. Figure 3 shows load-elongation diagrams for the three types of E thread.

Table 20. Physical Properties of Dacron Thread Specification MIL-T-4855 Size E (Equivalent to Nylon Specification MIL-T-7807 Size E)

	Dacron Spec.	Equivalent Nylon Spec.	Unprocessed Control U	Processed HS-HR	Heat Relaxed**
Number of plies	3	3	3	3	3
Twist direction	Z	Z	Z	Z	Z
Yd/lb	4550 min	5600 min	6380	6720	5260
Equivalent denier	985 max	800 max	702	667	847
Strength (lb)	6.8 min	8.5 min	9.4	9.8	9.2
Equivalent tenacity (g.p.d.)	3.1 min	4.8	6.1	6.7	4.9
Elongation (%)	35 max	22 max	14.9	18.2	33.4
Shrinkage (%) @ 350° for 1 hr	3% max	____	15.9	1.3	2.4*
Diameter (in.)			0.0078	0.0094	0.0112

*After 1/2-hr exposure.
**From TR 55-135, Table XXIV, p. 43.

Table 21 gives repeated stress properties of HS-HR and HR threads after five loading and unloading cycles to 5% and 15% strain levels, respectively. After cyclical straining to both of these levels, subsequent breaking strengths are not reduced. Indeed there is a slight increase in absolute strength, probably due to cold drawing.

After 5% strain, percent secondary creep values are 1.6 and 1.0 for the HS-HR and HR threads, respectively--a negligible difference. Corrected residual elongations are 16.2 and 38.1% for the HS-HR and HR yarns, respectively.

Approved for Public Release

Contrails

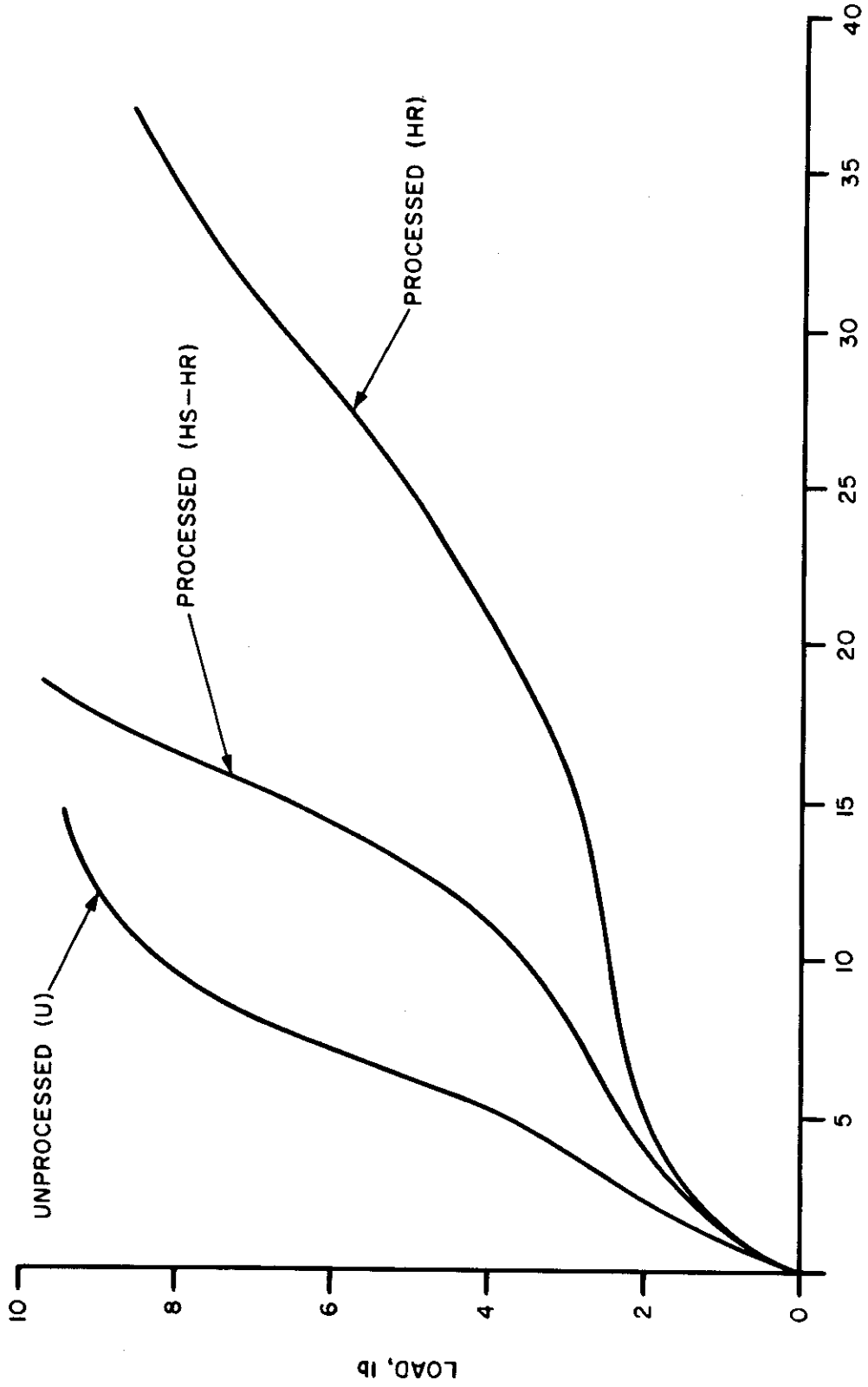

Figure 3 Typical Load-Elongation Curves of Dacron Type E Threads Specification MIL-T-4855

Approved for Public Release

Table 21. Physical Properties of Dacron Thread Specification MIL-T-4855 Size E (Equivalent to Nylon Specification MIL-T-7807 Size E) Before and After Heat Ageing at 350°F for 24 Hours

	Unprocessed Control	Processed HS-Hr 24-hr Oven Ageing at 350°F		Heat Relaxed HR ** 24-hr Oven Ageing at 350°F	
Single Load to Rupture		Before	After	Before	After
Breaking strength (lb)	9.4	9.8	7.5	8.5	7.27
Rupture elongation (%)	14.9	18.2	15.1	36.8	38.9
Denier	702.	667.	664.	849.*	849.*
Tenacity (g.p.d.)	6.05	6.67	5.12	4.6	3.9
Energy absorption (in-lb/in.)	.819	.762	.496	1.53	1.60
Energy per denier (in-lb/in./den x 10^{-3})	1.17	1.14	.746	1.81	1.88
Modulus (g.p.d./unit strain)	92.1	75.7	75.2		
Shrinkage (%) after 1 hr @ 350°F	15.9	1.3	0	2.4	0
Diameter (in.)	.0078	.0094	.0112		
Repeated Stress Properties					
Breaking strength (lb) after 5% strain		9.7	9.4	8.7	7.2
15% strain		10.0	9.2	8.6	7.1
Tenacity (g.p.d.) after 5% strain		6.5	6.3	4.7	3.8
15% strain		6.7	6.1	4.6	3.8
Energy absorption (in-lb/in) after 5% strain		.683	.772		
15% strain		.494	.489		
Energy per denier (in-lb/in./den x 10^{-3}) after 5% strain		1.02	1.14		
15% strain		.74	.72		
Modulus (g.p.d.) after 5% strain		77.3	68.6	46.3	38.1
15% strain		80.9	75.3	51.1	44.6
Secondary creep (%) after 5% strain		1.6	1.3	1.0	1.2
15% strain		7.9	8.3	9.3	8.8
Corrected residual elongation % after 5% strain		16.2	16.9	38.1	38.6
15% strain		9.7	10.4	25.6	29.4

*Since the HR thread was essentially heat stable and shrinkages were less than 2%, the denier was presumed constant.

**From TR 55-135, Table XLV .

Approved for Public Release

Goodrich

Contrails

Therefore if in use, threads are strained only to the 5% level the HR type would be the better, since its higher residual elongation after repeated straining would be manifested as greater energy absorption. After 15% strain, percent secondary creep values are 7.9 and 9.3 for the HS-HR and HR threads, respectively--again a relatively minor difference. Corrected residual elongations are 9.7% and 25.6% for the HS-HR and HR threads. Again at the 15% strain level the HR thread retains a greater amount of residual elongation and concomitant energy absorption. Saying it another way, after five loading and unloading cycles to either the 5 or 15% strain level, both the HS-HR and the HR threads have the same amounts of secondary creep or permanent set; but the HR threads have considerably more residual elongation and hence more energy absorption--of obvious potential advantage in an arrestation parachute. The HS-HR thread reaches 5% strain at about 2-1/4 lb load, or 23% of rupture load. The HR thread reaches 5% strain at about 2-lb load, also 23% of rupture load. Thus for both threads, percent load levels are about equal at 5% (equal) strain levels, and percent secondary creep values, whether considered from equal percent strain or percent stress levels, are about equal. At 15% strain, however, the HS-HR thread assumes a 7-lb load or 72% of rupture. The HR thread assumes a 3-lb load or 35% of rupture. At equal strain (15%) the load on the HR thread is considerably lower and this might be advantageous. Consider the situation now at equal percent load levels. Here the HR thread would extend a considerably greater amount and its secondary creep would be significantly higher than for the HS-HR thread. Thus, the HS-HR yarn would be preferred. The important question to answer becomes one of determining whether threads (and other end items) in use are subjected to specific loads (stresses) or specific elongations (strains). This question must be answered before a decision is reached as to whether the HS-HR process is better than the HR process.

Possibly neither stress nor strain level is the governing criterion but rather energy absorption. The determination of secondary creep magnitudes and dimensional stability at selected energy absorption levels might give some indication of relative merit. Some of the data needed to make such an analysis are available from the load-elongation diagrams already compiled, and it is recommended that any future work include such calculations. Furthermore, measurement of energy absorption under impact loading and the determination of secondary creep, residual elongation, and thermal shrinkage after such impact loading would certainly aid in the ultimate evaluation of the two processes. After heat ageing for 24 hours at 350°F as was the case for the HS-HR 220-denier yarn, retention of physical properties for the HS-HR Type E thread ranges from 80% to 100%, with the exception of energy and energy per denier. Here the combination of lower strength and lower elongation reduces the energy absorption properties. The HR thread shows a strength retention of 86% and a slight gain in elongation because of a slight gain in shrinkage. Thus energies are somewhat increased.

Repeated stress properties after heat ageing also fall into the 80% to 100+% range. Heat ageing therefore causes no unexpected changes in subsequent repeated stress characteristics of either the HS-HR or the HR threads. Both types of yarn appear to perform equally well insofar as retention of properties after heat ageing is concerned.

2.4.3.3 Dacron Thread, Specification MIL-T-4855, Type 3 Cord. Table 22 lists properties of U, HS-HR and HR Type 3 cord threads. As was the case with the Type E thread, the HS-HR 3 cord thread meets the equivalent nylon specification in all respects, while the HR type does not.

Approved for Public Release

Contrails

Table 22. Physical Properties of Dacron Thread Specification MIL-T-4855 Size 3 Cord (Equivalent to Nylon Specification MIL-T-7807 Size 3 Cord)

	Dacron Spec.	Nylon Spec.	Unprocessed Control U	Processed HS-HR	Heat Relaxed HR*
Number of plies	3	3	3	3	3
Twist direction	Z	Z	Z	Z	Z
Yd per lb	1450 min	1800 min	2090	2110	1690
Equivalent denier	3100 max	2500 max	2133	2114	2666
Strength (lb)	20.4 min	24.0 min	27.1	27.3	24.6
Equivalent tenacity (g.p.d.)	3.0	4.4	5.8	5.9	4.2
Elongation (%)	15.0 min	22.0 min	13.6	19.7	37.0
Shrinkage (%) @ 350°F for 1 hr	3%	--	20.0	1.6	0.8 (after 1/2 hr)
Diameter (in.)	---	--	0.017	0.018	0.028

*From TR 55-135, p. 97.

Table 23 gives repeated stress properties of HS-HR and HR threads after five loading and unloading cycles. Essentially the identical situation pertains as for the Type E threads discussed in Section 2.4 and the same conclusions, speculations and recommendations are made.

After heat ageing,retention of repeated stress properties is somewhat higher for the HS-HR thread than for the HR thread. There is a tendency for higher retention of original properties where the aged specimens are then repeatedly stressed. This is not unexpected, since the heat ageing in a relaxed condition causes "disorientation" with accompanying strength loss and greater ultimate elongation. Subsequent repeated stressing "cold works" the filament to give greater orientation, higher strength, and lower elongation.

In summary, heat ageing either the HS-HR or HR thread causes no serious loss in single load to rupture or repeated stress properties.

2.4.3.4 Dacron Webbing Equivalent to Type X (Modified) of Nylon Specification MIL-W-4088B. Table 24 compares the HS-HR and HR webbings. Note that 394 ends were used in the HS-HR type as compared with 329 ends for the HR type. The greater number permitted a strength of over 10,000 lb at just about the weight maximum. It is suggested that any future webbing sample composed of HS-HR yarns be woven with about 5% fewer ends (if possible), thus reducing the strength to about 9,500 lb and the weight and thickness to within the specifications.

Table 25 shows single load to rupture and repeated stress properties. Cyclically loading the webbing to 90% of rupture produces a secondary creep of 11.2%. Corrected residual elongation is 8.2%. The limited repeated stressing caused no loss in breaking strength due to fatigue.

Approved for Public Release

Table 23. Physical Properties of Dacron Thread Specification MIL-T-4855 Size 3 Cord (Equivalent to Nylon Specification MIL-T-7807) Before and After Heat Ageing at 350°F for 24 Hours

Single Load to Rupture	Unprocessed Control U	Processed HS-HR 24-hr Oven Ageing Before	Processed HS-HR 24-hr Oven Ageing After	Heat Relaxed HR ** 24-hr Oven Ageing Before	Heat Relaxed HR ** 24-hr Oven Ageing After
Breaking strength (lb)	27.1	27.3	21.8	24.6	19.2
Rupture elongation (%)	13.6	19.7	18.9	45.2	45.1
Denier	2133	2114	2047	2666*	2666*
Tenacity (g.p.d.)	5.77	5.87	4.83	4.2	3.3
Energy absorption (in-lb/in.)	1.78	2.30	1.84	5.58	5.10
Energy per denier (in-lb/in. den x 10^{-3})	0.84	1.09	0.90	2.09	1.91
Modulus (g.p.d./unit strain)	78.5	53.7	52.1	37.6	30.3
Shrinkage (%) after 1 hr @ 350°F	20.0	1.6	0	0.8	0
Diameter (in.)	0.017	0.018	0.020	0.028	--
Repeated Stress Properties					
Breaking strength (lb) after 5% strain		26.0	24.3	24.5	19.1
15% strain		27.0	24.8	24.3	17.8
Tenacity (g.p.d.) after 5% strain		5.60	5.13	4.2	3.3
15% strain		5.81	5.24	4.1	3.0
Energy absorption (in-lb/in.) after 5% strain		0.185	0.204	--	--
15% strain		0.135	0.143	--	--
Energy per denier (in-lb/in./den x 10^{-3}) after 5% strain		0.877	0.950	--	--
15% strain		0.644	0.670	--	--
Modulus (g.p.d.) after 5% strain		63.1	54.0	32.5	32.1
15% strain		69.9	66.6	37.2	39.0
Secondary creep (%) after 5% strain		1.4	1.1	1.1	1.4
15% strain		8.2	8.4	9.1	8.6
Corrected residual elongation (%) after 5% strain		16.7	18.9	44.6	44.8
15% strain		9.9	11.0	35.1	31.4

*Since the HR thread was essentially heat stable and shrinkage was less than 2%, the denier was presumed constant and was not measured after heat ageing.

**From TR 55-135, Table XLV, p. 97.

Approved for Public Release

Confidential

Contrails

Table 24. Physical Properties of Dacron Webbing (Equivalent Nylon Specification MIL-W-4088B Type X With Weave of Specification MIL-W-5665A)

		Equivalent Nylon Spec.	HS-HR Webbing	HR Webbing**
Width (in.)		1-23/32±1/16	1.81	1.82
Weight (oz/yd)		3.70 max	3.73	3.68
Strength (lb)		8700 min	10,000+*	8860
Elongation (%)		---	21.9	40.0
Energy absorption (in-lb/in.)		---	789	1273
Warp ends (total)		305 min	394	329
Binder		37 min	0	0
Picks (per in.)		22 min	19.0	20
Thickness (in.)		0.125 - 0.145	0.129	0.125
Shrinkage (%)		---	3.2	2.2
Weave		Double plain Single filling	As Type X MIL-W-5665A	As Type X MIL-W-5665A
Plied yarn No. of piles	Warp	10	10	10
	Binder	4	0	0
	Filling	3/3	3/3	3/3

*Load exceeded capacity of testing machine.
**From TR 55-135, Table XXV, p. 67.

Table 25. Physical Properties of HS-HR Dacron Webbing (Equivalent to Nylon Specification MIL-W-4088B Type X With Weave of Specification MIL-W-5665A)

Single Load to Rupture	Before Ageing	After Heat Ageing @ 350°F for 24 hours	Percent Retention of Property (%)
Picks per in.	19.0	19.7	103
Weight (oz/yd)	3.7	3.9	105
Shrinkage % after 1 hr @ 350°F	3.2	0	--
Breaking strength (lb)	10,000+*	8,427	80**
Breaking elongation (%)	21.9	19.4	89
Energy absorption (in-lb/in.)	789	553	70
Repeated Stress Properties			
Stress (load) level (lb)	9,000	7,884	--
Stress level (% of rupture)	90	90	--
Secondary creep (%)	11.2	16.8	150
Residual elongation (%)	9.1	11.3	124
Corrected residual elongation (%)	8.2	9.7	118
Breaking load (lb)	10,000+*	8,760	85

*Load exceeded capacity of testing machine.
**Approximately.

Approved for Public Release

Contrails

Heat ageing caused a loss in strength to 8,427 lb. After repeated stressing to 90% of rupture, the breaking strength rose to 8,760 lb. Again there is a tendency for repeated stressing to recover the strength lost by heat ageing. No serious loss of properties results from heat ageing.

2.4.3.5 Dacron Tubular Webbing, Equivalent to 9/16 in. Type of Nylon Specification MIL-W-5625. Table 26 tabulates Dacron tubular webbing properties. This end item was not previously prepared from HR yarns and so no comparison is possible.

Table 26. Physical Properties of Dacron Tubular Webbing (Equivalent to Nylon Specification MIL-W-5625)

	Equivalent Nylon Spec.	HS-HR Webbing	HS-HR After Heat Ageing @ 350°F for 24 hr	Percent Retention of Property (%)
Width (in.)	9/16 ± 1/16	10/16	9/16	90%
Weight (oz/yd)	.60 max	.61	.64	105%
Strength (lb)	1500 min	1570	1416	90%
Elongation (%)	---	22.2	28.5	128%
Warp ends (total)	65 min	79	79	100%
Picks (per in.)	26 min	26	27	104%
Thickness (in.)	0.090 max	0.070	0.090	114%
Shrinkage (%) 1 hr @ 350°F	---	3.8	0	---
Weave	Tubular,	Plain Tubular,	Plain Tubular,	Plain
No. of plies Warp	8	8	8	
Filling	4	4	4	

The webbing essentially meets all requirements of the equivalent nylon specification. Shrinkage at 350°F for one hour is 3.8%--slightly higher than desired. After heat ageing this is manifested as increased elongation.

Strength retention after heat ageing is again about 90%.

2.4.3.6 Dacron Type V Coreless Braid, Equivalent to Nylon Specification MIL-C-7515. Table 27 lists physical properties of Type V braid made from HS-HR type yarns. Equivalent nylon specifications are also listed. The HS-HR braid meets all specifications except the shrinkage where the 9% is excessive. Plied yarns removed from the braid showed a shrinkage of only 2%. Thus, the additional shrinkage is not explainable and further study is necessary to ascertain the cause.

Repeated stressing to 90% of rupture load (Table 28) produces a secondary creep to 13.0% in the HS-HR and 26.0% in the HR. This confirms the results found for the Dacron thread where secondary creep values for HS-HR and HR threads were equal at equal strain levels, but HS-HR threads showed advantageously at equal but high load levels. The corrected residual elongation of the HS-HR braid was found to be lower than that of the HR braid.

Table 28 lists the effect of heat ageing at 350°F for 24 hours for HS-HR and HR braids. Strength retentions are about 90%. Excessive shrinkage

Approved for Public Release

Contrails

Table 27. Physical Properties of Dacron Type V Coreless Braids (Equivalent to Nylon Specification MIL-C-7515)

	Equivalent Nylon Spec.	HS-HR Braid	HR Braid*
Weight (yd/lb)	25 min	27.6	22.9
Strength (lb)	1500 min	1556	1557
Elongation (%)	20 min	21.3	39.1
Shrinkage (%) 1 hr @ 350°F	0	9.0	1.8 (1/2 hr)
Construction			
Number of carriers	16	16	16
Ends per carrier	9	10	10
Total ends of plied yarn	144	160	160
Yarn ply	4	4	4
Total ends of singles	576	640	640
Picks (per in.)	6.5 - 8	5.2	5

*From TR 55-135, p. 106.

Table 28. Physical Properties of Dacron Type V Coreless Braid (Equivalent to Nylon Specification MIL-C-7515) Before and After Heat Ageing at 350°F for 24 Hours

	HS-HR		Heat Relaxed*	
Single Load to Rupture	Before Heat Ageing	After Heat Ageing 24 hr @ 350°F	Before Heat Ageing	After Heat Ageing 24 hr @ 350°F
Picks per in.	5.2	5.8	5.0	5.5
Weight (yd/lb)	27.6	24.9	22.9	21.5
Shrinkage (%) 1 hr @ 350°F	9.0	0	1.8 (1/2 hr)	0 (1/2 hr)
Breaking strength (lb)	1556	1343	1557	1220
Breaking elongation (%)	21.3	36.3	39.1	48.1
Energy absorption (in-lb/in.)	148.4	180.0	274.4	282.2
Repeated Stress Properties				
Stress (load) level (lb)	1460	1260	1400	1150
Stress level (% of rupture)	90	90	90	94
Secondary creep (%)	13.0	26.3	26.0	37.5
Residual elongation (%)	11.2	12.4	12.9	10.1
Corrected residual elongation (%)	8.5	7.5	10.2	10.1
Breaking load (lb)	1478	1313	1475	1185

*From TR 55-135, p. 106.

in the HS-HR braid causes significant increases in elongation and energy absorption.

Repeated stressing after oven ageing causes an apparent decrease in strength of both the HS-HR and HR braids. The dimensional stability of a braid can critically influence ultimate strength via small changes in diameter or pick-

Approved for Public Release

Contrails

age. Therefore, thermal stability in braids should be a prime requisite, and the apparent strength loss upon ageing and repeated stressing may stem from incomplete thermal stability.

2.4.3.6 Dacron Type IV Tape, Equivalent to Nylon Specification MIL-T-5038. Table 29 lists physical properties of Type IV tape made from HS-HR and HR type yarns. Equivalent nylon specifications are also listed.

Table 29. Physical Properties of Dacron Type IV Tape (Equivalent to Nylon Specification MIL-T-5038)

	Equivalent Nylon Spec.	HS-HR Tape Type IV	HR Tape Type IV*
Width (in.)	1 ± .03	1.03	1.03
Weight (oz/yd)	0.50 max	0.44	0.53
Strength (lb)	1000 min	1013	1250
Elongation (%)	18 min	18.8	33.7
Warp ends	197 min	197	197
Binder	16	17	16
Picks (per in.)	48 min	43.3	52
Thickness (in.)	0.035 to 0. 045	.034	.034
Shrinkage (%) 1 hr @ 350°F	--	3.4	0
Weave	Plain with Binder	Plain with Binder	Plain with Binder
No. of plies Warp	2 min	2	2
Binder	2 min	2	2
Filling	2 min	2	2

*From TR 55-135, p. 147.

Table 30 lists the effect of heat ageing. Strength retentions are in the 75-80% category. Due to some shrinkage in the HS-HR tape, elongation and pickage increase.

Table 30. Physical Properties of Dacron Type IV Tapes (Equivalent to Nylon Specification MIL-T-5038) Before and After Heat Ageing at 350°F for 1 Hour

	HS-HR 24 hr-Heat Ageing at 350°F		Heat Relaxed* 24-hr Heat Ageing at 350°F	
	Before	After	Before	After
Picks per in.	43	45	52	54
Weight (oz/yd)	0.44	0.45	0.53	0.54
Shrinkage (%) after 1 hr @ 350°F	3.4	0	0	0
Breaking strength (lb)	1013	785	1250	1013
Breaking elongation (%)	18.8	24.1	36.1	33.7
Energy absorption (in-lb/in.)	92.9	92.6	205.2	178.6

*From TR 55-135.

Approved for Public Release

Contrails

2.4.4 Conclusions

Comparison and evaluation of the HS-HR and HR processes yarns with particular reference to their use for Dacron parachute components show that: Unprocessed Type U has high tenacity, low elongation, and high heat shrinkage; Type HR has low tenacity, high elongation, and essentially no shrinkage; Type HS-HR has high tenacity, intermediate elongation, and essentially no shrinkage.

End items were heat aged for 24 hours at 350°F and properties compared against those of the unaged. For both HR and HS-HR types, strength losses range from 10 to 20%. However, it should be noted that the absolute strength of the HS-HR type is still higher than the HR.

Repeated stressing for five cycles to selected strain or load levels up to 90% of rupture shows no significant strength loss for either type.

Repeated stress produces "secondary creep" or "permanent set" in both types. This is the non-recoverable elongation or "stretch" which may develop upon loading. At equal percent strain (elongation) levels, permanent set is about equal for both HR and HS-HR yarns. At equal low stress (load) levels, permanent set is also about equal for both types. Under both of these conditions, the remaining elongation and energy absorption is greater for the HR type.

At equal high stress (load) levels, permanent set is much greater in the HR type and it is presumed that this is a disadvantage because it may result in excessive parachute distortion upon deployment.

It is not known whether parachute component deformations are governed by limiting strains, limiting stresses, or limiting energy absorption. It is suggested that the latter is the controlling factor. Until the strain levels for a deployed parachute are known, and until such knowledge is related to deformation and recovery characteristics in repeated use, no specific statements can be made as to the relative merits of the HS-HR vs the HR process.

Heat aged samples were also repeatedly stressed. Beyond the 10-20% strength loss occasioned by the ageing, the subsequent cyclical loading and unloading sequence caused no additional loss. Obviously the number of repeated stress cycles was not severe, since the purpose was to determine non-recoverable elongation rather than failure or weakening due to fatigue. There seemed to be some tendency for greater strength retention in heat aged samples after repeated stressing. This may be due to the fact that heat ageing in a relaxed condition can result in "disorientation" with accompanying strength loss and elongation increase. Subsequent repeated stressing "cold works" the filaments, causing increased orientation, greater strength, and lower elongation.

Those materials made either from HR or HS-HR yarns which were completely thermally stable exhibited no increased elongation after heat ageing for 24 hours at 350°F. Those materials which were not completely thermally stable, but which had low shrinkages (2-5%), manifested this shrinkage after heat ageing as increased rupture elongation.

While the effect was not investigated it is apparent that prolonged heat ageing would ultimately cause both lower strength and lower elongation for both HS-HR and HR materials.

2.4.5 References

Approved for Public Release

Contrails

WADD TR 60-584, pp. 13 to 44 and 340 to 368; WADC TR 55-264, pp. 135 to 137 and 153 to 154.

2.5 Some Principles of Parachute Fabric Construction with Respect to Fabric Strength, Weight, Bulk, and Air Permeability

The often expressed desire of textile engineers to design fabrics for specific end uses has long been frustrated by two disturbing factors: (1) the extreme difficulty in defining the problem, and (2) a lack of "handbook" data on the physical constants of fiber, yarn, and fabric. Military textiles, especially parachutes, appear to be susceptible to engineering treatment. There appear to be certain obvious fiber-yarn-fabric relationships which can be established either qualitatively or quantitatively which ultimately can lead to the development of properly engineered textile structures. Certain important requirements of parachute fabrics, namely strength, weight, bulk, and air permeability were quantitatively analyzed with the objective of designing parachute fabrics with specified physical properties. The analysis was prepared by W. A. Corry, Wright Air Development Center, and is reported in Technical Note WCRT 54-181, November 1954 .

2.5.1 Factors Influencing the Performance of Parachute Fabrics

2.5.1.1 Strength. Fabric strength is dependent almost entirely upon yarn strength and weight. Since it is such an overriding consideration for the more critical fabrics, the selection of fibers is narrowed to high strength continuous filament fibers such as silk, nylon, Dacron and the various high strength rayons. The calculation for strength of a fabric is straightforward and simple, and except for jammed structures can be made with confidence. Basically, the strength of the warp or filling is equal to the product of the strength of the individual yarns, the number of yarns, and some efficiency factor. Since most parachute fabrics are rather open, and high crimps are uncommon, this efficiency factor is high, usually well above 90%. The usual calculation is:

$$\text{B. S. (lb)} = \frac{T_y \times TC \times N \times E}{453.6}$$

where

B. S. = Breaking strength in pounds per inch as determined by the ravelled strip method.
T_y = Yarn tenacity in grams per denier.
TC = Thread count.
N = Yarn denier.
E = Efficiency factor.

A tantalizing sidelight of the strength problem is the loss of strength suffered in proceeding from filament to sewn seam. It has been demonstrated by Perry[1], that single yarn strength is typically from 50% to 80% less than the sum of the strengths of the filaments which compose it.

Fabric efficiencies are typically 92-95%. Seam efficiencies are typically 85-90%. Thus, at seams, filaments with a tenacity of, say, 9.0 g/den have an effective strength of only about 5.8 g/den when they become part of the parachute structure (9.0 x 0.80 x 0.95 x 0.85 = 5.8).

2.5.1.2 Weight. Weight calculations may be made with good accuracy, if the shrinkage is known. A simplified calculation for warp weight is:

Approved for Public Release

Contrails

$$W = TC_w \times N_w \times k \times (1 + C) \times (1 + S)$$

where

W = Weight of the warp in ounces per square yard.
C = Crimp (fractional, not %).
S = Shrinkage (fractional, not %).
N = Total yarn denier.
k = A constant (equal numerically to $10^{-4} \times 1.291$, where N is in deniers).

Crimp cannot be accurately calculated unless the configuration of yarn within the fabric is known.

2.5.1.3 Bulk. The bulk of continuous filament fabrics is dependent principally on 4 factors:

(1) Size of yarn (e.g., denier).
(2) Twist of yarn.
(3) Specific gravity of the yarn filament.
(4) Texture of the fabric.

The experiments of Taylor, et al.[2] have established the relationship between yarn diameter and twist for raw, uncompressed nylon, Orlon, Dacron and viscose rayon. It was shown that yarn diameters first decrease with increasing twist for all the deniers and polymer types tested to a minimum value at about 10 to 15 turns per inch and then they increase slightly at higher twists. In this investigation no attempt was made to measure yarn dimensions under various pressures. Taylor's data therefore probably represent the minimum widths and maximum thicknesses obtainable with the various yarns investigated as they would lie in the cloth. Figure 4 shows the effect of twist on nylon yarn diameter.

As these data were determined on uncompressed and, hence, essentially round yarns, the following should predict the minimum width of raw yarns:

$$d = k\sqrt{N}$$

where

d = diameter in inches.
N = denier.
k = a constant dependent upon the specific gravity of the filament and other factors (numerically equal to 5.1×10^{-4} for nylon).

The maximum width of a yarn as it lies in the fabric will obviously be the sum of the diameters of the filaments. If nylon is assumed to have perfectly circular filaments a fairly accurate prediction of maximum yarn width can be made as follows:

$$d_e = k \sqrt{\frac{N}{Z}} \times Z \qquad \text{or } d_e = k \sqrt{N}\sqrt{Z}$$

where

d_e = effective yarn width in inches.
k = is a constant (numerically equal to 4.37×10^{-4} for nylon).
N = yarn denier.
Z = number of filaments per yarn.

Table 31 gives calculated values for maximum and minimum width and the observed widths for raw nylon yarns twisted to about 15 turns per inch. As

Approved for Public Release

Contrails

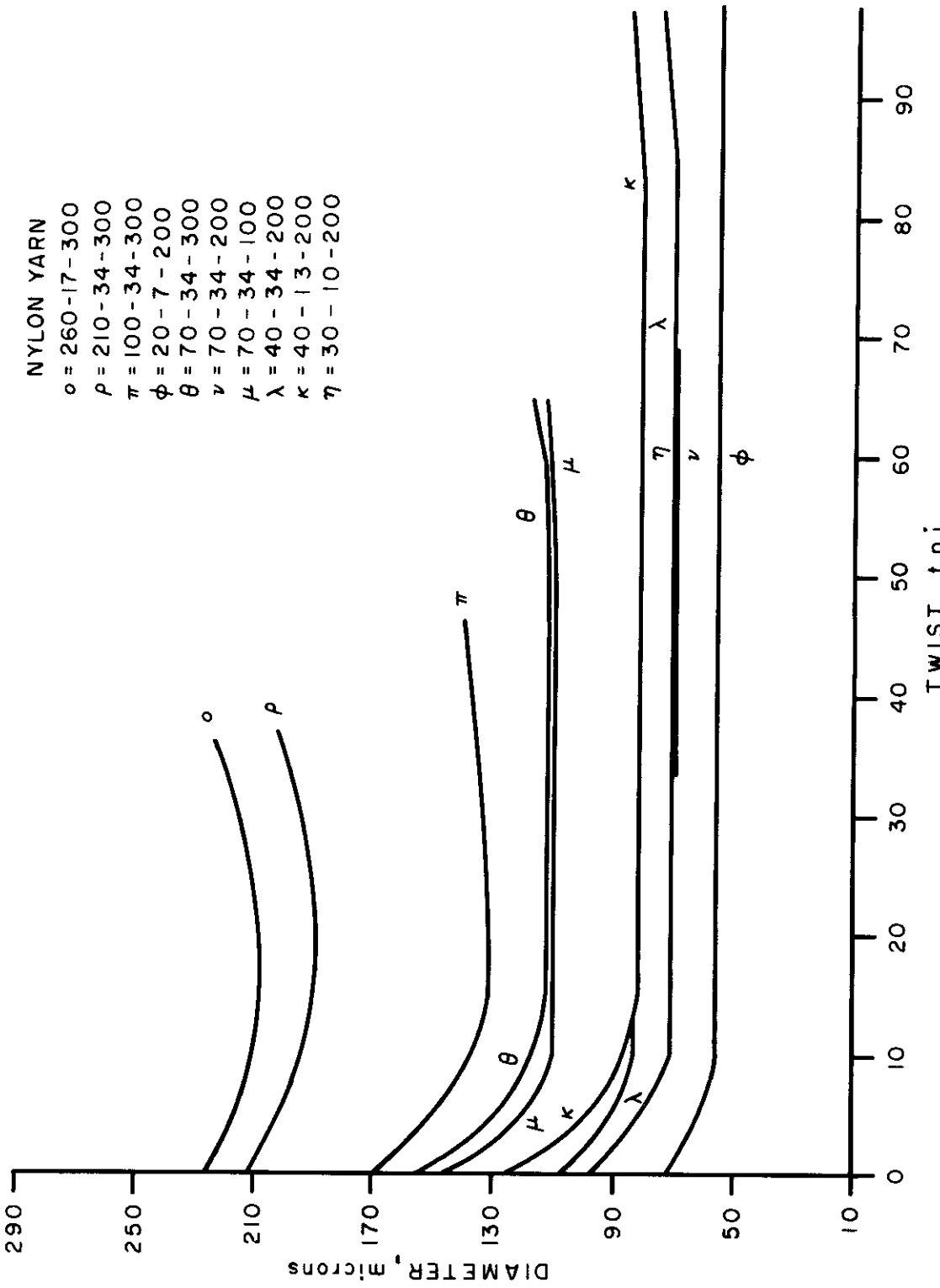

Figure 4 Effect of Twist on the Diameter of Nylon Yarns

Approved for Public Release

Contrails

Table 31. Theoretical Maximum and Minimum Widths of Nylon Yarns Compared to Measured Widths

Yarn Denier and Filament Count	Maximum Theoretical Width (mils)	Minimum Theoretical Width (mils)	Measured Width (mils)
20/7	5.2	2.28	2.16
30/10	7.6	2.79	2.71
40/13	10.0	3.22	3.27
50/17	1.28	3.61	-
70/34	21.4	4.26	4.35
100/34	25.6	5.10	5.26
210/34	37.0	7.40	7.48
260/17	29.1	8.23	8.15
840/140	150.3	14.80	-

all yarns are compressible the absolute minimum yarn width is, practically, unobtainable in a woven structure. Hence yarn widths within the fabric are normally intermediate between the maximum and minimum.

One limitation which faces the textile designer is the limited availability of yarns and filament size combinations. Commercial nylon yarns available for parachutes are:

Denier	Filaments	Approximate Tenacity (grams per denier)
30	10	5.0
40	13	5.0
50	17	5.0
70	34	5.0 and 6.5
100	34	6.5
210	34	7.5

Since strength is the primary consideration we must incorporate sufficient yarn and therefore a definite number of filaments to meet this requirement. Having settled on strength we can then determine what minimum fabric thickness may be obtained. It is obvious that for bulk determinations for filament fabrics one should not consider the entire yarn, but rather the filament as the basic unit. For example, taking a fabric with a construction of 76 ends and picks of 100 denier 34 filament yarns and using idealized, perfectly symmetrical, perfectly even filaments, the minimum thickness may be calculated as follows for a plain weave cloth, assuming balanced crimp.

Yarn spacing (center to center of the filament bundles)

$$P = \frac{1}{\text{thread count}} \text{ (warp or filling)}$$

which for a thread count of 76 equals 0.0132 in. Now calculating the maximum width (which would give minimum thickness)

$$d_e = 4.37 \times 10^{-4} \sqrt{N}\sqrt{Z}$$
$$= 4.37 \times 10^{-4} \sqrt{100}\sqrt{34}$$
$$= 0.0254 \text{ inches, which exceeds the available lateral space.}$$

It becomes obvious then that even in this idealized structure the fila-

Approved for Public Release

Contrails

ments must therefore be piled on top of each other. Two possible combinations of the 34 filaments are shown in Figure 5, and again idealizing, they are shown as nesting. The lateral dimensions are 17-1/2 and 12 times the filament diameter, respectively. Thicknesses are respectively 2 and 3 times the filament diameter, reduced by about 10% to account for the nesting.

The filament diameter is given by

$$d_z = 4.37 \times 10^{-4} \sqrt{\frac{N}{Z}}$$

where d_z = the diameter of a nylon filament, which in a 100 denier 34 filament yarn is about 0.00075 in.

For a plain weave we must provide an additional space in the plane of the fabric equal to the thickness of the yarn for each crossing thread to pass. Referring to Figure 5 we see that the minimum lateral dimension for a two filament layer configuration is

$$d_e = 0.00075 \text{ in.} \times (17\text{-}1/2 + 2) = 0.0146$$

and for a three layer configuration

$$d_e = 0.0075 \times (12 + 3) = 0.0112$$

It appears then that for the specified conditions a minimum fabric thickness would be twice the thickness of the three layer configuration.

$$G_{mn} = 2(L \times 4.37 \times 10^{-4} \times \sqrt{\frac{N}{Z}})$$

or

$$G_{mn} = 2(3 \times 0.00075) = 0.0045$$

where

G_{mn} = minimum fabric thickness
L = number of layers of filaments,

which, if we consider that the filaments could "nest" would be about 0.0041.

Again making the simplifying assumptions we may calculate maximum thickness, for balanced crimp,

$$G_{mx} = 2(k \times \sqrt{N})$$

and for the above fabric

$$G_{mx} = 2(0.00051) \sqrt{100} = 0.0102$$

where

G_{mx} = maximum thickness (except that in jammed structures, which occur in parachute fabrics, the thickness might be increased beyond this figure).

Theoretically, at least, a fabric having 76 ends and picks of 100 denier 34 filament nylon can be varied in thickness from about 0.0041 in. to 0.0102 in. The limits of thickness can be obtained practically only with extreme difficulty, but the lower limit was actually approached when a recent experimental fabric woven with 76 ends and picks of 100 denier 34 filament nylon yarns having producer's twist in both directions and calendered at moderate pressure, showed an actual thickness of only 0.0043 in. Similar fabrics now in use, having twisted warp and filling yarns, have a thickness

Approved for Public Release

Contrails

TWO LAYER CONFIGURATION

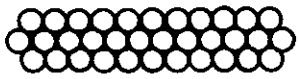

THREE LAYER CONFIGURATION

Figure 5 Idealized Yarn Configuration

Approved for Public Release

Contrails

of about 0.060 in.

Certain manufacturing factors also affect bulk appreciably. The best known of these is calendering, which flattens out the yarn bundle and, with nylon and Dacron at least, appears to set the structure fairly permanently. No evidence of flattening of the filament itself has ever been observed by the author. Cross sections of nylon yarns extracted from cloth calendered at 80 tons failed to reveal any distortion of the filaments. Another factor which affects thickness is tension. All the yarns in use today are given a slight twist, and it is obvious that tension on the twisted bundle of filaments will tend to make them round, and hence thicker.

2.5.1.4 Air Permeability. Air permeability is extremely sensitive to fabric structural change. Great ranges can be obtained with minor adjustments in twist, texture, or finishing. Figure 6 shows the effect of varying filling yarn twist over a range of 1/2 to 35 turns per inch, and the effect of calendering, on a widely used 40 denier warp, 70 denier filling construction.

One would expect the degree of openness to be the major factor in determining the air flow characteristics of fabrics. Perry[3] has shown that an essentially straight line relationship exists between air flow and percent open area for a series of nylon twill fabrics, at pressures of from 2 to 18 in. of water (Figure 7).

Several methods of treatment of air flow data have been suggested. Goglia's[4] relative porosity equation provides a comparison between actual flow through the fabric and flow which would occur through the permeability device if the fabric were not in place (and if the discharge coefficient of the device were equal to one). He defines relative porosity as

$$\frac{2V_1}{\sqrt{\frac{P_1 - P_2}{\rho}}}$$

where

V = Down stream velocity of air (feet/sec).
$P_1 - P_2$ = Pressure differential against the cloth (pounds/ft^2).
ρ = Density in slugs.

Heinrich[5] defines a similar relationship as "Effective Porosity" $\frac{V_2}{V_1}$

where

V_2 = down stream velocity of air.
V_1 = up stream velocity calculated from the pressure differential as follows:
$V_1 = \sqrt{\frac{2\Delta\rho}{\rho}}$

Data developed from these relationships, while valuable to the parachute designer, do not provide the textile engineer with information useful in predetermining the permeability of a given cloth. The problems and the interdependent variables are so numerous that handbook data must be compiled on yarn dimensions in the fabric and a rather wide use of simplifying assumptions must be made in regard to air flow before even approximations can be made.

Let us tabulate some of the variables so that the magnitude of the problem may be realized.

a. Yarn dimensions vary with twist, tension, filament count, and

Approved for Public Release

Contrails

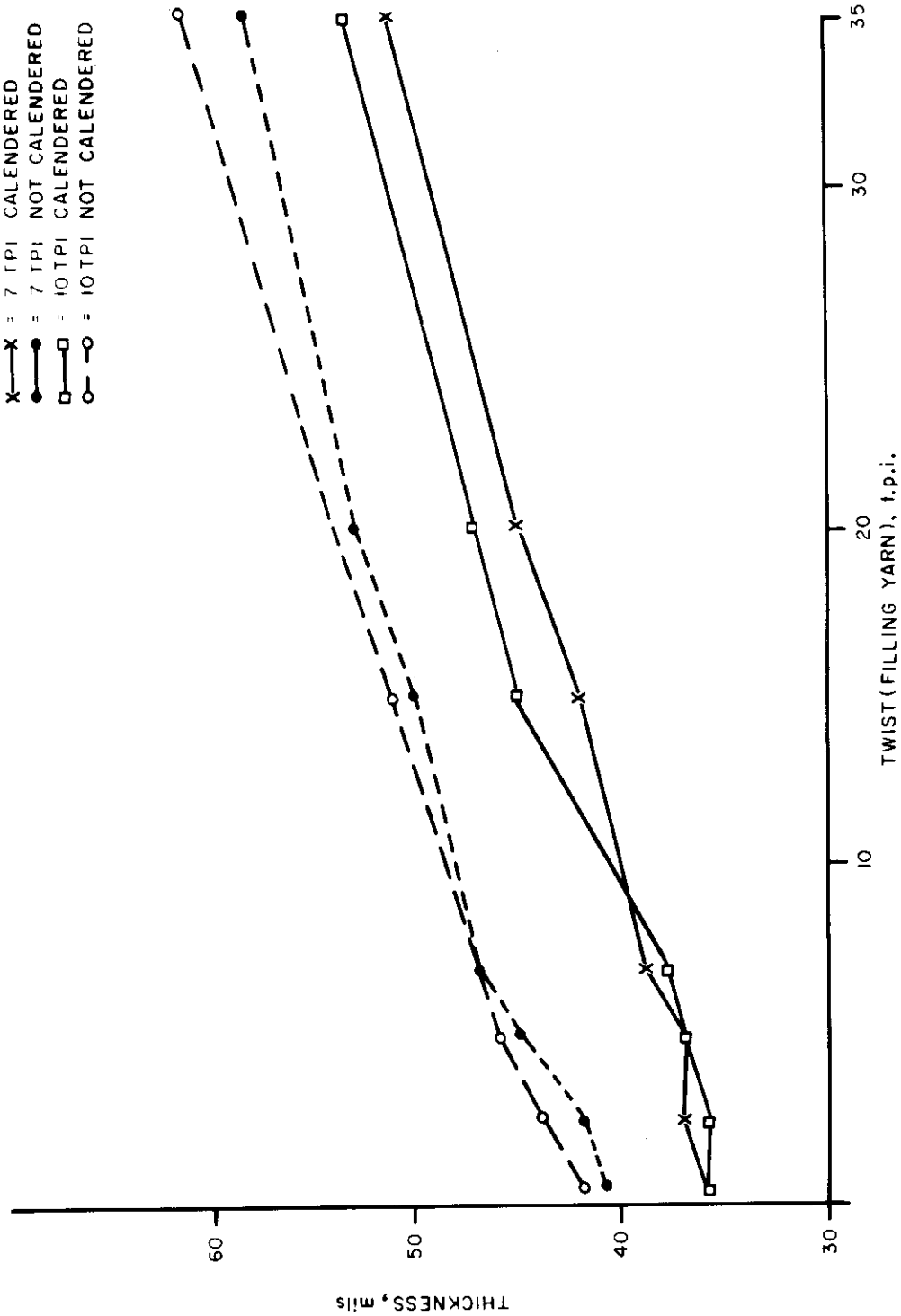

Figure 6 Effect of Twist and Calendering on Thickness of Specification MIL-C-7020, Type II Nylon Parachute Cloth

Approved for Public Release

Contrails

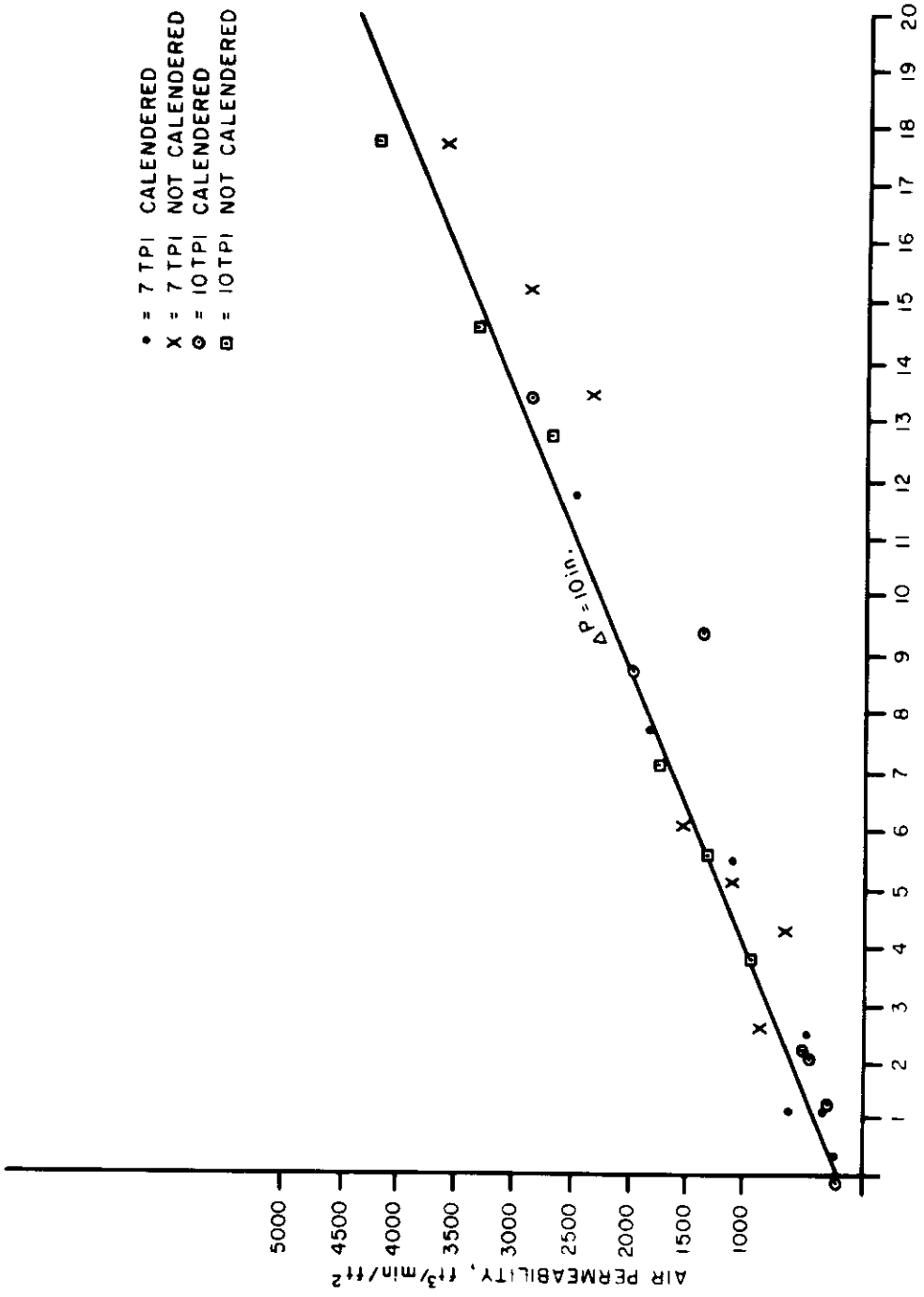

Figure 7 Percent Open Area vs. Air Permeability (at 10 in. water pressure drop)

Approved for Public Release

Contrails

yarn denier.

b. There is a change in the type of flow with changing pressure differential. Goglia[4] has indicated that at low pressures the flow behavior is largely viscous, at high pressures the flow is largely inertial and at intermediate pressures the flow is a combination of both.

c. As the cloth is subjected to air pressure it is biaxially strained, which in itself probably causes the following changes:

(1) An "opening-up" of the fabric interstices due to wider thread spacing.

(2) A tendency for the yarn to "bundlize" due to increased tension on the yarns, tending to make the yarn thicker (and narrower in the plane of the fabric) and thus to make the fabric more open.

(3) A tendency for the yarn to be flattened by the pressure, making it thinner, wider in the plane of the fabric, and less open.

2.5.2 Conclusions

Fabric strength, weight, bulk, thickness, and air permeability are important factors to be controlled in the proper design of parachute fabrics.

Sufficiently accurate calculations of weight and strength of fabrics may be readily made. Methods are given for determining the practical maximum and minimum fabric thickness for a given construction. Methods are given for calculating maximum and minimum yarn dimensions within a fabric. A method is proposed for approximating air flow at moderate pressure differentials when the yarn denier and filament count are known.

2.5.3 Bibliography

1. Perry, W. O., Unpublished data developed at WADC Materials Laboratory, Directorate of Research (Wright Air Development Division).

2. Taylor, J. L., et al., WADC Technical Report 53-12, March 1952.

3. Perry, W. O., WADC Technical Note WCRT 53-203, October 1953.

4. Goglia, M. J., Air Permeability of Parachute Fabrics, WADC Technical Report 52-283, Part I, November 1953 (Georgia Institute of Technology).

5. Heinrich, H. G., Experimental Parameters in Parachute Opening Theory, Paper presented at 196th Symposium, Shock and Vibration, September 1952.

6. Peirce, F. T., Journal of the Textile Institute, Vol. 28, No. 3, 1937.

2.5.4 References

The reader is referred to Section 5 which discusses the influence of yarn and fabric geometry on air permeability. Particularly, Sections 5.1, and 5.2 report on research conducted subsequent to this report (Section 2.5.) Also see WADD TR 60-584, pp. 191-237. The information contained in these later reports adds considerable knowledge to the subject of proper design of parachute fabrics.

Approved for Public Release

Contrails

Section III

FRICTION, ABRASION AND WEAR

3.1 Development of Nylon Webbings of Improved Abrasion Resistance

Previous study on the development of abrasion resisting treatments for nylon and Dacron webbings (see WADD TR 60-584, pages 164 to 176) demonstrated that a considerable increase in abrasion resistance was obtainable by proper resin application. In addition it was apparent that yarn and webbing structural geometry would also certainly have an effect on breaking strength, and abrasion resistance. Therefore a rational series of thirty-two experimental nylon webbings, meeting the general dimensional requirements of Specification MIL-W-4088B, Type XIII, were designed and constructed with systematic variations in constructional geometry. The webbings were then tested for breaking strength before and after abrasion on a standard laboratory abrasion machine in order to determine the influence of yarn and fabric construction on abrasion resistance. The study was conducted by C. C. Chu, E. R. Kaswell and D. J. Doull at Fabric Research Laboratories, Inc. and is reported in WADC TR 58-509, April 1959 (Contract AF 33(600)-34381).

3.1.1 Materials

Yarn: High tenacity Type 300 nylon 66 (du Pont):
210-denier, 34-filament (6.2 den/fil)
260-denier, 17-filament (15.3 den/fil)
840-denier, 140-filament (6.0 den/fil)

High tenacity Caprolan nylon 6 (National Aniline):
210/32* (6.56 den/fil), 1.0Z, Type HB, Commercial
210/32 (6.56 den/fil), 1.0Z, Type HBT, Experimental
560/32 (17.50 den/fil), 1.0Z, Type HBT, Experimental
840/136 (6.18 den/fil), 0.5Z, Type HBT, Commercial
2100/408 (5.15 den/fil), 0, Type HB, Commercial
2100/408 (5.15 den/fil), 0, Type HBT, Experimental
2100/112 (18.75 den/fil), 0, Type HB, Commercial

*Yarn denier 210, 32 filaments, 1.0 turns per inch, Z twist.

Webbings: The majority of the samples woven were based upon Specification MIL-W-4088B, Type XIII webbing. They were woven to comply with dimensional and strength requirements, but of course constructional factors were varied as experiment design dictated. A few Types VIII and XVIII webbings were also prepared and evaluated.

Table 32 lists the samples and identifies the variables investigated.

3.1.2 Variables Examined

Constructional effects investigated were those which resulted from varying denier, singles twist, ply twist, helix angles, warp ends, filling picks, and weave type.

3.1.3 Test Procedures

The samples were designed and constructed according to the planned outline, and delivered to Fabric Research Laboratories, Inc. for testing.

Approved for Public Release

Table 32. Summary of Experimental Webbings

Sample No.	Webbing Type	Variable	Warp Yarn Construction	Singles Twist	Ply Twist	Nylon	Type
0A	XIII[c]	Control	210/32/102	0	2.5	6	HBT
0B	"	"	"	"	"	"	"
0C	"	"	"	"	"	"	HB
1A	"	Picks: max weavable	"	"	"	"	HBT
1B	"	" min "	"	"	"	"	"
1B2[a]	"	"	"	"	"	"	"
1C	"	" (half between 22 and min weav.)	"	"	"	"	"
1C2[a]	"	"	"	"	"	"	"
2A	"	Modified weave: MIL-W-4088B (par. 3.2.1)	"	"	"	"	"
2B	" "	weave: MIL-W-4088B (par. 3.2.3)	"	"	"	"	"
2C	" "	weave: MIL-W-4088B (par. 3.2.4)	"	"	"	"	"
2D	" "	weave: MIL-W-4088B (par. 3.2.5)	"	"	"	"	"
3A	"	Ends	"	"	"	"	"
3B	"	"	"	"	"	"	"
4A	"	Yarn plies	2100/408/1	0	0	"	"
4B[b]	"	" "	840/136/3	0.5	2.5	"	"
4C	"	" "	560/32/4	1.0	2.0	"	"
4D	"	" "	210/32/3/3	1.0	5.0	"	"
5A	"	Singles twist (helix angle 7.5°)	2100/408/1	2.0Z	0	"	"
5B	"	Singles twist (helix angle 15°)	"	4.1Z	"	"	"
5C	"	Singles twist (helix angle 22-1/2°)	"	6.3Z	"	"	"
5D	"	Singles twist (helix angle 30°)	"	8.8Z	"	"	"
6A	"	Yarn twist	840/136/3	0.5Z	2.58	"	"

Approved for Public Release

Table 32. (Continued)

Sample No.	Webbing Type	Variable	Warp Yarn Construction	Singles Twist	Ply Twist	Nylon	Type
6B	XIII[c]	Yarn Twist	840/136/3	0.5Z	6.0S	6	HBT
6C	"	" "	"	0.5Z	11.5S	"	"
6D	"	" "	"	5.5Z	2.5S	"	"
6E	"	" "	"	5.5Z	4.0S	"	"
6F	"	" "	"	5.5Z	6.0S	"	"
6G	"	" "	"	5.5Z	8.5S	"	"
6H	"	" "	"	5.5Z	11.5S	"	"
6I	"	" "	"	13.0Z	2.5S	"	"
6J	"	" "	"	13.0Z	6.0S	"	"
6K	"	" "	"	13.0Z	11.5S	"	"
7A	"	Fiber denier	2100/112/1	2.0	0	"	HB
7B	"	" "	2100/408/1	"	"	"	"
8A	VIII	Weave	210/34/10	1.0	2.8	66	300
8B	"	Picks	"	1.1	"	"	"
8C	"	Dyeing	"	1.4	2.9	"	"
13A	XIII	Picks	"	1.1	2.8	"	"
13B	"	"	"	1.0	3.0	"	"
13C	"	Dyeing	"	1.3	3.2	"	"
18A	XVIII	Weave	"	1.2	3.4	"	"
18B	"	Picks	"	1.1	2.9	"	"
18C	"	Dyeing	"	1.1	3.0	"	"

a. 1B2 and 1C2 were intended to be repeats of 1B and 1C but they do not have identical properties.
b. 4B is the same sample as 6A.
c. Specifications for Type XIII webbing: 225 ends, 26 binders, 22 picks.
d. Helix angle = angle formed by fiber and singles yarn axis.

Approved for Public Release

Confidential

Contrails

Breaking Strength and Elongation were determined on an Instron tester using capstan jaws and a jaw speed of 0.5 in./min.

Energy Absorption was determined by measuring the area under the load-elongation diagram, and converting to units of in-lb/in.

Abrasion Resistance was determined by flex abrading the webbing over an hexagonal steel bar for a selected number of cycles (usually 5,000). The abrasion machine is that described in Section 4.10.2 of Specification MIL-W-4088B. The percent strength loss after abrading was used as a quantitative measure of abrasion resistance.

Webbing Analyses: Standard textile tests of weave, weight, thickness, pick and ends, and twist were determined according to prescribed textile testing practice.

Microscopic Studies: This consisted of (1) measuring surface helix angles formed by the axes of individual fibers appearing on the webbing surfaces and the webbing selvedge; (2) cross sections of both warp and filling. The information obtained from these observations was useful in studying the effect of fiber and yarn positions in the webbing as they influenced abrasion resistance.

3.1.4 Test Results

3.1.4.1 Effect of Picks per Inch on Strength and Abrasion Resistance.

Table 33 tabulates pertinent data.

Effect on Original Strength. Since webbing strength is theoretically governed by the product of yarn strength and the cosine of the crimp angle, it might be predicted that the fewer the picks per inch, the smaller the crimp and the stronger the webbing. The data did not entirely bear this out. A plot of strength vs. pickage gave a straight line with slope m of -62.5 lb per pick indicating that the strength does fall off as the pickage increases. However, the total range in going from 20 to 27 picks is only 444 lb (theoretical) or about 5% of the total strength of the webbing; thus pickage is not considered a critical variable.

Effect on Abrasion Resistance. Figure 8 shows plots of strength vs. pickage before and after abrasion. Over the 20-27 pick range a gain in abraded strength from 3,700 to 4,700 lb is seen. The corresponding percent losses in breaking strength due to abrasion fall from 55% to 35%.

A possible explanation is that with increasing picks, the webbing becomes a tighter structure, the span of yarn between interstices is shorter, thus reducing the opportunity for the fiber to become snagged by the sharp edges of the abradant bar. Another possible explanation is concerned with the energy absorbed in the abrasion process. This energy is probably absorbed by the abraded webbing at the bulging yarn spans between interstices. The energy absorbed by each pick probably diminishes as the free space per pick decreases, i.e., on a spatial basis it would be anticipated that the closer the picks, the relatively smoother the fabric surface and hence the lower the imposed energy. Thus the energy per pick varies in an inverse manner to the picks per inch. In the higher picks per inch samples, smaller magnitudes of energy will naturally cause less abrasive damage.

A third explanation deals with the ability of the webbings to absorb

Approved for Public Release

Table 33. Effect of Pick Variation on Webbing Performance

	Sample Numbers										
	1B	13B	13A	1B2	13C	0A	1C	0C	1C2	1A	0B
General											
Thickness (in.)	0.097	0.095	0.102	0.098	0.095	0.100	0.100	0.098	0.106	0.110	0.101
Weight (oz/yd)	2.21	2.20	2.21	2.15	2.40	2.32	2.27	2.29	2.32	2.37	2.35
Picks (per in.)	19.9	20.7	21.9	22.4	22.7	23.6	25.0	25.6	26.0	26.6	27.0
Width (in.)	1-26/32	1-27/32	1-24/32	1-27/32	1-23/32	1-23/32	1-26/32	1-25/32	1-26/32	1-21/32	1-25/32
Warp yarn properties											
Number of ends	225	225	225	225	225	225	225	225	225	225	225
Yarn denier	2218	a	2175	2215	a	2209	2202	2204	2218	2191	2208
Filament denier	6.56	6.56	6.56	6.56	6.56	6.56	6.56	6.56	6.56	6.56	6.56
Number of plies	10	10	10	10	10	10	10	10	10	10	10
Ply twist (t.p.i.)	2.5	3.0	2.8	2.4	3.2	2.6	2.4	3.0	2.5	2.6	2.6
Singles twist (t.p.i.)	1.2	1.0	1.1	1.3	1.3	1.1	1.2	1.2	1.2	1.2	1.2
Performance characteristics											
Unabraded strength (lb)	7150	7890	7748	6900	7375	7795	7340	7238	6790	7131	7228
Eff. tenacity (g.p.d.)	6.51	7.34	7.19	6.29	6.31	7.12	6.73	6.63	6.18	6.56	6.61
S.W.R.[1] x 10-3 (yd)	51.8	57.5	56.1	51.4	49.7	53.8	51.7	50.6	56.8	48.1	49.2
Abraded strength (lb)	3875	3644	3433	3695	4333	4034	4332	4388	4370	4704	4425
Strength loss (%)	45.8	53.8	55.7	46.5	41.2	48.3	41.0	39.4	35.6	34.0	38.8
Unabraded elongation (%)	24.7	23.2	23.8	25.9	34.0	28.4	26.5	28.8	30.8	29.3	30.6
Abraded elongation (%)	24.9	a	a	28.7	a	32.0	31.6	28.1	31.5	34.2	32.2
Contraction[2] (%)	7.6	a	a	9.5	a	8.2	8.7	7.8	8.5	6.2	7.4

1. S.W.R. = strength to weight ratio = unabraded breaking strength (lb) ÷ webbing weight in lb/yd.
2. Warpwise contraction after abrasion.
3. Effective tenacity = webbing strength (g) ÷ total warp end denier.

a. Not recorded.

Approved for Public Release

Confidential

Contrails

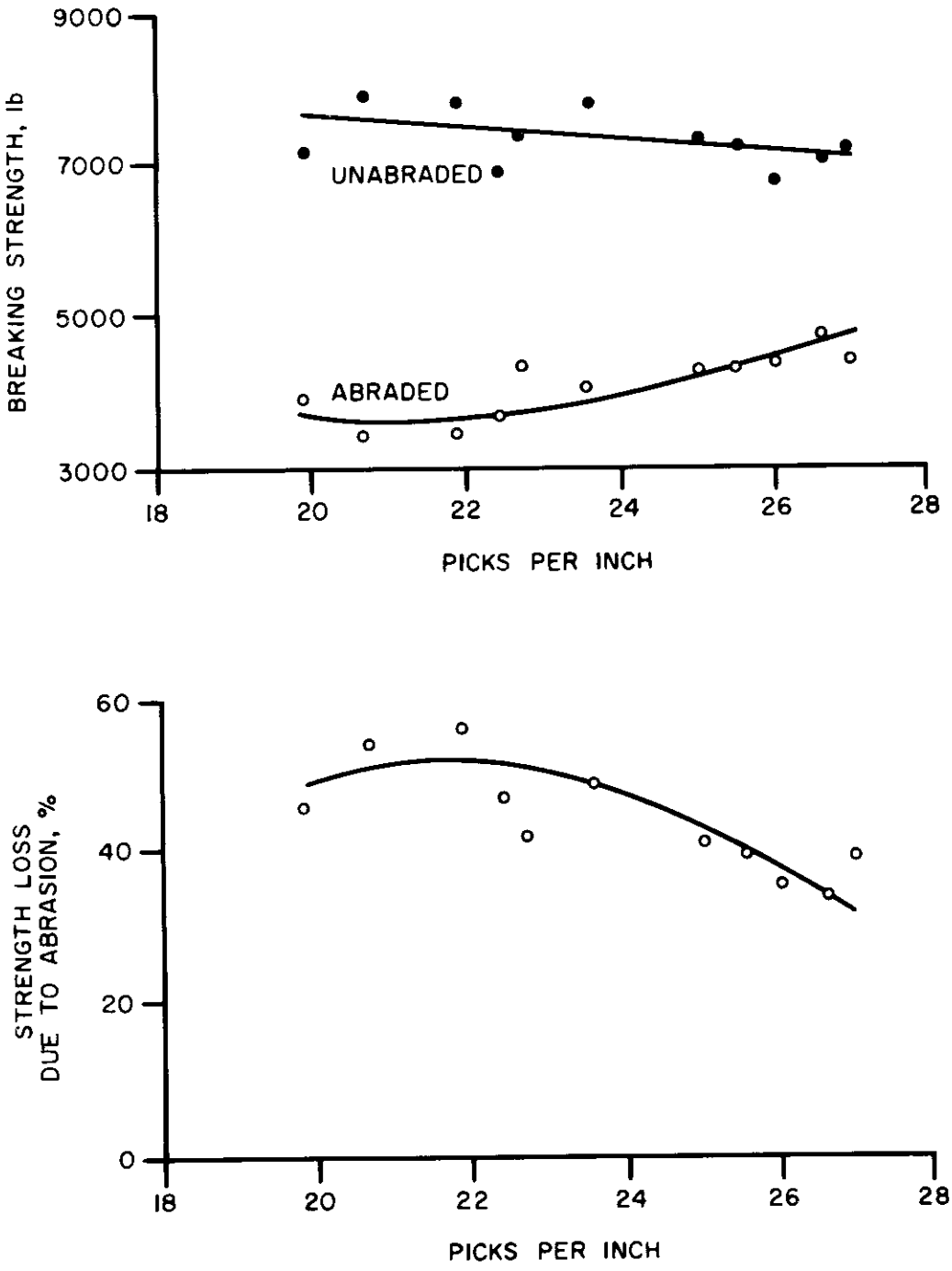

Figure 8 Effect of Pick Variation on Webbing Strength

Approved for Public Release

Contrails

the above mentioned abrasive energy. Hamburger* has shown that abrasion resistance is correlative with the energy absorption of mechanically conditioned secondary creep-free fibers; the greater the area (energy) under the mechanically conditioned stress-strain diagram, the higher the abrasion resistance. No repeated stress tests were made on these webbings to remove secondary creep or permanent set, but since all webbings are nylon it can be assumed that the energy to break in single load application might be a criterion of abrasion resistance. A plot of the approximate energy of all the webbing samples evaluated versus the corresponding strength loss percentages after abrasion shows a definite correlation and indicates that high abrasion strength losses are to be expected from webbings of low energy absorption characteristics.

The effects of pick variation on webbing performance may be summarized as follows:

	Increasing Picks per Inch	Decreasing Picks per Inch	Remarks
Unabraded strength	Down	Up	Effect is slight
Abraded strength	Up	Down	Effect is pronounced
% Strength loss	Down	Up	Effect is very pronounced

3.1.4.2 Effect of Weave Type on Webbing Performance. Of the nineteen webbings listed in Specification MIL-W-4088B, only five different weave types are used. They are:

a. A two up, two down herringbone twill with one reversal at the center of the webbing. This weave is used for webbing Types I, II, III, IV, V, VI, VIII, XII, XV, XVI, and XVIII; and is represented in this study by Sample No. 2A.

b. A double plain weave with a single filling. Separate binder warp ends are woven two up and two down, one end as one. All other warp yarns are woven two ends as one. This weave is used for webbing Types VII, IX, X, and XIII, and is the weave selected as the standard for this study. Sample No. 0A is the control for the group.

c. The weave for Type XI webbing is shown in Figure 1 of MIL-W-4088B and is represented by Sample No. 2B.

d. The weave for Type XIV webbing is a five up, one down, one up, five down herringbone twill with one reversal at the center of the webbing and is represented by Sample No. 2C.

e. The weave for Types XVIII and XIX webbings is shown in Figure 3 of MIL-W-4088B and is represented by Sample No. 2D.

Since MIL-W-4088B requirements for the nineteen different types of webbings embrace a wide variety of number of ends, picks per inch, yarn sizes, widths, thicknesses and strength requirements, it is difficult to arrive at a common basis for the purpose of evaluating the effects of weave alone. Lacking a rational denominator, one was chosen for convenience as well as conformity with the other experimental samples. Thus, Sample No. 2A, 2B, 2C, and 2D were woven with the different weaves cited above to match Type XIII in the number of ends, picks per inch (except 2A which being a single fabric rather than a double fabric, only half of the nominal picks was required), and width. Consequently, the various cover factors as they existed in configurations of the original webbing types were drastically altered. For

*Hamburger, W. J. Mechanics of Abrasion of Textile Materials. Textile Research Journal, Vol. 15, p. 169 (1945).

Approved for Public Release

Contrails

example: the weave of Sample No. 2D is normally specified for Type XVIII webbing, which webbing consists of 208 ends, and has a width of one inch. When this weave was used for Type XIII webbing, 225 ends were place in a width of 1-3/4 in., producing a much more open structure than the "specification construction." Therefore, the cover factor for this experimental Type XIII webbing with Type XVIII weave may be far too low, and any conclusion drawn that the Type XVIII weave is inferior to the standard specified Type XIII weave may be entirely erroneous. Perhaps use of the Type XVIII weave with the proper (increased cover factor) number of picks and ends might produce a superior "Type XIII" webbing. Thus the complexity of the interaction of more than one variable is pointed out, and the difficulty of drawing conclusions from this phase of the work is obvious.

The experimental data on these samples are given in Table 34 and are represented graphically in Figure 9. The conclusions drawn from these results are that while Sample No. 0A appears to have the highest original strength, the strength retained after abrasion is only a little over 50%. Sample No. 2B, on the other hand, is about 1,600 lb weaker to start with, but after abrasion it is 200 lb stronger than Sample No. 0A. Sample No. 2A is a very poor webbing; not only does it have low initial strength, but also the strength loss due to abrasion is in excess of 60! In light of the above, the merits of the different weave types cannot and should not be judged exclusively from the data presented. One is again reminded that these weaves are superimposed on a Type XIII configuration and they may or may not be the most efficient.

Previous discussions mentioned that Specification MIL-W-4088B constructions were not based upon rational engineering designs, but rather they apparently evolved via trial and error methods. Although there is nothing "sacred" about these specification constructions, such empirically developed "recipes" can frequently yield optimum properties through "natural evolution." Therefore, some, or all, of the standard MIL-W-4088B webbings could be at or near the optimum for a selected weave type--arbitrary as the weave type may be. The effects of weave type cannot be precisely determined unless each weave is represented in the form of its optimum construction. The best weave type is worthless unless the proper number of picks and ends is utilized.

3.1.4.3 Effect of Number of Warp Ends on Webbing Performance. To investigate the relative efficiencies of webbings woven with more or fewer ends than the specified 225 ends of Type XIII webbing, one sample was made with 257 ends, the maximum that could be woven into a webbing of the desired width. This was 32 ends more than the minimum so another webbing was woven with only 193 ends, i.e., 32 less than the minimum specified, reeded out to the same nominal width. Webbing Sample No. 1C was selected as the standard for comparison on the basis of having nearly the same picks per inch. The data on these three webbings are given in Table 35 and Figure 10, together with the strength values normalized to the identical number of warp ends. Such a normalization procedure permits comparison of strength efficiencies of webbings with different numbers of supporting ends.

The translation of yarn strength to webbing strength decreases in efficiency as the number of ends increases, as indicated by effective tenacities and strength to weight ratios. The loss in efficiency is primarily due to the difficulty in stressing a large number of ends uniformly such that each yarn bears its apportioned load.

The abrasion resistance, on the other hand, improves with increased

Approved for Public Release

Contrails

Table 34. Effect of Weave Variation on Webbing Performance

	Sample Numbers				
	0A	2A	2B	2C	2D
General					
Thickness (in.)	0.100	0.094	0.100	0.103	0.114
Weight (oz/yd)	2.32	2.08	2.30	2.19	2.20
Picks (per in.)	23.6	11.7	26.0	23.9	27.0
Width (in.)	1-23/32	1-25/32	1-26/32	1-26/32	1-24/32
Warp yarn properties					
Number of ends	225	225	225	225	225
Yarn denier	2209	2209	2216	2249	2211
Filament denier	6.56	6.56	6.56	6.56	6.56
Number of plies	10	10	10	10	10
Ply twist (t.p.i.)	2.6	2.6	2.7	2.6	2.5
Singles twist (t.p.i.)	1.1	1.3	1.2	1.3	1.2
Performance characteristics					
Unabraded strength (lb)	7795	5983	6126	6144	6668
Eff. tenacity (g.p.d.)	7.12	5.47	6.06	5.51	6.08
S. W. R.[1] x 10^{-3} (yd)	53.8	46.0	42.6	44.9	48.5
Abraded strength (lb)	4034	2234	4275	3312	3997
Strength loss (%)	48.3	62.7	30.2	46.1	40.1
Unabraded elongation (%)	28.4	24.8	28.8	25.1	24.7
Abraded elongation (%)	32.0	24.4	28.4	22.2	20.7
Contraction[2] (%)	8.2	22.4	4.2	10.8	12.5

1. S.W.R. = strength to weight ratio.
2. Warpwise contraction after abrasion.

number of ends. Since the abrasion energy input is constant, by virtue of the test conditions the strength losses due to abrasion should theoretically be inversely proportional to the number of ends. Thus:

	Ratio of Ends	Ratio of Losses
1C vs. 3B	$\frac{225}{193} = 1.17$	$\frac{48.0}{41.0} = 1.17$
1C vs. 3A	$\frac{257}{225} = 1.14$	$\frac{41.0}{36.4} = 1.13$
3A vs. 3B	$\frac{257}{193} = 1.33$	$\frac{48.0}{36.4} = 1.32$

Since the ratios of ends do agree in all cases with the ratio of losses, it may be concluded that the abrasion resistance is directly proportional to the number of ends, within the range studied.

3.1.4.4 Effect of Singles Yarn Twist Variation on Webbing Performance. The structural design of yarns going into the webbings is of paramount importance with respect to strength and abrasion resistance. Yarns made from the same filament size may have entirely different properties depending on the number of plies, the singles twist, and the ply twist. This section is concerned with the simplest case--the effect of twist in single yarns.

Approved for Public Release

Contrails

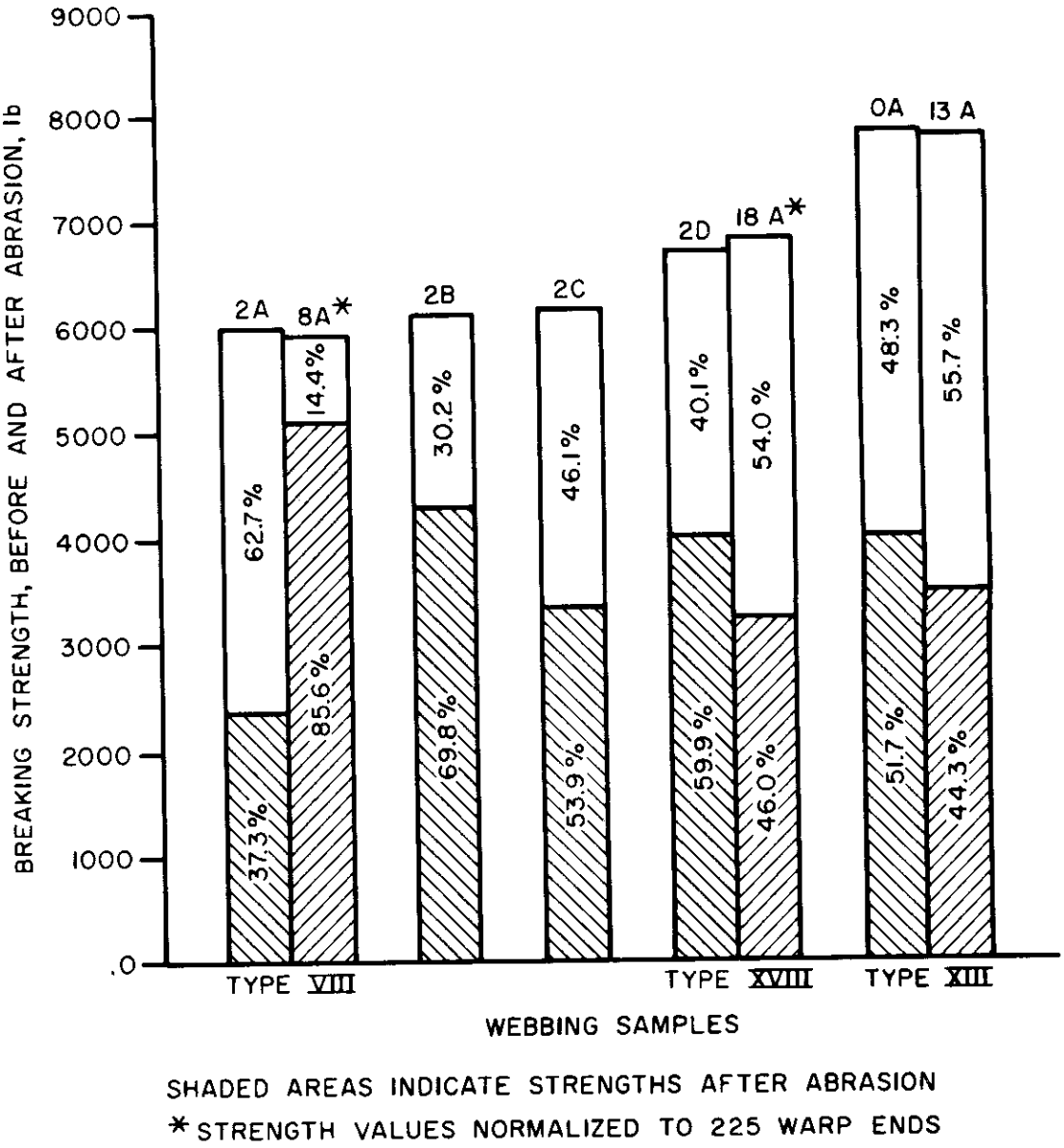

Figure 9 Effect of Weave on Webbing Strength

Approved for Public Release

Contrails

Table 35. Effect of Number of Ends on Webbing Performance

	Sample Numbers 3B	1C	3A
General			
Thickness (in.)	0.087	0.100	0.113
Weight (oz/yd)	1.93	2.27	2.55
Picks (per in.)	24.7	25.0	24.8
Width (in.)	1-29/32	1-26/32	1-26/32
Warp yarn properties			
Number of ends[3]	193	225	257
Yarn denier	2201	2202	2207
Filament denier	6.56	6.56	6.56
Number of plies	10	10	10
Ply twist (t.p.i.)	2.3	2.4	2.3
Singles twist (t.p.i.)	1.2	1.2	1.3
Performance characteristics			
Unabraded strength (lb)	6724[a]	7340	7900[a]
Eff. tenacity (g.p.d.)	7.19	6.73	6.32
S.W.R.[1] x 10^{-3} (yd)	55.7	51.7	49.6
Abraded strength (lb)	3495[a]	4332	5026[a]
Strength loss (%)	48.0	41.0	36.4
Unabraded elongation (%)	25.4	26.5	31.7
Abraded elongation (%)	25.1	31.6	33.6
Contraction[2] (%)	8.0	8.7	8.5

a. Strength values corrected for the number of ends are as follows: 3B (7839, 4075): 3A (6916, 4400).
1. S.W.R. = strength to weight ratio.
2. Warpwise contraction after abrasion.
3. Binder ends not included.

The range of twists (turns per inch) studied was such that the surface fiber helix angles varied from zero to approximately 30 deg.

Manufacturing tolerances and calculation inaccuracies (the yarns were assumed to be circular in cross section) resulted in relatively minor differences between the specified and the actual helix angles.

Table 36 is a tabulation of the physical and mechanical properties of the five webbing samples woven from yarns with varying twists. The performance characteristics are plotted against filament inclination in Figure 11. The term "filament inclination" is possibly more suitable than "helix angle" since the latter usually refers to the angle formed by the fiber and yarn axis. In the case where the yarn axes are parallel to the selvedge, the two terms may be correctly interchanged. The angles in question were measured with respect to the webbing selvedge; the straightness of the yarn path was not investigated.

The effect of yarn twist on the unabraded strength is very apparent: strength decreases with increasing yarn twist; indeed it varies as the cosine of the helix angle, with a surprising accuracy.

Approved for Public Release

Contrails

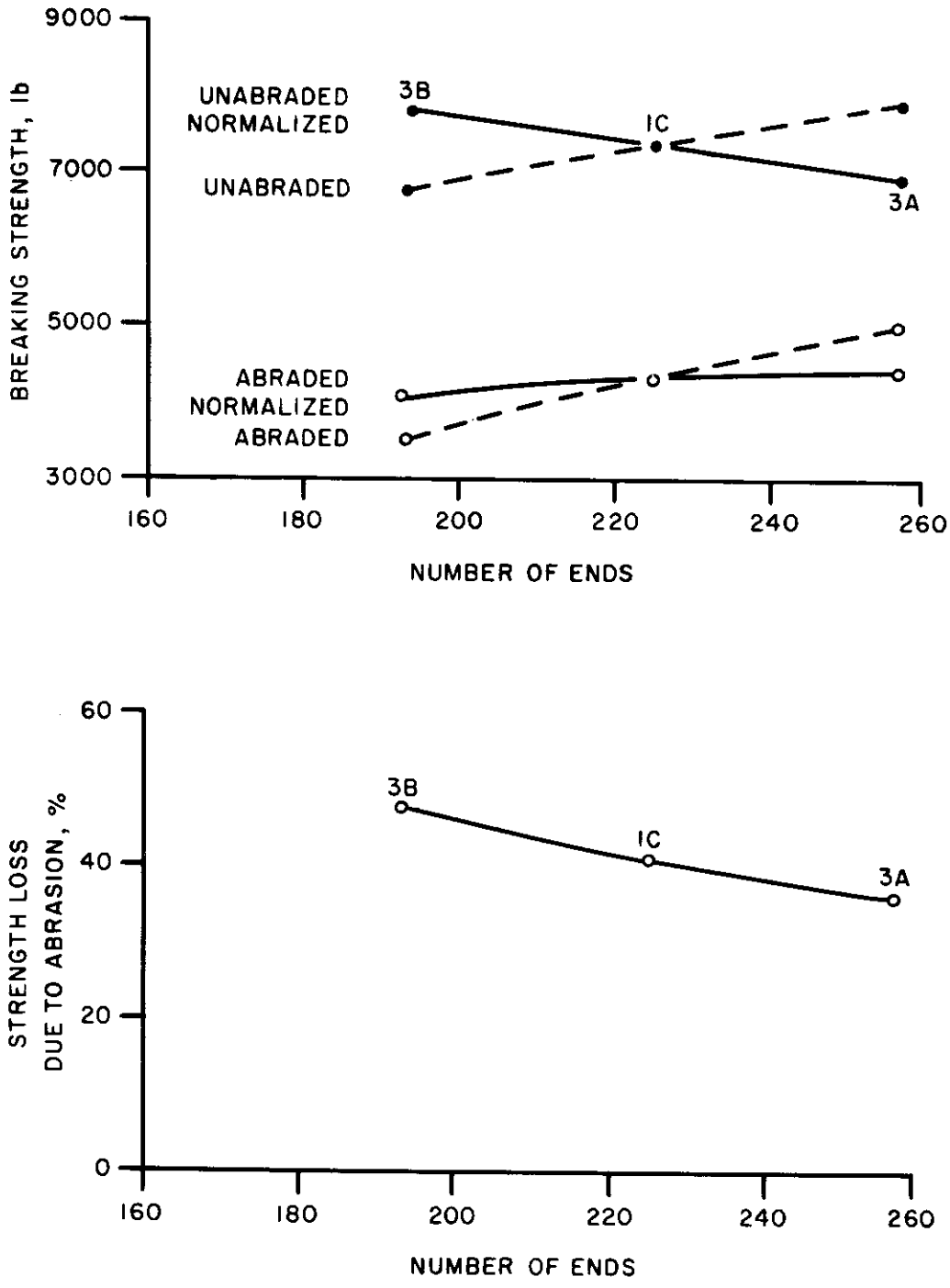

Figure 10 Effect of Number of Ends on Strength

Approved for Public Release

Contrails

Table 36. Effect of Singles Yarn Twist on Webbing Performance

	Sample Numbers				
	4A	5A	5B	5C	5D
General					
Thickness (in.)	0.097	0.097	0.102	0.113	0.112
Weight (oz/yd)	2.21	2.26	2.35	2.45	2.51
Picks (per in.)	25.1	25.9	26.9	26.8	26.7
Width (in.)	1-23/32	1-24/32	1-24/32	1-24/32	1-23/32
Warp yarn properties					
Number of ends	225	225	225	225	225
Yarn denier	2099	2135	2204	2289	2381
Filament denier	5.15	5.15	5.15	5.15	5.15
Number of plies	1	1	1	1	1
Singles twist (t.p.i.)	0	2.5	4.8	6.7	9.6
Performance characteristics					
Unabraded strength (lb)	7090	7194	6794	6202	5842
Eff. tenacity (g.p.d.)	6.82	6.80	6.22	5.47	4.95
S.W.R.[1] x 10^{-3} (yd)	51.3	50.9	46.3	40.5	37.2
Abraded strength (lb)	3687	4143	4038	4743	4604
Strength loss (%)	48.0	42.4	40.6	39.6	21.2
Unabraded elongation (%)	28.5	30.8	34.2	36.3	42.3
Abraded elongation (%)	32.5	30.7	31.9	35.1	44.8
Contraction[2] (%)	13.8	7.9	5.0	3.8	4.8

1. S.W.R. = strength to weight ratio.
2. Warpwise contraction after abrasion.

Webbing Number	Calculated Helix Angle	Cosine of the Helix Angle	Calculated Strength (lb)	Actual Strength (lb)
4A	0	1.000	----	7090
5A	9.9	0.985	6984	7194
5B	18.5	0.948	6724	6794
5C	25.1	0.906	6421	6202
5D	33.8	0.831	5983	5842

Another effect is the increase in elongation with increase in yarn twist; however, this is not quite as predictable as the loss in strength. The rate of change in extensibility is faster than the change in the values of the cosines. Thus, the areas under load-elongation diagrams, or the energies, actually increase while the breaking strengths decrease.

The abrasion resistance of the webbings increase with increasing yarn twist. This may be attributed to a variety of possible causes:

1. Increased energy absorption characteristics as discussed in Section 3.1.4.1.
2. Dimensional stability of the webbing during abrasion. It was observed that while breaking strengths decrease due to abrasive action, elongations almost always increase. It is postulated that this results from a "contraction" caused by the abradant bar acting as a rake on the "knuckles" at the yarn crossovers. Repeated raking pushes the "knuckles" closer to-

Approved for Public Release

Contrails

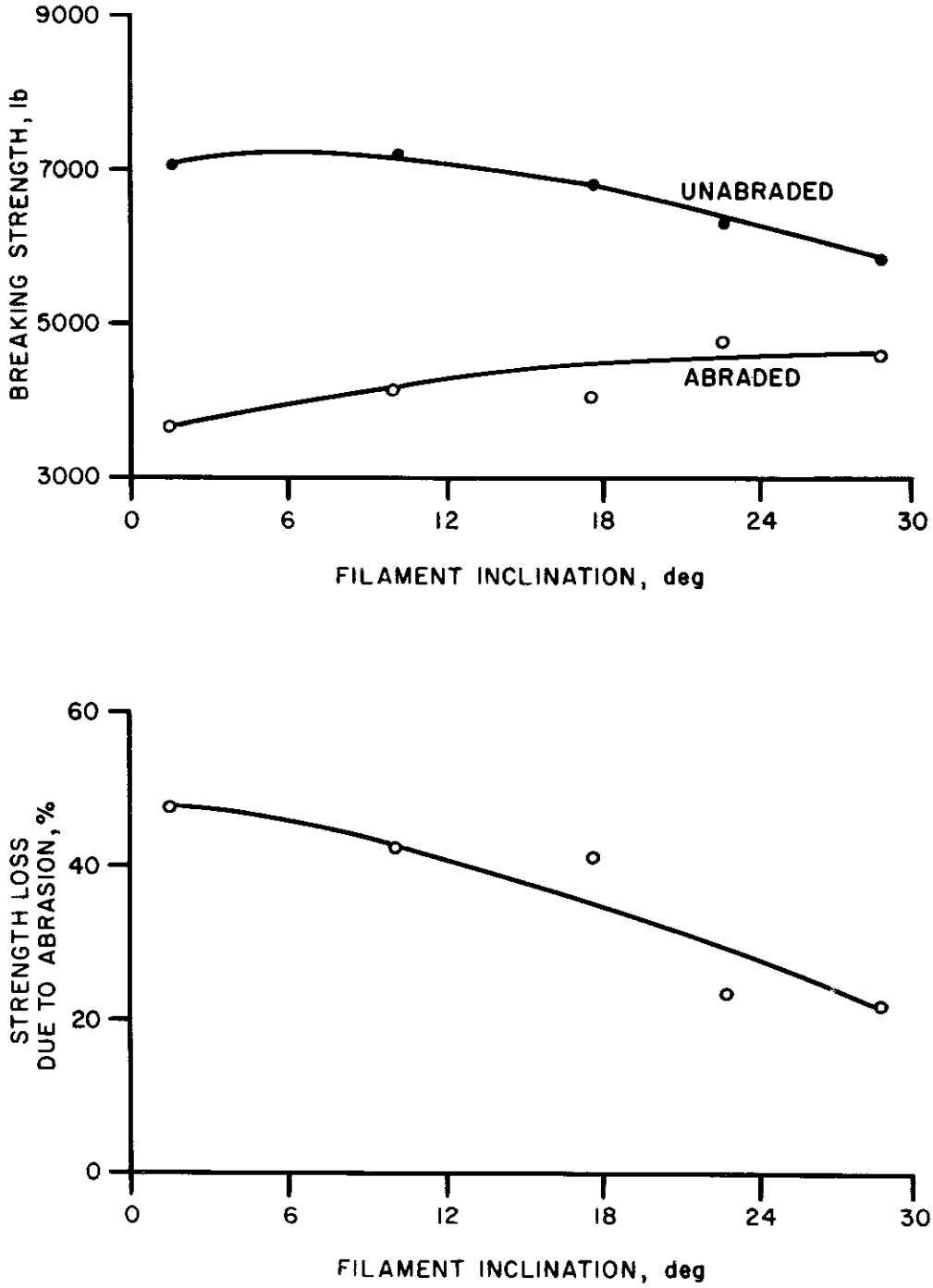

Figure 11 Effect of Filament Inclination in Singles Yarns on Webbing Strength

Approved for Public Release

Contrails

gether thereby reducing the webbing length. This contracted length takes the form of increased warp crimp. Examination of the abraded specimens revealed that the increased crimp causes the warp yarns to protrude from the plane of the webbing, and the yarns frequently opened up as individual filaments became abraded. Further opening of the yarn facilitated even greater damage due to abrasion. Thus it is obvious that the smaller the contraction, the less the yarns will move out of the plane of the webbing, and the less they will be snagged and abraded by the abradant bar.

3. The changes in yarn cross section shape are very pronounced. At very low twists the yarns are very loose and the individual filaments form almost flat surfaces which are in contact with the abradant. As the twist increases, the cross section becomes more and more circular; the area of contact with the abradant diminishes, hence fewer fibers are abraded.

4. The role of flexing: The action of the webbing abrasion machine is not solely abrasion; rather abrasion is accompanied by flexing of the webbing specimen. If the yarn has zero twist, the filaments are flexed with the webbing. On the other hand, if the yarn has some degree of twist the filaments are flexed through larger radius of curvature. In the course of the abrasion test, the specimen is flexed and unflexed 5,000 times. The differences in the radius of curvature could be of importance.

3.1.4.5 Effect of Plied Yarn Twist Variation on Unabraded Strength and Abrasion Resistance. The geometric and performance characteristics of this series of experimental webbings are tabulated in Table 37. Because of the complexity, the webbing strength is not a simple function of the filament inclination as was the case in the singles yarns. However, the general trend still holds, i.e., the breaking strength decreases with increasing filament inclination.

With the plied yarn construction, the webbings are considerably heavier in weight due to twist take-up. The consequence is that both the effective tenacities and the strength-to-weight ratios are substantially depressed. On the other hand, for the same reason, the elongations are greatly increased.

Figure 12 shows percent strength loss due to abrasion vs. the various singles and ply twists. In the upper graph, the effect of ply twist at constant singles twist is seen; the lower graph plots the effect of singles twist at constant ply twists.

The conclusions given for singles yarns also hold true here. However, two additional observations are worthy of note: First, the increase in elongation due to helix effects far surpasses those for single yarns, resulting in much higher energy absorption capacities of the webbings; second, in examining webbing cross sections a startling revelation comes to light. Since the weave type requires that two warp ends be woven as one, the two separate ends are usually found side by side. But in the case of the webbings with higher twist combinations (6B, 6C, 6H, 6J, and 6K) the "wildness" in the yarns made the yarns pile one on top of the other. This condition protects half of all the warp yarns from abrasion. A combination of these circumstances explains the outstanding abrasion resistance of webbing sample 6K which has lost only 8.1% of its strength after abrasion.

3.1.4.6 Effect of Yarn Denier and Ply Variation on Webbing Performance. Other yarn structural parameters that influence webbing performance are the yarn denier, the number of plies, and the filament denier. If certain requirements in the specifications are to be met, i.e., thickness, width and strength, the choice of yarn size becomes rather limited. More-

Approved for Public Release

Table 37. Effect of Yarn Twists on Webbing Performance

	Sample Numbers										
	6A	6B	6C	6D	6E	6F	6G	6H	6I	6J	6K
General											
Thickness (in.)	0.114	0.123	0.182	0.120	0.121	0.136	0.148	0.169	0.152	0.147	0.171
Weight (oz/yd)	2.72	2.99	3.39	2.75	2.80	2.96	2.94	3.25	3.05	3.10	3.16
Picks (per in.)	28.0	28.2	25.3	27.9	27.7	26.9	23.9	24.4	27.0	27.2	24.9
Width (in.)	1-23/32	1-24/32	1-23/32	1-25/32	1-24/32	1-23/32	1-24/32	1-24/32	1-24/32	1-24/32	1-25/32
Warp yarn properties											
Number of ends	225	225	225	225	225	225	225	225	225	225	225
Yarn denier	2581	2744	3132	2597	2619	2686	2853	3113	2774	2818	3054
Filament denier	6.18	6.18	6.18	6.18	6.18	6.18	6.18	6.18	6.18	6.18	6.18
Number of plies	3	3	3	3	3	3	3	3	3	3	3
Ply twist (t.p.i.)	2.5	6.2	11.1	3.2	4.2	6.8	9.4	12.9	4.1	6.3	11.5
Singles twist (t.p.i.)	0.5	0.6	0.6	5.1	5.2	5.3	5.7	6.0	13.7	13.6	15.8
Performance Characteristics											
Unabraded Strength, (lb)	7730	7310	6095	7955	7474	7019	7640	6254	6896	6460	7220
Eff. tenacity (g.p.d.)	6.04	5.38	3.93	6.18	5.76	5.27	5.40	4.05	5.02	4.61	4.77
S.W.R.[1] x 10^{-3} (yd)	55.5	39.1	28.8	46.3	42.7	37.9	41.6	30.8	36.2	33.5	36.5
Abraded Strength (lb)	5622	6112	5160	5282	5764	5575	6025	5220	5842	5658	6636
Strength loss (%)	27.3	16.4	15.3	33.6	22.9	20.6	21.1	16.5	15.3	12.4	8.1
Unabraded elongation (%)	30.9	43.5	58.8	34.3	34.8	38.6	42.9	52.6	42.7	42.3	62.0
Abraded elongation (%)	35.5	41.3	59.6	35.7	38.7	43.3	47.3	60.2	43.3	47.4	49.5
Contraction[2] (%)	7.5	3.9	3.8	6.5	1.9	7.4	6.9	4.0	3.0	2.3	1.2

1. S.W.R. = strength to weight ratio.
2. Warpwise contraction after abrasion

Approved for Public Release

Confidential

Contrails

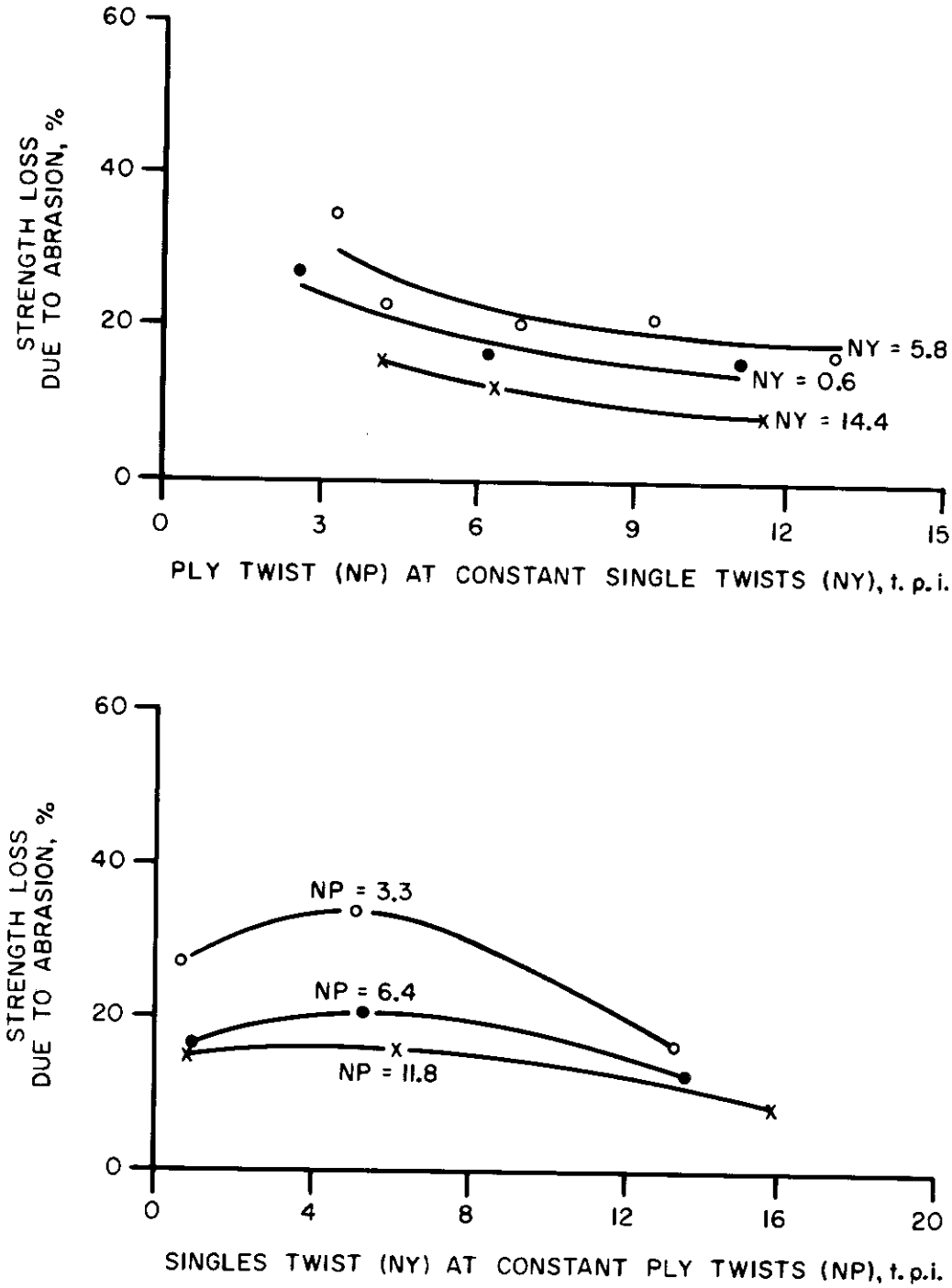

Figure 12 Effect of Twist on Webbing Strength

Approved for Public Release

Contrails

over, commercial yarns suitable for webbing use are restricted to a few selections. Thus, it is very difficult, if not altogether impossible, to study the effects of yarn size alone without studying the effects of plying at the same time by virtue of the fact that smaller yarns must be plied together to meet dimensional and strength demands.

From the available materials, certain combinations of yarn sizes and number of plies capable of yielding the desired final yarn size were possible. Webbings woven from such combinations were:

Sample 0B woven from 210/32 10 ply yarns, total denier = 2100
Sample 4A woven from 2100/408 singles yarns, total denier = 2100
Sample 6A woven from 840/136 3 ply yarns, total denier = 2520
Sample 4C woven from 560/32 4 ply yarns, total denier = 2240
Sample 4D woven from 210/32 3 cord yarns, total denier = 1890

Evaluation results on the above webbings are tabulated in Table 38. Since the total deniers of the yarns are not all the same, the strength values are also given after normalizing adjustment to a common basis of 2100 denier. Attention is called to the superior abrasion resistance of Sample 4C with the 4 ply yarn. It is doubtful, however, that the credit is due to the number of plies since the filament denier is much higher than the rest of the group. (See Section 3.1.4.7 on the effect of filament denier.) Comparison of the remaining four samples reveals that 4D, made with the 3 cord yarns, is strongest in the unabraded state and 6A, woven from 3 ply yarns, is the most abrasion resistant.

3.1.4.7 Effect of Filament Denier. Although five filament sizes are used in the experimental samples, there are actually only two that have significantly different deniers. The other differ very slightly from the two; further, their plied constructions preclude them from any direct comparison. The two studied are:

Webbing 5A woven from 2100/408 yarns, 5.15 denier per filament.
Webbing 7A woven from 2100/112 yarns, 18.75 denier per filament.

Data on these two webbings are given in Table 39. The effect of fiber denier is very evident: the finer fibers give a higher original breaking strength while the coarser filament performed much better in abrasion resistance.

The principal reason for the better strength in 5A is that yarns made with smaller filaments tend to have higher tenacities than those having large filaments. This is borne out by strength tests of the various yarns:

Yarn	Filament Size (denier per filament)	Tenacity (grams per denier)
2100/408	5.15	7.40
840/136	6.18	7.47
210/32	6.56	7.50
560/32	17.50	6.45
2100/112	18.75	6.68

The better abrasion resistance offered by the larger filament yarn is probably due to: (a) greater dimensional stability as evidenced by lower contraction figure upon abrasion. The smaller crimp interchange minimizes the tendency for the yarns to protrude out of the plane of the webbing and become abraded; and (b) the larger filaments slip over the irregularities of the abradant bar, whereas the smaller filaments become snagged and ruptured.

Here again, as on several other occasions, a paradox exists where high

Approved for Public Release

Contrails

Table 38. Effect of Yarn Plies on Webbing Performance

	Sample Numbers				
	0B	4A	6A	4C	4D
General					
Thickness (in.)	0.101	0.097	0.114	0.107	0.099
Weight (oz/yd)	2.35	2.21	2.72	2.32	2.15
Picks (per in.)	27.0	25.1	28.0	26.6	26.9
Width (in.)	1-25/32	1-23/32	1-23/32	1-23/32	1-24/32
Warp yarn properties					
Number of ends	225	225	225	225	225
Yarn denier	2208	2099	2581	2230	2007
Filament denier	6.56	5.15	6.18	17.50	6.56
Number of plies	10	1	3	4	3/3
Ply twist (t.p.i.)	2.6	--	2.5	2.3	3.7/2.7
Singles twist (t.p.i.)	1.2	0	0.5	1.3	1.2
Performance characteristics					
Unabraded strength (lb)	7228	7090	7730	6710	6922
Normalized strength (lb)	7228	7090	6442	6291	7691
Eff. tenacity (g.p.d.)	6.61	6.82	6.04	6.07	6.96
S.W.R.[1] x 10^{-3} (yd)	49.2	51.3	55.5	46.3	51.5
Abraded strength (lb)	4425	3687	5622	6058	4107
Normalized strength (lb)	4425	3687	4685	5679	4563
Strength loss (%)	38.8	48.0	27.3	9.7	40.7
Unabraded elongation (%)	30.6	28.5	30.9	29.6	32.3
Abraded elongation (%)	32.2	32.5	35.5	32.4	32.4
Contraction[2] (%)	7.4	13.8	7.5	4.7	9.4

1. S.W.R. - strength to weight ratio.
2. Warpwise contraction after abrasion.

initial strength and good abrasion resistance seem incompatible; one must be sacrificed for the other.

3.1.4.8 Effect of Dyeing on Webbing Performance. The significance of the effects of dyeing on webbing performance was discussed in WADC TR 56-151 wherein it was speculated that the difference in abrasion resistance between dyed and undyed webbings may be due to structural changes induced by the dyeing processes. In the initial phases of this project, several samples were prepared and evaluated both in the dyed and undyed states. The findings from these tests are given in Table 40, from which the following observations are made:

In the process of dyeing the webbings shrank. This is evidenced by the increase in weight of approximately 10%, increased pickage also of 10%, decreased width, and an increase in elongation of almost 50%!

There does not appear to be any definite trend in the original unabraded strength. Two of the three lost an insignificant amount of breaking strength after dyeing, but the third showed a slight gain. The much higher extensibilities of the dyed webbings give correspondingly greater energy absorptions.

Approved for Public Release

Contrails

Table 39. Effect of Filament Size on Webbing Performance

	Sample Numbers 5A	7A
General		
Thickness (in.)	0.097	0.106
Weight (oz/yd)	2.26	2.22
Picks (per in.)	25.9	26.4
Width (in.)	1-24/32	1-23/32
Warp yarn properties		
Number of ends	225	225
Yarn denier	2135	2156
Filament denier	5.15	18.75
Number of plies	1	1
Ply twist (t.p.i.)	--	--
Singles twist (t.p.i.)	2.5	2.2
Performance characteristics		
Unabraded strength (lb)	7194	6090
Eff. tenacity (g.p.d.)	6.78	5.69
S.W.R.[1] x 10^{-3} (yd)	50.9	43.9
Abraded strength (lb)	4143	5275
Strength loss (%)	42.4	13.4
Unabraded elongation (%)	30.8	27.5
Abraded elongation (%)	30.7	28.3
Contraction[2] (%)	7.9	3.7

1. S.W.R. = strength to weight ratio.
2. Warpwise contraction after abrasion.

The abrasion resistance of the dyed webbings should theoretically be better than the undyed ones because of higher energy absorption. This is true in two cases (weave Types VIII and XIII); in the third, the weave was such that the exposed yarn floats were so long that they were easily snagged by the abradant bar, so much so that no amount of increased energy was of any assistance in keeping the unprotected filaments from rupturing.

Dyeing improves abrasion resistance with a concomitant increase in elongation. The higher extensibility is probably caused by shrinkages induced by the high temperatures encountered in the dyeing processes as well as via the possible use of carriers or dyeing assistants which normally swell the fibers. These shrinkages would occur regardless of whether yarn or piece dyeing methods were used. For applications where low elongation is desirable, the increased elongation due to dyeing can be removed via hot stretching or via use of dope dyed yarn.

3.1.4.9 Comparison of Yarn Types. Although most of the experimental webbings studied in this project were woven from Type HBT (high tenacity, bright, thermally stable) Caprolan nylon 6 yarns, a few had to be woven from Type HB yarns because the particular sizes were not available in the HBT type. Webbings 5A and 7A were designed to evaluate the influences of filament size. However, 5A was woven from Type HBT yarns while 7A was woven from HB yarns. The natural question is whether the differences observed

Approved for Public Release

Contrails

Table 40. Effect of Dyeing on Webbing Performance

	Sample Numbers					
	8B	8C	13B	13C	18B	18C
General						
Weave type	VIII	VIII	XIII	XIII	XVIII	XVIII
Dyed	No	Yes	No	Yes	No	Yes
Thickness (in.)	0.062	0.060	0.095	0.095	0.126	0.129
Weight (oz/yd)	1.39	1.54	2.19	2.42	1.85	1.99
Picks (per in.)	16.6	18.5	20.7	22.7	17.0	18.4
Width (in.)	1-28/32	1-24/32	1-27/32	1-23/32	1-3/32	1-0/32
Warp yarn properties						
Number of ends	132	132	225	225	208	208
Yarn denier	2179	2328	2170	2360	2174	2368
Number of plies	10	10	10	10	10	10
Ply twist (t.p.i.)	2.8	2.9	3.0	3.2	2.9	3.0
Singles twist (t.p.i.)	1.1	1.4	1.0	1.3	1.1	1.1
Performance characteristics						
Unabraded strength (lb)	3990	3810	7890	7375	6040	6635
Eff. tenacity (g.p.d.)	6.30	5.63	7.34	6.31	6.06	6.12
S.W.R.[1] x 10^{-3} (yd)	45.8	39.5	57.5	48.7	52.2	53.2
Abraded strength (lb)	2940	3409	3644	4333	2746	2754
Strength loss (%)	26.3	10.5	53.8	41.2	54.5	58.5
Unabraded elongation (%)	24.1	40.8	23.2	34.0	20.8	30.0
Energy absorption (in-lb/in.)	362	575	619	924	475	773

1. S. W. R. = strength to weight ratio.

were due to fiber type or filament size. Data show that no significant differences may be seen either geometrically or performance wise. Therefore, the differences between webbings 5A and 7A should be attributed to filament size effects.

3.1.5 Conclusions

The following is a resumé of the effects of varying constructional parameters on webbing performance:

Picks per Inch. Increasing the picks per inch produces a slight decrease in original strength; but the abrasion resistance is improved.

Weave Type. Of the five weave types investigated the standard Type XIII weave is best with respect to strength and abrasion resistance in the Type XIII webbing. The other four weaves are inferior in the Type XIII construction. The standard Type VIII weave in the Type VIII construction gives excellent strength and abrasion resistance. The Type XVIII weave is poorer in the Type XVIII construction than it is in the Type XIII construction.

Number of Ends. Increasing the number of ends increases the original webbing strength but is not linearly proportional to the number of ends added. The abrasion resistance, however, is greatly improved.

Singles Yarn Twist. Increasing the turns per inch in the singles reduces

Approved for Public Release

Contrails

the original webbing strength because of the helix effect. The abrasion resistance is improved.

Ply Yarn Twist. Here again, as in the above case, increasing the ply twist causes a decrease in strength. The improvement in abrasion resistance is more pronounced here than for singles twist. In fact, the webbing made with the highest singles and ply twist yarn (Sample 6K) had the highest strength after abrasion of all webbings studied.

Number of Plies and Yarn Size. Results of the study of yarn sizes and number of plies are not readily apparent. Sample 4D has the highest normalized original strength, while 6A has the highest normalized abraded strength. These webbings were woven from 3/3 cord and 3 ply yarns respectively. The performance of webbing Sample 4A woven from singles yarns appears to be the poorest of the group. Hence it may be concluded that plied yarns are better than singles yarns for webbing use.

Filament Denier. Increasing the filament denier produces a significant decrease in original strength, concomitant with greatly improved abrasion resistance.

Dyeing. The effect of dyeing on webbing performance is a slight decrease in the original strength and a similarly slight improvement in abrasion resistance.

Yarn Type. There is no indication that yarn types HB and HBT are different from each other.

3.1.6 Optimum Webbing Design

The foregoing summary indicates that the design for maximum original strength does not coincide with the requirements for maximum abrasion resistance. Thus, the design of an improved webbing must be a compromise between high initial strength and high abrasion resistance, each representing less than the maximum were either the sole consideration.

It is speculated that an optimum webbing design may be engineered by proper selection of the best features of each of the constructional variables listed in Section 3.1.5 above. However, the various improvements may be cumulative, but not necessarily additive, e.g., if a 6% strength gain is realized by reducing the number of picks per inch, and a 4% gain by adding a few more ends, combining both may not yield a 10% total improvement. The exact effect cannot be anticipated quantitatively unless actual samples are constructed and evaluated.

3.1.7 References

Sections 2.1, and 6.1 and WADD TR 60-584 , pp. 85 to 88, 164 to 176, 292 to 328.

Approved for Public Release

Contrails

Section IV

IMPACT LOADING

4.1 Comparative Drop Tests of Chemstrand and du Pont Nylon Parachutes

While previously nylon 66 was obtainable only from the du Pont Company a new source is now available from the Chemstrand Corporation. For competitive purchasing reasons this new source was investigated. Object of the program was to compare the performance of new Chemstrand nylon parachutes against standard du Pont nylon parachutes. Twenty-five parachutes composed of Chemstrand nylon canopy cloth, and twenty-five identical parachutes composed of du Pont nylon canopy cloth were manufactured (AF Part No. 50C7024-12, 30 ft-diameter guide personnel canopies, Type C-1, AF drawing No. 52J6026-2) and tested by drop tests, Whirltower tests, and Textile Laboratory air permeability tests.

The study was conducted by J. V. Waite, 6511th Test Group (Parachute) N.A.A.S., El Centro, California, and is reported in AFFTC-TN-58-17, September 1958.

4.1.1 Materials

The Chemstrand and du Pont nylon were woven into fabrics of Specification MIL-C-7020, Type I. The fabrics were then assembled into standard parachutes as noted above.

4.1.2 Test Procedures

Four basic types of tests were conducted: (a) twisted line tests; (b) opening shock tests; (c) life tests; (d) laboratory measurements of fabric air permeability before and after the various deployments. From these tests (described below) the following data were obtained: (1) Parachute opening time; (2) snatch and opening forces; (3) the relationships between the number of test drops on a parachute and the change in fabric air permeability.

a. Twisted Line Tests: These tests consisted of dropping a 200-lb drop test dummy to which the test parachute was attached from the rear ramp of a flying aircraft. Each canopy was subjected to a minimum of one test with twisted lines. All canopies that failed to open or had abnormally long opening times were given additional tests, as the manner in which the dummies were launched from the aircraft had a definite bearing upon the success or failure of the test. The utmost care was exercised to launch the dummies without inducing rotation. The tests were conducted at 500-ft altitude at approximately 100 knots.

b. Opening Shock Tests: These tests were made with a Whirltower. This facility has a rotating vertical central shaft to which a horizontal boom is attached. A gondola, rigged for the attachment of a parachute-equipped test dummy, is anchored to the tower boom by means of a 114-ft length of heavy flexible steel cable. In operation, the gondola moves in a circular path 344 ft in diameter at a vertical distance of 120 ft above the ground. Centrifugal force is applied to the dummy and parachute while the gondola is in motion.

Approved for Public Release

Contrails

Sixteen assemblies, eight Chemstrand and eight du Pont, were selected for opening shock tests after completing the twisted line tests. These tests were conducted from the Whirltower at speeds ranging from 125 to 300 knots. Tensiometers were used to record the snatch and opening forces.

c. Life Tests: These tests were also made with a Whirltower at 150 knots. Thirteen assemblies, six Chemstrand and seven du Pont were repeatedly deployed until failure occurred or a test was discontinued.

d. Air Permeability: This was determined under ASTM conditions as specified in Federal Specification CCC-T-191b. Air flow is measured in cubic feet per minute (cfm.) per square foot of fabric at 0.5 in. water pressure across the fabric.

4.1.3 Test Results

a. Twisted Line Tests: Forty-two tests each were made for both the Chemstrand and du Pont canopies. (One Chemstrand canopy failed to open because of dummy rotation; this test was discarded and is not considered germane to the evaluation.) Average opening times were slightly shorter for the Chemstrand than for the du Pont canopies, but these two types of nylon are not considered significantly different with respect to this test.

b. Opening Shock Tests: Forty tests each were made for both the Chemstrand and du Pont canopies. The opening and snatch forces, and opening times of the Chemstrand and du Pont canopies were approximately equal at equivalent air speeds (Figures 13 and 14).

c. Life Tests: A total of 130 life tests each was made for both the Chemstrand and du Pont canopies (Table 41).

The results are so variable as to be inconclusive. It is apparent, however, that no significant difference in life exists between the two nylon types.

d. Air Permeability Tests: Table 42 shows air permeability ranges and averages for the original fabrics, and after a total of 127 drop tests for the Chemstrand parachutes and 115 drop tests for the du Pont parachutes respectively. Results indicate no significant difference between the two types of nylon.

4.1.4 Conclusions

Test results show no significant difference between parachute canopies fabricated with Chemstrand nylon and those fabricated with du Pont nylon in respect to service life, opening shock, opening time, damage, and air permeability .

4.1.5 References

None.

Approved for Public Release

Contrails

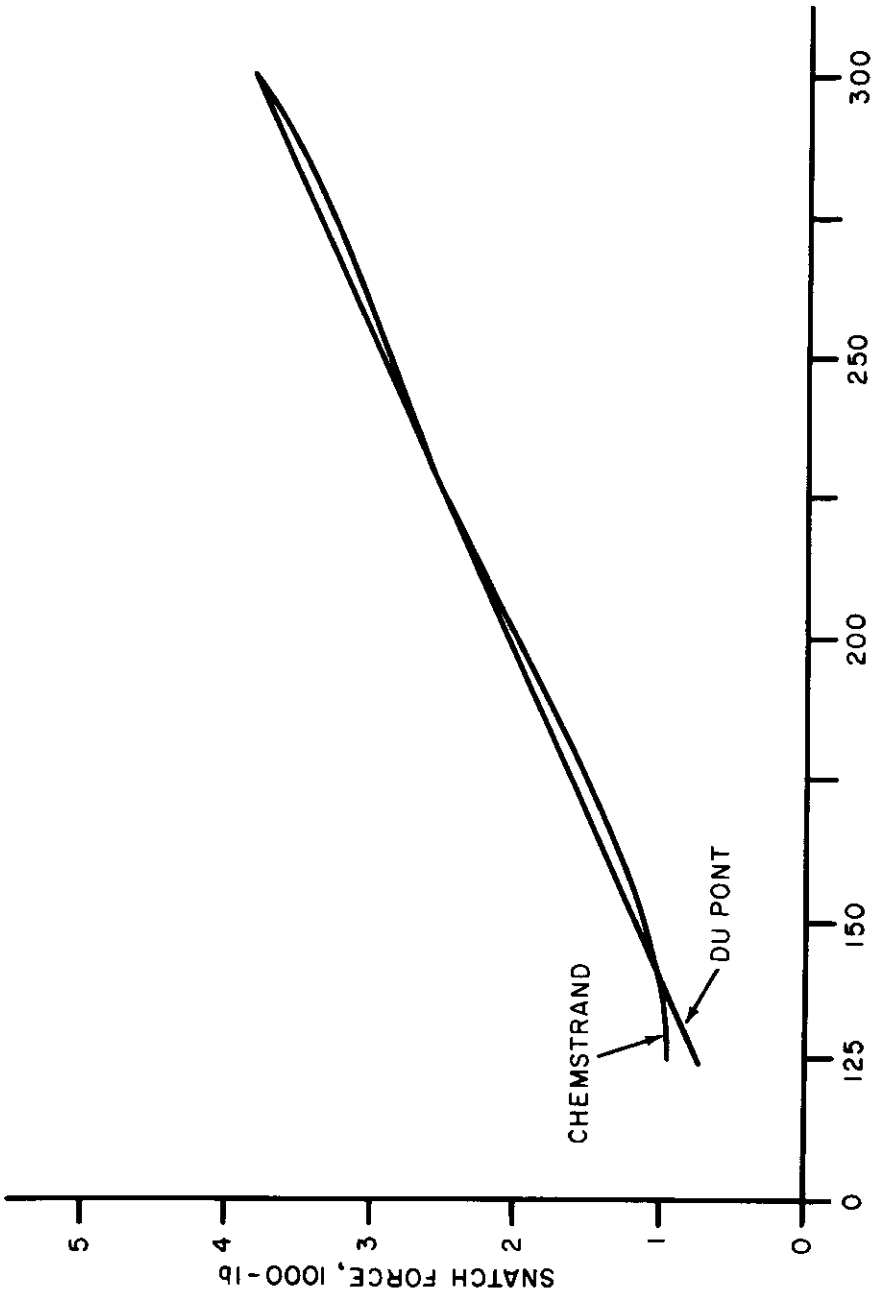

Figure 13 Snatch Force vs. Launching Speed for Chemstrand and du Pont Nylon Canopies

Approved for Public Release

Contrails

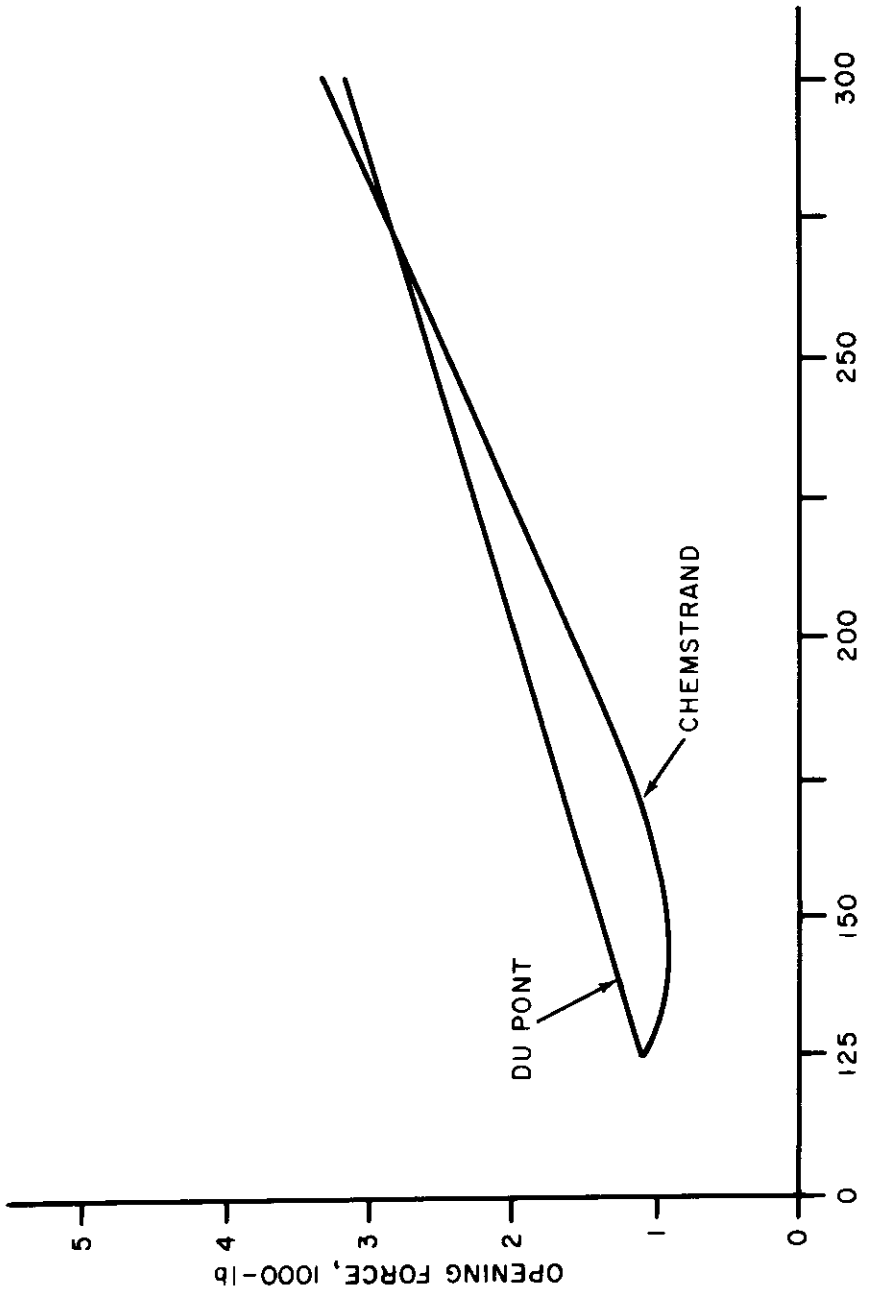

Figure 14 Opening Force vs. Launching Speed for Chemstrand and du Pont Nylon Canopies

Approved for Public Release

Contrails

Table 41. Life Tests of Chemstrand and du Pont Canopies

Canopy No.	No. of Tests	Remarks
C-1*	39	Tested to destruction
C-2	13	Tested to destruction
C-3	5	Tested to destruction
C-4	22	Not tested to destruction
C-7	41	Not tested to destruction
C-13	10	Not tested to destruction
D-1**	13	Tested to destruction
D-2	1	Tested to destruction
D-3	39	Not tested to destruction
D-4	7	Tested to destruction
D-5	19	Not tested to destruction
D-7	41	Not tested to destruction
D-13	12	Tested to destruction

* = Chemstrand
** = du Pont

Table 42. Air Permeabilities of Fabrics Before and After Drop Tests

	Permeability cfm./ft^2	
	C*	D**
Original		
Range	108-136	103-141
Average	123	123
Number of drop tests	127	115
After drop tests		
Range	108-133	106-132
Average	122	120

*C = Chemstrand
**D = du Pont

Approved for Public Release

Contrails

4.2 Effect of Repeated Deployments on the Properties of B-47 Deceleration Parachutes

The purpose of the investigation was to determine the safe number of uses to which a B-47 D-1 deceleration parachute can be put so that maximum safety and dependability can be insured. Parachutes were use tested (deployed) in increments of 10 through 60 tests at MacDill Air Force Base, Florida, and were then tested for strength and dimension changes at the WADC Materials Laboratory. The work was conducted by J. C. McGrath and is reported in WADC Technical Note 57-326, November 1957.

4.2.1 Materials and Test Procedure

Seven parachutes, all made by the same company between October 1952 and May 1953 were selected. Elongation marks 36 in. in length were placed on 12 suspension lines and 12 vertical radial ribbons so that elongation or shrinkage between gage marks after deployment could be measured. Parachute No. 1 was retained as a control; parachute No. 2 was deployed 10 times; parachute No. 3 was deployed 20 times, etc.; parachute No. 7 was deployed 60 times. The parachutes were returned to the Materials Laboratory where components were tested according to applicable specifications:

(1) Lower Lateral Bands, (skirt band) Specification MIL-W-4088B, nylon webbing, Type VI (1,800-lb min breaking strength). Sections were cut from the band so that the test point would be at each third panel attachment, i.e., the junction of the radial bands and the suspension lines. Twelve samples were broken.

(2) Vertical Radial Bands. Specification MIL-T-5038 nylon reinforcing tape, Type IV, 1-1/2 in. wide (1,500-lb min breaking strength). Specimens were cut from every third vertical ribbon (12 total breaks).

(3) Suspension Lines. Specification MIL-W-5625, nylon tubular webbing, 3/4 in. wide (2,250-lb min breaking strength). All 36 lines were tested with each specimen being cut from the section of line adjoining the skirt band.

(4) Ribbon. Specification MIL-T-5608, nylon ribbon, Type V, Class C (300-lb min breaking strength). Five test specimens were cut from every third panel of each parachute. Sixty samples were broken.

Test data from the lower lateral bands and the vertical radial ribbons cannot be compared to specification requirements due to the stitching and layer of ribbons combined in the structure.

Breaking strengths of riser webbings are not included in this report.

4.2.2 Test Results

Table 43 shows breaking strengths as a function of number of deployments. Also shown are the percents increase (+) or decrease (-) from the original 36 in. of the line and ribbon gage marks. Table 44 tabulates percent loss in strength after the specified number of deployments.

Approved for Public Release

Contrails

4.2.3 Conclusions

Breaking strength comparison tests of ribbons show the percent losses to be very erratic. This may be due to the amount of oil, grease or dirt which had accumulated on the ribbons. Five adjacent ribbons, for testing, were cut from every third panel of the parachute approximately one-third the distance from the bottom of the skirt. No allowance was made for the degree of dirt or stain for the particular panel.

The majority of low individual breaking strength values for the suspension lines was caused by abrasion of the lines. The variation of percent loss for both the lower lateral bands and the vertical radial tapes cannot be explained.

Results of tests on B-47 deceleration parachutes from 10 through 60 uses indicate that the parachutes can be used for 60 or more deployments if handled, inspected and repaired correctly. The most important factor in determining the usability of the parachute will still be visual inspection.

4.2.4 References

Sections 1.1, 1.2, 4.1, 4.3, and WADC TR 55-264, pp. 63 to 68.

4.3 Effect of Repeated Deployment on the Properties of F-100 Deceleration Parachutes

The purpose of the investigation was to obtain data to establish the service life of test parachutes. Parachutes were use tested (deployed) in increments of 5 through 35 tests at Nellis Air Force Base, Nevada, and were then tested for breaking strength, dimensional change, and air permeability at the WADC Materials Laboratory. The work was conducted by J. C. McGrath and is reported in WADC Technical Note 58-20, January 1958.

4.3.1 Materials Tested

Ten parachutes, all made by the same company between June 1955 and February 1956 were deployed according to the following schedule:

No. 1. Control
2. 5 uses
3. 10 uses
4. 15 uses
5. 20 uses
6. 25 uses
7. 30 uses
8. 35 uses
9. intended for 40 uses; failed on the 10th use.
10. intended for 45 uses; failed on the 25th use.

4.3.2 Test Procedures

Prior to deployment selected panels were tested for air permeability, each area being marked so a re-test could be made after deployments were completed. Riser webbings, radial seam tapes, and suspension lines were gage marked so that the elongation or shrinkage resulting from the deployment could

Approved for Public Release

Table 43. Breaking Strength of Component Parts of B-47 Deceleration Parachutes after Specified Number of Deployments

Component Parts	Number of Deployments							Specification Requirement
	0 Control	10	20	30	40	50	60	
Ribbons MIL-T-5608 Type V, Class C Breaking strength (lb)	313	167.8	214.9	222.8	208.8	229.0	228.5	300 min
Suspension lines, MIL-W-5625, 3/4-in. width Breaking strength (lb)	2641.1	2521.2	2357.8	2553.0	2339.0	2409.7	2263.7	2250 min
Gage length change (%)	*	-1.2	-1.7	-1.3	-2.1	0.1	-2.2	None
Lower lateral bands, MIL-W-4088B, Type VI Breaking strength (lb)	2105.8	2029	1568.2	1657.0	1359.5	1818.7	1494.1	1800 min**
Vertical radial tapes, MIL-T-5038, Type IV, 1-1/2 in. width Breaking strength (lb)	2205	2187.5	1870.0	1879.0	1930.0	2156.6	1857.0	1500 min**
Gage length change (%)	*	-0.5	-1.2	-1.3	-0.2	0.1	-2.4	None

*Original length, 36 in. (-) signifies shrinkage.

**Used for comparison only due to stitching and layers of ribbon combined in the structure.

Approved for Public Release

Contrails

Table 44. Percent Loss in Strength After Use

Component Parts	Percent Loss in Strength After Deployment (uses)					
	After 10 Uses	After 20** Uses	After 30 Uses	After 40** Uses	After 50 Uses	After 60*** Uses
Ribbons	46.45*	31.43	28.9	33.37	26.93	27.09
Suspension lines	4.54	10.72	3.34	11.44	8.76	14.29
Lower lateral bands	3.64	25.52	21.31	35.44	13.63	29.05
Vertical radial tapes	0.79	15.19	14.78	12.47	2.19	15.78

*Ribbons were very dirty and oil or grease stained.
**Entire parachute oil and grease stained.
***This parachute lost from station for over one year, part of the time overseas.

be determined.

After deployment under normal daily flight conditions the parachutes were returned to the Materials Laboratory where components were tested according to applicable specifications:

(1) Fabric. Specification MIL-C-7350, Type I, Cloth, Nylon for Drag Parachutes. Warp and filling specimens were taken from selected panels and tested for breaking strength. Air permeability was rechecked in the same area as before the deployment tests.

(2) Risers. Specification MIL-W-4088B, Type X, Webbing Nylon (8,700-lb min breaking strength). Six specimens were broken from each riser assembly.

(3) Lower Lateral Bands. MIL-T-5038, Tape, Nylon (1,000-lb min breaking strength) test specimens were cut from the skirt band so that the test point would be at every other panel attachment (total of 10 breaks) i.e., the junction of the radial seams and the suspension lines.

(4) Radial Seams. Specification MIL-T-5038, Tape, Nylon, Reinforcing (1,000-lb min breaking strength) plus MIL-T-5038, Tape (500-lb min breaking strength.)

(5) Vertical Tapes. Specification MIL-T-5038, Tape, Nylon, Reinforcing (500-lb min breaking strength.)

(6) Suspension Lines. Specification MIL-W-5625, Tape, Nylon, Tubular (1,500-lb min breaking strength.) All twenty lines were broken with the specimens being cut from the section of line adjoining the skirt band.

An experimental solid webbing suspension line of nylon (1,500-lb min breaking strength) was substituted on parachute Nos. 5 (20 uses) and 9 (10 use supplemental.)

Approved for Public Release

Contrails

4.3.3 Test Results

4.3.3.1 Deployment Data. Table 45 shows the ranges of deployment speeds, duration of flight, after burner time, and damage reported.

Table 45. Ranges of Deployment Data: F-100 Deceleration Parachutes

Parachute	No. of Deployments	Deployment Speed Range (knots)	Flight Duration Range (minutes)	After Burner Time Range (minutes)	Damage
2	5	136-160	55-80	1-7	small holes in panel
3	10	130-165	55-60	1-5	none
4	15	100-160	55-70	1-5	two panels damaged
5	20	120-170	50-70	1-4	2 lines broken
6	25	125-160	45-80	1-4	small holes in panel
7	30	105-160	25-70	1-5	broken lines, small holes, ripped panel
8	35	135-160	45-70	1-5	lines broken
9	10	135-210	20*-70	1-3	friction burns
10	25	125-160	45-75	1-5	lines broken, panels damaged, parachute collapsed

*Canopy opened while airborne, could not be jettisoned.

4.3.3.2 Physical Property Changes. Table 46 lists breaking strengths and gage length changes of lines, radial seams and tapes, and risers after deployment. Table 47 tabulates percent loss in strength for these items. Table 48 lists fabric air permeability, breaking strength, and breaking elongation.

4.3.4 Conclusions

The parachute used as a control does not give a true picture for comparison purposes. The filling breaking strength fails to meet minimum strength requirements of Specification MIL-C-7350, Type I. Breaking strength of the lower lateral bands fail to meet the minimum requirements of the webbing used in the band (MIL-T-5038 tape, 1,000-lb min). It is believed that the low breaking strength of the lower lateral bands (control parachute) was due to poor construction and not to the webbing itself, inasmuch as the same type webbing was used in all parachutes.

Approved for Public Release

Table 46. Breaking Strength and Gage Length Change of Component Items of F-100 Brake Parachute

No. of Uses	Suspension Lines		Radial Seams		Radial Tapes	Lower Lateral Bands	Risers	
	Breaking Strength (lb)	Gage Length Change[a]	Breaking Strength (lb)	Gage Length Change[a]	Breaking Strength (lb)	Breaking Strength (lb)	Breaking Strength (lb)	Gage Length Change[a]
Specification	1500 (min)	-	-		500 (min)	1000(min)	8700 (min)	
Control	1642	-	1915		593	831	8962	
5 Use	1601	0.36	1840	0.22	566	1206	9108	0.83
10 Use	1429	0.19	1762	(-) 0.05	547	930	8211	1.61
15 Use	1572	0.27	1690	0.69	541	1246	No test	No test
20 Use	1449***	0.55	1859	0.27	525	1002	6865	2.22
25 Use	1333	0.55	1799	0.72	538	1016	7036	2.61
30 Use	1300	0.38	1615	0.91	468	1162	6956	0.70
35 Use	1345	0.33	1552	(-) 0.13	489	989	6651	2.16
10 Use *	1834***	0.27	1486	0.16	449	799	7769	1.38
25 Use **	1408	(-)0.14	1455	0.28	508	1177	7371	2.28

*Parachute deployed in flight on 10th use test. Could not jettison. Not reparable.

**Parachute damaged during 25th use test. Not reparable.

***Experimental lines.

[a]Gage length change as result of deployment. (-) indicates shrinkage.

Approved for Public Release

Contrails

Table 47. Percent Loss in Strength, Component Items of F-100 Brake Parachute

	Percent (%) Loss in Strength				
No. of Uses	Suspension Lines	Radial Seams	Radial Tapes	Lower Lateral Bands**	Risers
5	2.43	3.91	4.55	45.1 Increase**	1.62 Increase
10	12.9	7.93	6.07	11.9 "	8.38
15	10.3	11.22	8.68	49.9 "	No test
20	11.7*	2.95	11.48	20.5 "	23.41
25	12.7	6.08	9.2	22.06 "	21.49
30	20.7	15.63	21.8	39.8 "	22.37
35	18.08	18.4	17.47	19.0 "	25.78
10	11.7*	22.4	24.28	3.8	13.32
25	14.2	24.04	14.23	41.6 Increase	17.86

*Experimental lines.

**Percent loss in strength of lower lateral bands is not a true picture. Breaking strength of bands in the control parachute was very low probably due to faulty construction.

Fabric used in six of the ten parachutes met the requirement of MIL-C-7350, Type I for air permeability. Fabric with high original permeability showed less change after deployments than the fabric with low original permeability. The strength of the fabric was not affected seriously by the number of deployments. When compared with the minimum strength of 90 lb/in., the greatest loss in strength was 7.6% (filling wise) for the ten use parachute which deployed in flight at high speed. Specimens taken from areas which were very soiled and grease or oil stained gave lower strength results than other areas. Breaking elongation of the fabric changed very little after deployments.

Losses in strength of suspension lines, radial seams and tapes, lower lateral bands and riser webbings after use are well within limits. Low individual breaking strength values, in most cases caused by abrasion, have lowered the overall average in some instances.

4.3.5 References

Sections 1.1, 1.2, and 4.2, and WADC TR 55-264, pp. 63 to 68.

Approved for Public Release

Table 48. Physical Properties of Fabric from F-100 Brake Parachutes

No. of Uses	Air Permeability ($ft^3/min/ft^2$) Before Use Test	Air Permeability ($ft^3/min/ft^2$) After Use Test	Breaking Strength (lb/in.) Warp	Breaking Strength (lb/in.) Filling	Breaking Elongation (%) Warp	Breaking Elongation (%) Filling
Control	134		95.8	89.1	20.4	26.6
5 Use	139.3	175.8	105.8	103.7	21.9	27.7
10 Use	141.0	155.8	104.7	96.8	22.1	26.6
15 Use	149.2	173.1	94.3	94.2	20.3	26.3
20 Use	165.8	175.8	95.4	93.6	20.1	26.8
25 Use	139.5	179.0	97.9	92.4	19.6	24.1
30 Use	158.8	144.9	94.6	91.1	19.5	24.3
35 Use	164.0	176.5	89.4	86.1	19.4	25.7
10 Use*	155.3	161.7	92.1	83.1	20.8	24.1
25 Use**	149.6	151.1	91.2	87.7	20.4	22.2
Spec. Requirements	100-150		90 min	90 min	20 min	20 min

*Parachute deployed in flight on 10th use test. Could not jettison. Not reparable.

**Parachute damaged during 25th use test. Not reparable.

Approved for Public Release

Confidential

Contrails

Section V

POROSITY AND AIR PERMEABILITY

5.1 Development of Design Data on the Mechanics of Air Flow Through Parachute Fabrics

Section 2.5, and WADD TR 60-584, pp. 191 to 237 have traced the development of a quantitative engineering approach to the design of parachute fabrics of specified air permeability. Pages 201 to 234 report work by Fabric Research Laboratories, Inc. on the influence of yarn and fabric geometry on fabric air permeability. Factors studied were: (1) the effect of yarn twist on fabric properties; (2) the mechanics of air flow through fabrics; (3) compilation of data. Continuing that work, Klein, Lermond and Platt of Fabric Research Laboratories, Inc. present additional information on the mechanics of air flow in WADC TR 56-576, September 1957 (Contract AF33(616)-2977).

Objective of the study was a thorough determination of the factors involved in parachute fabric permeability, and the quantitative prediction of their influence with a view to rational engineering design of such materials.

5.1.1 Materials Tested

A rational series of nylon parachute fabrics as listed in Table 49, page 203 of WADD TR 60-584.

Example: Fabric R20C5
R = rip-stop weave
20 t.p.i. warp twist
C = calendered
5 t.p.i. filling twist

5.1.2 General Approach

The development of a procedure for the quantitative prediction of air flow through textile materials involves two problems. First, it is necessary to know how flow varies as a function of the size and shape of the areas available for flow; and second, the shape and size of these areas must be known as a function of the flow. It is this inter-dependence of pertinent flow parameters wherein the test itself creates variables, that makes a purely empirical flow-pressure correlation equation of no value. Thus, the relation between permeability and pressure drop across a given fabric is not a unique one, but may depend to a large degree on test parameters such as size and shape of specimen. Clearly, a synthesis of the sort required to design parachute fabrics to permeability specifications must be preceded by a rather critical analysis in order that as many as possible of these variables be separated and evaluated individually.

The first step in such an analysis has been to develop, in terms of fabric parameters, a restatement of the classical relations describing incompressible fluid flow through an orifice. From these it becomes clear what sort of investigation is required in order to obtain, if such exist, unique relations among the chosen variables. A variety of experimental data is then analyzed in an attempt to obtain verification of the assumptions made and the numerical constants required for practical application of the theory.

Approved for Public Release

Contrails

5.1.3 Test Methods

Air Permeabilities at low pressures up to 10 in. of water were determined on a Frazier Permeometer. Air permeabilities at high pressures up to 50 in. of water were determined on a Georgia Institute of Technology permeometer.

Light Penetrability was used as a measure of the Free Area (FA) or open area of the fabric. This is a measure of the open area (i.e., the area not occupied by fiber or yarns) of the fabric as a percentage of the total fabric area. Light Permeability (LP) was measured by means of an ultraviolet spectrophotometer fitted to the 50-inch permeometer. LP's of the fabrics were measured simultaneously with air permeabilities. Thus, the LP's indicated the open area of the fabric while the fabric was being distorted by the application of air pressure.

Biaxial Testing was conducted on the Fabric Research Laboratories, Inc. Biaxial Tester as described in WADD TR 60-584, page 370.

5.1.4 Development of a Theoretical Flow Equation

In arriving at a theoretical form of an equation to express the flow of air through a parachute fabric the following procedure is used:

a. The classical equation for incompressible fluid flow through an orifice is stated.

b. The meaning of each term is defined with respect to a fabric analogy.

c. The use of such a formula is provisionally justified, the real criterion of its validity being its subsequent test against experimental results.

d. The classical formula is rewritten in a form more easily applicable to fabric structures.

e. The experimental work necessary for practical application of the theory is outlined.

To obtain independent relationships among the several variables considered, the following information must be found:

a. Fabric strain as a function of fabric stresses.

b. Fabric stresses as a function of pressure differential and geometric configuration of sample.

c. Fabric pore size and shape as a function of fabric strain.

d. Air flow through the fabric as a function of pore geometry and pressure differential.

It is the determination of the above four relationships and their application to flow prediction in parachute fabrics that comprise this report.

Approved for Public Release

Contrails

5.1.5 Theoretical Analysis of Structural Changes During Permeability Tests

When a fabric is mounted in the permeometer and subjected to a pressure differential, two separate but related phenomena take place.

a. Air flow in accordance with the fabric geometry and pressure differential.

b. Fabric geometry changes as a result of biaxial stresses set up by the pressure differential.

Geometric changes must be measurable or predictable before the mechanics of flow can be investigated. Biaxial tensioning of a fabric under a hydrostatic pressure would be relatively simple to analyze if two conditions were satisfied: (1) the specimen under test were free of the boundary effects caused by the clamping restraint at the edges, and (2) if the specimen were truly square mechanically, i.e., possessed identical properties in the warp and filling directions. For the approximate analysis to follow, both of these conditions will be assumed to be satisfied.

One form of the classical expression for incompressible fluid flow through an orifice is:

$$Q' = \left[\frac{A\, C_c\, C_v}{\sqrt{1 - C_c^2 \left(\frac{A}{A_1}\right)^2}} \right] \sqrt{\frac{2g}{\rho} (p_1 - p_2)} \qquad (1)$$

where:

Q' = volume rate of flow
A = orifice area
C_c = coefficient of contraction
C_v = coefficient of velocity
A_1 = approach area
ρ = fluid density, assumed constant
P_1 = upstream pressure
P_2 = downstream pressure
g = acceleration of gravity. (See Table 52 for symbols.)

Two questions immediately arise in adapting such a formula for use with flow through fabrics: (1) Can the flow through a fabric be considered as being entirely through orifices (pores) or must the flow through the yarns be considered? (2) Is the use of a formula for incompressible flow justified?

To the first question it can be answered that photomicrographs of parachute fabric cross-sections show a denseness of yarn structure sufficient to preclude any appreciable intra-yarn flow compared to that of the relatively large pore area. Also, experimental data of air flow through parachute fabrics indicate a relationship between total pore area and air flow at a given pressure differential which is sufficiently close to a direct proportionality to make the assumption of intra-yarn flow improbable. These

Approved for Public Release

Contrails

two points are demonstrated by photomicrographs and tabulations. It can then be concluded that at least for the type of fabric being studied here, the flow may be considered as being entirely through the open pores.

The answer to the question of compressibility is much more direct. Here it is only necessary to compare compressible and incompressible formulations and show that a negligible difference exists between them for the conditions studied. For an adiabatic compressible flow it can be shown that Equation (1) would then become:

$$Q' = \frac{A\, C_c\, C_v}{\sqrt{1 - C_c^2\left(\frac{A}{A_1}\right)^2}} \times \sqrt{\frac{2g}{\rho_1}} \times \sqrt{p_1\left(\frac{k}{k-1}\right)\left[\left(\frac{p_2}{p_1}\right)^{\frac{k-1}{k}} - 1\right]} \qquad (2)$$

where ρ_1 is the density corresponding to upstream conditions and k is the isentropic exponent for air.

It has been the convention to express flow in terms of cubic feet per minute per square foot of original fabric sample area. Under this convention and with the necessary numerical substitutions for the permeometer used (employing a six-inch circular specimen):

$$Q = \frac{Q'}{A_{fo}} = 1106\, C_D(FA)\, \frac{\Delta p^{1/2}}{\rho^{1/2}} \left(\frac{A_f}{A_{fo}}\right) \qquad (3)$$

where Q is flow (cfm/ft^3); Q', vol. flow rate (cfm); ρ, air density (lb/ft^3); Δp, pressure diff. across fabric (in. water); A_{fo} initial or zero flow sample area.

In general metering practice, the pressure differential can be easily and accurately measured, the orifice area is known, and discharge coefficients are well tabulated in terms of the geometries of standard metering orifice assemblies and the Reynolds number of the flow. In dealing with flow through fabric pores, a much more difficult problem exists because here an orifice does not lie in a single plane, nor are the various orifices uniform in shape or size. Since there has been no previous work relating to experimental correlations of flow parameters such as the Reynolds number and discharge coefficient for such geometries, it is impossible to make any practical use of a theoretical calculation until such a relation can be at least approximately established.

Now consider a circular specimen clamped by a ring and subjected to a pressure differential Δp. Under the given assumptions the fabric must deform spherically. This is illustrated, together with the geometric symbols to be used, in Figure 15. If the specimen is mounted flat but unstressed, then from purely geometric considerations it can be shown mathematically that:

$$\sigma = \frac{\Delta p\, r}{2} \times \left[3 \frac{1}{\sqrt{\frac{3\Delta p\, r}{K}} - \frac{\Delta p\, r}{2K}}\right] \qquad (4)$$

Approved for Public Release

Contrails

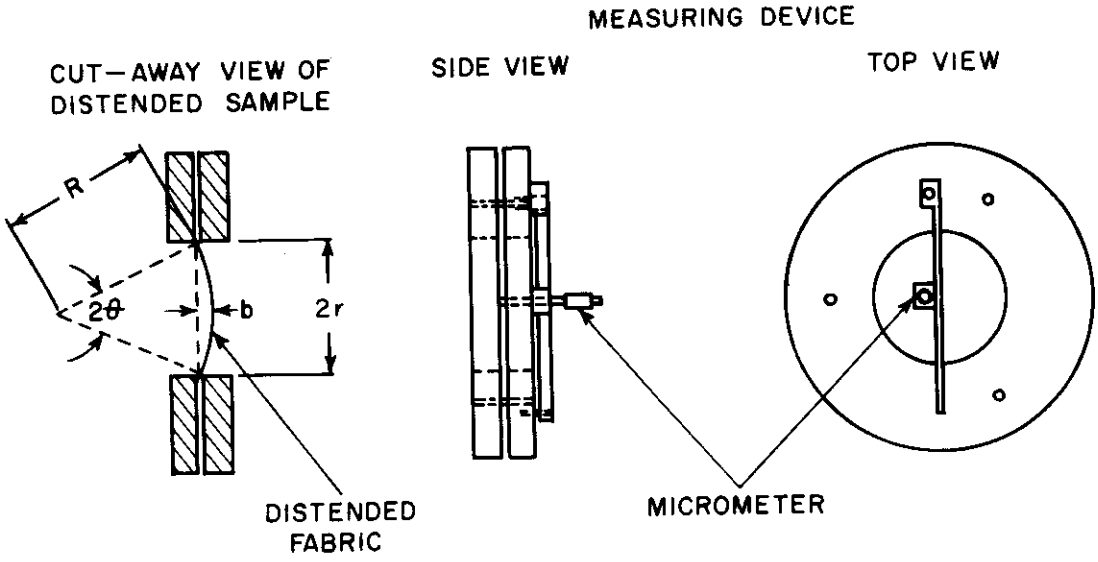

Figure 15 Diagrammatic Sketch of Distended Fabric Sample and Device for Distention Measurement

Approved for Public Release

Contrails

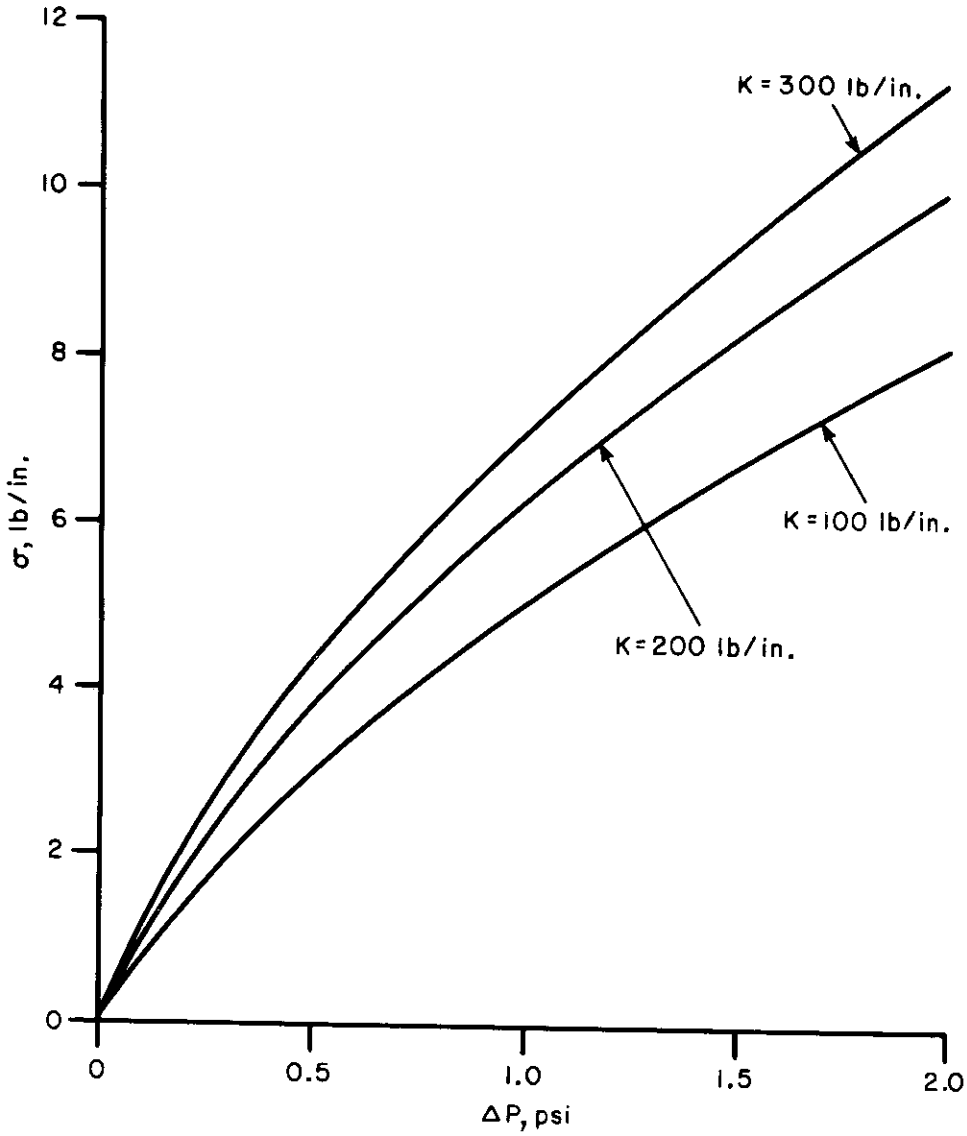

Figure 16 Fabric Stress vs. Δ p as a Function of the Biaxial Modulus

Approved for Public Release

Contrails

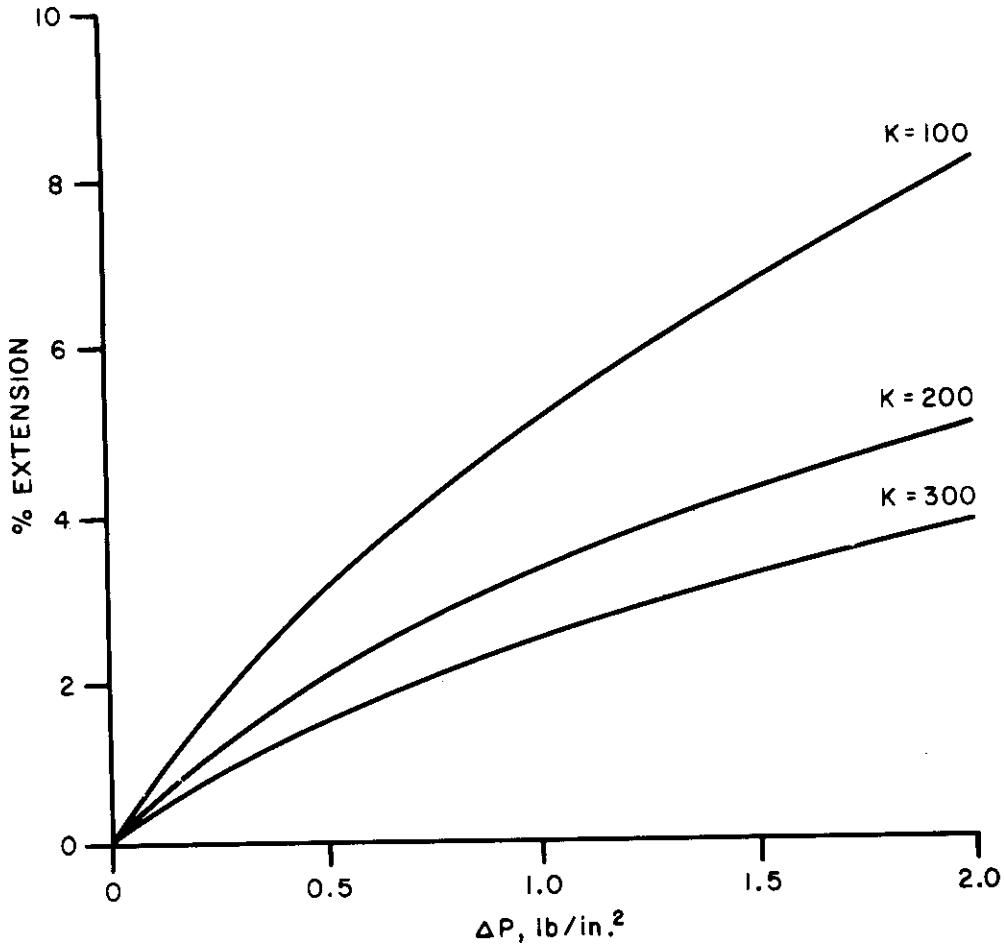

Figure 17 Fabric Strain vs. Δ p as a Function of Biaxial Modulus

Approved for Public Release

Contrails

where:

σ = fabric stress in force per unit width of fabric
Δp = pressure differential
r = radius of test specimen
K = biaxial modulus (equal biaxial loads and square fabrics)

Stress vs. pressure results of this equation are presented graphically in Figure 16 for a test specimen with a radius of three inches. Figure 17 expresses similar strain vs. pressure data.

While the results cannot be quantitatively used without a knowledge of the biaxial K's, it is immediately obvious from Equation (4) that since pressure differential and specimen radius always occur together as $\Delta p\, r$, this product must be the same for different tests of the same sample for cloth geometry to be the same. For example, if two specimens were tested, one twice the size of the other, the smaller specimen would require a pressure differential twice that of the larger one in order that the geometries be the same.

5.1.6 Theoretical Change in FA with a Change in Fractional Strain (e)

The importance of gross geometric changes in fabric structure is primarily in their relation to the finer changes which are prime influences on the air flow. An analysis will now be made showing the theoretical relation between (FA) and e under the following assumptions:

a. The yarn strain is the same as the fabric strain (very nearly true for low crimp fabrics) and

b. The yarn undergoes a constant volume extension with a constant shape.

As shown in WADD TR 60-584 (page 204)

$$(FA) = (1 - d_w t_w)(1 - d_f t_f) \tag{5}$$

where d_w, d_f, t_w and t_f are the warp and filling yarn diameters and threads per inch, respectively.

For a square fabric:

$$(FA) = (1 - dt)^2 \tag{6}$$

If the fabric extension is e,

$$t = t_o/(1 + e) \tag{7}$$

and from assumptions (a) and (b) above:

$$d = d_o\left(1 - \frac{e}{2}\right) \tag{8}$$

where the zero subscripts indicate initial values. The latter expression may be deduced by recognizing that the Poisson ratio for a constant volume deformation is 1/2. Combining Equations (6), (7) and (8) it can be shown

Approved for Public Release

Contrails

that

$$FA = FA_o + 3\,e\left(\sqrt{(FA)_o - (FA)_o}\right) \qquad (9)$$

where FA_o = initial fractional free area.

5.1.7 Investigation of the Discharge Coefficient, C_D

In Section 5.1.5 a formula was derived for the flow of air through a fabric. This equation was

$$Q = 1106\, C_D\, (FA)\left(\frac{\Delta p^{1/2}}{\rho^{1/2}}\right)\left(\frac{A_f}{A_{fo}}\right) \qquad (3)$$

An important unknown in this expression is C_D, the coefficient of discharge. A procedure for determining this factor experimentally and correlating it with fabric parameters will now be described.

Once again making the assumption of squareness,

$$\frac{A_f}{A_{fo}} = (1 + 2\,e) \qquad (10)$$

where A_f is fabric area under pressure, A_{fo} is its area at rest, and e is the linear extension of the fabric. Then:

$$C_D = \frac{Q\ \rho^{1/2}}{1106\ (FA)\ \Delta p^{1/2}\ (1 + 2\,e)} \qquad (11)$$

The experimental evaluation of C_D obviously requires a knowledge of all the factors on the right-hand side of Equation (11). From normal test procedure Q, ρ, and Δp are known. By means of the measurement of "b," the fabric distention in inches, the fractional strain e can be determined. The Free Area (FA) was determined by measuring the ultraviolet light transmission of the fabric. This method is based on the principle that ultraviolet light passes only through the yarn or fabric interstices, and not through the fibers.

With all quantities on the right-hand side of Equation (11) known, the value of C_D for the given conditions is established. Discharge coefficients for standard orifice flow (i.e., round orifices in round ducts) are correlated experimentally with a dimensionless quantity, Re, the Reynolds number of the flow. Re is defined by:

$$Re = \frac{V\,D}{\upsilon} \qquad (12)$$

where V is the average velocity through the orifice, D is the diameter of the orifice, and υ, the kinematic viscosity of the fluid. For fabric pores it would be desirable if a similar relationship could be found. In an effort to obtain such a relation the following assumptions will be made:

Approved for Public Release

Contrails

a. The free area can be determined by light penetrability techniques.

b. The dimensions of a fabric pore can be taken as the average dimensions of the pores of the sample.

c. Variations in length to breadth ratios of the pores have negligible effect as such on the flow. Only the smallest dimension appears in the analysis as the characteristic dimension of the Reynolds number.

Assumption (a) is good insofar as a good correlation can be shown between free area as measured by LP (Light Penetrability) techniques and microscopic determination by yarn size, and pick and end count, and in subsequent portions of this report the two will be used interchangeably. The dubious point is that both methods are actually planar and a pore does not lie in a single plane. Possible errors because of this are discussed in Section 5.1.11.

Assumption (b) is probably correct if there is not a very great difference in pore sizes within a sample. Of course, the whole point of the Reynolds number here is to be able to include pore dimension in the analysis, but over a small range the effect of variations can be considered linear so that no large error should be introduced by averaging.

The third assumption is justified by what meager experimental results there are in the literature on the effect of flow of length and breadth ratio of a slot where it is shown that the effect is not great. This seems reasonable because the effects of viscosity are primarily concerned with the most constricted part of the flow, corresponding to the smallest dimension.

Now define:

$$Re = \frac{V\,w}{\upsilon} \tag{13}$$

where w is the minimum pore dimension and V is the average air velocity through a pore. V can be found from the expression:

$$V = \frac{Q}{(FA)\quad(1 + 2\,e)} = \frac{Q}{(LP)\,(1 + 2\,e)} \tag{14}$$

and w is found by direct measurement. Figure 18 plots Re vs. C_D. It would be supposed that there would be a general trend for fabrics with higher (FA) to have higher C_D's at the same Reynolds number. It would also be anticipated from experience with orifice flow that C_D would be an increasing function of Re. The latter is clearly true from Figure 18 but reference to Table 49 which gives (FA)'s, shows that the relative magnitude of the C_D's is not properly ordered with respect to (FA).

5.1.8 Experimental Measurements of Flow and LP Under Pressure

The most basic measurement in this investigation is the actual

Approved for Public Release

Contrails

measurement of flow. For the material discussed in this report these measurements were made on a permeometer designed to test a six-inch circular specimen up to a maximum pressure differential of 50 in. of water. The machine was modified during the course of the work to enable measurements of LP (light penetrability, a measure of Free Area FA) to be made simultaneously with those of Δp and flow in order that the flow might be investigated on the basis of individual pores.

Figures 19 and 20 show typical permeability curves of twenty-five experimental fabrics, both Type I and Type II, expressed as cubic feet per minute per square foot of initial area plotted vs. Δp, the pressure differential, in inches of water. Qualitatively these curves exhibit nothing unusual or informative. Those curves representing fabrics of higher LP (see Figures 21 and 22 for LP's) show higher permeabilities, and the permeability increases roughly as the square root of the pressure differential.

Figures 21 and 22 show graphically the relation between LP and Δp for eleven different Type I and Type II fabrics. Here again the qualitative picture is not particularly informative. LP rises with a rise in pressure differential. It is the quantitative application of these data to the determination of basic parameters which is important. First, these curves are used to find the proper values of FA to use in Equation (11) in order to determine C_D. Second, data of Δp vs. e as calculated from the fabric distention under test, and those of Figures 21 and 22 described above are combined to give a plot of e vs. LP under test conditions for five different Type I and Type II Fabrics. The results are plotted in Figure 23.

5.1.9 Determination of Pore Dimensions

To apply Equation (13) to determine the Reynold's number of flow through a pore as defined by the average minimum pore dimension, it is necessary to know the minimum pore dimension. This is derived as:

$$w_{av} = \sqrt{\frac{(FA)}{\gamma t_w t_f (144)}} \qquad (15)$$

where:

w_{av} = average minimum pore dimension in feet
FA = Free area
γ = ratio of minimum to maximum pore dimension
t_w, t_f are numbers of warp and filling threads per inch

or using as before LP for (FA)

$$w_{av} = \frac{1}{12} \sqrt{\frac{LP}{\gamma t_w t_f}} \qquad (16)$$

Approved for Public Release

Contrails

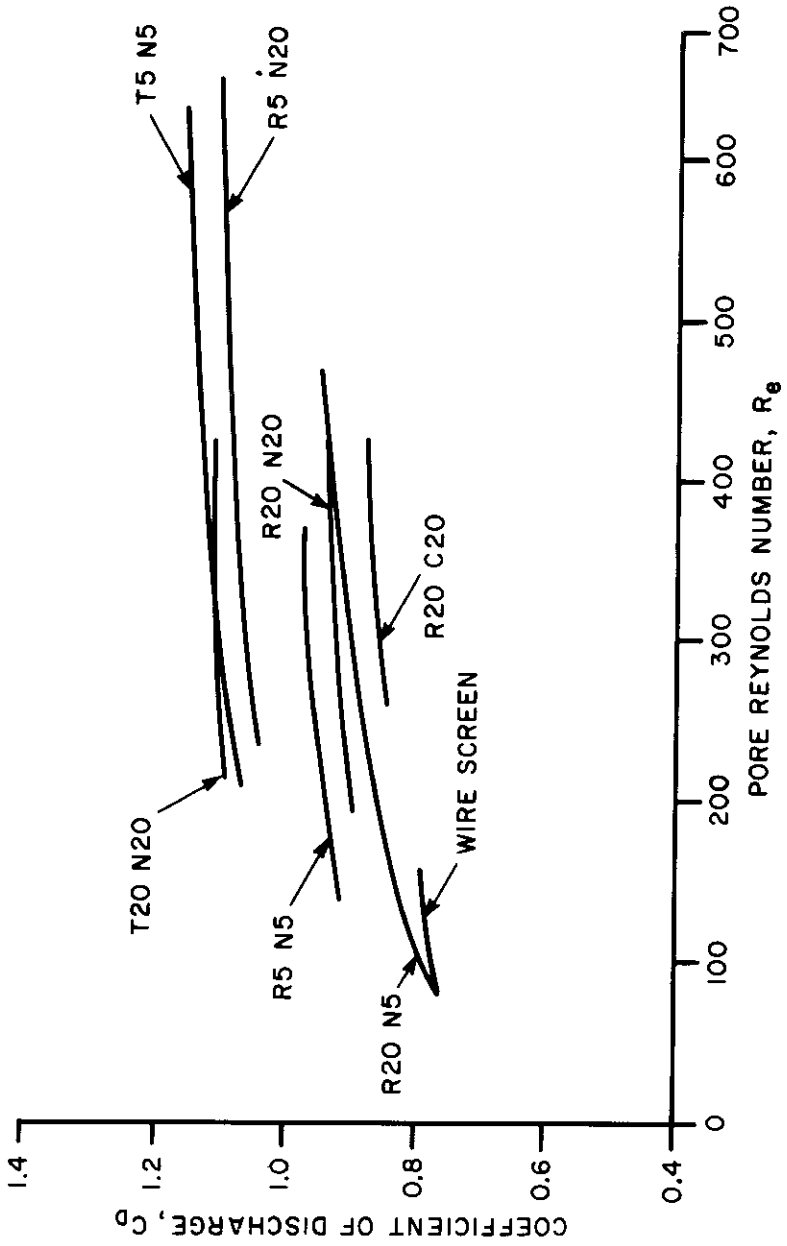

Figure 18 The Pore Reynolds Numbers and Corresponding Discharge Coefficients for Seven Experimental Fabrics and a Wire Screen

Approved for Public Release

Table 49. Rip-Stop Fabric Parameters

Fabric	t_w x t_f	Yarn Diameter (in.) Warp	Yarn Diameter (in.) Filling	Yarn Twist(t.p.i.) Warp x Filling	Yarn Denier Warp x Filling	Fractional FA	Fractional LP
R1/2N1/2	120.0 x 124.4	0.004696	0.006728	1.5 x 1.7	31.0 x 31.6	0.072	0.068
R1/2N20	120.2 x 123.2	-------	--------	1.4 x 23.4	31.0 x 31.9	-----	0.224
R1/2N30	120.4 x 121.8	-------	--------	1.3 x 34.4	31.3 x 31.9	-----	0.263
R5N5	121.2 x 124.2	0.004234	0.005412	6.3 x 7.1	30.8 x 32.1	0.160	0.144
R5N20	120.0 x 121.8	--------	--------	6.7 x 22.9	30.9 x 32.1	-----	0.248
R20N1/2	121.4 x 120.0	0.003336	0.006898	22.4 x 1.2	30.9 x 31.5	0.103	0.118
R20N5	120.6 x 119.6	--------	--------	22.5 x 6.6	31.2 x 32.0	-----	0.187
R20N20	120.4 x 116.8	0.003199	0.004243	22.4 x 22.9	30.6 x 30.7	0.310	0.304
R30N1/2	121.0 x 119.4	0.003029	0.005538	32.1 x 1.5	30.9 x 31.7	0.216	0.151
R30N30	120.0 x 115.8	0.003000	0.003618	32.0 x 34.2	30.6 x 32.1	0.371	0.370
R1/2C1/2	121.4 x 126.8	0.005779	0.006978	1.5 x 1.4	30.7 x 33.3	0.034	0.030
R1/2C20	120.0 x 122.8	--------	--------	1.4 x 23.5	30.8 x 32.1	-----	0.136
R1/2C30	120.6 x 124.2	--------	--------	1.5 x 33.8	31.3 x 32.9	-----	0.158
R5C5	121.0 x 125.2	0.004783	0.006569	6.1 x 6.7	31.1 x 32.7	0.075	0.075
R5C20	121.0 x 122.0	--------	--------	7.0 x 23.6	30.6 x 32.8	-----	0.156
R20C1/2	121.6 x 122.4	0.003814	0.006964	23.2 x 1.0	30.8 x 32.0	0.080	0.067
R20C5	121.0 x 121.4	--------	--------	22.5 x 6.6	31.5 x 32.7	-----	0.102
R20C20	121.4 x 119.2	0.004138	0.004945	22.8 x 23.4	31.4 x 31.9	0.205	0.186
R30C1/2	121.6 x 121.4	0.003797	0.006740	33.0 x 1.5	30.6 x 32.1	0.099	0.076
R30C30	120.8 x 117.4	0.003726	0.004252	32.7 x 33.9	31.9 x 32.6	0.276	0.254

Approved for Public Release

Confidential

Contrails

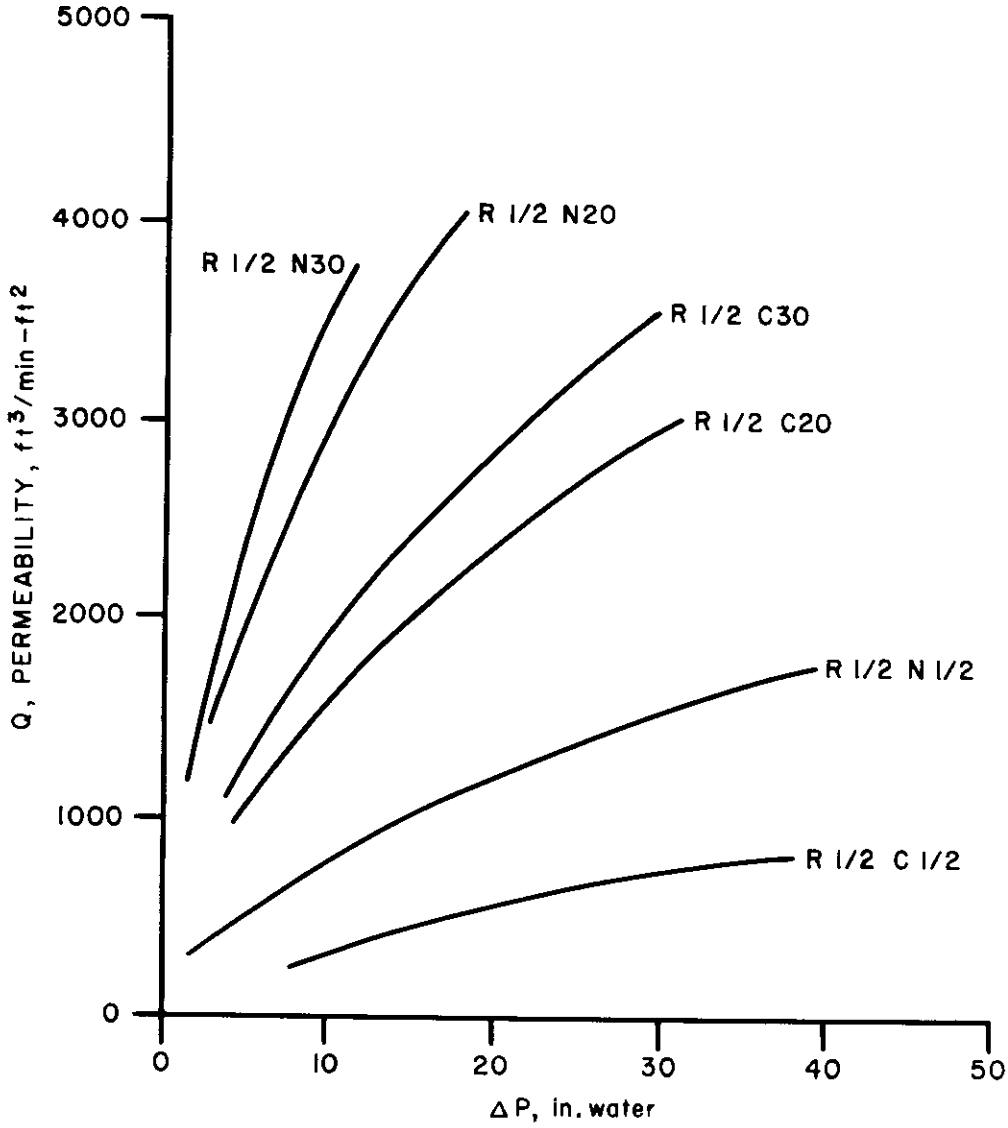

Figure 19 Air Permeability vs. Pressure Differential for Experimental Type I Fabrics With 1/2 Turns per Inch in the Warp

Approved for Public Release

Contrails

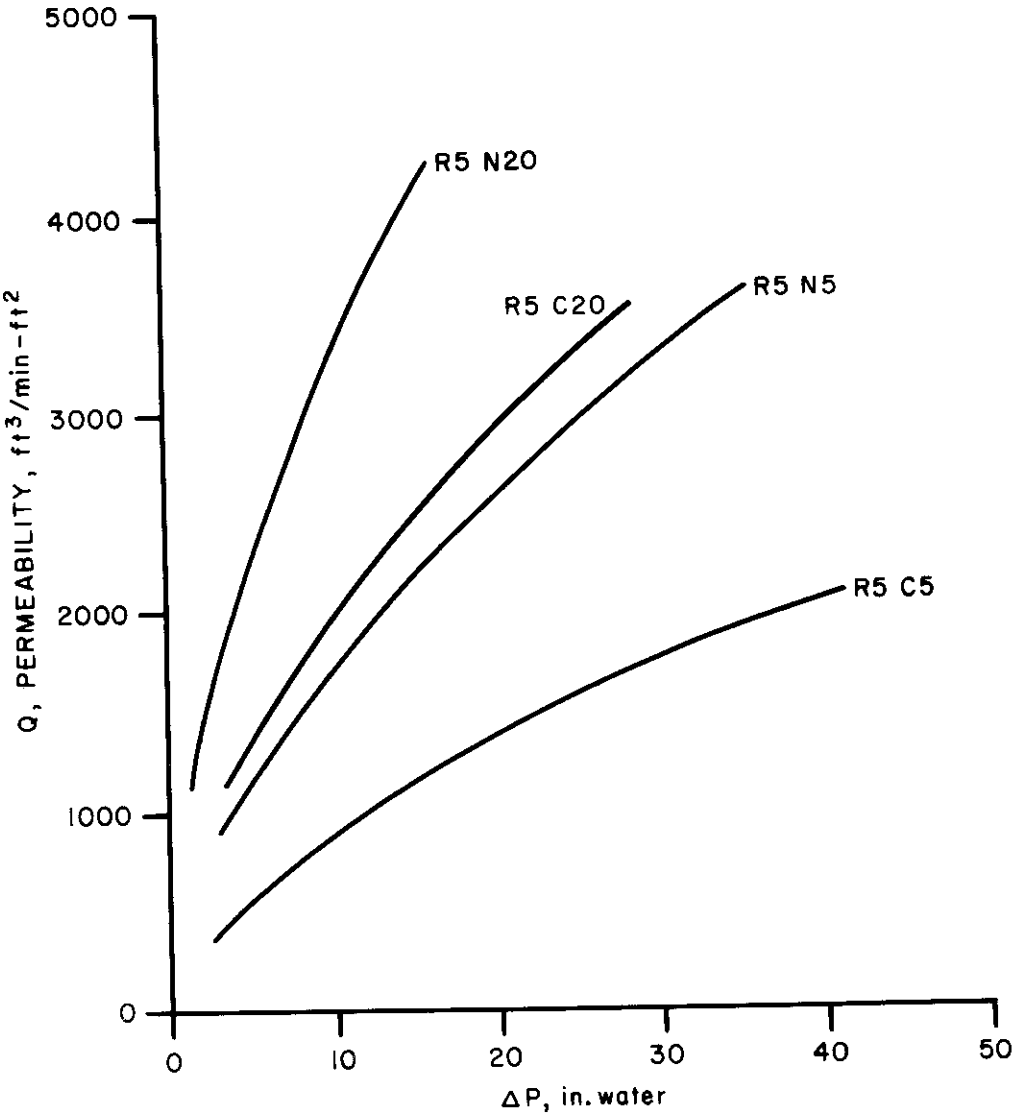

Figure 20 Air Permeability vs. Pressure Differential for Experimental Type I Fabrics With 5 Turns per Inch in the Warp

Approved for Public Release

Contrails

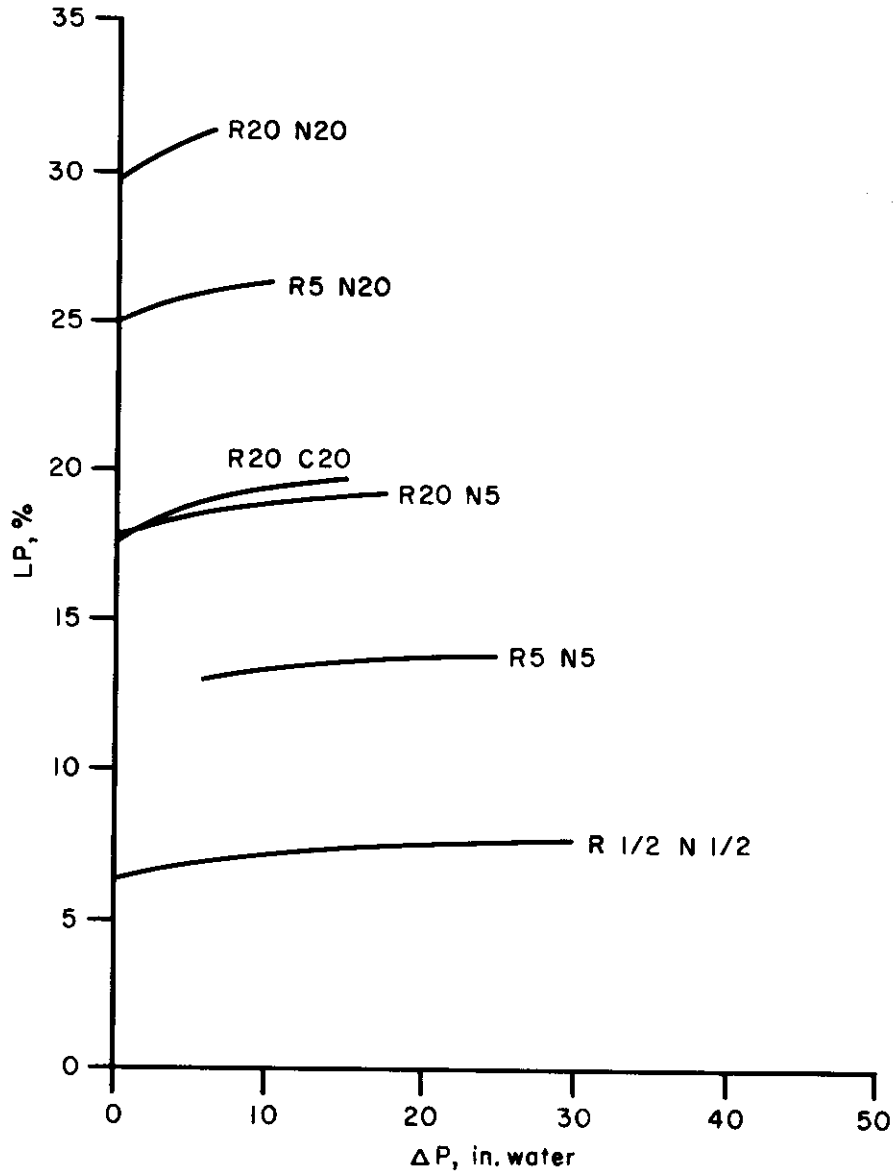

Figure 21 Light Penetrability vs. Pressure Differential Under Permeability Test for Type I Experimental Fabrics

Approved for Public Release

Contrails

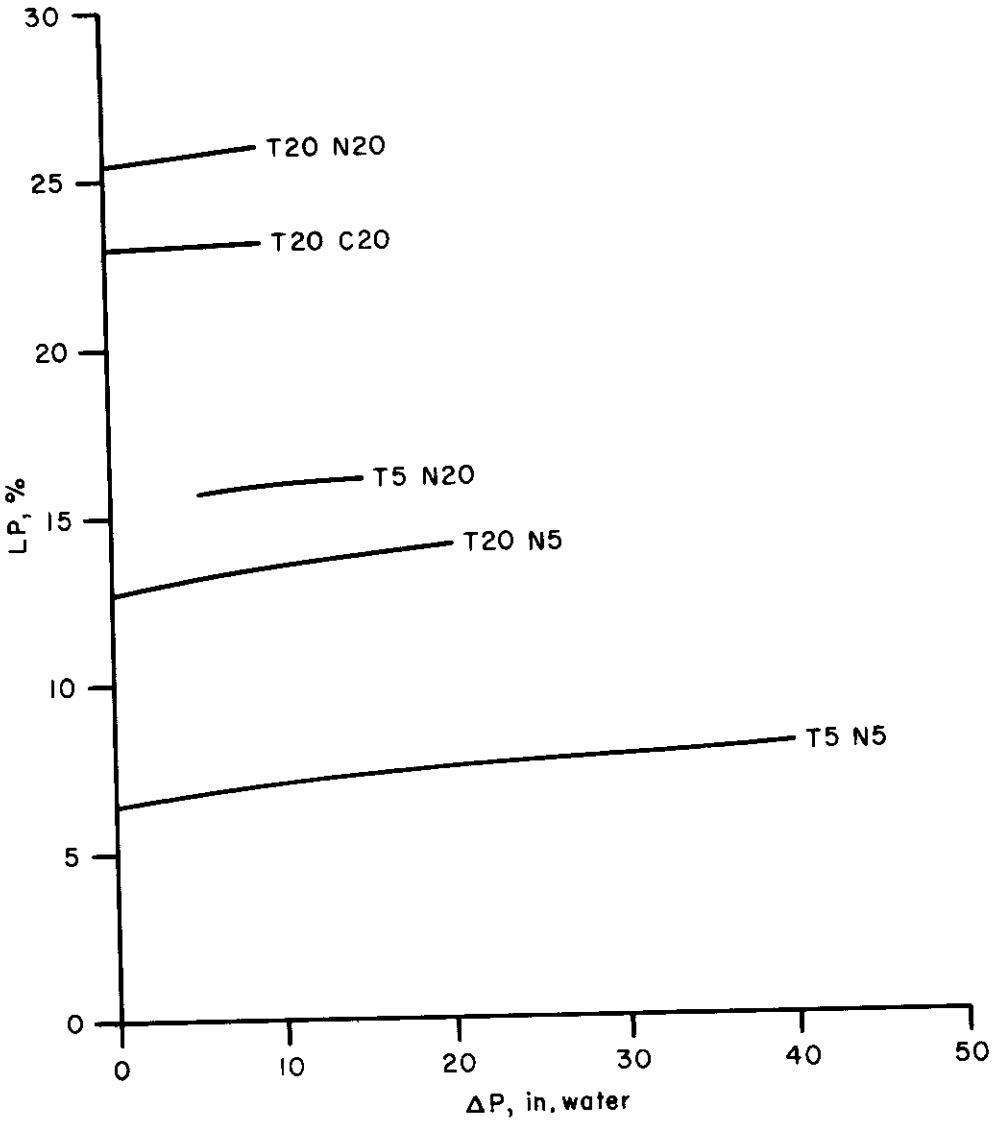

Figure 22 Light Penetrability vs. Pressure Differential Under Permeability Test for Type II Experimental Fabrics

Approved for Public Release

Contrails

γ, the ratio of average pore length to average pore width, is found by direct measurements from enlarged photographs, as exemplified by Figure 24.

5.1.10 Biaxial Tensile Tests

To correlate mechanical properties of fabrics with performance under flow it is necessary to evaluate these mechanical properties separately so that strains and the effect of strains in a fabric may be known functions of stresses alone and not conditioned by unknown variables of a particular test procedure. Since a hydrostatic pressure induces biaxial stresses, the biaxial characteristics must be investigated. Moreover, a hydrostatic pressure over a uniform (square) fabric would give rise to a spherical deformation and uniform stresses and strains, i.e., the warp and filling stresses and strains would be identical.

The biaxial tester imposes stresses simultaneously in the warp and filling direction such that the ratio of these stresses remains constant. For the case described above, a uniform stress distribution, this ratio is unity. Accordingly, the biaxial tests performed under this contract have all been done at a warp to filling stress ratio of one.

A brief description of the test procedure will be found in WADD TR 60-584 (page 370).

Four types of biaxial tests were performed. (a) Load to break measuring extension simultaneously; (b) load to break measuring LP simultaneously; (c) repeated loading measuring extension and (d) repeated loading measuring LP.

The load-extension to break curves for fabrics R1/2N1/2, R5N5, R20N5, R20N20, T5N5, and T20N20 are typified by Figure 25. By themselves the only important point they exhibit is the lack of correspondence of warp and filling characteristics, that is, non-squareness.

The load vs. LP to break curves for the same six fabrics are given in Figures 26 and 27. These curves by themselves can be used to predict LP under given conditions of uniform biaxial stress. Figure 28 plots Light Penetrability (LP) vs. average strain.

The repeated loading, load-extension curves for a maximum stress of 20 lb/in. are typified by Figure 29. The companion curves giving LP as a function of stress for 20 lb/in. repeated loading are typified by Figure 30.

Extension measurements presented some difficulty in the repeated loading work, particularly at very low loads. This is because the measurement is made by sensing the position of small pins inserted into the fabric and initially at a separation of 1/2 in., thus yielding a motion of 0.005 in. for each one-percent extension. It is very easy for the yarns at the insertion point to reorient themselves slightly, perhaps to the extent of a few thousandths of an inch, when the fabric is slacked off before reloading. Thus the uncertainty of strain measurement could be as high as one percent.

Approved for Public Release

Contrails

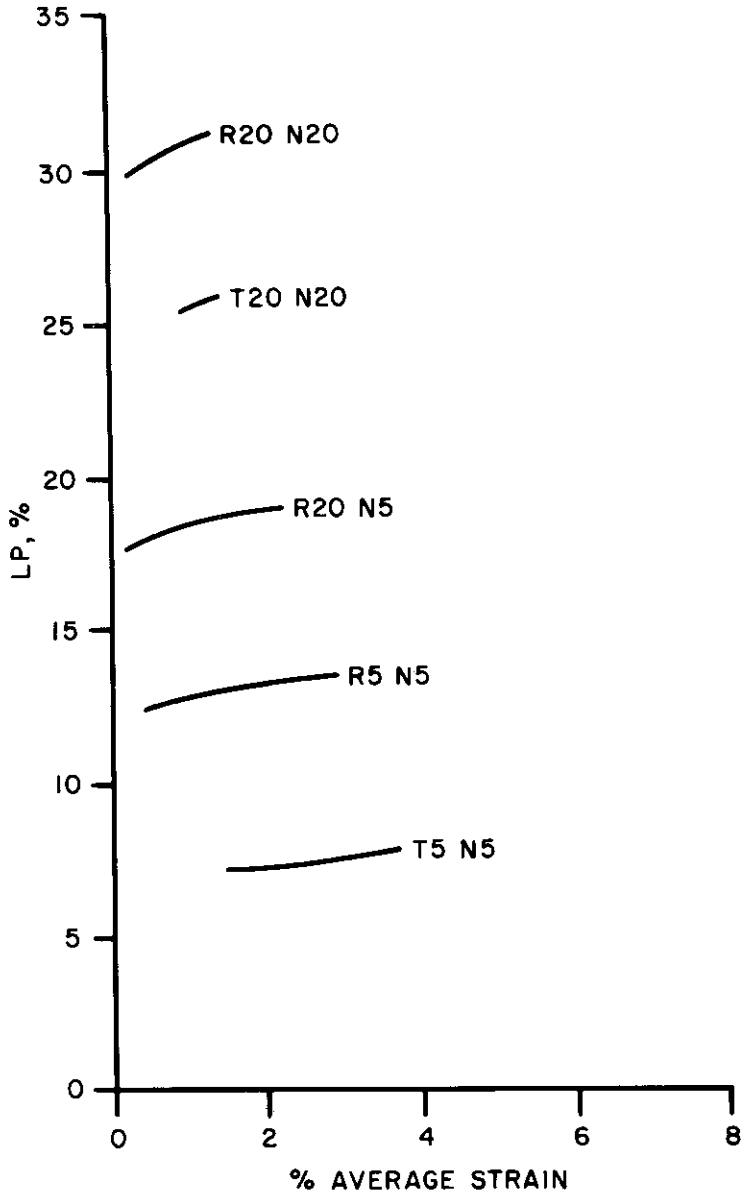

Figure 23 Light Penetrability vs. Fabric Strain Measured Under Permeability Test

Approved for Public Release

Contrails

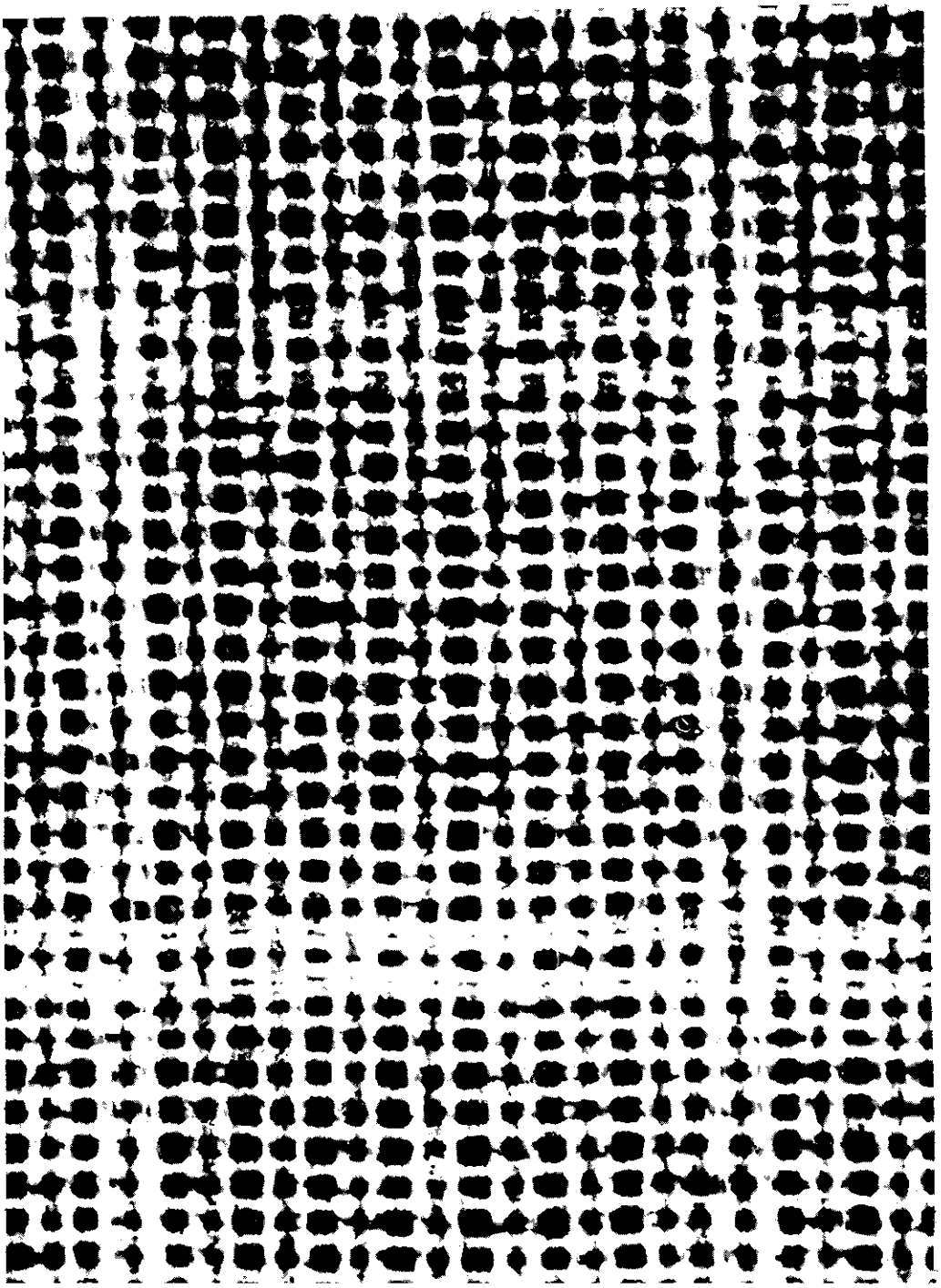

Figure 24 Planar Photomicrograph of R5N20

Approved for Public Release

Contrails

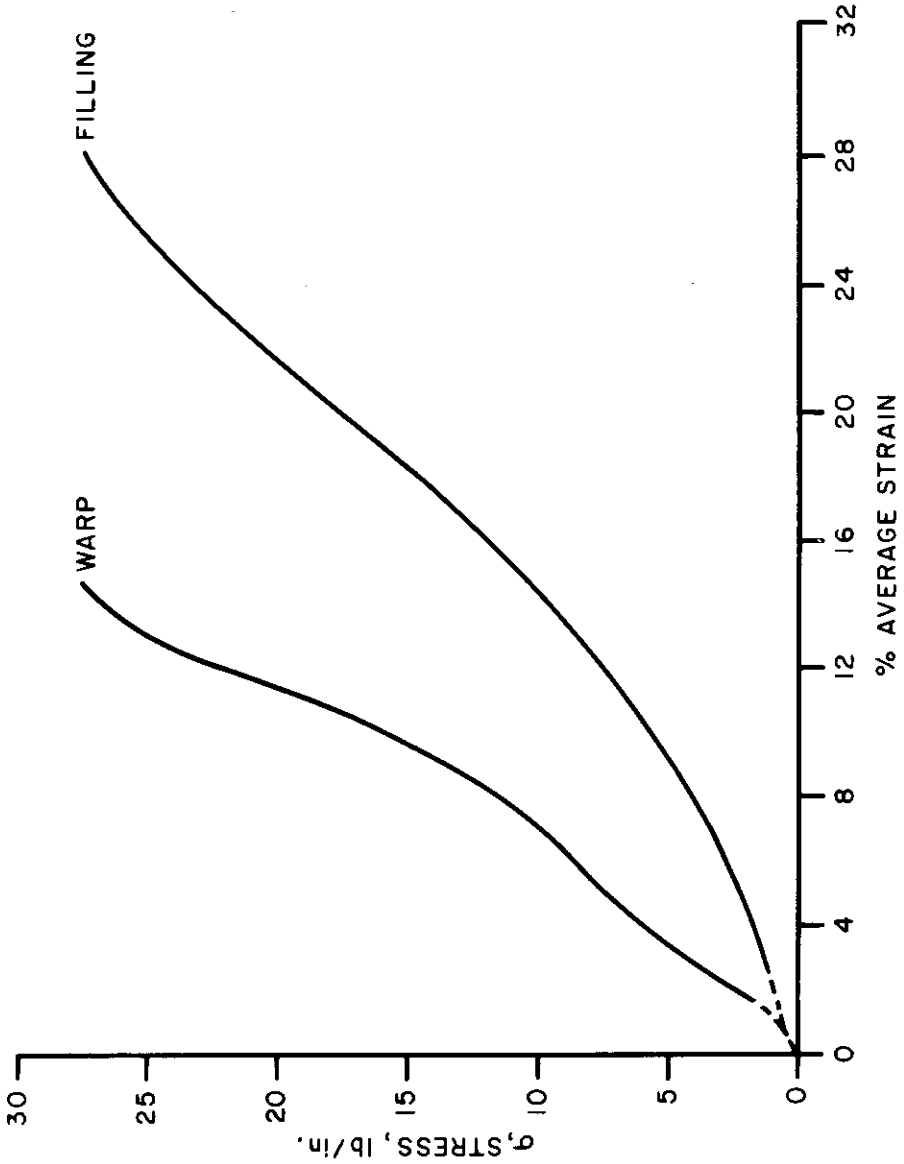

Figure 25 Average Biaxial Load Elongation Diagram for R5N5

Approved for Public Release

Contrails

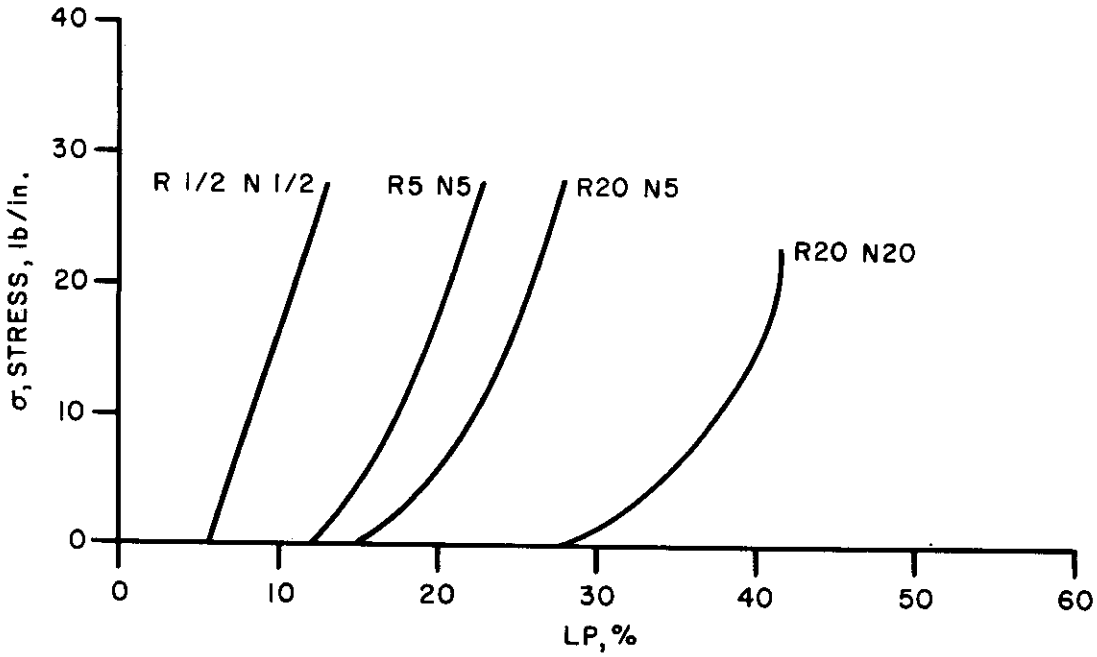

Figure 26 LP vs. Biaxial Stress Determined From Biaxial Tests for Type I Experimental Fabrics

Approved for Public Release

Contrails

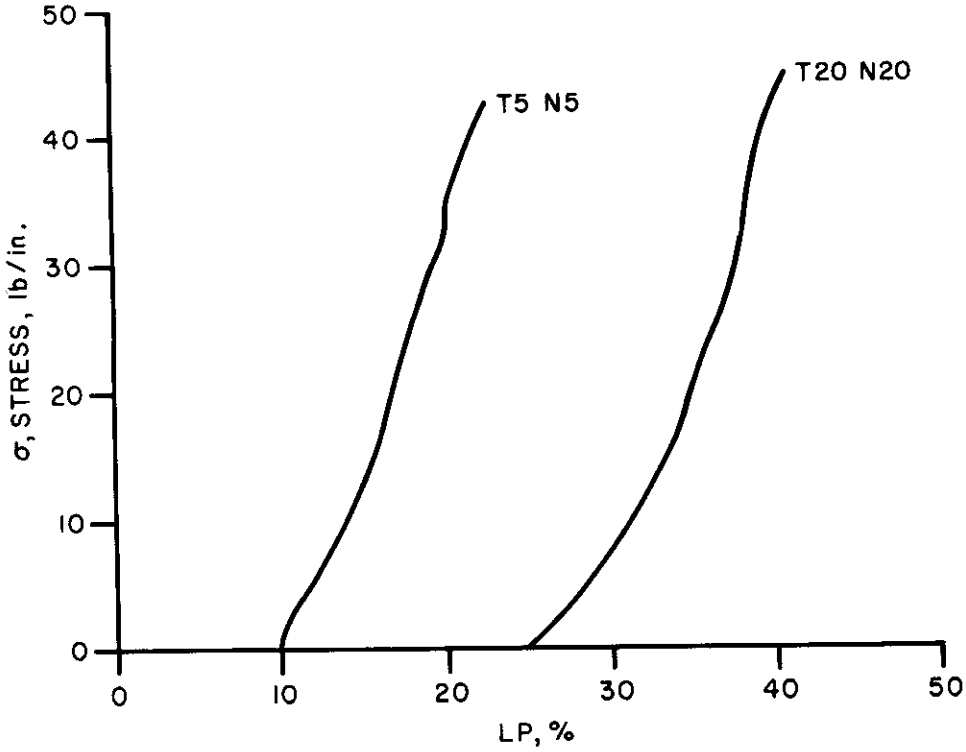

Figure 27 LP vs. Biaxial Stress Determined From Biaxial Tests for T5N5 and T20N20

Approved for Public Release

Contrails

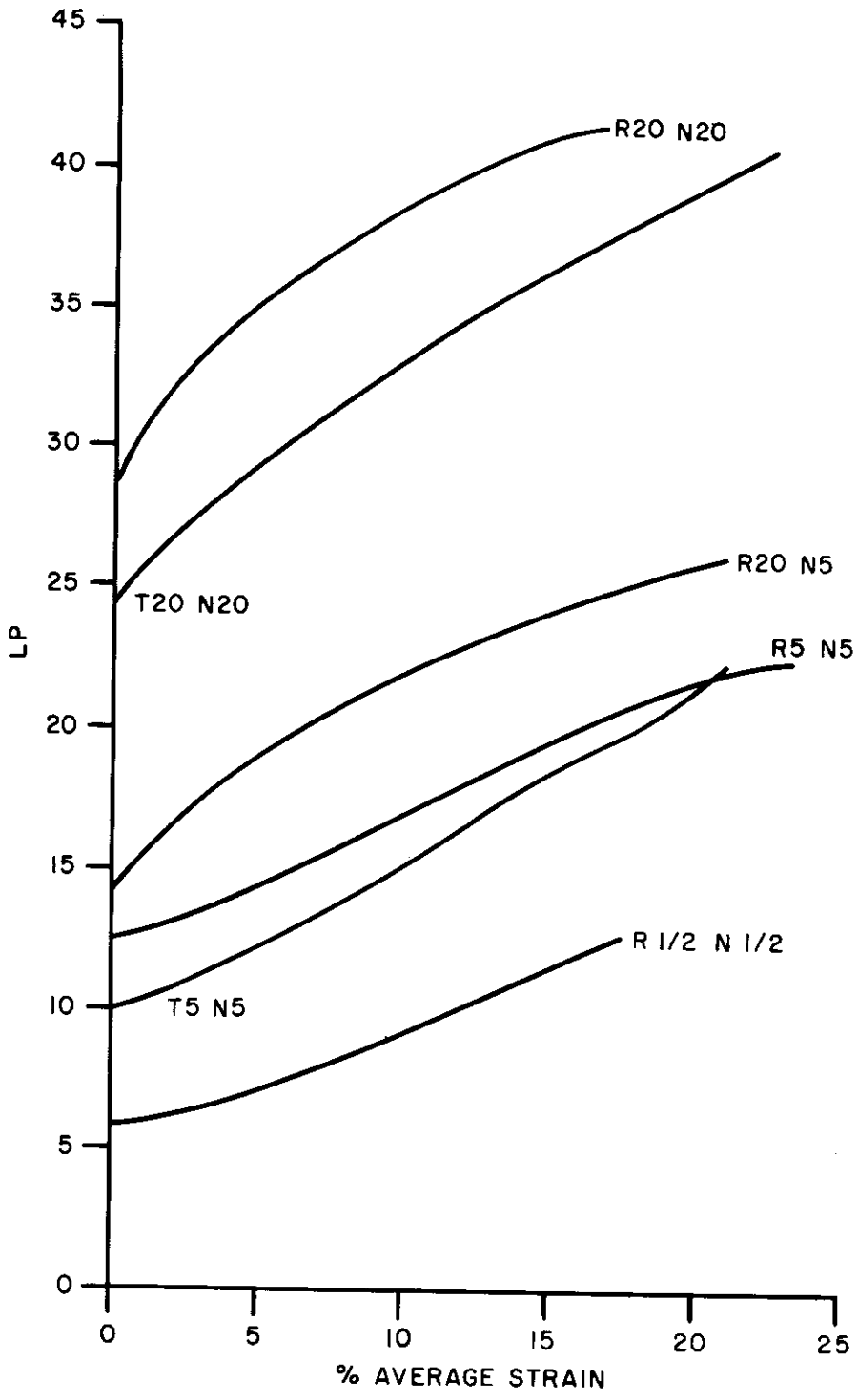

Figure 28 Light Penetrability vs. Average Strain Determined From Biaxial Tests

Approved for Public Release

Contrails

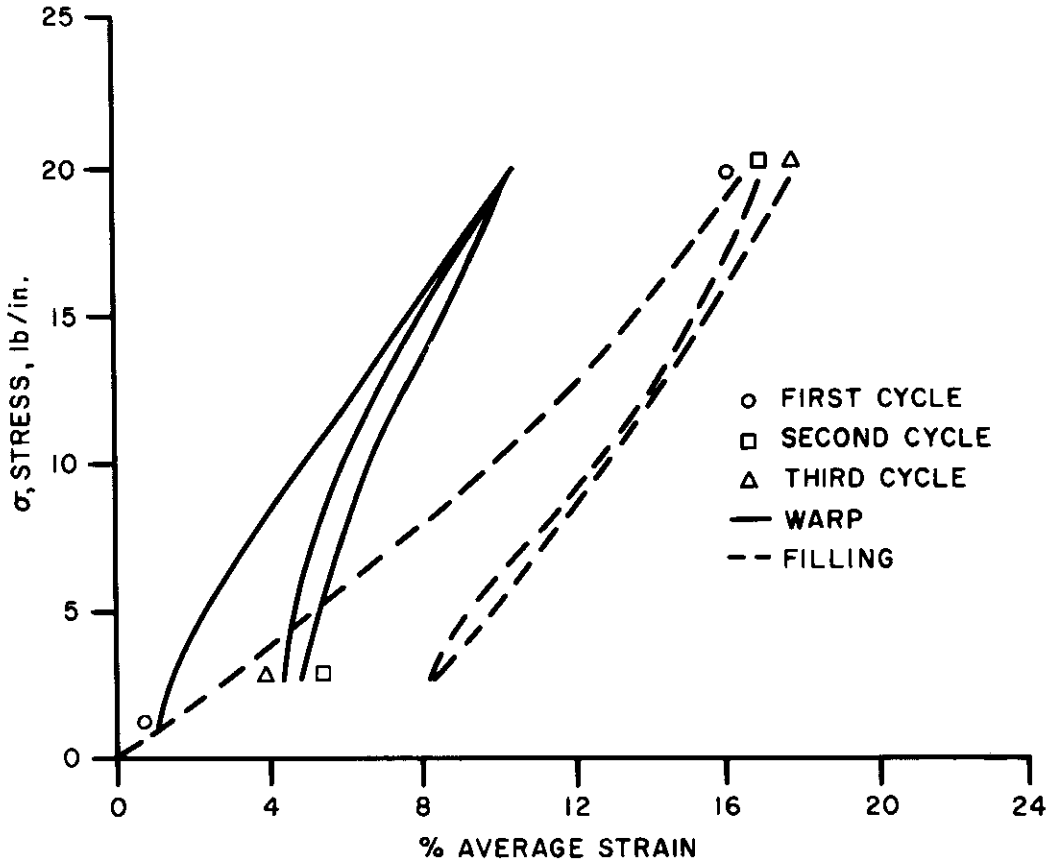

Figure 29 Load Elongation Diagram for Repeated Biaxial Loading to 20 Pounds per Inch of R1/2N1/2

Approved for Public Release

Contrails

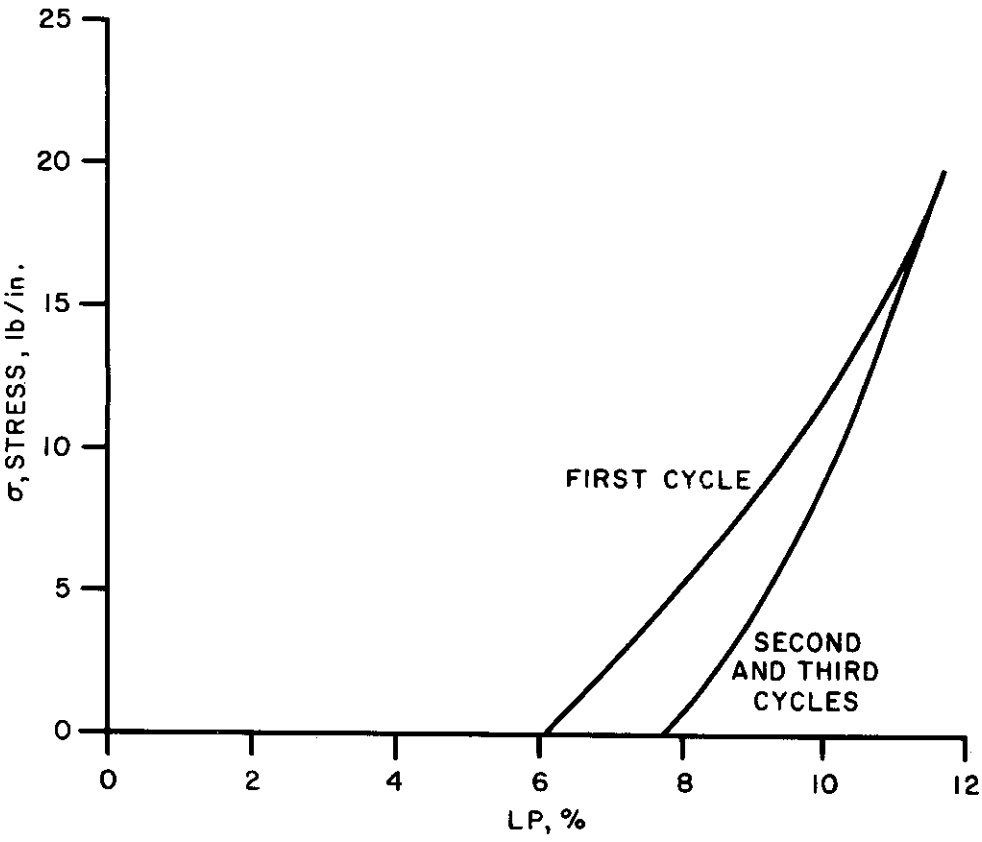

Figure 30 Light Penetrability as a Function of Biaxial Stress for Repeated Loading to 20 Pounds per Inch for R1/2N1/2

Approved for Public Release

Contrails

At the 20 lb/in. level both LP and strain curves exhibit essentially the same thing. A small set (non-recovery) occurs on the first loading but does not increase thereafter for the conditions of the test. At the 10 lb/in. level R1/2N1/2, chosen because it should be among the most susceptible to a set of the fabrics studied, showed essentially the same set that it did at 20 lb/in. At the 5 lb/in. level LP tests indicate essentially zero set for R1/2N1/2. The measurement uncertainties described above made it impossible to obtain a consistent set of data for extension measurements at this low load level, but there was no recognizable trend toward a set. This is consistent with the permeability tests performed here wherein no flow hysteresis was exhibited at pressure differentials up to 50 in. of water, corresponding to a biaxial tension of the order of a few pounds per inch. In future work, at higher pressure differentials this set must be reckoned with in making analyses and predictions, but it is not possible to tell from tests of the duration performed here to what extent this set is permanent.

5.1.11 Correlation of Theoretical and Experimental Data

In the preceding several sections, the mechanism of air flow through parachute materials has been analyzed in an approximate way, and a considerable amount of experimental data compiled for the purpose of determining the validity of the theoretical approach and reducing it to a practical usefulness. The correlation, integration and examination of the several aspects of this work will now be considered.

Following is a list of the various individual relationships derived theoretically or determined experimentally:

a. Q vs Δp, the fabric permeability as a function of the pressure differential, for specific test conditions.

b. LP vs. Δp, the fabric light penetrability as a function of the pressure differential, for the same conditions as (a).

c. e vs. Δp, the average fabric strain calculated from distention under pressure, vs. pressure differential.

d. σ vs. LP, the fabric uniform biaxial stress from biaxial tests vs. LP measured simultaneously.

e. σ vs. e, the fabric uniform biaxial stress vs. the strains in the warp and filling directions, both for loading to break and repeated stressing.

f. (FA) vs. e, the theoretical free area of a fabric as a function of its strain and initial geometry.

g. σ vs. Δp, the theoretical relation between σ and Δp for the test conditions of this report.

From these seven individual relationships a number of others can be derived. In some cases the same quantity can be found by more than one method, each involving different assumptions, thus allowing a check of the validity of the assumptions and analyses. Several such relations will be now derived.

Approved for Public Release

Contrails

From (b) to (c) a plot can be made of e vs. LP, e calculated from fabric distention under test and LP measured at a corresponding Δp. This information was given in Figure 23 of Section 5.1.8. From biaxial tests, (d) and (e), the same relation can be plotted but determined purely from externally imposed stresses. Here e is defined as the average value of the warp and filling e's. The results of this computation were given in Figure 28. Comparison between Figures 23 and 28 shows that while the results of the biaxial tests cover a much wider range of strains than those of the permeability tests, the agreement over the mutually covered range is very good. Apparent exceptions are fabrics R20N5 and T5N5 but such is not actually the case. The discrepancy can be shown to be based completely on the rest (FA) which varies by a considerable amount in different parts of the fabric bolt. That is, for the permeability tests, the rest LP's of the R20N5 and T5N5 were approximately 17% and 7%, respectively, while the specimens of the same fabric samples used for biaxial tests showed rest LP's of approximately 15% and 10%. Lacking an agreement on initial open areas it could hardly be expected that these curves could superimpose. They do, however, parallel each other.

On the basis of these results it can be concluded that the average extension of the specimen under test can, at least for the magnitude of distortions involved here, be approximated from measurement of distention and the assumptions of a spherical deformation.

Having established the validity of a test strain measurement through a correlation of LP with known strains, the next step is to establish the numerical relationship between LP (or (FA)) and e as in relation (f). On a theoretical basis it was shown in Section 5.1.6 that:

$$(FA) = (FA)_o + 3\,e\,(\sqrt{FA_o - FA_o}) \qquad (9)$$

This derivation included the assumptions that the yarn shape remained constant and that the Poisson ratio was 1/2. It can be easily be shown that for no contraction, or a Poisson ratio of zero, the coefficient 3 in the above equation would be 2. Since the ratio for polymeric materials should be close to 1/2, corresponding to a constant volume deformation, an experimental fitting of Equation (9) may be made using experimental values of e and (FA) and substituting for the coefficient 3 an unknown constant M. The results of this fitting should yield the following information about yarn shape under test: If M is 3, no shape change; if M is less than 3, flattening occurs; and, if M is greater than 3, rounding or consolidation occurs. The equation used for calculating M is:

$$M = (FA) - (FA)_o \Big/ e\left(\sqrt{FA_o - FA_o}\right) \qquad (17)$$

Table 50 presents the results of these and associated calculations for six fabrics in the following manner: The first two columns give the average e and LP determined from biaxial tests; the third column, LP calculated from Equation (9) where M is taken as 3; the fourth column, M calculated from Equation (17); and the fifth column, (FA) calculated using the value M = 2.56, the average of all M's in the fourth column.

Several points are worthy of note in this table. First, most values of M are less than 3; thus, the yarns tend to flatten at the port boundaries.

Approved for Public Release

Contrails

Table 50. Evaluation of Equation (17) as a Means of Determining LP Changes

Fabric	From Biaxial Measurement e*	From Biaxial Measurement LP*	LP From Equation (17)*	M Required For Experimental Fit	LP Calculated From Equation (17) and M = 2.56*
R1/2N1/2	0.00	0.056	0.056		
	0.05	0.080	0.084	2.56	0.080
	0.10	0.107	0.111	2.78	0.103
	0.15	0.173	0.137	2.43	0.126
T5N5	0.00	0.101	0.101		
	0.05	0.130	0.132	2.78	0.128
	0.10	0.160	0.165	2.79	0.155
	0.15	0.188	0.197	2.73	0.183
	0.20	0.218	0.229	2.74	0.210
R5N5	0.00	0.123	0.123		
	0.05	0.140	0.158	1.40	0.153
	0.10	0.173	0.191	2.15	0.182
	0.15	0.193	0.225	2.01	0.211
	0.20	0.218	0.259	2.06	0.240
T20N20	0.00	0.249	0.249		
	0.05	0.298	0.296	4.00	0.280
	0.10	0.335	0.323	3.48	0.312
	0.15	0.365	0.361	3.39	0.344
	0.20	0.393	0.398	2.90	0.376
R20N20	0.00	0.289	0.289		
	0.05	0.350	0.324	3.65	0.332
	0.10	0.385	0.362	3.24	0.364
	0.15	0.410	0.400	2.84	0.396

*Values given are on a fractional basis.

Approved for Public Release

Contrails

Second, while most values are less than 3, M in some cases approaches and even exceeds 3 at low extensions of fabrics with high twist yarns, indicating an initial tendency toward consolidation of yarn structure. Third, the relative magnitude of M should be an index of the integrity of the yarn structures, values near 3 corresponding to "solid" yarns. This is fairly well borne out by the table, the higher twist structures yielding values nearer to 3 than the lower. T5N5 shows a higher M than might be anticipated, but it is a moderately "cohesive" sort of fabric in spite of its low twist. (The twills are in general less "sloppy" than their rip-stop counterparts.) Lastly, the column showing the value of LP predicted from an average value of M shows that even for this rather unjustifiable procedure of using an average value which should in fact vary from fabric to fabric, a satisfactory numerical agreement exists between theory and experiment.

Since the value of M is closely related to fabric structure, it can be approximated much more closely for a given synthesis by taking the structure into consideration. Thus in design work the number 2.56 would not be used, but rather a value known to be typical for the sort of fabric to be made. The agreement between calculated and actual LP changes as a function of e should then be very good.

From (a) above, the theoretical relation between σ and Δp as derived in Section 5.1.5 (e) above, the results of the biaxial stress-strain tests and (c) above, the relation already fairly well justified between e and Δp by distention measurements, the assumptions involved in the theoretical analysis of the specimen deforming under given test conditions can be examined.

In 5.1.5 it was shown that for a square fabric and for the given assumptions the uniform biaxial stress could be expressed as:

$$\sigma = \frac{\Delta p\, r}{2} \qquad \frac{3}{\sqrt{\frac{3\,\Delta p\, r}{K}} - \frac{\Delta p\, r}{2K}} \qquad (4)$$

Since the fabrics are not square, in using this equation the additional assumption is made that an average K may be used. It is defined as the average value of the warp and filling K's determined individually. All other quantities in Equation (4) are as previously defined. Computations have been made for the maximum test, Δp obtained for five different fabrics and the corresponding e's found from:

$$e = \frac{\sigma}{K} \qquad (18)$$

where K is the average value of the biaxial moduli. Table 51 compares calculated vs. measured fractional strain (e).

It is noted that for the lower twist constructions the value of e found by this method is too high, whereas for the higher twist constructions

Approved for Public Release

Contrails

the agreement is remarkably good between the e's as determined by the two methods. Since the validity of the distention type measurement as a means of determining e has already been fairly well established, the conclusion must be reached that the lowest twist constructions are effectively stiffer under the given permeability test conditions where the orthogonal stresses cannot be identical, than they are under a uniform biaxial test. A number of reasons might be advanced for this, but probably the most logical is that the lower twist fabrics are much tighter and thus less able to move within themselves to help accomodate for the immovable boundary. That is, while the fabric is trying to extend over-all, it is not permitted to at the clamped region. A certain skewing of trellising must then take place which is considerably inhibited if the fabric is tightly woven. This additional restraint placed upon the yarn motions can only increase the stiffness of the fabrics. To check this hypothesis it would be necessary to use a much larger specimen than is at present used since a very large specimen should show less effect of boundary restraint. Another, though probably less sensitive test, would be to use a smaller sample and see if the effect increased.

Great care should be exercised in characterizing the geometric condition of a fabric under test and theoretical methods applied only after they are clearly validated by experimental evidence for the type of fabric and type of test involved. Extrapolation of experimental data is in general not justified.

A most important correlation, C_D vs. Re, has already been presented in Section 5.1.7. Certain discrepancies existed and were pointed out there. Now, on the basis of the validation of the more simple relations on which this correlation depends, it is possible to assign probable causes for these discrepancies.

The chief difficulty lay in the fact that there was no regular arrangement of the curves with respect to fabric parameters considered. That is, it would be anticipated that fabrics having a higher LP would show less effect of air viscosity and thus higher C_D's. Apparently the problem is in the assumption that the LP or (FA) as previously defined is actually the area available for flow. The true area available can in fact never be less than this, but can easily be more. It is easy to see this from photomicrographs where the non-planar character of pores is obvious. An LP or (FA) measurement determines areas by the projected pore dimensions whereas the actual minimum spacing between yarns is usually more. The effect is exaggerated in the cross-sections presented because they were made at yarn cross-overs rather than in the free pore area. Clearly, there can be no adjacent yarn overlap in the pore section as exhibited here at some of the cross-overs, but this is a matter of degree only. The situation is analogous to that of a partial light baffle wherein the passage of light is much more restricted than that of a fluid.

The implication of the above is that the C_D based on the projected area is higher than a true C_D based on actual area available for flow. The numerical difference depends on the relative magnitudes of the apparent and true (FA)'s. This consideration of tortuosity of path would seem to be a very complex one for engineering purposes, and indeed in the general case it is. For given fabric and yarn types, however, the configurations are fairly restricted and the above effect can be quantitized without the

Approved for Public Release

Contrails

Table 51. Evaluation of Theoretical Method for Determining Fabric Strain Under a Pressure Differential

Fabric	Pressure Differential (psi)	Fractional e Calculated	K_{av}	Calculated lb/in σ	Fractional e From Experimental Distention Measurement
R5N5	0.91	0.048	98	4.7	0.029
R20N5	0.54	0.037	82	3.0	0.022
R20N20	0.27	0.012	209	2.5	0.0125
T5N5	1.09	0.034	187	6.4	0.0295
T20N20	0.31	0.014	202	2.9	0.0134

expenditure of an exorbitant amount of time. This restriction within a type is demonstrated in Figure 18, where it can be seen that the Type I fabrics are grouped at a different level from the grouping of Type II's.

5.1.12 Conclusions

The general approach, followed in an attempt to determine and characterize quantitatively the fabric and flow parameters of importance in air permeabilities, has been validated. In the single case where quantitative agreement between theory and experiment was not satisfactory (C_D vs. Re), reasonable cause has been assigned and a subsequent investigation should correct this deficiency.

Practical design utilization of the basic flow equation given in Section 5.1.5.

$$Q = 1106\ C_D\ (FA)\ \frac{\Delta p^{1/2}}{\rho\ 1/2}\ \left(\frac{A_f}{A_{fo}}\right) \qquad (3)$$

requires a prior knowledge of the change in fabric dimensions with changes in pressure. This necessitates a theoretical formulation or empirical correlation for biaxial deformation on the basis of stress and fabric parameters. The analysis required to assemble such information for the general case would be most formidable, but for the restricted sort of construction used in parachutes, it should not be a large task to obtain such information with engineering accuracy. When such information is available, and with the results of this report and suggested corrections to the free area calculations, it should be possible to design parachute cloth to meet permeability specifications within a reasonably close tolerance.

Much of the foregoing work has been confined to investigations of phenomena up to only 50 in. of water pressure differential. Future work should be conducted which will extend such investigations to much higher pressures, at the same time making such corrections in approach as have been indicated to be necessary by the past phases of the work.

Approved for Public Release

Contrails

5.1.13 References

Sections 2.5, 5.2 and 5.3, and WADD TR 60-584, pp. 191 to 237 and 370.

Table 52. List of Symbols

a_p	Area of a single pore (sq ft).
b	Fabric distention (in.) measured during permeability tests.
d_f, d_w	Filling and warp yarn diameters (in.).
d_o	Yarn diameter at rest (in.).
e	Fractional linear extension.
g	Acceleration due to gravity.
k	Isentropic exponent for air.
l_{av}	Average maximum pore dimension (ft).
Δp	Pressure differential across the fabric (in. of water).
p_1	Upstream pressure.
p_2	Downstream pressure.
r	Radius of test specimen (in.).
t_f, t_w	Number of filling and warp threads per inch.
t_o	Number of threads per inch at rest.
w_{av}	Average minimum pore dimension (ft).
A	Orifice area (sq ft).
A_1	Approach area (sq ft).
A_f	Total fabric area (sq ft).
A_{fo}	Initial sample area (sq ft).
A_p	Total pore area (sq ft).
A_t	Total specimen area (sq ft).
C_c	Coefficient of contraction.
C_D	Coefficient of discharge.
C_v	Coefficient of velocity.
D	Orifice diameter (ft).
FA	Fractional free area.
FA_o	Initial fractional free area.
K	Biaxial modulus.
LP	Fractional light penetrability.
M	An index of yarn flattening.
Q	Flow (cfm/ft^2).
Q'	Volume rate of flow (cfm).
Q'_p	Volume rate of flow for a single pore (cfm).
R	Radius of curvature of a spherically deformed fabric (in.).
Re	Reynolds number.
V	Average velocity (ft/sec).

Approved for Public Release

Contrails

γ	Ratio of minimum to maximum pore dimension
θ	Angle of half arc formed by distended sample.
θ_o	Angle of half arc formed by sample at rest.
ν	Kinematic viscosity.
ρ	Fluid density
σ	Fabric stress (force per unit width).

5.2 Development of a Design Procedure to Engineer Parachute Fabrics

The work described below is concerned primarily with the theoretical aspects of fabric design to meet permeability specifications, and is a logical continuation of the work presented in Section 5.1 (WADC TR 56-576). At present the ability to design is apparently far ahead of the ability to construct a parachute fabric of desired properties. It is possible to predict air permeability of a known structure with considerable accuracy, but it is not possible to predict exactly some of the important geometric properties of a fabric that will result from a nominal design. This continuation again has been conducted by Klein, Lermond and Platt of Fabric Research Laboratories, Inc. and is reported in WADC TR 58-65, May 1958 (Contract AF 33(616)-3845). The significant difference from prior work is that the fabric is treated as a three- rather than two-dimensional structure, thus permitting a more accurate characterization of the actual flow region.

5.2.1 General Approach

Section 5.1 presented the relationship between pressure drop and fabric permeability as being functional with the Reynolds number of the flow through the fabric pores and the fabric open area. Whereas a much better correlation between flow and fabric parameters was obtained than has been found by any previous method, sufficient inaccuracies existed to warrant a more careful analysis; also, the pressure range over which flow has been investigated had been limited to a maximum of 50 in. of water.

Briefly, this previous work consisted of developing a flow equation and obtaining an experimental correlation curve which together could be used to predict air flow with the pressure differential and certain fabric parameters known.

This equation is:

$$Q = 1106\, C_D\, (FA) \left(\frac{\Delta p}{\rho}\right)^{1/2} \left(\frac{A_f}{A_{fo}}\right) \qquad (1)$$

where:

Q	=	flow (cfm/ft^2) based on area of test specimen at rest
C_D	=	coefficient of discharge
FA	=	free area, the projected open area as seen by an observation normal to the plane of the fabric
Δp	=	pressure differential (in. of water)
ρ	=	air density (lb/ft^3)
A_f/A_{fo}	=	ratio of specimen area under test to its area at rest
1106	=	a constant consistent with a six-inch circular specimen.

Approved for Public Release

Contrails

Note: See Table 53 for complete list of symbols.

An experimental correlation curve related C_D and Re for certain ripstop fabrics, Re defined by:

$$Re = \frac{V\,w}{\upsilon} \qquad (2)$$

where:

V = the average air velocity through a pore
w = the width of minimum dimension of a pre
υ = the kinematic viscosity of the air.

Table 53. List of Symbols

d_o	Yarn diameter at rest (in.).
e	Linear extension of the fabric under test.
h	Vertical distance between centers of adjacent filling yarns.
ℓ	Maximum projected pore dimension.
Δp	Pressure differential (in. of water).
r	Radius of a fiber.
t_w	Warp (threads per inch).
t_f	Fillings (threads per inch).
w	Width of minimum dimensions of a pore.
A_f/A_{fo}	Ratio of specimen area under test to its area at rest.
A_p	Projected pore area.
A_θ	Total pore area.
$A_\theta A_p$	Area increase factor.
C_D	Coefficient of discharge.
C_f	Percent filling crimp.
FA	Free area, the projected open area as seen by an observation normal to the plane of the fabric.
LP	Fractional light penetrability.
Q	Flow (cfm/ft^2) based on area of test specimen at rest.
Re	Reynolds number.
S_t	Projected distance between centers of the nearest fibers of adjacent filling yarns.
S	Distance between filling yarns at the angle θ.
ν	Average air velocity through a pore.
β	Reciprocal of the Poisson ratio.
θ	Angle between the plane of the fabric and the line joining the nearest points of adjacent filling yarns in plane perpendicular to the fabric and parallel to the warp yarns.
υ	Kinematic viscosity.
ρ	Air density (lb/ft^3).

Approved for Public Release

Contrails

It was pointed out in the previous work that the concept of flow being proportional to the projected free area might be in error, due to the fact that the open area actually available for flow is larger than this projected free area, considerably so in tightly woven fabrics. Accordingly, a development which takes this factor into account will now be presented.

5.2.2 Consideration of Inclined Areas

Consider Figures 31 and 32 which are sketches of fabric surfaces of plain and twill weaves respectively. In each case the upper picture is a view normal to the fabric surface and the lower, at an acute angle. From these it is at once clear that the spaces between the yarns as seen by a fluid are indeed larger than those seen by any projected measurements. The following analysis gives a means for finding approximately the open area as seen by the air.

Consider the diagram of Figure 33. It shows an idealized view of the filling cross-section of a fabric with low twist filling yarns and very low warp crimp. (The results of this analysis will apply equally well to fabrics where the filling yarns are not ribbon-like as shown; but the restriction of very low warp crimp is necessary and generally met in parachute fabrics.) The circles represent individual fibers of the filling yarns; r is the radius of these fibers; w, the spacing between adjacent filling yarns; S_t, the projection between centers of the nearest fibers of adjacent filling yarns; θ, the angle between the plane of the fabric and the line joining the center of these fibers, S_θ, the distance between these fibers; and h, the vertical distance between centers of adjacent filling yarns. The magnitude of h will vary from h_o where the filling crosses the warp to zero at a point half-way between the cross-overs. At the same time θ and S_θ will vary from their maximum values to zero and w respectively.

The assumption is made that the area available for flow is at any point proportional to S_θ rather than w, the projected spacing. Thus the total pore area, A_θ, is the integral of S_θ over the spacing between filling yarns rather than the product of warp and filling spacings ℓ and w. This value is developed analytically, and can be shown to be the following:

$$\frac{A_\theta}{A_p} = \left(1 + \frac{2r}{w}\right) f(\theta) - \frac{2r}{w} \qquad (3)$$

where:

- A = total pore area
- A_p = projected pore area
- $\frac{A}{A_p}$ = area increase factor
- r = radius of a fiber
- w = width or minimum dimension of a pore
- f_θ = area inclination factor. It is a function of θ where θ = angle between the plane of the fabric and the line joining the nearest points of adjacent filling yarns in plane perpendicular to the fabric and parallel to the warp yarns. $f(\theta)$ is obtained from Figure 34.

Approved for Public Release

Contrails

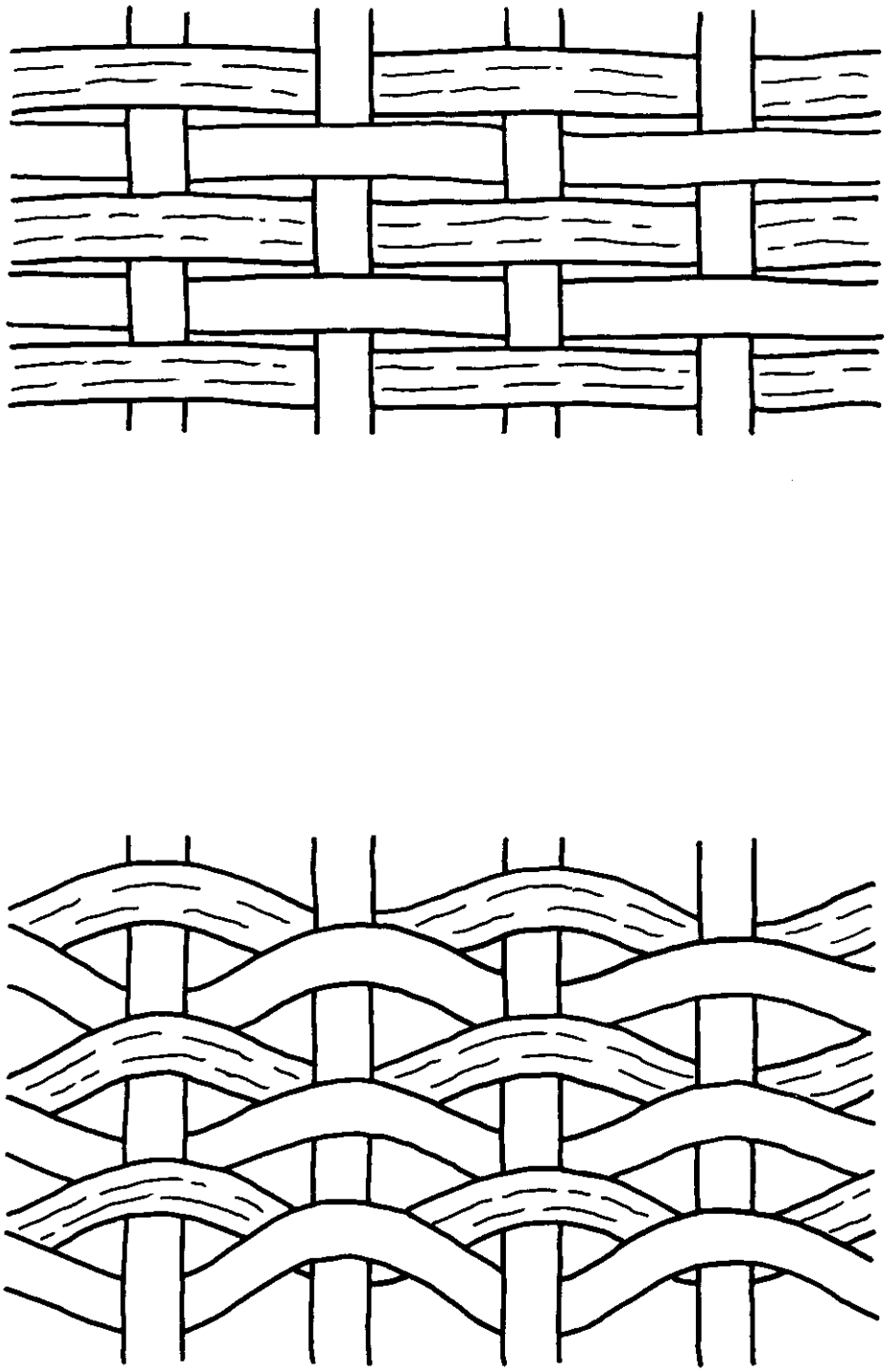

Figure 31 Normal and Oblique Views of Plain Weave

Approved for Public Release

Contrails

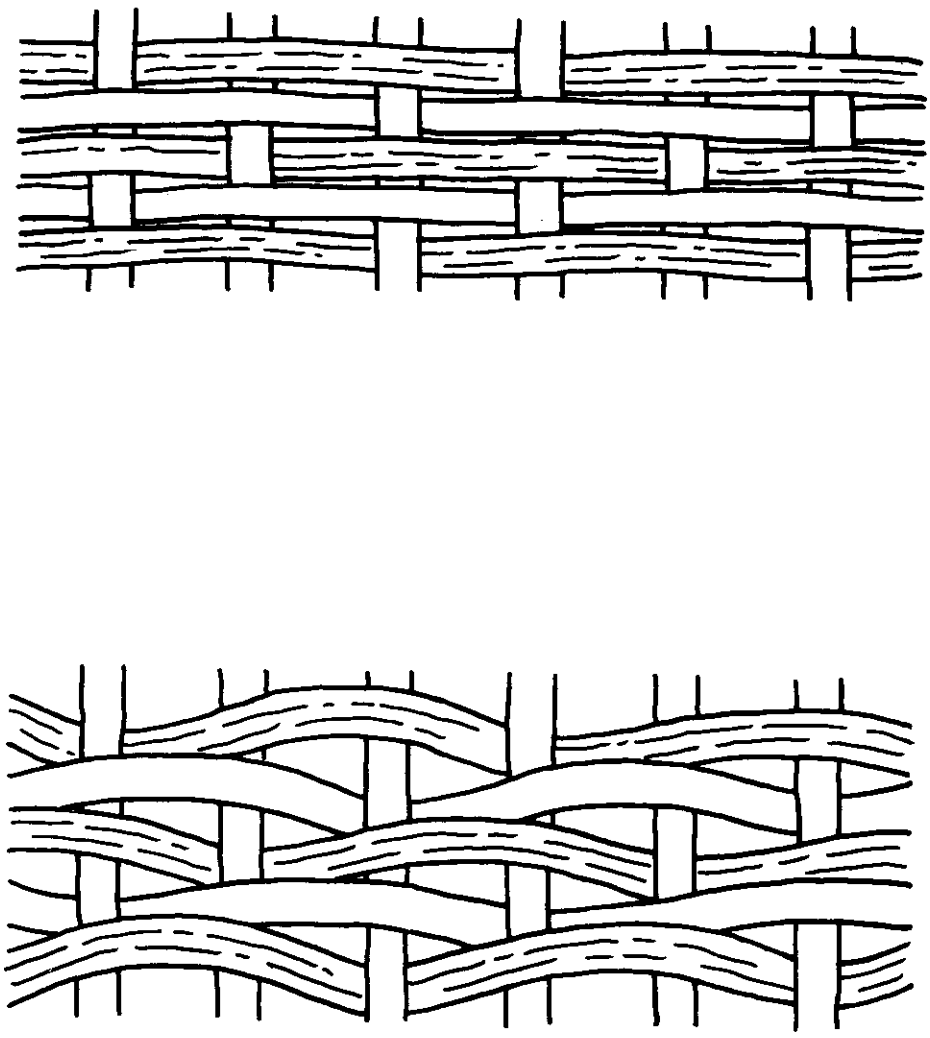

Figure 32 Normal and Oblique Views of Twill Weave

Approved for Public Release

Contrails

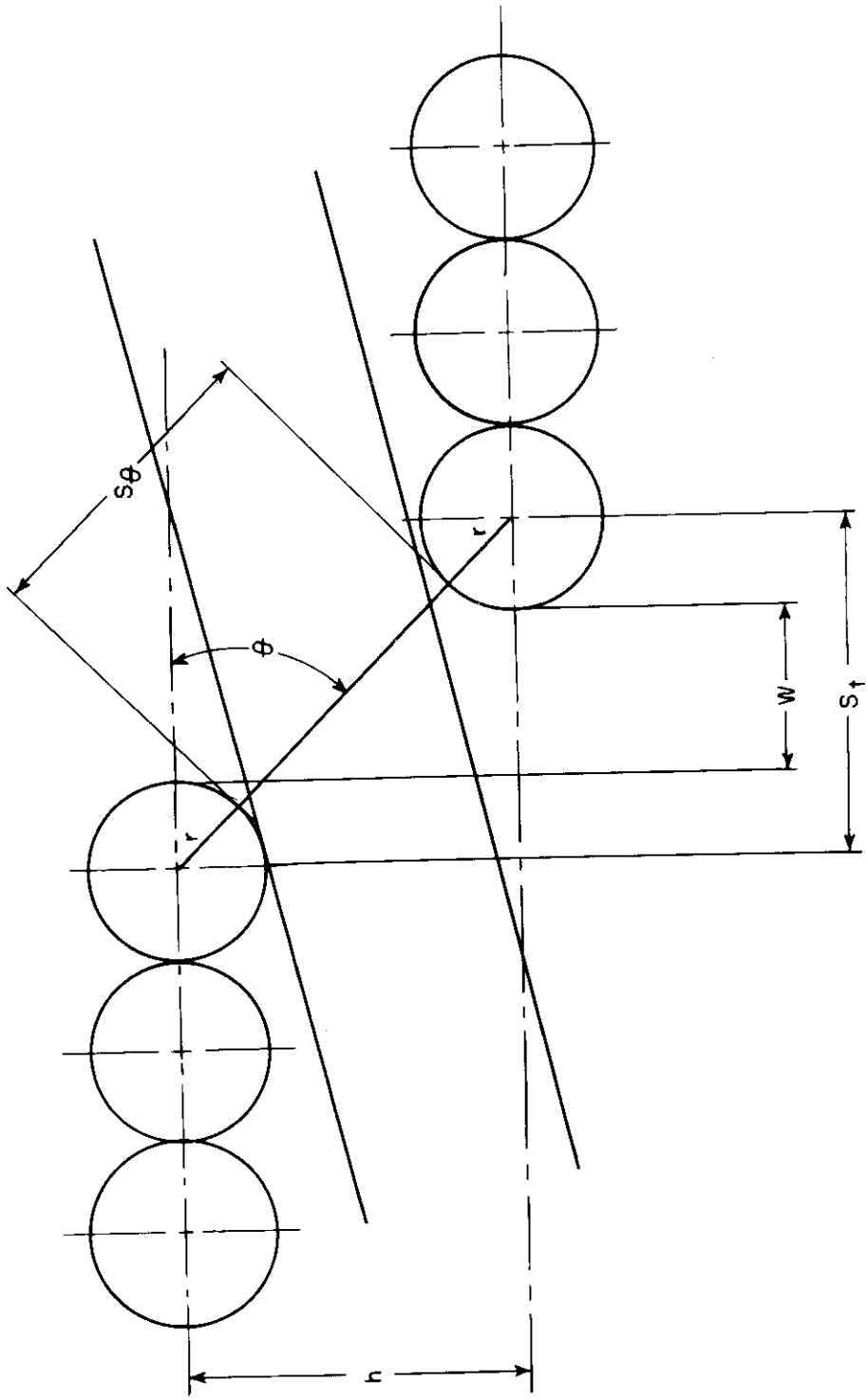

Figure 33 Idealized Filling Cross-Section

Approved for Public Release

Contrails

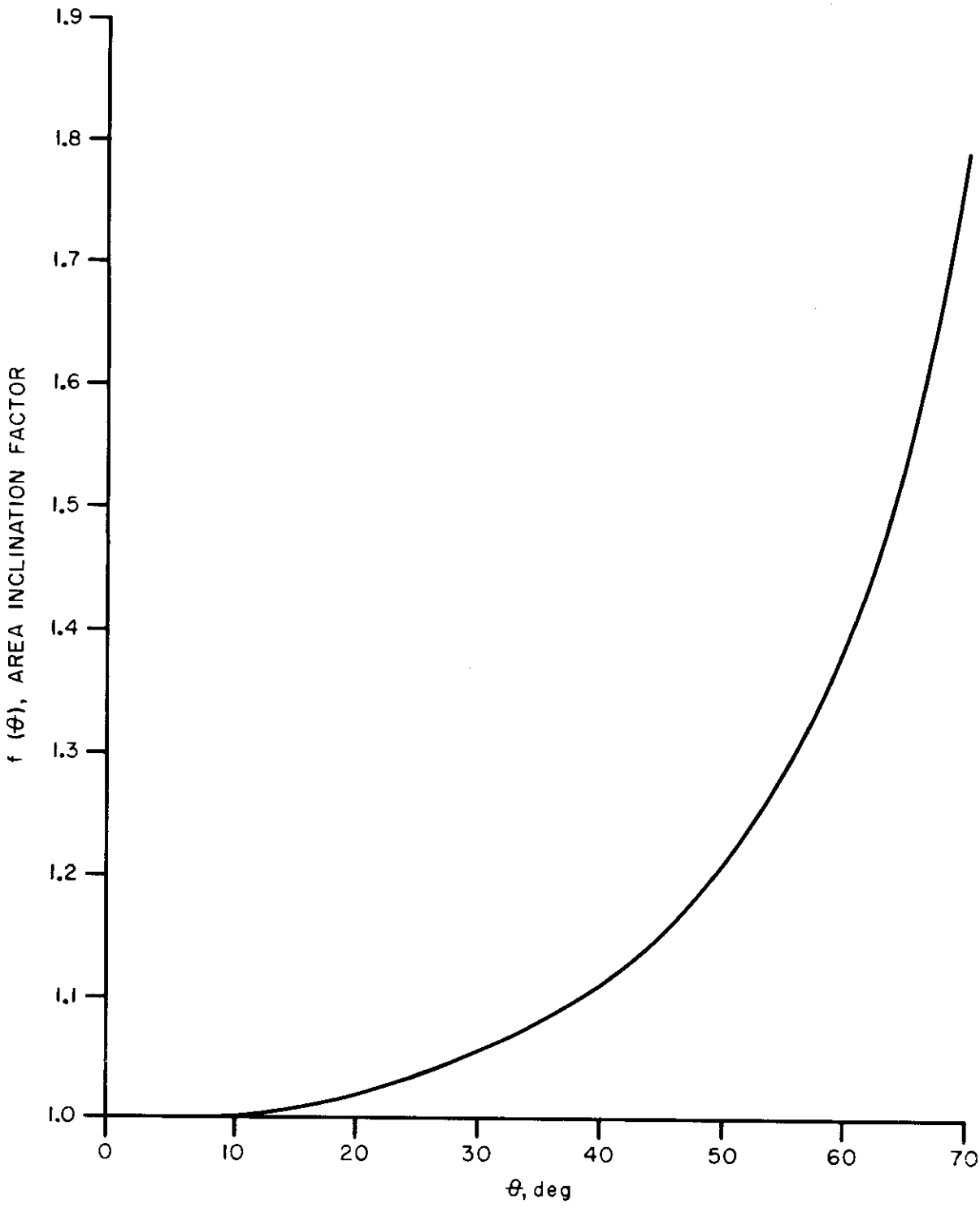

Figure 34 Area Inclination Factor vs. Pore Angle

Approved for Public Release

Contrails

When the value of A_p is already known, as for example from light penetrability measurements as is the case in this report, it is usually more convenient to find A by multiplying A_p by A_θ/A_p, but if good microscopic measurements are available the formula for A_θ may be used directly. When FA, or A_p in the present terminology, is very small, $f(\theta)$ may be quite large. In such cases A_θ/A_p is very sensitive to small changes in θ as can be seen from Figure 34, and large errors in calculated inclined areas could result from small errors in physical measurement. Here the A_θ formula must be used directly.

Logically, if an inclined area is to be used to characterize the fabric, an inclined width should be specified as the characteristic dimension in the determination of the Reynolds number. This width, w_{av}, is defined as the arithmetical average between the pore width at its point of maximum inclination and its minimum value which occurs at the pore center, this minimum value being equal to the previously defined w. There results:

$$w_{av} = \frac{w(1 + \sec \theta_{max}) + 2r(\sec \theta - 1)}{2} \qquad (4)$$

The pore Reynolds number then becomes:

$$Re = \frac{V w_{av}}{\nu} \qquad (5)$$

V, the average velocity through a pore, is calculated on the basis of the inclined area. It is in general necessary to correct the values of the geometric quantities involved for the changes occurring as a result of the loading under test. These changes result from both yarn and fabric deformation. Their influence will be discussed below.

It will be noted from Figure 34 that the angle θ, necessary for computing w_{av}, is influenced by the fabric height, h. It has been found that for the fabrics considered here the expression:

$$h = \frac{136\sqrt{C_f}}{t_w} \qquad (6)$$

where:

C_f = percent filling crimp
t_w = warp threads per inch
h = mils

correlates very well with values of h determined microscopically.

Approved for Public Release

Contrails

The coefficient of discharge is determined from the following modification of Equation (1).

$$C_D = \frac{Q \rho^{1/2}}{1106 \left(\frac{A_\theta}{A_p}\right)\left(\frac{A_f}{A_{fo}}\right) (LP) (\Delta p)^{1/2}} \qquad (7)$$

But

$$A_f/A_{fo} = (1 + 2e)$$

where e is the linear extension of the fabric under test. So

$$C_D = \frac{Q \rho^{1/2}}{1106 (A_\theta / A_p) (1 + 2e) (LP) (\Delta p)^{1/2}} \qquad (8)$$

Again, the change in geometry under test may exert considerable influence on the calculations.

Using the above outlined procedure, a series of curves of C_D vs. Reynolds number was plotted for four experimental and four commercial Type I fabrics. The free area (projected) of these fabrics varied from about 5 to 30%, and the angles θ, from about 25 to 50 deg. Using these curves, several curves of C_D vs. θ at constant Reynolds numbers were constructed. These curves, parallel straight lines within the precision of the data, were extrapolated to zero and the ordinates so found designated as $(C_D)_o$. This formation was used to plot a curve of $(C_D)_o$ vs. Re (Figure 35). From the slope of the lines of the constant Reynolds number plot it was found that

$$C_D = (C_D)_o - 0.0041 \theta_{max} \qquad (9)$$

where θ_{max} is in degrees. It should be carefully noted that this is an experimental correlation for data embracing θ from 25 to 50 deg and Re from 180 to 300. Extrapolation far beyond these limits is probably not justified. The extrapolation to zero described above is solely a calculating expedient; the value of $(C_D)_o$ so found is not necessarily the true value of C_D at $\theta = 0$, but is only a base from which C_D's in the known range of θ's can be easily found.

Physically, the inclination of the pore areas to the average flow path introduces losses due to tortuosity and mixing.

5.2.3 Mechanics of Solution and Results

In each case, the geometry of the fabric used in making the calculations of θ and A_θ was found in the following manner:

(1) Yarn diameters were taken from graphs which give the experimental relation between yarn diameter and twist for the yarns used in the parachute fabrics.

Approved for Public Release

Contrails

(2) Warp and filling threads per inch were measured directly.

(3) Corrections were made for the measured changes in fabric size and light penetrability under test.

(4) The height h was determined from the expression, $136\sqrt{c_f}/t_w$. From the above data, all the information necessary can be found for substitution into Equations (5) and (8). This was done for four experimental and four commercial Type I fabrics mentioned in the previous section and discharge coefficient so found was plotted vs. the individual averages found experimentally for each fabric. This is shown in Figure 36. Clearly, this method gives a very good result, over the range studied.

Various methods were used for the determination of crimp, none ideal. The most satisfactory means seemed to be to dead-load marked yarns removed from a fabric, successively reducing the dead-load and noting the extension at each load. An extrapolation of the load-extension diagram to zero load should give a fair approximation of the yarn crimp.

As an example of the method of C_D-Re computation, a fabric designated as FRL #2 will be used. This is an experimental low permeability fabric described fully in Section 5.2.4. It is used as an example here because it was not used in developing the relationship of Figure 36, and also because it has a very low permeability. It thus serves the two-fold purpose of exemplifying the method and testing the hypotheses involved.

The present method of analysis uses in its final form the following quantities:

(a) Area and dimensions of fabric pores

(b) Inclination of fabric pores

(c) Pressure differential across fabric

(d) Rate of air flow through fabric.

In addition to the fabric data given in Table 54 of Section 5.2.4, it is necessary to know the relationships given in Figures 37 and 38. Figure 37 gives the fabric extension vs. Δp; Figure 38, the fabric light penetrability vs. Δp; Figure 39, derived from Figures 37 and 38, the fabric extension vs. LP; and Figure 40, the flow in cfm/ft^2 as a function of Δp.

The easiest way to proceed is as follows: Pick a value of extension, one percent for example, and from Figures 37, 38, 39, and 40, find the Δp, LP, and Q associated with this extension. They will be found to be $\Delta p = 3.8$, LP = 0.0244, and Q = 195. From previously developed techniques involving pore shape and LP, the pore width, w, is found to be 8.33×10^{-5} in.; the fiber diameter for this yarn is 3.1×10^{-5} in.; the filling yarn crimp is initially 5.9%, and the end count is 174 per inch. By making the assumption that for small extensions the reduction in filling crimp is equal to the fabric extension, all the geometric variables required are at hand. Application of Equation (3) yields $\theta = 45^\circ$ and $A_\theta / A_p = 1.26$.

Approved for Public Release

Contrails

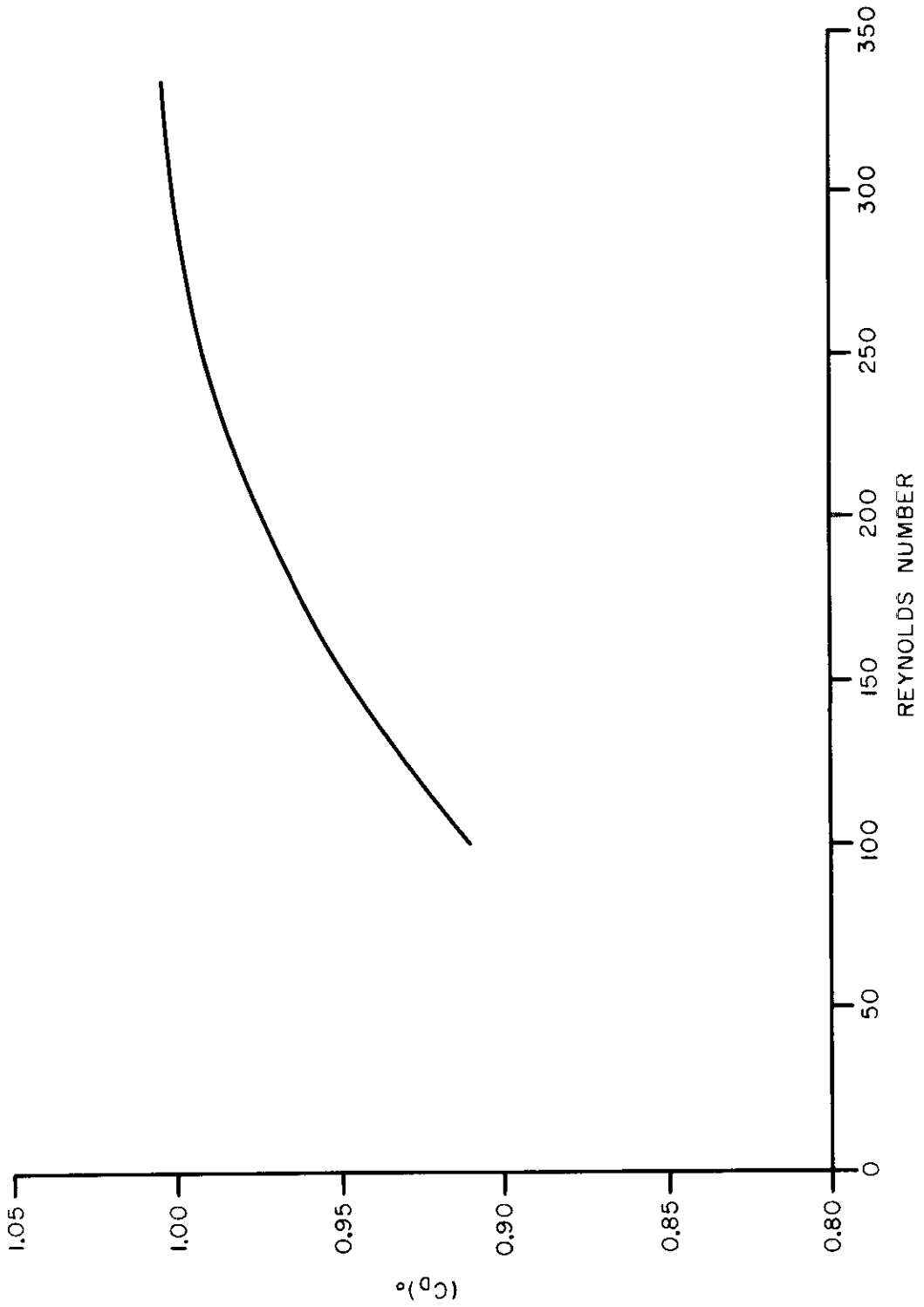

Figure 35 $(C_D)_\delta$ vs. Reynolds Number

Approved for Public Release

Contrails

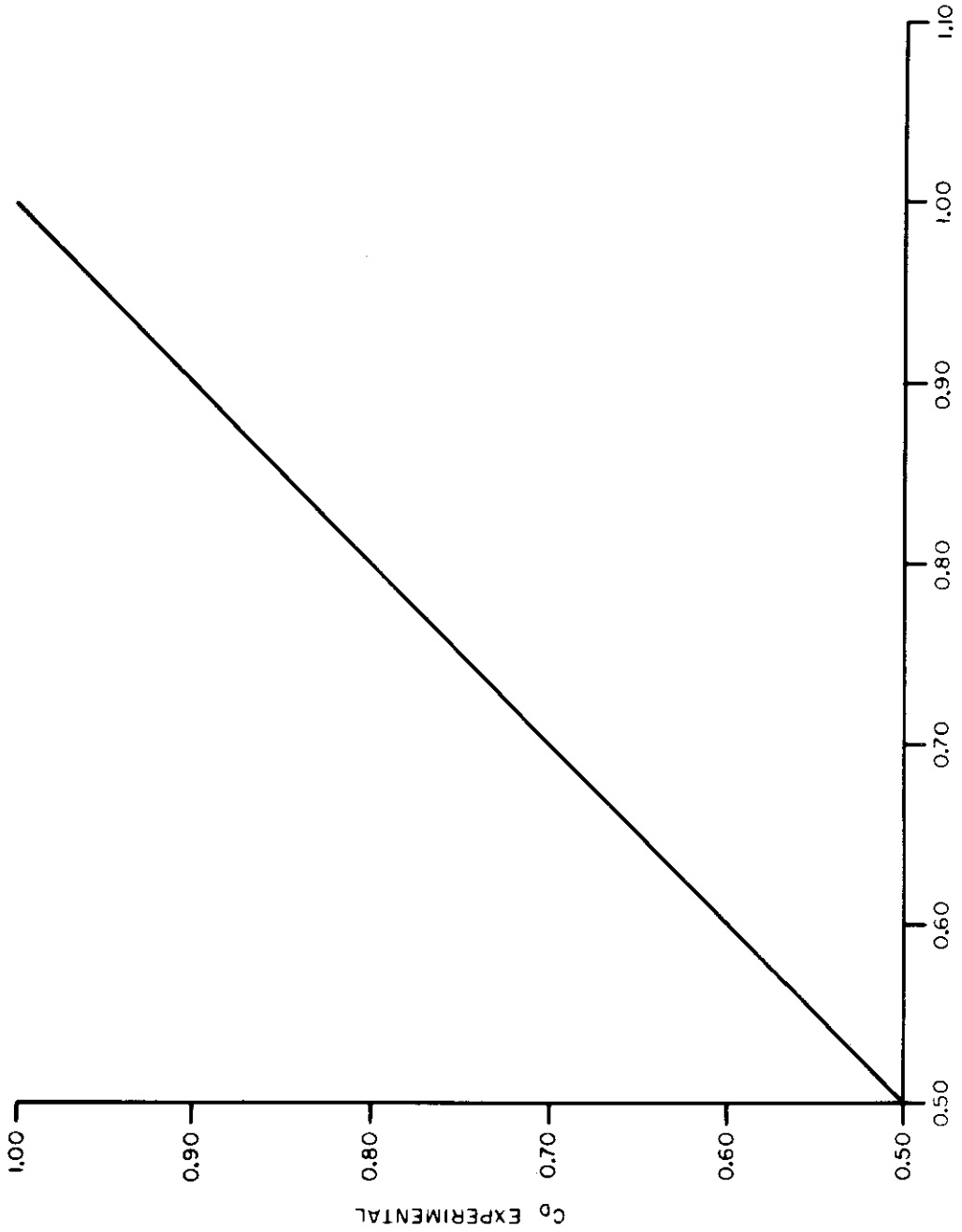

Figure 36 Correlation of Experimental and Calculated Discharge Coefficient

Approved for Public Release

Contrails

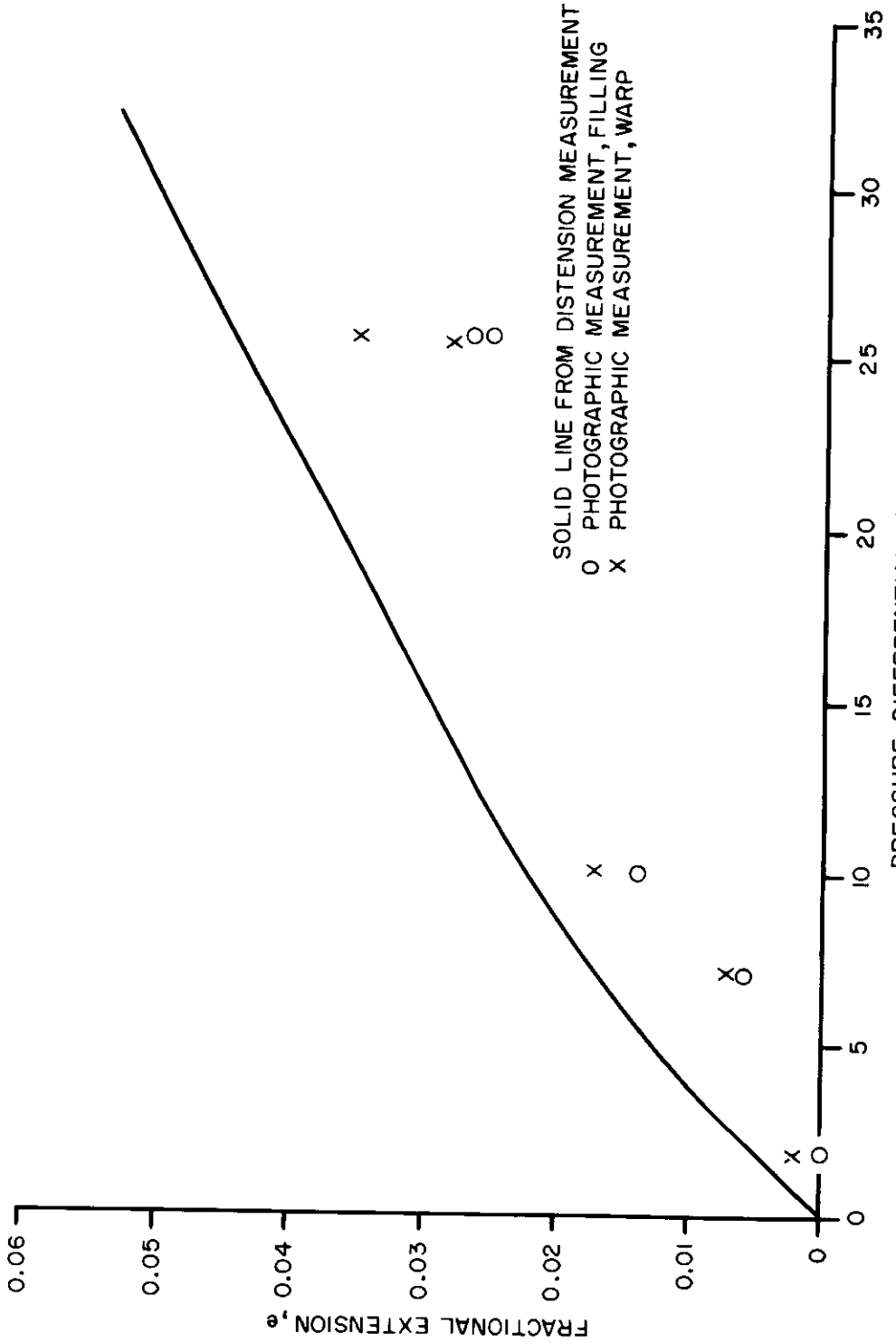

Figure 37 Fractional Extension vs. Δ p for Fabric 2

Approved for Public Release

Contrails

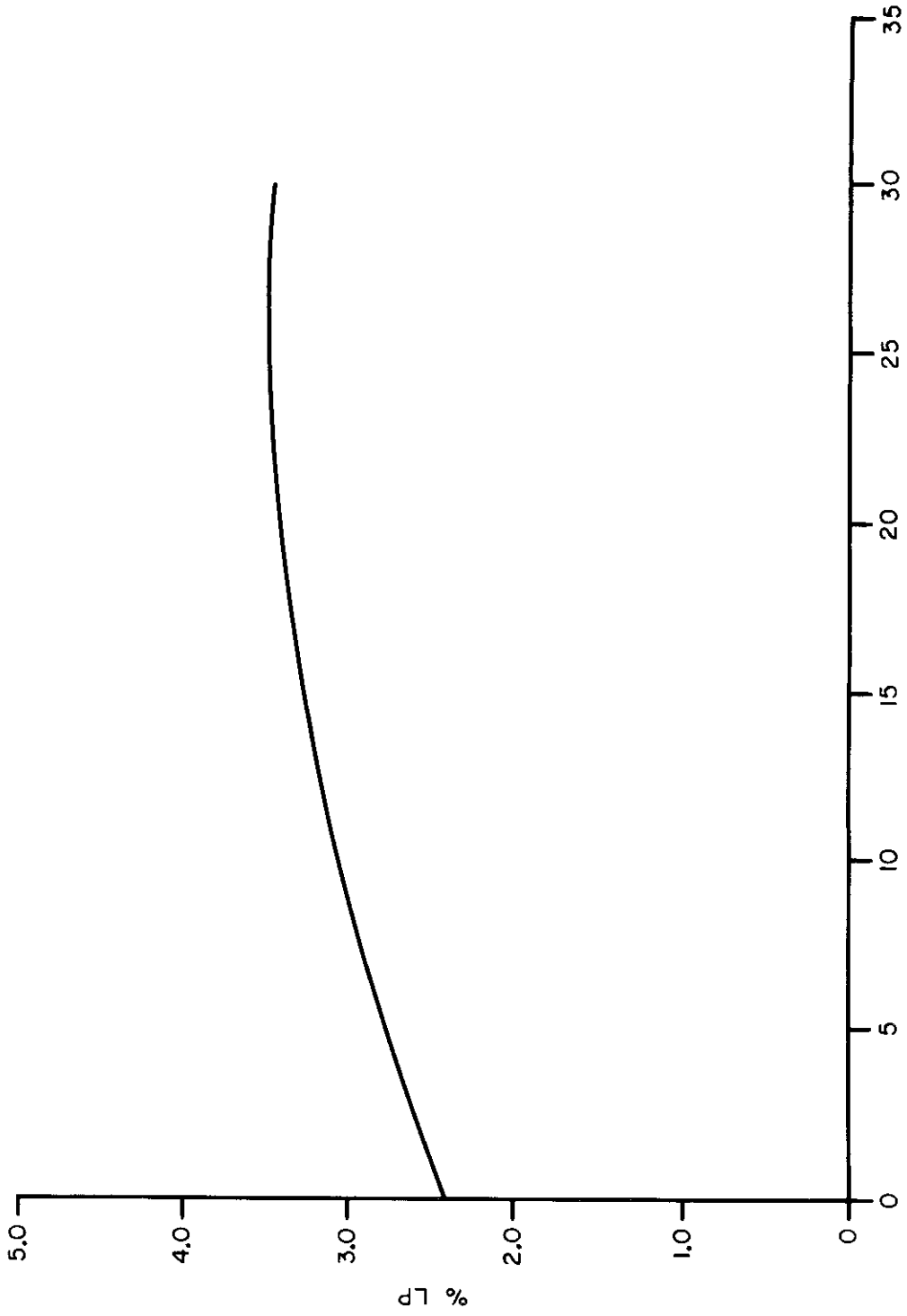

Figure 38 Percent LP vs. Δ p for Fabric 2

Approved for Public Release

Contrails

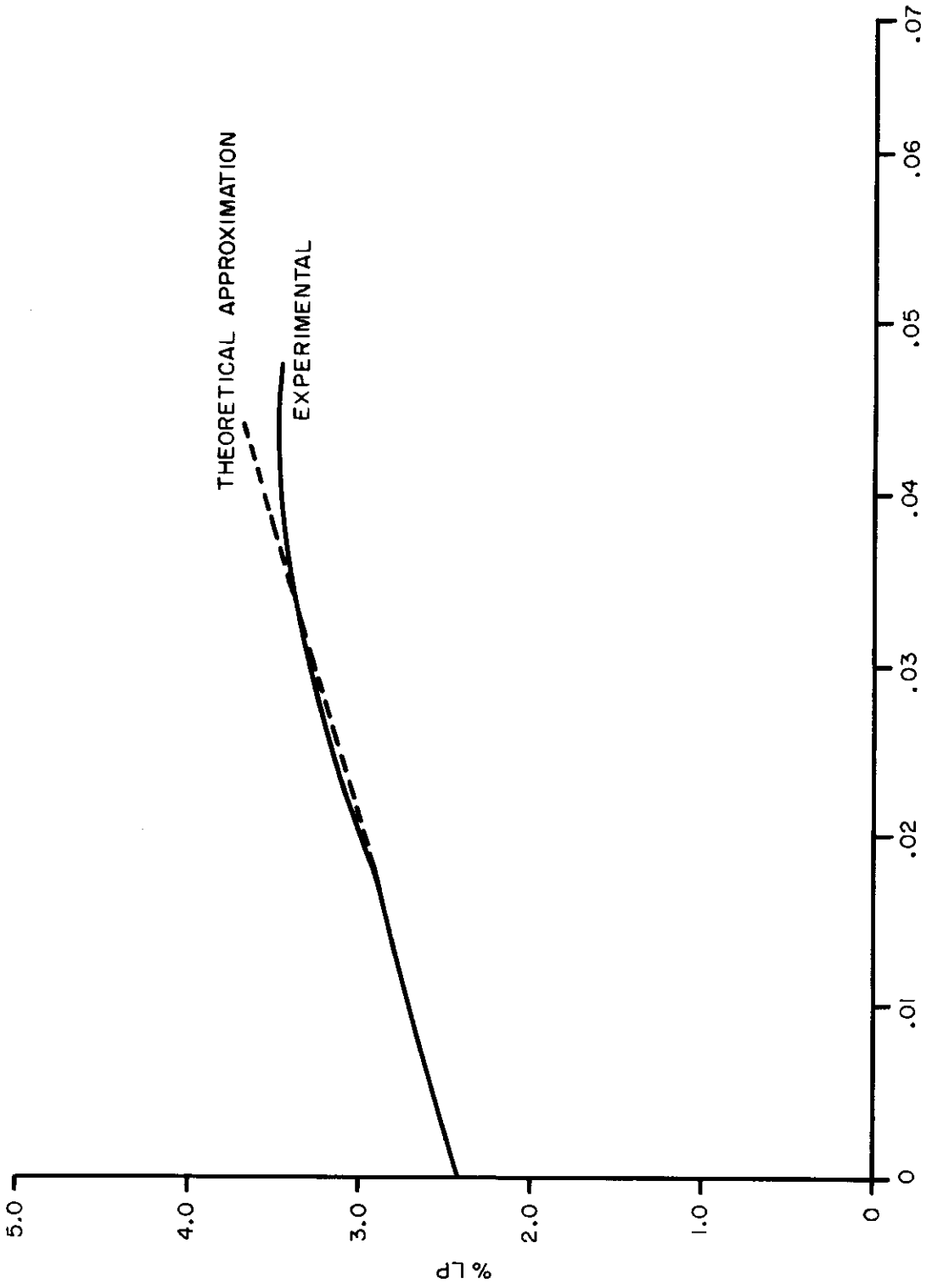

Figure 39 Percent LP vs. Fractional Extension for Fabric 2

Approved for Public Release

Contrails

Now apply Equation (8)

$$C_D = \frac{Q \rho^{1/2}}{1106 \frac{A_\theta}{A_p} (LP)(1 + 2e)(\Delta p)^{1/2}} \qquad (8)$$

For this case the result is:

$$C_D = 0.69$$

Calculation of the Reynolds number of the flow is accomplished by means of the foregoing data and Equation (5)

$$Re = \frac{V w_{av}}{\nu} \qquad (5)$$

The Reynolds number so found is 59. By referring to Figure 36 and extrapolating slightly, it can be seen that $(C_D)_o = 0.87$.

Now applying the correlation relationship, Equation (9):

$$C = (C_D)_o - 0.0041 \theta_{max} \qquad (9)$$

there results C = 0.69 -- a perfect agreement with the experimental determination.

Similar calculations were carried out at extensions of 2% and 4%, with experimental vs. correlation formula results of 0.78 vs. 0.74, and 0.84 vs. 0.86 respectively.

An important feature of the above results is that the formulas involved were originally derived from data obtained on fabrics of much higher LP than that of Fabric FRL #2, yet the correlation is still good for this fabric. This tends to substantiate the physical importance of the variables considered and justify the use of the Reynolds number as here defined and the angle θ as independent flow parameters.

Some thoughts should now be given to the manner in which the relationships shown by Figure 37 through 39 were obtained.

The solid line of Figure 37 represents the average fabric extension as a function of Δp as found by fabric distention measurements made under test as described in Section 5.1.4. The crosses and circles represent, respectively, warp and filling extensions as determined from photographs taken under test. The photographs used for this computation are typified as Figure 42. Backlighting was used so that the brightest portions are open areas and the darkest ones, double yarn thicknesses, that is, where warp and filling cross. While the same specimens were not used in the two different methods, it is clear that lower readings are obtained by the photographic technique. Since distension measurements have in the past been considered fairly accurate, it is this calculation which is used in this work, but the difference in results between the methods certainly bears investigation.

Approved for Public Release

Contrails

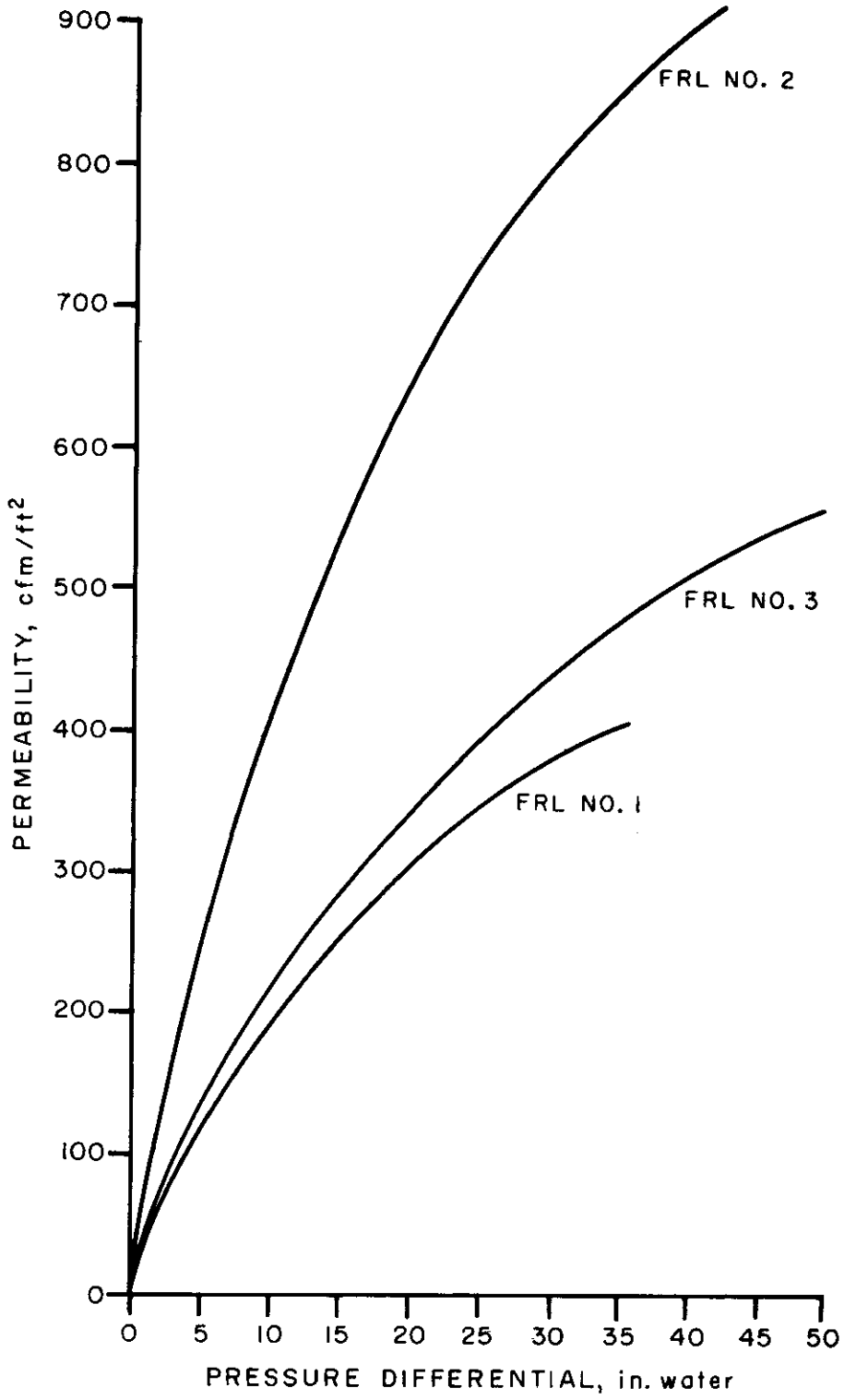

Figure 40 Permeability of Fabrics FRL 1, 2 and 3

Approved for Public Release

Contrails

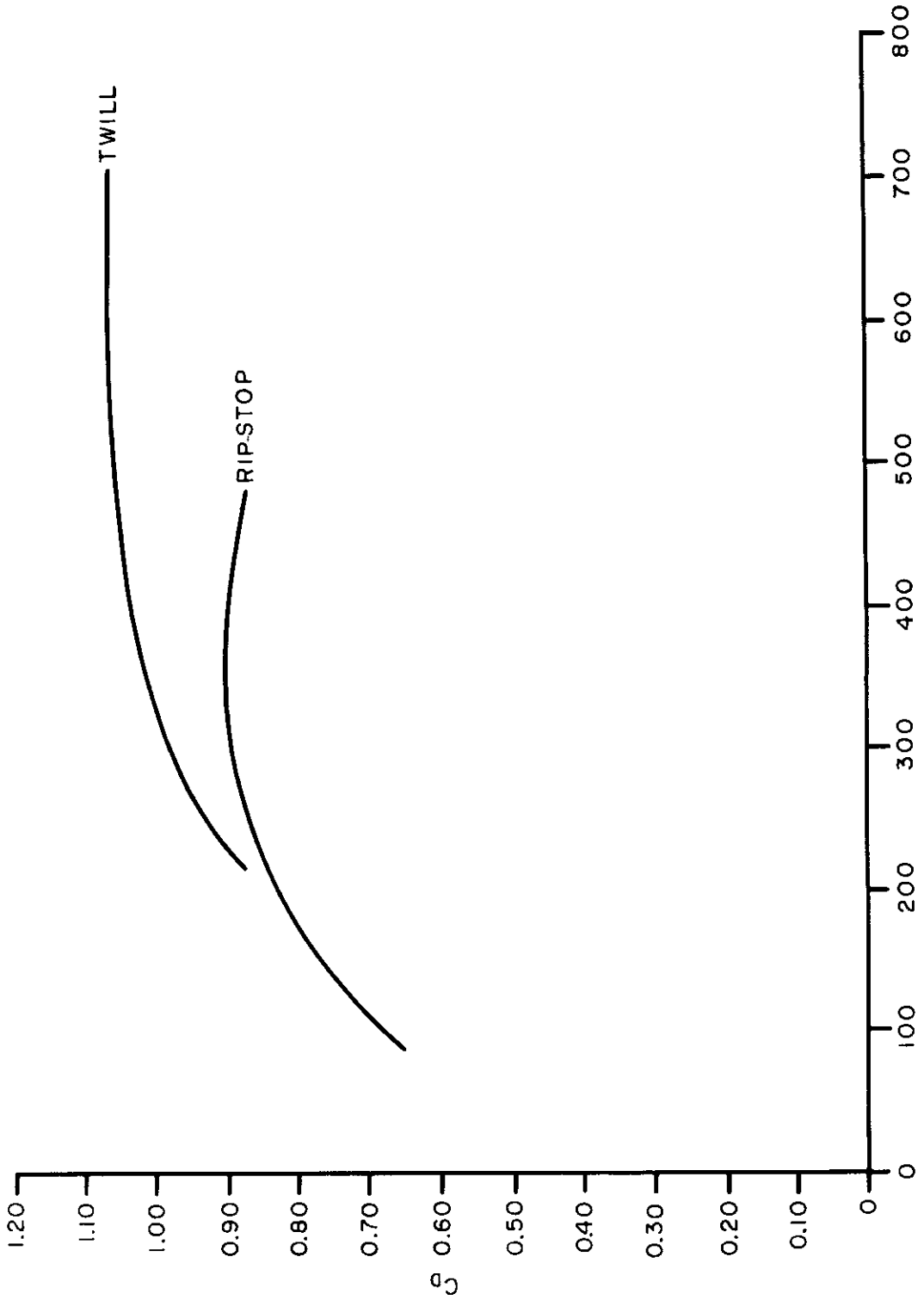

Figure 41 C_D vs. Reynolds Number of Twill and Rip-stop Fabrics

Approved for Public Release

Contrails

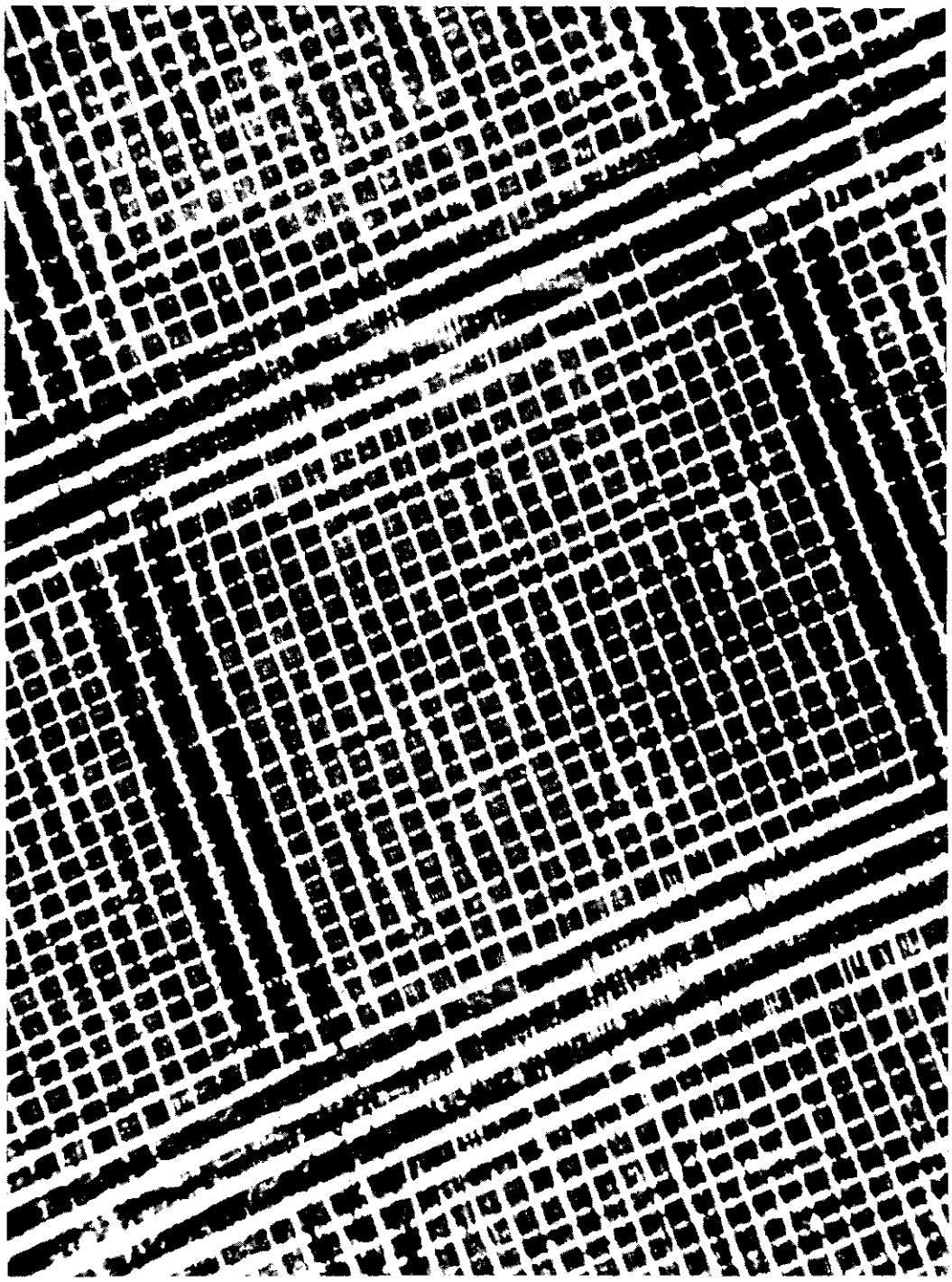

Figure 42 Surface Photograph of Fabric FRL-2 at p = 25.6, inches of H_2O

Approved for Public Release

Contrails

Figure 38 shows LP as a function of Δp under test conditions. The reason the curve has been shown to pass directly through the LP at zero Δp point is because this point represents the average of several rest LP readings and is more reliable than the rather variable LP readings at very low pressure drops. The variability of low LP readings is in general large, larger than the flow variation from specimen to specimen. Thus a good part of the variation between values of LP at given Δp is probably experimental in origin and not real.

In Figure 39 the solid line shows the relationship between LP and e as derived from Figures 37 and 38, while the dotted curve shows the same relationship derived from a mathematical expression developed below.

Consider a square fabric with yarns of width d_o and count per inch t_o. The FA or LP of this fabric at rest is:

$$(LP)_o = (1 - d_o t_o)^2 \tag{10}$$

If under test the fabric extends by an amount e the count will change to $t_o/(1 + e)$. In addition, the yarn diameter may change due to a Poisson effect so that the new diameter is $d(1 - e/\beta)$. β is defined as the reciprocal of the Poisson ratio. The expression for LP under test then becomes:

$$LP = \left[1 - d_o t_o \frac{1 - \frac{e}{\beta}}{(1 + e)}\right]^2 \tag{11}$$

It should be understood that β is a geometric as well as a material function here and will change with construction:

Solving the above two expressions for β one obtains:

$$\beta = \frac{e(1 - \sqrt{LP_o})}{(LP)_o(e - 1) + \sqrt{LP} - e} \tag{12}$$

The significance of the value of β is that positive values indicate a decrease in yarn diameter with fabric extension; negative values an increase, that is, flattening; and the larger the value, the smaller the effect. A value of 2 corresponds to a constant volume, constant shape deformation, the familiar Poisson ratio of 1/2.

Solutions of the above β equation for fabric FRL #2 were made using the data from Figures 32 and 33. The following pairs of values are for e and β respectively: .01, ∞ ; .02, ∞ ; .03, 25; .04, -11.3. All of these values are quite large enough which means that the average yarn diameter remains essentially constant. Using this fact a solution for LP is found in the form:

Approved for Public Release

Contrails

$$(LP) = \left[\sqrt{(LP)_o} + e\left(1 - \sqrt{LP_o}\right)\right]^2 \qquad (13)$$

It is this expression which is plotted as a dotted line in Figure 39.

Where different types of yarns are to be used, a knowledge of their behavior by an analysis similar to the above is required for design purposes.

In Figure 41 the results of C_D vs. Re calculations on the following fabrics are presented:* R1/2N1/2, R5N5, R20N5, R20N20, T1/2N1/2, T5N5, T20N5, T20N20, FRL #1, FRL #2 and FRL #3.

These correlation curves are for C_D and not $(C_D)_o$. Thus they include the effect of inclination on the magnitude of the area, but do not include the effect of inclination as such. On the basis of the previous success with the use of θ, the inclination, as an independent parameter, it might be supposed that consideration of this would lead to a better fit of the experimental points.

It should be noted that curve for the twill fabrics lies at a higher level than for the rip-stops (plain weave). It has been found in general that twill weaves exhibit higher discharge coefficients than plain weaves. A probable explanation for this is that for equivalent total open area, the area is less broken up by reversals in inclination than is that of the plain weave. This can be seen by observation of Figures 31 and 32. Other weaves would undoubtedly possess different C_D- Re characteristics.

Some crude experiments were performed to indicate approximately the physical mechanisms underlying the assumptions made in the above developments.

The experiments were as follows: Two plates were drilled with two rows of small, closely spaced holes through each, the only difference being that in one of the plates, the two rows were drilled at angles of 45 deg to the plate, toward each other, while in the other all the holes were normal to the plate. Thus, under an air pressure differential the air streams through the holes at an angle could be made to converge or diverge depending on which side of the plate was placed upstream. All tests were run at pressure differentials near 50 in. of water using from one to ten holes and keeping the others covered. The following results, all of significant magnitude were calculated.

(1) The flow per hole decreased with increasing number of holes or lesser spacing of holes.

(2) The flow per hole was greatest for the straight holes, slightly less for the divergent, and considerably less for the convergent.

(3) Based on the actual hole area, discharge coefficients of the order of 0.7 were found but were about 1.0 on the basis of the projected area.

Certain conclusions can be drawn from these data:

---

*R indicates rip-stop; T, twill, N, non-calendered; the first number, the warp yarn twist; and the second number, the filling yarn twist.

Approved for Public Release

Contrails

(1) There are considerable losses involved where a number of holes discharge close together and the magnitude of this loss is dependent on angle and spacing of the air jets.

(2) The losses involved in angulation and mixing are not so great as to compensate for the erroneous FA measured by a projection, and an unrealistically high value of the discharge coefficient will result if the projected area is used.

Thus the consideration of inclined area and θ as independent flow parameters is shown to be reasonable by a method independent of the correlations presented above.

5.2.4 Design of a Minimum Permeability Type I Fabric

As a part of the research the Type I fabric was to be redesigned to have an air permeability of 50 cfm/ft^2 at one-half inch of water pressure differential without the use of calendering. This fabric was to meet as nearly as possible all the other requirements of MIL-C-7020. Since it seemed that the Air Force was contemplating uses for parachute fabrics of very low permeability, it was deemed advisable to find the lowest limit of permeability to which a Type 1 fabric could be constructed. This was not possible to predict on the basis of prior work because the exact geometry which different yarns will assume under different constructions must at present be determined primarily by empirical means. For example, yarn diameter, a very important parameter in permeability considerations will vary with twist, number of filaments and tightness of weave, all of which effects must be determined experimentally. (Processing variables will be considered later.)

Qualitatively it is clear that up to a certain point a fabric could be made less permeable by decreasing yarn denier or fiber denier while maintaining total weight constant. This is because a more complete filling of open areas can be effected with a more finely subdivided blocking medium. Accordingly, the present Type I fabric using 30 denier, 10 filament yarns was redesigned in three different ways, all maintaining the same weight specification - (1.1 oz/sq yd). The yarns were as follows:

(a) 20 denier, 20 filament

(b) 20 denier, 7 filament

(c) 30 denier, 21 filament.

The three fabrics manufactured from these yarns will subsequently be designated as FRL #1, FRL #2, and FRL #3 respectively. Compared with the present Type I construction they permit evaluation respectively of the effects of:

(a) Finer yarns and finer filaments

(b) Finer yarns alone

(c) Finer filaments alone.

Approved for Public Release

Contrails

Table 54 summarizes the physical properties of the three fabrics. It can be seen that only FRL #3 comes close to meeting the specification of MIL-C-7020, the others failing badly on both tear strength and filling tensile strength. The reason for the low filling tensile strengths is that the filling yarns themselves are of low strength. The cause for this is undoubtedly processing damage, since warp and filling yarns are nominally identical. Thus, it should be possible to raise these strengths to acceptable levels. In the case of the low tear strengths, however, there appears to be little hope of significant improvement, the cause residing in the fine yarns. Henceforth, only FRL #3 will be considered as having any practical utility, but the other two can be used to extend the application of permeability prediction equations.

Figure 40 shows the permeabilities of fabric FRL #1 to FRL #3 as a function of Δp on the 50-in. permeometer. These results are the average of five tests each. Experimental points are not shown because the calculations were performed more rapidly by averaging procedures prior to determination of the flow. The coefficient of variation in each case lies between 5 and 10%. FRL #3, the fabric meeting the required physical specification, exhibits a permeability of about 25 cfm/ft^2 at one-half inch of water. Thus it is clear that the target of 50 cfm/ft^2 is a feasible one. Also to be noted from these curves is that whereas reduction of filament denier and reduction of yarn denier both reduce the permeability of a constant weight fabric (current nominal design is for 100 cfm/ft^2 at one-half inch of water), the reduction in filament denier has a much stronger effect. This is fortunate because it permits the use of a normal sized yarn in a low permeability fabric, thus maintaining tear strength.

The foregoing three fabrics were also studied at higher pressure differentials. These results will be discussed together with the high pressure results on the other fabrics considered.

5.2.5 High Pressure Testing

A number of fabrics were tested on a high pressure permeometer located at Massachusetts Institute of Technology. It was not possible to reach the target value of 750 in. of water pressure differential on any of the samples because failure occurred before that point. This is not to say that the maximum pressure values shown on the graphs following could not be exceeded in practice; the test procedure necessarily introduced non-uniform strains which are probably in excess of those imposed under the operating conditions of a parachute. This non-uniform straining is largely an edge effect, so its influence on permeability was eliminated by the use of a flexible rubber membrane over the specimen which permitted flow only through a one-inch square in the center of the four-inch specimen.

Figure 43 plots pressure differential vs. permeability, and is a composite of average curves for each fabric.

Since the contract was terminated during the high pressure testing work, very little has been done in using these results. Certain gross tendencies can, however, be noted.

(1) The higher permeability fabrics exhibit a higher degree of uniformity than the lower ones.

Approved for Public Release

Table 54. Experimental Fabric Parameters

Fabric	t_w	t_f	Weight oz/sq yd	d_{yarn}	N_f	$(LP)_o$	c_f	S_w	S_f	e_w	e_f	TS_w	TS_f	Q 1/2"
FRL #1	203	181	1.15	20	20	0.0091	10.2%	46	35	32%	44%	2.4	1.7	17.8
FRL #2	195	178	1.10	20	7	0.0244	5.9	41	23	29	30	2.4	2.0	35.3
FRL #3	129	120	1.07	30	21	0.0168	5.1	40	39	26	36	5.6	4.0	24.5

t_w, t_f = warp and filling thread/inch; rip-stop yarns counted as two

d_{yarn} = yarn denier

N_f = number of filaments/yarn

$(LP)_o$ = rest LP, fractional

C_f = % crimp, filling

S_w, S_f = warp and filling 1-in. tensile strength lb/in.

e_w, e_f = warp and filling ultimate elongation, %

TS_w, TS_f = warp and filling tongue tear strength, lb

Q 1/2" = cfm/ft^2 at 1/2 in. water pressure differential.

Approved for Public Release

Confidential

Contrails

(2) Permeabilities at high pressures are usually very nearly proportional to the square root of the pressure differential, slightly higher for low permeability fabrics, slightly lower for high ones.

While no calculations on fabrics or yarn deformation have been made at the higher pressures, it seems clear that such deformations rather than any basic difference in flow character are responsible for the above. All the fabrics are operating at Reynolds numbers where C_D should become slightly smaller with increased flow. In the case of the high permeability fabrics this is exhibited, but in the tighter fabrics where small geometric increases are proportionately greater in their effects, the increased area due to tensioning is noticeable. The greater uniformity of the fabrics with more highly twisted yarns can be explained on the basis of the above and also the greater structural integrity accompanying higher twists.

In addition to the conventional permeability tests some experiments were run on a selected group of fabrics to determine hysteresis susceptibility as a function of construction. Three types of tests were run:

(a) The fabric was cyclically loaded between zero and 80% of the pressure required to break it; flow and pressure measurements being taken at frequent intervals of pressure.

(b) The fabric was held for 15 minutes at 80% of bursting pressure, then investigated for permeability vs. Δp.

(c) The fabric was suddenly and repeatedly loaded and unloaded to approximately 80% of bursting strength, the loading and unloading cycles occupying about 3-5 seconds each. Permeability was then checked.

Within the range of normal fabric variability and experimental error no difference could be found between one time loading and any of the above procedures. It must be concluded that these fabrics, both twill and ripstop, are quite stable against the effects of repeated loading, at least under these circumstances. Since the Air Force has not always observed such stability, it is probable that variations in permeability with age and use are occasioned by other mechanical influences such as folding and rubbing.

5.2.6 Conclusions: Present Status of Design to Permeability Specifications

From the foregoing work it is apparent that if the pertinent physical parameters of a fabric are known, its air permeability can be predicted with a considerable degree of accuracy. Conversely, it should be true that the physical parameters could be specified to produce a fabric of given permeability characteristics. The former has been well demonstrated at least at low pressure differentials, but the latter presents considerable problems in that certain dimensional tolerances must be achieved which are apparently commercially unobtainable at present.

Consider the case of the LP or FA of fabric FRL #1. It was found to be 0.0091. Now suppose the number of filling yarns is reduced by 2%. Using the known fabric parameters and altering only the filling threads per inch,

Approved for Public Release

Contrails

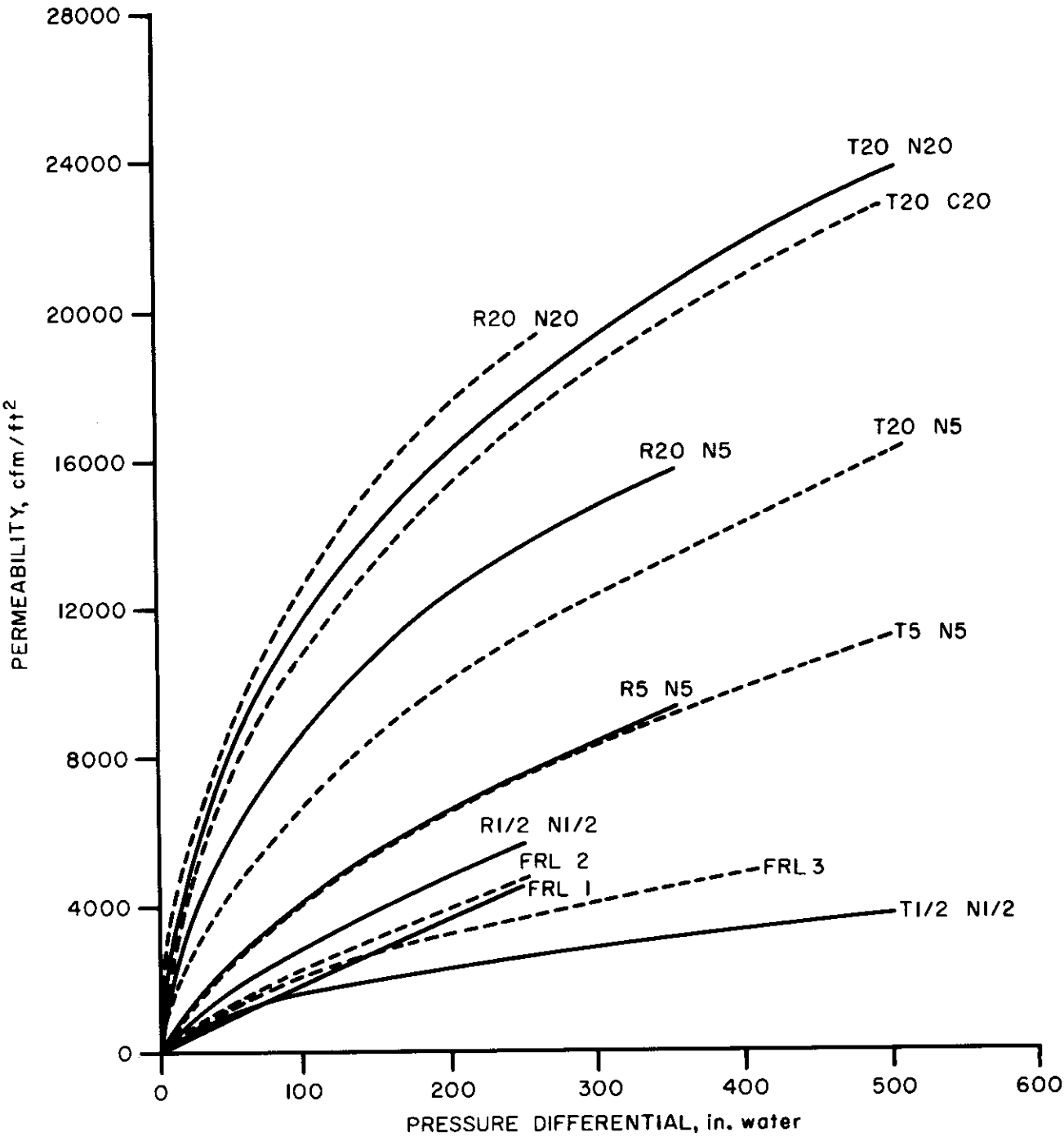

Figure 43 Permeability of Experimental Fabrics

Approved for Public Release

Contrails

it is calculated that the new FA would be 0.0394, a tremendous increase and a very strong influence on air permeability, yet 2% is not a large processing variation. The effect of such a change in warp or filling thread count would of course not be so great on a more open fabric, but many other factors, equally hard to control, have a significant influence on permeability. It is well known and has been clearly presented that yarn diameters are of the highest significance. Reference to yarn twist vs. diameter graphs shows that even at a given yarn twist the diameters cannot be accurately predicted, possibly the result of different weaving tensions or finishing procedure.

Many more examples could be given, all pointing to a very important conclusion, that the ability to define the flow through a parachute fabric is far ahead of the ability to produce a fabric to a given specification.

The implications are obvious. A balanced program leading toward the engineering of a parachute fabric to given permeability specifications must concentrate for the present on control of unwanted variables. From the work reported in this section and in Section 5.1 the most important of these variables seem to be threads per inch, yarn diameter and yarn crimp. An additional and closely allied area of study should be the stability of various constructions under conditions to which they are normally subjected.

5.2.7 References

Sections 2.5, 5.1, 5.3 and WADD TR 60-584, pp. 191 to 237 and 370.

5.3 A Study of the Air Permeability Properties of Commercially Produced Parachute Fabrics

In conjunction with the study of the mechanics of air flow through parachute fabrics as reported in Section 5.1, a study was made of the variability in air permeability and light penetrability of Type I and Type II MIL-C-7020A parachute fabrics. The work was conducted by Klein, Lermond and Platt of Fabric Research Laboratories, Inc. and is reported in WADC TR 56-576, September 1957 (Contract AF 33(616)-2977). Object of the work was to determine the degree to which the fabrics met permeability specifications, and where such requirements were not met, the reasons therefore.

5.3.1 Materials Tested

Parachute Fabrics Specification MIL-C-7020A
Type I 20 samples
Type II 19 samples

5.3.2 Test Procedure

All 39 fabrics were tested for air permeability at 0.5-in water pressure differential, and for light penetrability at rest.

5.3.3 Test Results

Table 55 tabulates data. Of the samples tested, only 60% of the rip-stops (Type I) and 42% of the twills (Type II) were within the specifications. Within a given sample the twills showed far more varia-

Approved for Public Release

Table 55. Air Permeability and Light Penetrability Values for Commercial Fabrics

Type I				Type II			
Source	Air* Permeability ($ft^3/min/ft^2$)**	% Coefficient of Variations	Fractional Light Penetrability**	Source	Air* Permeability ($ft^3/min/ft^2$)**	Coefficient of Variations	Fractional Light Penetrability**
1 a	136	9.1	0.0771	1 a	113	18.5	0.0422
b	178	3.4	0.0817	b	93	10.7	0.0300
c	180	3.5	0.0816	c	89	13.8	0.0256
2 a	123	2.2	0.0792	2	90	5.7	0.0235
b	113	3.7	0.0629	3	102	8.9	0.0422
3	109	6.6	0.0661	4	97	7.9	0.0405
4	125	4.5	0.0738	6 a	98	11.8	0.0337
5	260	5.0	0.0126	b	94	13.8	0.0277
6 a	95	2.4	0.0596	7	40	17.3	0.0136
b	87	4.0	0.0447	8 a	124	14.7	0.0406
7	87	5.8	0.0511	b	114	11.1	0.0385
8 a	102	6.2	0.0535	9	91	13.4	0.0317
b	103	8.2	0.0592	10	77	4.7	0.0185
9	111	5.9	0.0709	11	139	9.4	0.0533
10	76	8.2	0.0447	12 a	107	14.5	0.0301
11 a	100	3.0	0.0563	b	109	11.7	0.0371
b	113	3.1	0.0506	13	119	10.8	0.0447
12 a	134	7.2	0.0732	14 a	157	22.3	0.0611
b	110	8.2	0.0546	b	165	37.8	0.0509
13	101	7.5	0.0597				
Average	122		0.0663		106		0.0360
Specification	80-120				100-160		

*Measured at 1/2 in. water pressure differential.

**Average of five tests.

Approved for Public Release

Confidential

Table 56. Fabric Parameters of Selected Commercial Fabrics

Type I

Source	t_w x t_f	Yarn Diameter (in.) Warp*	Yarn Diameter (in.) Filling*	Yarn Twist (t.p.i) Warp x Filling	Air** Permeability ($ft^3/min/ft^2$)	Fractional FA	Fractional LP
1	120.4 x 116.8	0.00446	0.00732	7.4 x 1.0	136	0.0657	0.0771
2 a	120 x 114.8	0.00436	0.00726	7.4 x 1.0	123	0.0794	0.0792
b	118.2 x 116.4	0.00458	0.00752	7.3 x 1.1	113	0.0555	0.0629
3	130.8 x 121.6	0.00435	0.00714	7.0 x 1.1	109	0.0570	0.0661
4	126.8 x 121.2	0.00407	0.00690	7.8 x 1.3	125	0.0791	0.0738
5	120.4 x 121.6	0.00412	0.00622	8.0 x 1.1	260	0.0123	0.0126
7	122 x 116.8	0.00540	0.00763	7.6 x 1.1	87	0.0369	0.0511
11 a	117.2 x 122.8	0.00463	0.00713	6.7 x 0.8	100	0.0482	0.0563
13	120 x 120	0.00461	0.00778	14.5 x 3.8	101	0.0414	0.0597

Type II

1	128 x 75	0.00457	0.01284	7.7 x 1.0	113	0.0355	0.0422
2	128 x 75.2	0.00514	0.01265	8.1 x 1.0	90	0.0174	0.0235
3	130.0 x 74.4	0.00504	0.01151	7.4 x 1.2	102	0.0495	0.0422
4	127.2 x 76	0.00425	0.01187	5.6 x 1.1	97	0.0449	0.0405
7	120.8 x 67.6	0.00533	0.01374	8.1 x 0.9	40	0.0110	0.0136
11	125.2 x 74.4	0.00456	0.01145	7.0 x 1.4	139	0.0719	0.0533
13	122.8 x 76	0.00485	0.01222	8.6 x 1.3	119	0.0201	0.0447
14 a	125.6 x 79.6	0.00439	0.01029	7.4 x 3.2	157	0.0812	0.0611

*For Type I Fabrics the diameter reported = $14/18\ D_{\text{plain weave yarn}} + 2/18\ D_{\text{rip-stop yarn}}$.

**At 1/2-in. water pressure differential.

Approved for Public Release

Confidential

Contrails

bility than the rip-stops. As a general rule the Type I fabrics had permeabilities on the high side and Type II fabrics were on the low side even for those fabrics meeting specifications.

Table 57. Relative Flow of Selected Commercial Fabrics

Type I			Type II		
Source	$Q_{1/2}$*	$Q_{1/2/LP}$*	Source	$Q_{1/2}$*	$Q_{1/2/LP}$*
1	136	1760	1	113	2570
2 a	123	1560	2	90	3890
b	113	1800	3	102	2370
3	109	1650	4	97	2390
4	125	1700	7	40	2950
5	260	2060	11	139	2610
7	87	1710	13	119	2680
11 a	100	1780	14 a	157	2570
13	101	1680			

*Permeability in cubic feet per minute per square foot of fabric at a pressure differential of 1/2-in. of water and LP expressed on a fractional basis.

As a means of determining the cause of failure to meet specifications, nine of the Type I and eight of the Type II fabrics were studied further to determine certain of the fabric parameters. The tabulation of these parameters is shown in Table 56.

Since the warp and filling twists show little or no difference from sample to sample and the yarn deniers are also essentially the same for all the fabrics, differences in fabric geometry should offer an explanation as to the reasons for difference in air flow. It has been shown previously in Section 5.1 that the permeability of a fabric should be approximately proportional to the free area under the test conditions. Since a half inch of water pressure drop causes little fabric extension, the ratio, Q/LP should be approximately constant for all fabrics of the same weave. This ratio for the 17 fabrics of Table 56 is close to being constant for a given weave type for the fabrics as shown in Table 57. It must be concluded, then, that the fabrics differ in permeability primarily as a result of differences in fabric geometry (yarns diameters and threads per inch). Reference again to Table 56 shows that for the most part those fabrics that do not meet specifications differ from the average for either the warp or filling diameter. There are also slight differences in the thread counts from sample to sample. It must be remembered that a slight difference in any one of these parameters can cause a large change in the fabric free area, particularly for low (FA) values.

The ratio of Q/(FA) for the twills is not quite as constant as that for the rip-stops. One reason for this may be that the true air channel deviates more from the apparent one than in the case for the rip-stops. Thus the sensitivity to change in geometry will be greater.

Pictorially, the differences in fabric geometry may be observed by

Approved for Public Release

Contrails

photomicrographs of cross-sections from high, medium and low permeability fabrics of both types. For the most part, the filling yarns show little or no difference from fabric to fabric as far as distribution of the individual filaments is concerned with the exception, perhaps, of the most open fabric. The warp yarns, on the other hand, show pronounced differences. In going from low to high permeability fabrics the filaments become more compacted and the area occupied by a given yarn becomes less. Thus the difference in permeability of the various fabrics can be ascribed to differences in either yarn or fabric geometry. Since there is no pronounced difference in twist, the differences in yarn diameters must be ascribed to such things as variation in warp tension from one manufacturer or one run to another. The higher the tension, the more slender is the yarn. In the case of the filling yarns the differences in diameter could be caused by different degrees of heating. The yarn is of low twist (1 turn per inch) and thus would generally be broad and flat. Excessive heating would cause the filaments to be more compact although still perhaps maintaining their ribbon-like character.

5.3.4 References

Section 5.1.

5.4 The Air Permeability and Biaxial Stress Properties of Parachute Fabrics

Previous studies of the mechanics of air flow through parachute fabrics, as reported in Sections 5.1 and 5.2 and WADD TR 60-584 have dealt with air pressure differentials ranging from 0.5 in. of water in standard permeability testers to 50 in. of water with the Georgia Institute of Technology permeometer. Air Force requirements for parachute fabrics have made it necessary to study cloth permeabilities at pressure differences ranging from 50 to 1,000 in. of water.

In the WADC sponsored program at the Georgia Institute of Technology, specimen diameters were increased to 6 in. and in certain airflow tests square clamps were used. The increase in fabric area due to the induced stresses was manifest in these experiments and so there emerged a need to measure biaxial stresses during high-pressure-difference airflow tests. Simultaneous measurement of fabric deformation should then fix the state of fabric stress and strain thereby allowing a more realistic judgment of fabric resistance to airflow under known conditions of deformation.

The Textile Division at Massachusetts Institute of Technology has designed and constructed suitable instrumentation for measurement of fabric stress and strain at pressure differentials encountered in airflow tests. This instrumentation has been incorporated in a high pressure permeometer, capable of testing airflow through parachute cloths over the range of 0 to 1,000 in. of water pressure differential. The system described has been successfully used to characterize the flow-stress-strain behavior of selected standard and experimental fabrics. The work was conducted by Krizik, Victory, Cheatham and Backer, and is reported in WADC TR 57-443, December 1957 (Contract AF 33(616)-3253).

5.4.1 Materials Tested

Table 58 lists properties of the fabrics studied.

Approved for Public Release

Contrails

Table 58. Description of Test Parachute Fabrics

Fabric	Threads per Inch (W x F)	Weave	Yarn Denier (W x F)
E1 Nylon 100 lb/in. strength	72 x 71	Plain	105 x 107
E2 Nylon 200 lb/in. strength	68 x 72	2/2 R Twill	225 x 225
E3 Nylon 300 lb/in. strength	55 x 52	See note	520 x 521
E4 Nylon 400 lb/in. strength	41 x 41	2/2 R Twill	685 x 686
E5 Nylon 600 lb/in. strength	48 x 47	2 x 2 Basket	905 x 905
E6 Nylon 600 lb/in. strength	47 x 45	2 x 2 Basket	903 x 917
E7 Dacron 100 lb/in. strength	78 x 72	Plain	119 x 119
E8 Dacron 200 lb/in. strength	78 x 73	2 x 2 Basket	252 x 258
E9 Dacron 600 lb/in. strength	42 x 43	2 x 2 Basket	1246 x 1288
S1 Nylon Spec. MIL-C-7020 B (ASG) Type 1 Natural	123 x 117	Rip-stop	30 x 31
S2 Nylon Spec. MIL-C-7020 B (ASG) Type II Natural	125 x 70	2/1 L Twill	38 x 72
S3 Nylon Spec. MIL-C-7350 (ASG) Type I Natural	70 x 70	See note	106 x 104
S4 Nylon Spec. MIL-C-7350 (ASG) Type II Natural	51 x 52	See note	220 x 220
S5 Nylon Spec. MIL-C-8021 (ASG) Type I Natural	70 x 73	2/2 R Twill	225 x 227
S6 Nylon Spec. MIL-C-8021 (ASG) Type II Natural	53 x 47	See note	441 x 456

Note: Weave Designs:

E3	S3	S4	S6
OOXO	XOXOXO	OXOXOX	OXOXOX
OOOX	OXOOXX	XXXOXO	XXXOXO
OXOO	XOOXOO	OXOXOX	OXOXOX
XOOO	OOXOOX	XOXOXO	XOXOXO
	XXOOXO	OXOXXX	OXOXXX
	OXOXOX	XOXOXO	XOXOXO

X warp end up
O warp end down

Approved for Public Release

Contrails

5.4.2 Apparatus

The permeometer instrumentation was built to supplement fixed compressor and steam ejector equipment of the M.I.T. Gas Turbine Laboratory. The compressor was of 75 HP capacity furnishing 450 std cu ft of air at pressures up to 120 psi. The main steam ejector of the laboratory, operating with a 2-in. throat, is capable of drawing 0.9 lb air per second or 670 std cu ft per min from atmospheric conditions down to pressures of 7.5 psi.

The M.I.T. permeometer consists of an orifice metering unit and a cloth specimen clamp assembled in series with the compressor or the ejector, and with necessary duct work. A parallel-metering orifice system is placed between the compressor and the test duct. This system allows for continuous flow measurements over the range of air velocities required. The orifice plates (diameters 0.6 and 1.4 in., respectively) are mounted in standard 2-in. pipes with suitable pressure taps placed fore and aft according to A.S.M.E. metering standards. The fabric sample clamping device simultaneously holds the specimen across the test duct (without leakage) and permits measurement of load build-up in the fabric during airflow tests. Strain gages are used to measure the stress resulting from the air flow. Manometers are used to measure pressure drops across the test specimen and the orifice plates. To restrict air flow measurements to those areas of the fabric specimen where the state of the stress is uniform and measurable, a pliable membrane was used. This membrane is fabricated out of two 6x6-in. square 0.010 in. thick rubber sheets with a 1.25x1.25-in. opening in the center and one 3x3-in. piece of rubberized 3 ply Fortisan fabric with a 1.00x1.00-in. hole in its center. The Fortisan fabric is loosely placed between the two sheets of rubber, which are in turn jaw-clamped with the test fabric (at its upstream face). Thus when the membrane-cloth sample assembly is subjected to a static pressure the Fortisan fabric maintains a constant flow area while the two rubber sheets extend and conform with the profile of the test sample, making a tight air seal against it.

For the study of prestressing effects on air permeability another special device was designed. As constructed and assembled a cylinder allows air from the main test duct to impinge on the opening in the Fortisan masking shield, hence limiting the sample flow area, for this special case, to a 1-in. diameter circle. Meanwhile, independent control of air pressure in a sealed annular chamber allows one to prestress the diaphragm, hence to prestress the test sample.

Finally, a hydrostatic pressure testing device was designed. It allows separate and more complete measurement of fabric distortion under varying pressure differentials. In this device, the hydrostatic pressure is supplied by a nitrogen tank (2,500 psi) through a pressure regulator to a relief-valved ballast tank equipped with a calibrated pressure gage (0-100 psi $\pm$ 0.5%). Water present in the lower part of the ballast tank is connected through a solenoid valve and damping valve to the sealed clamp fixture. A rubber membrane prevents flow through the test fabric. A contour tracer assembly fastened to the same base plate as the clamp fixture, rises above the fabric specimen and permits direct plotting of fabric deformation under hydrostatic pressure.

5.4.3 Test Procedures

The program of stress-flow testing called for the evaluation of

Approved for Public Release

Contrails

the test fabrics over a range of 0 to 1,000 in. of water pressure differential. Specifically, it was required that data be furnished on air permeability versus biaxial load and elongation at air pressure differentials of 0.5, 1.0, 2.0, 4.0, 8.0, 16, 32, 64, 128, 250, 500, 750 and 1,000 in. of water. Each specimen was retained in the sample clamp and was subjected to a succession of increasing pressures to give a test run of the flow and stress-strain behavior over the range of pressure differentials which the specimen could withstand without rupturing. When the maximum pressure was reached, the flow was then reduced until the pressure differential fell to zero. The flow was increased to maximum pressure, then reduced again to zero, increased, etc., for ten cycles, finally being brought to the maximum level. The cycling took approximately 15 min in all. At maximum pressure, readings were taken as in the case of the successively increasing pressure tests and included:

a. Pressure differential across the orifice.
b. Pressure upstream at the orifice.
c. Pressure upstream of the fabric sample.
d. Initial fabric slope, warp and filling.
e. Local elongation, warp and filling.
f. Center deflection.

Load during these tests was recorded continuously and marks were made on the Sanborn Chart (or time scale) to identify the moment of pressure readings. The pressure differential was then reduced in five increments and readings taken at each level. In the later stages of the program the cycling data were shown to be in close agreement with a single return cycle test and the latter procedure was substituted.

5.4.4 Test Results

5.4.4.1 Effect of Pressure Differential Upon Air Flow. Figures 44 and 45 plot air flows at pressures up to 16 in. of water. Table 59 tabulates air flow data at pressures from 32 to 1,000 in. of water.

5.4.4.2 Effect of Air Density Upon Air Flow. The majority of tests reported at high pressure differentials use atmospheric pressure at the backside of the fabric. In actual parachute usage, high pressure differentials often occur at extremely high altitudes, hence with relatively low backside pressures. It is therefore important to know the influence of average air density on flow characteristics for given pressure differentials.

Tests of this nature required use of the steam ejector in series with the compressor. Two basic conditions were achieved for specimens S2, S3, S6, E3, E6 and E8. In one instance the backside pressure was atmospheric and the front side pressure varied so as to give pressure differentials from 100 to 600 in. of water. In the other case, the backside pressure was retained at 10 cm of Hg (absolute) and the frontside pressure was varied to give the same 100 to 600 in. of water pressure drop across the sample. The ratio of mass flows with the 10-cm backside pressure to mass flows with atmospheric backside pressure is given in Figure 46. Since the Reynolds number is the dimensionless product of density, diameter, velocity and inverse viscosity, the ratio of mass flows is equivalent to the ratio of Reynolds numbers over the given pressure differential range.

5.4.4.3 Effect of Fabric Pre-stressing on Air Flow. The equipment

Approved for Public Release

Contrails

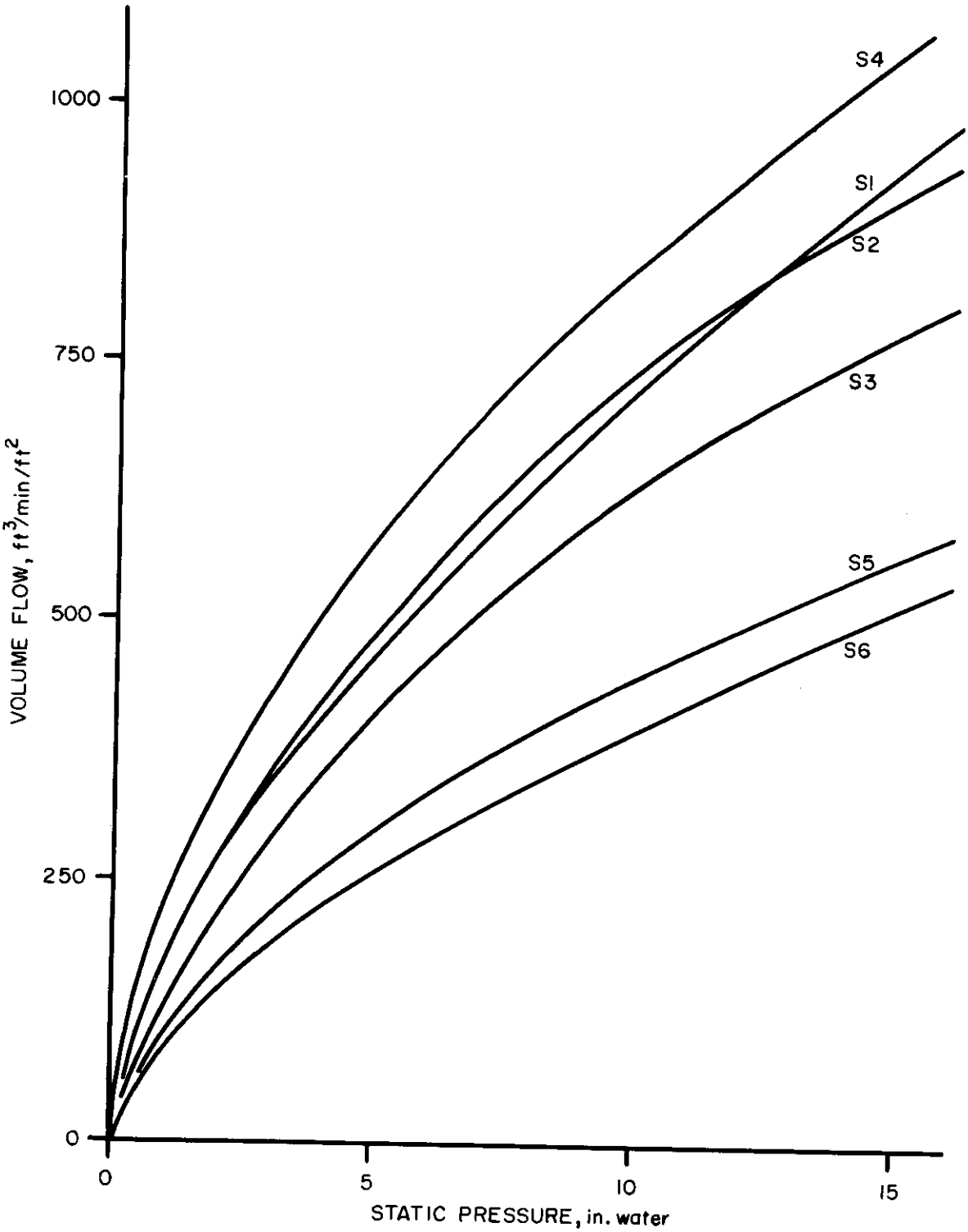

Figure 44 Volume Flow vs. Static Pressure Samples S1 - S6

Approved for Public Release

Contrails

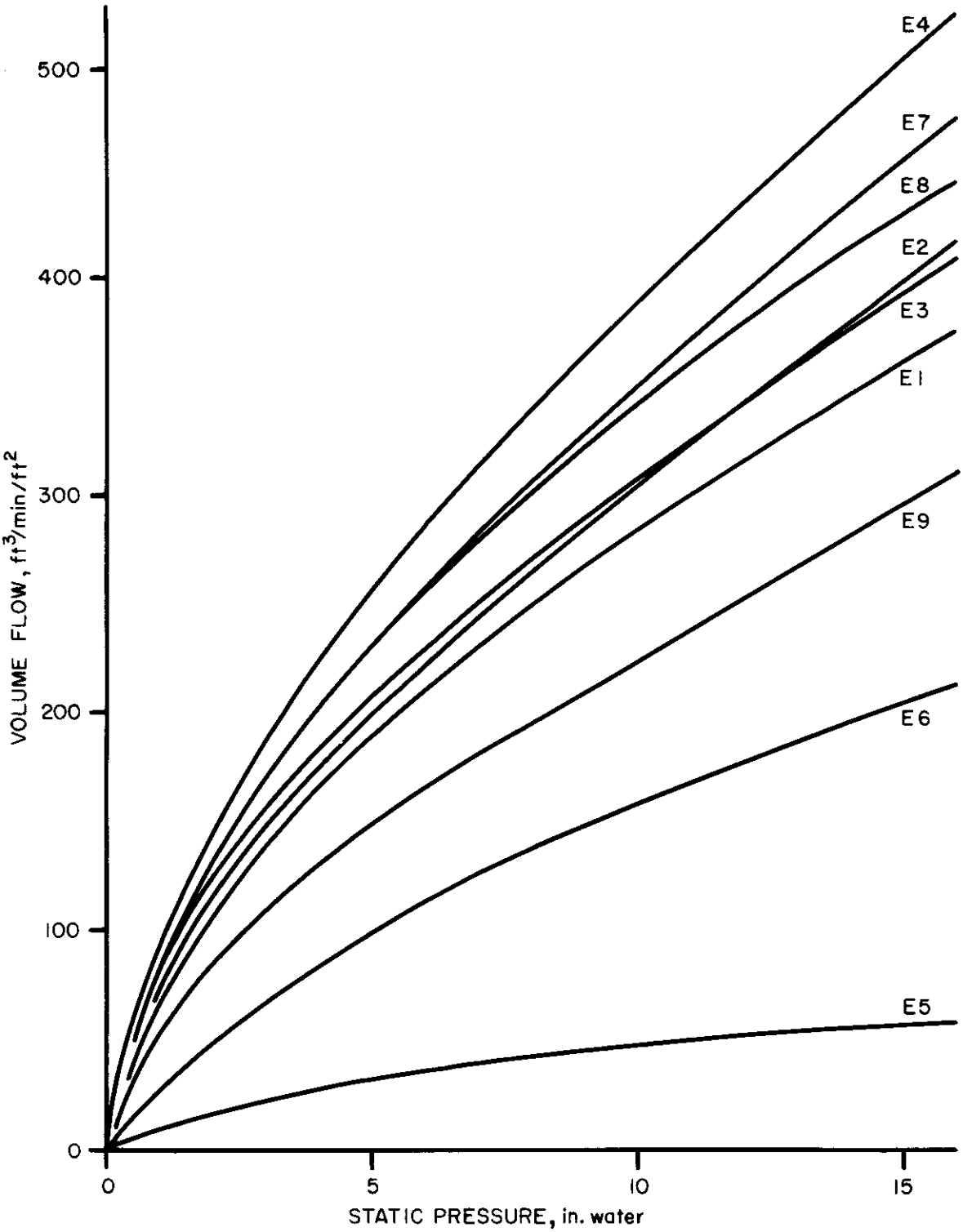

Figure 45 Volume Flow vs. Static Pressure Samples E1 - E9

Approved for Public Release

Contrails

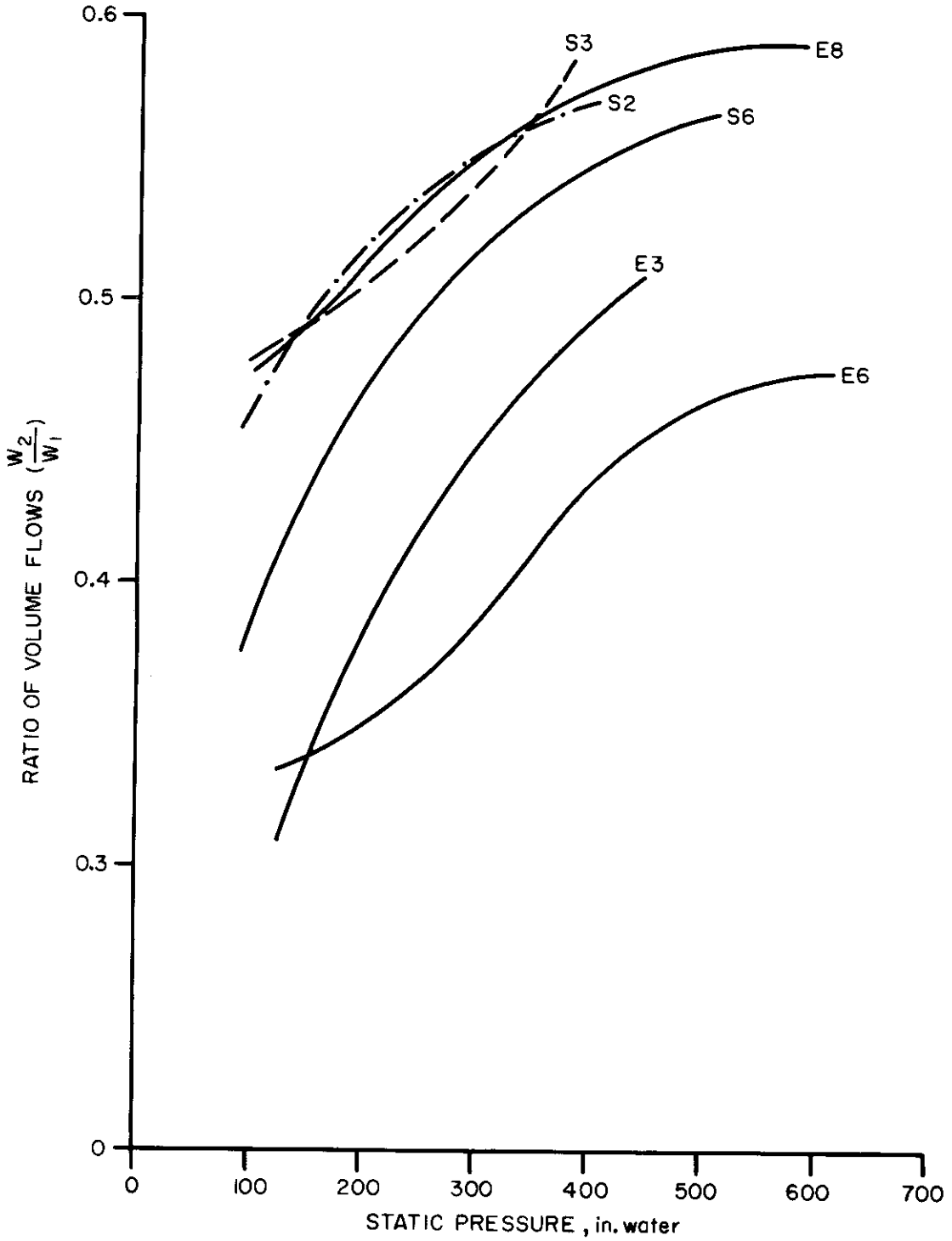

Figure 46 Ratio of Volume Flows vs. Static Pressure Various Samples

Approved for Public Release

Table 59. Summary of Permeometer Results

Static Pressure	Volume Flow	Load W	Load F	Strain W	Strain F	Center Deflection	Area Increase	Angle	Angle
in. water	$ft^3/min/ft^2$	lb/in.	lb/in.	in./in	in./in.	in.	%	θ	θ
Sample E1									
32	700	5.5	3.7	.011	.011	.225	1.20	13.0	14.5
64	1100	8.5	6.3	.022	.022	.390	3.00	19.0	20.5
128	1700	13.0	10.5	.042	.042	.510	5.70	26.5	29.5
250	2930	21.3	17.0	.072	.072	.670	11.30	36.0	39.5
Sample E2									
32	500	6.5	4.0	.010	.004	.202	.73	16.0	18.0
64	940	11.0	7.5	.015	.008	.275	1.50	19.0	23.0
128	1420	18.5	14.0	.022	.015	.375	3.10	26.0	28.5
250	2080	29.5	25.0	.035	.032	.502	6.20	34.0	37.0
500	3200	50.1	45.0	.054	.064	.680	11.00	43.5	48.5
Sample E3									
32	600	8.6	8.5	.0020	.0021	.165	.30	13.8	13.0
64	1000	14.5	12.0	.0030	.0034	.199	.65	17.0	16.0
128	1500	25.5	22.5	.0065	.0067	.245	1.51	19.5	19.5
250	2100	38.8	36.5	.0140	.0140	.320	3.10	23.5	25.6
500	3000	57.0	55.0	.0280	.0280	.453	6.40	32.0	34.5
750	4100	71.5	68.0	.0430	.0420	.586	9.70	40.5	39.0
1000	5200	90.0	83.0	.0580	.0558	.698	13.00	46.5	47.0

Approved for Public Release

Confidential

Table 59. Summary of Permeometer Results (Continued)

Static Pressure	Volume Flow	Load W	Load F	Strain W	Strain F	Center Deflection	Area Increase	Angle	Angle
in. water	$ft^3/min/ft^2$	lb/in.	lb/in.	in./in.	in./in.	in.	%	θ	
Sample E4									
32	1400	9.4	3.0	.0043	.0035	.230	.60	17.0	10.5
64	1800	17.0	6.0	.0078	.0058	.282	1.30	21.0	14.7
128	2300	27.0	11.0	.0150	.0120	.360	2.50	26.5	19.0
250	3200	43.0	22.0	.0310	.0235	.465	5.10	31.8	24.0
500	4720	65.0	39.0	.0620	.0475	.615	10.20	40.2	34.0
750	6400	85.0	50.0	.0920	.0750	.718	15.20	45.7	39.8
1000	8000	102.0	65.0	.1200	.0960	.805	20.00	50.9	44.5
Sample E5									
32	90	7.0	3.0	.0030	.0030	.150	.5	9.0	9.0
64	190	15.0	6.0	.0040	.0050	.210	1.0	15.5	20.0
128	390	23.0	10.5	.0090	.0085	.288	1.8	20.5	27.0
250	600	39.5	20.5	.0180	.0165	.365	3.5	25.5	32.0
500	920	60.0	38.8	.0370	.0330	.468	7.0	33.0	39.2
750	1200	82.0	56.5	.0550	.0500	.599	10.4	37.3	44.0
1000	1540	100.0	72.5	.0740	.0660	.680	13.9	40.5	50.5
Sample E6									
32	540	4.9	2.9	.0040	.0040	.165	.5	11.0	13.0
64	800	8.8	5.5	.0065	.0080	.232	1.0	14.5	17.5
128	1090	17.5	11.5	.0105	.0130	.305	2.0	18.5	21.5
250	1560	33.0	27.5	.0185	.0225	.395	4.0	23.0	26.5
500	2420	54.5	41.5	.0348	.0450	.520	7.8	33.0	34.5
750	3460	74.0	51.5	.0505	.0605	.605	11.8	38.8	40.0
1000	4150	92.5	71.5	.0615	.0780	.675	14.7	44.8	42.7
Sample E7									
32	920	8.2	4.0	.0040	.0040	.226	1.2	20.5	20.5
64	1140	14.0	8.3	.0070	.0070	.279	2.3	25.0	27.0
128	1680	20.7	13.5	.0130	.0130	.415	4.6	30.5	34.8
250	2442	27.5	19.5	.0365	.0365	.568	9.4	40.5	44.9
500	2920	40.5	31.0	.0820	.0820	.850	18.5	56.0	59.0

Approved for Public Release

Confidential

Table 59. Summary of Permeometer Results (Continued)

Static Pressure in.water	Volume Flow $ft^3/min/ft^2$	Load W lb/in.	Load F lb/in.	Strain W in./in.	Strain F in./in.	Center Deflection in.	Area Increase %	Angle θ	Angle θ
Sample E8									
32	650	5.5	3.5	.0020	.0020	.170	.50	6.5	8.0
64	1100	11.6	7.5	.0050	.0050	.215	1.20	9.0	13.0
128	1550	21.2	16.0	.0100	.0100	.275	2.10	14.5	17.5
250	2200	31.8	27.0	.0190	.0190	.370	4.05	20.5	24.0
500	3570	42.5	41.5	.0395	.0395	.550	8.20	30.5	35.0
750	5100	51.0	53.8	.0590	.0590	.705	12.20	40.0	44.0
1000	6700	58.0	68.0	.0780	.0780	.795	16.50	45.0	48.5
Sample E9									
32	920	9.0	4.0	.0005	.0005	.142	.12	13.9	15.0
64	1160	11.5	7.5	.0010	.0010	.180	.30	15.8	18.0
128	1310	29.1	14.0	.0030	.0032	.245	.70	18.5	22.5
250	1860	48.5	26.0	.0058	.0070	.305	1.40	22.5	27.5
500	2420	76.5	46.5	.0120	.0145	.390	2.88	23.5	28.9
750	3220	95.0	62.0	.0177	.0225	.465	4.34	32.5	37.0
1000	4040	--	76.0	.0240	.0303	.530	5.80	38.9	46.0
Sample S1									
32	1500	3.05	3.00	.017	.015	.310	2.1	14.5	20.0
64	2450	5.70	5.00	.035	.032	.500	4.6	23.0	27.5
128	4400	9.50	8.30	.064	.057	.670	12.0	36.5	44.5
250	6900	16.50	13.50	.097	.095	.785	20.0	45.0	55.5
Sample S2									
32	1450	4.50	3.0	.010	.010	.290	2.15	13.0	21.0
64	2100	8.00	5.5	.021	.023	.425	4.35	23.0	30.5
128	3202	13.50	10.6	.040	.043	.605	8.50	32.5	41.0
250	4800	21.50	19.0	.075	.087	.790	16.70	41.0	54.8
500	6200	34.00	31.5	.155	.165	.930	34.50	50.5	65.0

Approved for Public Release

Confidential

Table 59. Summary of Permeometer Results (Continued)

Static Pressure in. water	Volume Flow $ft^3/min/ft^2$	Load W lb/in.	Load F lb/in.	Strain W in./in.	Strain F in./in.	Center Deflection in.	Angle Increase %	Angle θ	Angle θ
Sample S3									
32	1470	5.50	3.5	.006	.006	.277	1.95	15.1	20.5
64	2050	9.00	6.2	.012	.012	.375	3.00	21.5	23.7
128	2900	13.00	9.5	.022	.023	.505	5.13	29.3	34.5
250	4670	23.50	17.5	.042	.046	.675	11.35	40.0	44.5
500	7070	41.50	31.5	.086	.090	.830	18.50	51.0	57.0
Sample S4									
32	2000	6.50	4.40	.0045	.0028	.245	0.90	16.50	19.40
64	2800	10.00	7.40	.0095	.0070	.319	1.80	22.00	24.10
128	4100	15.50	13.00	.0196	.0150	.422	3.70	28.50	30.80
250	5751	25.60	20.80	.0380	.0305	.578	7.18	37.00	39.80
500	7950	43.80	35.00	.0762	.0610	.782	14.20	46.50	52.50
Sample S5									
32	970	5.50	4.2	.0040	.0040	.250	0.6	10.5	15.50
64	1370	11.50	7.2	.0065	.0065	.305	1.2	20.5	21.50
128	1900	17.00	14.0	.0110	.0110	.395	2.2	26.5	28.50
250	2650	27.20	24.5	.0240	.0240	.530	4.7	35.0	37.50
500	3750	48.00	42.5	.0445	.0445	.700	9.5	46.5	49.00
750	4600	72.00	62.5	.0760	.0760	.805	16.1	53.5	56.00
Sample S6									
32	1270	4.5	3.5	.0020	.0020	.255	0.40	16.5	17.0
64	1720	10.0	7.0	.0065	.0065	.310	1.02	21.0	24.5
128	2360	18.0	12.5	.0120	.0120	.380	2.40	26.0	29.0
250	3370	27.5	23.0	.0235	.0235	.572	4.70	34.0	33.5
500	5000	47.0	40.5	.0480	.0480	.655	9.80	44.2	42.5
750	6750	70.9	61.0	.0770	.0770	.784	15.90	52.8	51.5
1000	8550	108.0	94.0	.1080	.1080	.890	22.00	59.5	60.0

Approved for Public Release

Confidential

Contrails

described for the prestress test is designed to permit independent variation of stress and pressure differential across the fabric. Test results obtained with such a device should be of value to the parachute designer who has on hand empirical data on fabric stresses and strains, and who wishes to correlate airflow behavior of a given cloth with stress and pressure differential data characteristic of that obtained in an actual chute. Six fabrics were tested with a pressure chamber prestress level equivalent of 100 in. of water. The pressure differential across the open fabric section was increased over a range of 0 to 140 in. of water. The fabrics tested were E1, E2, E3, S1, S2, and S3. Figure 47 shows typical curves for the relaxed and prestressed (PS) conditions.

If a similar set of curves were plotted for 200, 300, etc. to 1,000 in. of water the availability of air flow data depending on the two independent variables, pressure drop and stress, would then be realized. It is clear in these figures that air flow under prestress conditions significantly exceeds the air flow in the standard test.

A number of test combinations are possible with this device. The sample strain in the flow area can be kept constant for different pressure drops, by varying the chamber pressure. Or the flow, can within limits, be kept constant at different pressure drops by varying the chamber pressure.

5.4.5 Conclusions

A series of stress-flow studies have been conducted on a selection of standard and experimental parachute fabrics. Measurements of flow (in cubic feet of air, per square foot of fabric, per minute) have been reported in both tabular and graphical form. The basic independent variable in these tests was the pressure differential across the specimen. In addition, measurements of stress and area increase as determined by strain warpwise and filling-wise are reported.

The area increases have ranged from 5.8%, thus establishing firmly the magnitude of the pressure-stress effects on gross fabric geometry. Since air flow is specifically dependent on pore area rather than on gross fabric area, the changes specified above will have still greater effect on permeabilities. This follows from the fact that as the warp and filling yarns extend, the individual pore areas increase percentage-wise more than is indicated in the given 5 to 35% level. Offsetting this feature is the flattening tendency of individual yarns which reduces pore areas somewhat. The pore opening tendency is observed to be the dominant one. For if it were not, one would expect to find a choking taking place in the specimen pores at pore throat speeds corresponding to Mach number 1.0 and a flattening of the permeability-pressure curve. The Mach 1.0 speed should occur at a pressure ratio of 0.528 (aft pressure/fore pressure). The test conditions reported here include pressure ratios as low as 0.41. But in each case observed the permeability curve continues to rise at pressure ratios equal to or less than 0.528.

Parachute designers are faced with the difficult problem of extrapolating the behavior of a small specimen of fabric clamped rigidly in a permeometer to that of a large piece of parachute cloth held flexibly in a parachute canopy. The boundary conditions of the small specimen are critical in relating fabric stress to the pressure causing such a stress. One concludes

Approved for Public Release

Contrails

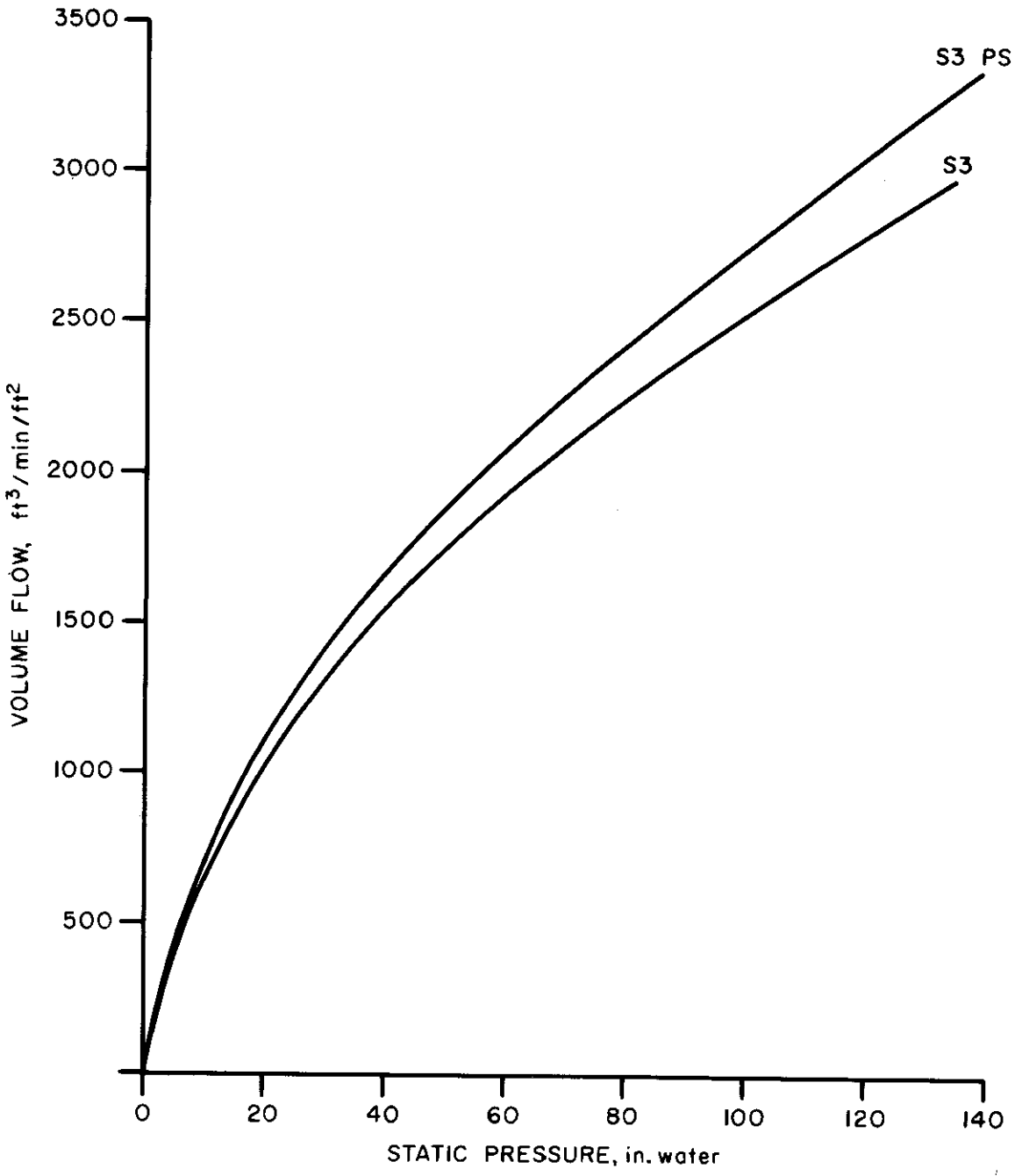

Figure 47 Volume Flow vs. Static Pressure Prestressed Sample S3

Approved for Public Release

Contrails

that there is too great a complexity of stress and strain in a given specimen to allow meaningful correlation of average specimen permeability and area distortion data. It remained to restrict the area of flow to a portion of the sample where stress and strain were essentially biaxial and uniform.

Restricting air flow by means of a membrane covering all but the center portion of the fabric raises several questions concerning the membrane effect. Questions related to effect of dynamic pressure, effect of the orifice discharge coefficient, equivalence of fabric loading and specimen center deflection have been considered. Calculations and some experimentation(with and without the membrane present) have shown the stress and strain influence of the membrane to be negligible. When flow is restricted to the center section of the specimen, the permeability is seen to be much higher than when flow takes place through the entire specimen. This follows from the fact that the center section is under maximum biaxial stress hence is the most porous part of the specimen.

The measurement of parachute cloth permeability at high levels of average pressure (and density) is unrealistic in terms of high altitude parachute work. The effect of densities on parachute permeabilities is by no means established. More tests reported to data have provided atmospheric pressure on the back side of the fabric and hence the pressure ratios and average pressures in test have been restricted in range. By introducing below atmosphere conditions behind the fabric, this study has allowed comparison of mass and volume flows at the same pressure drop but with different average densities. The density (or more specifically, the Reynolds number effect) is seen to be significant although the limited number of experiments does not allow generalization.

Local biaxial tensions of parachute cloth in a canopy are dependent on the pressure drop across the fabric and on local curvatures. In the small permeability test specimen the local curvature is related to pressure drop and sample geometry. It would be desirable to free the tensions and curvatures incurred during permeability testing from the effect of specimen geometry. Prestressing is one method of controlling the fabric stress and strain independently of pressure drops and specimen clamps. The prestressing data reported here merely show the magnitude of the effect present in certain specification and experimental fabrics and point the way to a complete characterization of fabric permeability with pressure drop and biaxial tensions as independent variables.

5.4.6 References

Sections 5.1, and 5.2, and WADD TR 60-584, pp. 191 to 234.

Approved for Public Release

Contrails

Section VI

SEWABILITY

6.1 Effect of Webbing and Sewing Thread Design, and Seam Types on Seam Efficiencies

A series of webbing seam specimens prepared with four different webbing or tape constructions, two types of threads and two seam types was tested for seam efficiences. The work was conducted by the WADC Materials Laboratory and is reported in WCLT 57-71, August 1957.

6.1.1 Materials Tested

Table 60 lists the seam samples prepared for test.

Table 60. Webbing Properties, Thread Types, and Seam Types

	Webbings (Experimental)						Tapes	
	A	B	C	D	E	F	G	H
Weave	*	*	*	*	*	*	Requirement same as MIL-T-5038, Type II	
Width (in.)	2	2	2	2	2	2		
Thickness (in.)	.028	.032	.023	.032	.023	.032		
Denier, W	420	420	210	420	210	420		
F	420	420	420	420	420	420		
Total ends	180/1	378/1	500/1	378/1	500/1	378/1		
Picks (per in.)	36	36	36	36	36	36		
Weight (oz/yd)	0.61	0.79	0.55	0.79	0.55	0.79		
Strength (lb)	1500	2000	1500	2000	1500	2000	1700	1700
Thread type	FF	FF	FF	3 Cord	FF	3 cord	FF	3 cord
Seam type	A	A	A	A	B	B	B	A

6.1.2 Test Procedure

Seam test samples (Fig. 48) were prepared according to Table 60 and tested for tensile strength and seam efficiency.

6.1.3 Test Results

Table 61 shows average seam strengths and efficiencies.

6.1.4 Conclusions

The highest seam efficiency (79.8%) was obtained with specimen "a." Specimens b, d, f have very nearly the same efficiency. If better efficiency is to be obtained with these webbings a revision in the seam design is necessary. Specimens c and e have the same efficiency. Since the warp for both g and h failed to break, it is possible that some improvement in efficiency can be

Approved for Public Release

Contrails

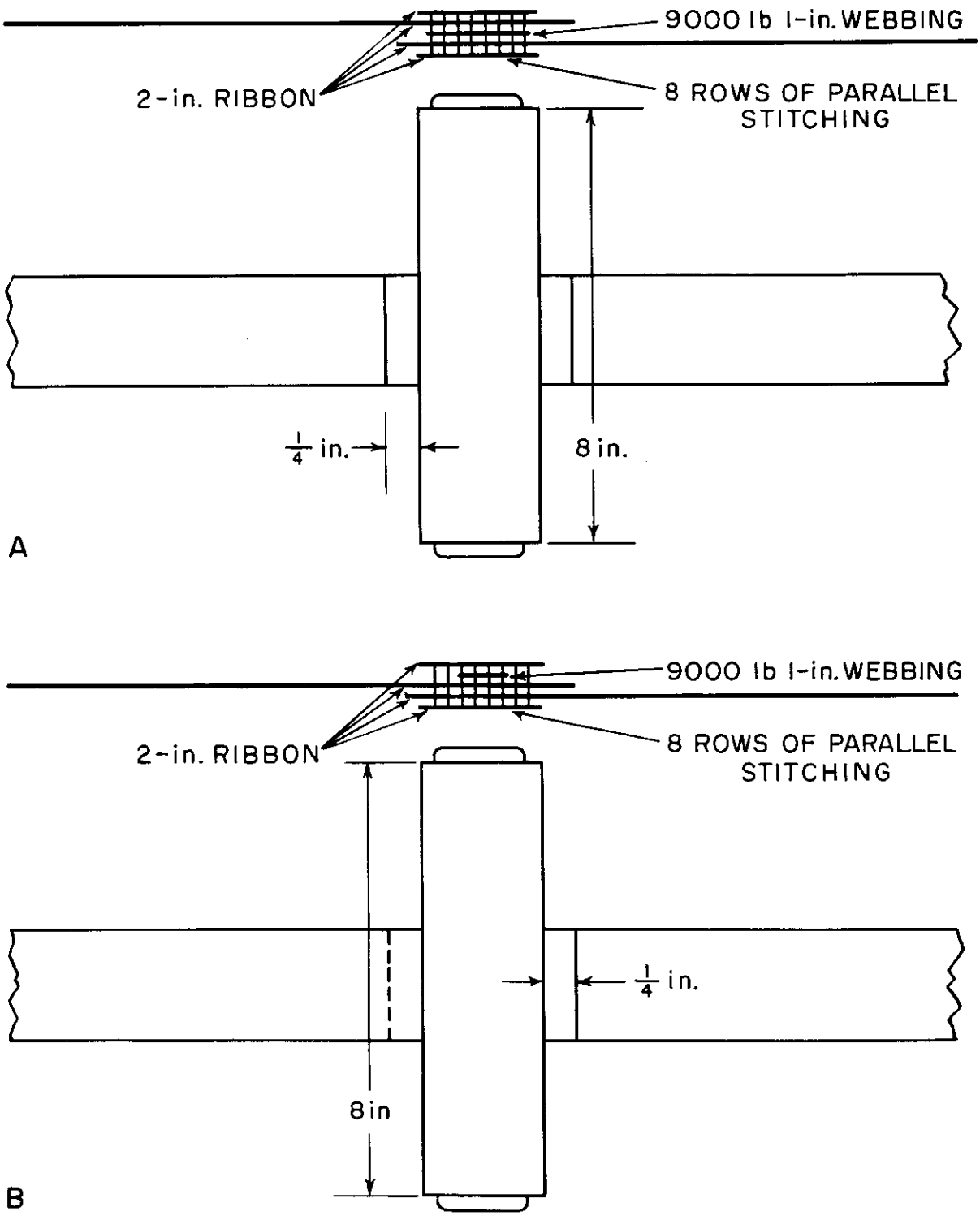

Figure 48 Stitching Patterns

Approved for Public Release

Contrails

Table 61. Average Seam Strengths and Efficiencies

	Strength (lb)		Efficiency (%)	Remarks
	Control*	Seamed Specimen		
(a)	1887	1505	79.8	Webbing broke at seam
(b)	2513	1433	57.0	Seam broke
(d)	2513	1564	62.2	Webbing broke at seam
(f)	2513	1520	60.4	Webbing broke at seam
(c)	1666	1245	74.7	Webbing broke at seams
(e)	1666	1247	74.8	Webbing broke at seams
(g)	2354	1336	56.8	Seam held but filling was stripped from warp
(h)	2354	1448	61.5	

*Control values are tensile tests on unsewn tapes or webbings.

achieved by finding a seam that will grip the warp more firmly.

6.1.5 References

WADD TR 60-584, pp. 244 to 328.

Approved for Public Release

Contrails

Section VII

SUNLIGHT AND WEATHER RESISTANCE

7.1 The Effect of Solar Radiation and Weather on the Breaking Strength of Outdoor Exposed Webbings

Sunlight, as one major factor in the exposure of textile materials to weathering, often is the cause of severe deterioration. Nylon is particularly susceptible. There is an increasing need for webbings with longer service life for use in aircraft runway barriers. A controlled series of outdoor exposure tests evaluating various types of Orlon and nylon in both natural and Olive Drab color, with and without ultraviolet protectors, was conducted at Dayton, Ohio (temperature, urban climate), Las Cruces, New Mexico (desert rural) and College, Alaska (sub-arctic rural). These sites were selected to provide a wide variety of amounts of solar radiation. Specimens were exposed for specified periods and were then tested for tensile strength retention. The program was conducted by WADC and is reported in WADC TR 58-201, November 1958.

7.1.1 Materials Tested

Fiber Types: Nylon Type 300 continuous filament, high tenacity bright yarn, natural and dyed Olive Drab.

Nylon Type 330 continuous filament, high tenacity bright yarn containing an ultraviolet inhibitor, natural and dyed Olive Drab.

Orlon continuous filament yarn, natural and dope dyed black.

7.1.2 Test Procedures

All specimens were installed on racks so that they were identically oriented at a 45-deg angle to ground level, facing south, and in such a manner that the center 18-in. portion of each webbing length was exposed to the sun's rays. Once the specimens were fastened to the racks they were not disturbed until their selected exposure periods had ended and it was time for their removal. Exposures continued for 360 days--from October 1955 to October 1956, with specimen series being removed at the end of 15, 30, 45, 60, 90, 120, 180, and 360 days. The total daily radiation in Langley units (g-cal/cm^2) was recorded at each site by use of a pyroheliometer. The approximate total dosages incident on 18x1-3/4-in. specimens for each exposure period are shown in Table 62.

After exposure the specimens were returned to the Materials Laboratory, conditioned and tested for breaking strength in an atmosphere of 65% ± 2% R.H. and 70° ± 2°F.

7.1.3 Test Results

Table 63 shows breaking strengths and percents of original strength retained for all samples under all conditions of treatment and exposure. (The original Technical Report WADC TR 58-201 plots comprehensive graphs of breaking strength and strength retention vs. days of

Approved for Public Release

Contrails

Sample	Webbings	Site and Sample
	MIL-W-4088B-XIX Webbings Woven From Type 300 Nylon Yarn	
1	Natural, Condition-U*	A1,® B1, C1
2	Natural, Condition-U* treated with catechol formaldehyde U. V. inhibitor	A2, B2, C2
3	Natural, Condition-R**	A3, B3, C3
4	Natural, Condition-R,**treated with catechol formaldehyde U. V. inhibitor	A4, B4, C4
5	Olive Drab, Condition-U*	A5, B5, C5
6	Olive Drab, Condition-U,* treated with catechol formaldehyde U. V. inhibitor	A6, B6, C6
7	Olive Drab, Condition-R**	A7, B7, C7
8	Olive Drab, Condition-R,** treated with catechol formaldehyde U. V. inhibitor	A8, B8, C8
	MIL-W-4088B-XIX Webbings Woven from Type 330 Nylon Yarn	
9	Natural, Condition-U*	A9, B9, C9
10	Natural, Condition-R**	A10, B10, C10
11	Olive Drab, Condition-U*	A11, B11, C11
12	Olive Drab, Condition-R**	A12, B12, C12
	Webbings Woven from Orlon Yarn	
13	4500 lb, Natural, Condition-U*	A13, B13, C13
14	4500 lb, Dope Dyed Black, Condition-U*	A14, B14, C14

*Condition U: No abrasion resisting resin finish.
**Condition R: Abrasion resisting resin finish.
®Site A, Dayton, Ohio.
Site B, Las Cruces, New Mexico.
Site C, College, Alaska.

Table 62. Exposure in Langleys

Exposure Period (days)	Total Langleys (g-cal x 10^4) Site A (Dayton)	Site B (Las Cruces)	Site C (College, Alaska)
15	105	198	31
30	203	395	63
45	294	588	102
60	375	726	120
90	518	1069	127
120	627	1335	160
180	769	1665	238
360	2589	4304	2296

exposure, and vs. amounts of solar radiation, but these are not included in this abstract since they can be derived from the data in Table 63.)

Effect of Webbing Weave: The nylon webbing of Specification MIL-W-4088B,

Approved for Public Release

Table 63. Webbings, Average Breaking Strengths and Percent Retention After Exposure

Sample	Webbing Description	Control (lb)	Number of Days Exposed (Dayton) Strength (lb) and Strength (%) Retained: 0 (lb)	15 days (lb)	15 days (% ret)	45 days (lb)	45 days (% ret)	90 days (lb)	90 days (% ret)	120 days (lb)	120 days (% ret)	180 days (lb)	180 days (% ret)	360 days (lb)	360 days (% ret)
A1	Nylon 300, Nat., U	10170	10099	99.3	8756	86.1	8154	81.2	6916	68.0	5540	54.5	1385	13.6
A2	Nylon 300, Nat., U,CF	10332	10258	99.3	10010	96.9	9876	95.6	9547	92.4	9058	87.6	6337	61.3
A3	Nylon 300, Nat., R	10209	10064	98.6	9445	92.5	9318	91.3	8875	86.9	7700	75.4	2654	26.0
A4	Nylon 300, Nat., R,CF	10688	10314	96.5	9852	92.2	9906	92.7	9469	88.6	8966[1]	83.9	5900	55.2
A5	Nylon 300, O.D., U	10207	10142	99.4	10195	99.9	10216	100.1	9979	97.2	9375	91.8	5788	56.7
A6	Nylon 300, O.D., U,CF	10149	10088	99.4	9725	95.8	10087	99.4	9399	92.6	9176	90.4	6853	67.5
A7	Nylon 300, O.D., R	10175	10395	102.2	9986	98.1	10087	99.1	9713	95.5	9219	90.6	6412	63.0
A8	Nylon 300, O.D., R,CF	10518	10378	98.7	10020	95.3	10015	95.2	9783	93.0	9612	91.4	7154	68.0
A9	Nylon 330, Nat., U	10199	9837	96.5	9940	97.5	9874	96.8	9609	94.2	9079[1]	89.0	5160	50.6
A10	Nylon 330, Nat., R	10129	9765	96.4	9949	98.2	9779	96.5	9537	94.2	9347	92.3	6056	59.8
A11	Nylon 330, O.D., U	9904	9800	98.9	10216	103.1	9718	98.1	9669	97.6	9317[1]	94.0	7456	75.3
A12	Nylon 330, O.D., R	10147	10204	100.6	9700	95.6	9602	94.6	9617	94.8	9204	90.7	6890	67.9
A13	Orlon, Nat., U	4917	4824	98.1	4956	100.8	4352	88.5	4749	96.6	4480	91.1	4113	83.6
A14	Orlon, Doped Black, U	4646	4689	100.9	4702	101.2	4114*	88.5	4575	98.5	4453	95.8	4350	93.6

Approved for Public Release

Confidential

Table 63. (Continued)

Number of Days Exposed (New Mexico)

Sample	Webbing Description	Average Breaking Strengths and Percents Retention After Exposure													
		0	15 days		45 days		90 days		120 days		180 days		360 days		
		Control (lb)	(lb)	(% ret)	(lb)	(% ret)	(lb)	(% ret)	(lb)	(% ret)	(lb)	(% ret)	(lb)	(% ret)	
B1	Nylon 300, Nat., U	10170	9272	91.2	8045	79.1	6198	60.9	5559	54.7	3579	35.2	1205	11.8	
B2	Nylon 300, Nat., U, CF	10332	10342	100.1	10353	100.2	9763	94.5	9272	89.7	8456	81.8	5353	59.8	
B3	Nylon 300 Nat., R	10209	9848	96.5	8582	84.1	8381	82.1	7781	76.2	5698	58.1	1815	17.7	
B4	Nylon 300, Nat., R, CF	10688	10283	96.2	9911	92.7	9283	86.9	8841	82.7	8192	76.6	4715	44.1	
B5	Nylon 300, O.D., U	10207	10142	99.4	10159	99.5	9816	96.2	9622	94.3	8354	81.8	4422	43.3	
B6	Nylon 300, O.D., U,CF	10149	10701	105.4	9964	98.2	9762	96.2	9427	92.8	8651	85.2	5595	55.0	
B7	Nylon 300, O.D., R	10175	10122	99.5	9906	97.4	9677	95.1	9602	94.4	8461	83.2	4798	47.1	
B8	Nylon 300, O.D., R,CF	10518	10229	97.3	10004	95.1	9708	92.3	9496	90.3	8024	76.3	6038	57.4	
B9	Nylon 300, Nat., U	10199	9927	97.3	9995	97.9	9465	92.8	9279	90.9	8689	85.2	5830	57.2	
B10	Nylon 330, Nat., R	10129	9948	98.2	9804	96.8	9864	97.4	9574	94.5	9322	92.0	6239	61.6	
B11	Nylon 330, O.D., U	9904	10291	103.9	10134	102.3	9715	98.1	9512	96.0	8676	87.6	5178	52.3	
B12	Nylon 330, O.D., R	10147	9839	96.9	9647	95.1	9140	90.1	9199	90.7	8221	81.0	4718	46.5	
B13	Orlon, Nat., U	4917	4839	98.4	4708	95.7	4888	99.4	4919	100.0	4952	100.7	4254	86.5	
B14	Orlon, Doped Black, U	4646	4657	100.2	4668	100.5	4703	101.2	4653	100.2	4687	100.9	4256	91.6	

Approved for Public Release

Confidential

Table 63. (Continued)

Number of Days Exposed (Alaska)
Strength (lb) and Strength (%) Retained

Sample	Webbing Description	0 Control (lb)	15 days (lb)	15 days (% ret)	45 days (lb)	45 days (% ret)	90 days (lb)	90 days (% ret)	120 days (lb)	120 days (% ret)	180 days (lb)	180 days (% ret)	360 days (lb)	360 days (% ret)
C1	Nylon 300, Nat., U	10170	9762	95.9	9941	97.7	9874[2]	97.2	9849[3]	96.9	9197[4]	90.4	2192	21.5
C2	Nylon 300, Nat., U,CF	10332	10040	97.2	10066	97.4	10261[2]	99.3	10134[3]	98.1	9702[4]	93.9	8101	78.4
C3	Nylon 300, Nat., R	10209	10050	98.4	10095	98.9	10044[2]	98.4	10162[3]	99.5	9672[4]	94.7	4976	49.0
C4	Nylon 300, Nat., R,CF	10688	10152	94.9	10348	96.8	10348[2]	96.8	10235[3]	95.8	9698[4]	90.7	7789	72.8
C5	Nylon 300, O.D., U	10207	9924	97.2	9979	97.8	10100[2]	98.9	9929	97.3	9372[4]	91.8	8350	81.8
C6	Nylon 300, O.D., U,CF	10149	10377	102.2	10338	101.9	10329[2]	101.8	10139[3]	99.9	9468[4]	93.3	8443	83.2
C7	Nylon 300, O.D., R	10175	10270	100.9	10032	98.6	10131[2]	99.6	10098	99.2	9791	96.2	8395	82.5
C8	Nylon 300, O.D., R,CF	10518	10187	96.9	10204	97.0	10284[2]	97.8	10020[3]	95.3	9879	93.9	8821	83.8
C9	Nylon 330, Nat., U	10199	9969	97.7	9879	96.9	9927[2]	97.3	9857[3]	96.6	9484	92.9	8517	83.5
C10	Nylon 330, Nat., R	10129	9948	98.2	10098	99.7	9937[2]	98.1	9745[3]	96.2	9544	94.2	8949	88.3
C11	Nylon 330, O.D., U	9904	10029	101.2	10092	101.8	9878[2]	99.7	9743	98.4	9480	95.7	9186	92.7
C12	Nylon 330, O.D., R	10147	9881	97.4	9732	95.9	9663[2]	95.2	9874[3]	97.3	9452	93.1	8719	85.9
C13	Orlon, Nat., Nat., U	4917	4882	99.3	5059	102.9	5034[2]	102.4	4885[3]	99.3	5055	102.8	4930	100.3
C14	Orlon, Doped Black, U	4646	4574	98.5	4658	100.3	4688[2]	100.9	4709[3]	101.4	4737	101.9	4624	99.5

U--No abrasion resisting finish.
R--Abrasion resisting finish.
CF--Catechol formaldehyde U. V. inhibitor.

*Samples inadvertently abraded by flapping against exposure rack.

1. Exposed 194 days.
2. Exposed 89 days.
3. Exposed 172 days.
4. Exposed 165 days

Approved for Public Release

Confidential

Contrails

Type XIX, has a weave that exposes all of the warp yarns to both the face and back surfaces of the webbing. Inasmuch as the warp yarns are the load bearing ones, the webbing weave as it influences the frequency of appearance of the warp yarns on the webbing surface, has a direct effect on the strength loss due to direct sunlight degradation. Therefore, the strength data presented in this report pertain only to the particular construction employed, and are not applicable to all nylon webbings. Of course, because the construction was held constant, the effect of fiber type, resin, finish, color, and U. V. inhibitor can be ascertained.

Strength Variability: The strength data in Table 63 show that some webbings after exposure have a higher breaking strength than the unexposed controls. This is explained by the 5-10% variability in webbing of this type.

Effect of Exposure Site: Table 62 shows that the largest amount of solar radiation (Langleys) was recorded at Site B (New Mexico). Of all three exposure sites the webbings exposed at Site B showed the least amount of strength retention after exposure. This was evident regardless of the type of yarn, color, condition or treatment of the webbing used. (Compare A vs. B vs. C respective samples.)

Comparison of Natural Type 300 vs. 330 Nylon: The samples made from Type 300 nylon yarn, natural color, Condition U and R showed the most strength loss after exposure. This was evident at all three exposure sites. When the samples of this webbing were woven with Type 330 nylon a substantial increase in strength retention after exposure was clearly noticeable. This increase was characteristic at all exposure sites. (Compare samples 1 vs. 9 and 3 vs. 10 for sites A, B, and C.)

Comparison of Olive Drab Type 300 vs. Type 330 Nylon: There are no natural colored nylon webbings used in aircraft runway barriers by the Air Force. Webbings used are Olive Drab (O. D.), Condition R, from Type 300 nylon yarn. The O. D. color produces a significant improvement in the degradation resistance of Type 300 nylon (compare 1 vs. 5 and 3 vs. 7 at A, B, C). With Type 330 nylon there is evidence of a possible superiority of the O. D. over the natural color (compare 9 vs. 11 and 10 vs. 12) but some reversals exist.

Comparing the standard Type 300 O. D. Condition R with the equivalent made from Type 330 nylon (7 vs. 12), no advantage in changing to the Type 330 is apparent.

Effect of Catechol Formaldehyde Inhibitor: The catechol formaldehyde causes a large improvement in the natural Type 300 nylon (1 vs. 2, 3, vs. 4). It causes a slight to nominal improvement in the O. D. Type 300 nylon, Conditions U and R (compare 5 vs. 6, 7 vs. 8). Since only O. D. webbing is used in the barriers, there is not enough improvement to warrant use of the catechol formaldehyde on the O. D. Type 300. The catechol formaldehyde was not applied to this Type 330 webbing.

Resistance of Orlon Webbings: Samples 13 and 14 (at Sites A, B, C) show that both the natural and black dope dyed Orlon exhibit good resistance to

Approved for Public Release

Contrails

weathering, but its tenacity is too low to permit its use for barrier webbings.

7.1.4 Conclusions

1. Natural color nylon webbings made from Type 300 yarns and without treatment of any kind have poor strength retention after exposure to solar radiation.

2. In resistance to sunlight degradation Type 330 nylon yarn is superior to Type 300 nylon yarn.

3. Catechol formaldehyde is a satisfactory sunlight inhibitor for nylon webbings made from Type 300 yarn, and shows to be more effective on the natural color nylon webbings than the O. D. color nylon webbings.

4. Olive Drab nylon webbings suffer considerably less degradation after exposure to solar radiation than natural color nylon webbings.

5. Continuous filament orlon webbings have very good resistance to sunlight degradation, but the yarn is no longer commercially available, and furthermore, webbing abrasion resistance is poor with no known treatment for improving it. Therefore, it is currently not suitable for runway barriers.

7.1.5 References

Sections 8, and 10, and WADD TR 60-584, pp. 2 to 8, 329 to 332.

7.2 Effect of Six Months Protected Outdoor Storage on the Breaking Strengths of Parachute Materials

One 24-ft and two 64-ft packed parachutes were stored out of doors under selected conditions of protection. After six months (from April through September) of such storage the textile components were tested for residual strength and comparison made with the specifications.

The work was conducted by Lt. C. F. Holmes, Jr., WADC Materials Laboratory and is reported in WCLT T-58-4, January 1958.

7.2.1 Materials Tested

Parachute I, Assembly 319398 (64 ft) was placed in a unit and covered with a canvas security cover which was supposed to be waterproof.

Parachute II, Assembly 391400 (64 ft) was placed in an uncovered shipping container.

Parachute III, Assembly 421628 (24 ft) was placed in a rubber covered sealed unit, which was then in turn covered with a canvas security cover which was supposed to be waterproof. The unit was not dessicated before sealing.

7.2.2 Test Procedures

The units containing the parachute assemblies were stored out of doors for 6 months under the following conditions of temperature and humidity:

Approved for Public Release

Contrails

Temperature

Month	Maximum	Minimum	Average
April	85	36	65.1
May	93	47	74.5
June	94	65	79.8
July	98	69	83.8
August	98	62	82.3
September	95	56	74.6

Relative Humidity

Ambient Relative Humidity %	April % of month	May % of month	June % of month	July % of month	August % of month	September % of month
90-100	30	19	30	30	9	39
80-90	20	22	20	23	19	25
70-80	16	17	16	15	17	14
50-70	19	30	30	28	32	29
30-50	15	12	4	4	23	3

The parachutes were then removed, and tested for residual strength.

7.2.3 Test Results

Table 64 lists breaking strengths after exposure, and compares the results with minimum strength specifications.

All average strengths are above the minimum specifications. Only two individual test specimens, as noted in the table failed to meet minimum specifications.

7.2.4 Conclusions

The exposure conditions did not cause strengths to drop below minimum strength requirements.

7.2.5 References

Sections 1.1, and 7, and WADD TR 60-584, pp. 2 to 4.

Approved for Public Release

Contrails

Table 64. Breaking Strength of Stored Parachute Materials

(Average of Five Tests)

Description	Specification Number	Strength Range (lb) (min)	(max)	(avg)	Strength Specification (lb) (min)
Parachutes 1 (64 ft)					
Shroud line ties	MIL-W-5665 Type I	398	418	411	350
Suspension line	MIL-W-5625 9/16 in.	1610	1610	1610*	1500
Suspension line	MIL-W-5626 1 in.	3830	3910	3848	3000
Radial seams	MIL-W-5625 1 in.	3890	4410	4150*	3000
Horizontal ribbons	MIL-R-5608 Type C-V	317	320	319	300
Vertical ribbons (ribbons were doubled and stitched together)	MIL-R-5608 Type C-III	207	235	221	90 (single ribbon)
Suspension line	MIL-W-4088 Type XVIII	6120	6270	6058**	6000
Horizontal ribbon	MIL-R-5608 Type E-II	1048	1160	1106	1000
Radial seams	MIL-W-4088 Type XVIII	8260	8280	8270*	6000
Parachute II (64 ft)					
Suspension line ties	MIL-W-5665 Type I	420	430	423	350
Suspension lines	MIL-W-4088 Type XVIII	6280	6310	6282	6000
Radial seams	MIL-W-4088 Type XVIII	8310	8560	8435*	6000
Horizontal ribbons	MIL-R-5608 Type E-II	1160	1210	1182	1000
Vertical ribbons (ribbons were doubled and stitched together)	MIL-R-5608 Type C-III	220	231	227	90 (single ribbon)
Parachute III (24 ft)					
Suspension line	MIL-W-5625 9/16 in.	1570	1590	1580*	1500
Suspension line	MIL-W-4088 Type XX	9260	9640	9457	9000
Radial seams	MIL-W-4088 Type XX	10280	11700	11164	9000
Horizontal ribbons	MIL-R-5608 Type E-II	1018	1162	1117	1000
Vertical ribbons stitched together (MIL-W-4088 Type I and MIL-R-5608 Type C-III)					
Tested according to Spec. MIL-R-5608		588**	622	607	590
Tested according to Spec. MIL-W-4088		650	675	662	590

*Two tests.

**One test out of five was below the minimum specification.

Approved for Public Release

Contrails

Section VIII

TEMPERATURE PROPERTIES

8.1 The Effect of Dead Loading and Low Temperature on the Elongation Characteristics of Nylon Braid

Nylon braid was dead loaded at forces ranging from 7 to 18% of rupture, and the resulting elongations determined with time. Tests were conducted at room temperature and at -76°F. The work was conducted by Lt. B. R. Fox, WADC Materials Laboratory and is reported in WCLT T-58-23, April 1958.

8.1.1 Materials Tested

Nylon braids, Specification MIL-C-7515A, Types IV and V.

8.1.2 Test Procedure

Standard Conditions Test (65% R.H. and 70°F): Vertically suspended lengths of braid, approximately 7 ft long were initially loaded with a 10-lb weight. One minute after loading two gage marks 36 in. apart were marked on the braid. This technique was used to establish an original fixed length.

The 10-lb weight was removed and a heavier test weight was applied, namely 70 lb for the 1,000-lb strength Type IV braid, and 276 lb for the 1,500-lb strength Type V braid. Distances between the gage marks were measured after 1 minute, and after 1/2, 1, 2 hr, etc. up to 4-1/2 hr.

Low Temperature Test (-76°F): At room temperature the specimens were originally marked under a 10-lb load exactly as described for the "Standard Conditions Test," above.

At Room Temperature: The 10-lb weights were removed and the 70- and 276-lb test weights, respectively, were applied. Distances between gage marks were measured at the end of 1 minute, 1/2, 1 and 2 hr. (Note that up to this point Standard Conditions prevailed.)

At the end of two hours the temperature in the test chamber was reduced to -76°F. This required about 15 min. Gage marks were then measured at the end of 2-1/2, 3, 3-1/2, 4, and 4-1/2 hr, counting time from the original applications of the test weights at room temperature.

8.1.3 Test Results

Table 65 tabulates percent elongations as a function of time.

8.1.4 Conclusions

There is a slight increase in elongation at the lower temperature. The order of magnitude is about 0.3 to 0.4 percent elongation. This difference, while possibly statistically significant, does not appear to be of any practical importance. It should be noted that because of the nature of the test, for both the "Standard Conditions Test" and the "Low Temperature Test," most of the elongation occurred at room conditions.

Approved for Public Release

Contrails

Table 65. Percent Elongation vs. Time For Nylon Braids Under Selected Dead Loads

Time	Type IV 1000-lb Braid 70-lb Dead Load				Type V 1500-lb Braid 276-lb Dead Load			
	70°F, 65% R.H.		70°F, 65% R.H.		70°F, 65% R.H.		70°F, 65% R.H.	
1 min	2.34		----		10.17		----	
1/2 hr	3.16		3.16		10.86		10.95	
1 hr	3.33		3.28		10.90		11.07	
2 hr	3.48		3.41		10.95		11.15	
2-1/2 hr	3.51		3.78		10.98		11.49	
3 hr	3.52		3.77		11.04		11.51	
3-1/2 hr	3.55		3.79		11.07		11.52	
4 hr	3.55		3.83		11.07		11.54	
4-1/2 hr	3.56		3.84		11.07		11.55	

8.1.5 References

None.

Approved for Public Release

Contrails

Section IX

CHEMICAL RESISTANCE

9.1 Effect of Duco Lacquer, 3661 Paint Thinner, on The Strength of Nylon Parachute Materials

Because parachute compartment cans may be cleaned with Duco Lacquer, 3661 Thinner, it was necessary to determine the effect of this chemical on the strength of nylon parachute ribbons. The work was conducted by WADC Materials Laboratory and is reported in WCRT T-57-14.

9.1.1 Materials Tested

Parachute ribbons Specification MIL-T-5608: Class E, Type 2, 2-in., 1,000-lb strength; Class C, Type 5, 2-in., 300-lb strength.

Duco Lacquer, 3661 Thinner.

9.1.2 Test Procedure

Specimens of the 300-lb ribbon were saturated with the thinner, immediately allowed to dry, and were then tested for tensile strength.

Specimens of each of the ribbons were immersed in thinner for three days, removed, allowed to dry, and were then tested for tensile strength.

9.1.3 Test Results

Table 66. Effect of Duco Lacquer, 3661 Paint Thinner, on the Strength of Nylon Ribbons

	1000-lb Ribbon		300-lb Ribbon	
	Strength (lb)	Strength Loss (%)	Strength (lb)	Strength Loss (%)
Control	1189.2	-	329	-
Saturated with thinner	Not tested	-	330	+0.3
Soaked 3 days in thinner	1175.6	1.1	318	3.3

9.1.4 Conclusions

Slight exposure of nylon materials in Duco Lacquer, 3661 Thinner, causes no strength loss in the materials tested.

Three-day soaking of the nylon materials in the same thinner will not cause appreciable strength loss in the materials tested.

9.1.5 References

WADD TR 60-584, pp. 428 to 454.

Approved for Public Release

Contrails

Section X

RADIATION PROPERTIES

10.1 The Effect of Thermal Radiation on Nylon Parachute Ribbons

A study of the effect of thermal radiation on the strength loss of nylon parachute ribbons was conducted by WADC Materials Laboratory, and is reported in Technical Memorandum TM-56-9, March 1956.

10.1.1 Materials Tested

1. Selected samples of Class E, Type II nylon ribbon, Specification MIL-T-5608 upon which were stamped blue ink stripes 1/8, 3/16 or 1/2 in. in width. Objective was to determine if the inked areas were more severely degraded by the radiation than were the un-inked areas.

2. Class E, Type II nylon ribbon, MIL-T-5608 having a double layer of Class C, Type III nylon ribbon MIL-T-5608 sewn perpendicularly to it with O. D. sewing thread.

3. The same as (2) above, except with white sewing thread.

10.1.2 Test Procedures

A carbon arc heat source was used to irradiate the samples with heat energies ranging from 5 to 25 cal/cm^2, the total amount being controlled by the length of exposure time. For example: Using a 25 cal/cm^2/sec source and exposing the specimen for 1/5 sec produced a total radiation of 5 cal/cm^2. Inked specimens were irradiated in the inked areas; sewn specimens were irradiated on the light ribbon at the intersection of the light and heavy ribbons. The maximum area of radiation was 1.1-in. diameter circle.

After irradiation all samples were tested for breaking strength. The seamed samples were tested as follows:

Series E and F: The heavy ribbon was placed in one jaw of the testing machine; the light ribbon in the other. This produced a shear type of break.

Series G, H, K and L: The light ribbon was subjected to a straight tensile pull, one end of the ribbon being fastened in each jaw.

10.1.3 Test Results

Visual inspection of exposed specimens showed that the following total calories/cm^2 are sufficient to destroy the specimens:

Ink striped specimens: 10-25 cal/cm^2 using a 25 cal/cm^2/sec heat energy source.

Series E (white) and F (O. D.) thread: Shear tensile; 10-25 cal/cm^2 using a 25 cal/cm^2/sec source.

Series G (white) and H (O. D.) thread: Straight tensile; 20-25 cal/cm^2

Approved for Public Release

Contrails

using a 5 cal/cm^2/sec source.

Series K (white) and L (O. D.) thread: Straight tensile; 15-25 cal/cm^2 using a 15 cal/cm^2/sec source.

Table 67 tabulates radiation exposure vs. resulting tensile or seam strengths.

Table 67. Effect of Thermal Radiation on the Strength of Ribbons and Ribbon Assemblies

Specimen Type Inked Strips: Radiation Source 25 cal/cm^2/sec	Average Strength (lb) for 1/8-, 3/16-, 1/2-, in. ink bands
Control	916
Radiated	
10 cal/cm^2	330
15 cal/cm^2	310
20 cal/cm^2	265
25 cal/cm^2	265

Seamed Ribbons: Shear Type Test	Strength (lb) 25-cal Source	
	O. D. Thread	White Thread
Control	50	60
Radiated		
5 cal/cm^2	35	58
10 cal/cm^2	40	40
15 cal/cm^2	40	50
20 cal/cm^2	30	40
25 cal/cm^2	30	25

Seamed Ribbons: Tensile Type Test	5-cal Source		15-cal Source	
	O. D.	White	O. D.	White
Control	215	200	215	200
Radiated				
5 cal/cm^2	217	210	212	198
10 cal/cm^2	213	190	203	199
15 cal/cm^2	201	218	137	158
20 cal/cm^2	181	187	138	140
25 cal/cm^2	126	172	127	152

Destruction occurred in lesser degree when the total radiation was lower than the quantities shown above. It was difficult to quantify the effect of lower amounts of radiation because the strength values were not conclusive.

The thermal radiation effect on a dark color such as the blue ink or the O. D. thread is much more severe than it is on a white color.

10.1.4 References

Approved for Public Release

Contrails

Sections 10.2, and 10.3 and WADD TR 60-584, pp. 2 to 8, 333 to 338, 360 to 369; WADC TR 55-264, pp. 105 to 156.

10.2 The Effect of Thermal Radiation on Nylon and Dacron Webbings

A study of the effect of thermal radiation on the strength loss of nylon and "Dacron" webbings is reported in WCRT T-56-20, April 1956. Specimens were exposed by the New York Naval Shipyard Materials Laboratory, and subsequent strength testing was conducted by WADC Materials Laboratory.

10.2.1 Materials Tested

Nylon Webbing: Specification MIL-W-4088B, Type XIII, O. D., Condition R (resin treated).

Dacron Webbing: Manufactured to meet nylon Specification MIL-W-4088B, Type XIII, white.

10.2.2 Test Procedure

A carbon arc heat source was used to irradiate the webbing specimens with radiation fluxes of 85, 42, or 20 cal/cm^2/sec. The principal purpose was to determine the radiant exposure capable of producing strength losses.

Phase I consisted of establishing the critical thermal energies necessary to initiate melting of the webbings. For these exposures 1-3/4-in. wide specimens were irradiated full width with a 2-mm band of radiation, until melting occurred.

Phase II consisted of exposing specimens to 125, 150, 175, and 200% of the critical radiation necessary for melting. The specimens were then tested for breaking strength loss.

10.2.3 Test Results

See Tables 68 and 69.

Table 68. Critical Thermal Energies Required for Initial Melting of Nylon and Dacron Type XIII Webbings

Radiation Flux (cal/cm^2/sec)	Total Radiation Required to Induce Melting (cal/cm^2)	
	Nylon (O. D.)	Dacron (white)
85	6.7	16.0
42	7.8	15.0
20	12.0	24.0

Using a radiation flux of 85 cal/cm^2/sec both the nylon and Dacron webbings were exposed up to 107 cal/cm^2 without completely melting through. The white Dacron ignited at 40 cal/cm^2 and continued to burn after the ex-

Approved for Public Release

Contrails

Table 69. Effect of Thermal Radiation on Breaking Strength of Nylon and Dacron Type XIII Webbings

Nylon			Dacron		
Total Radiation Exposure (cal/cm^2)	Breaking Strength (lb)	Percent Loss (%)	Total Radiation Exposure (cal/cm^2)	Breaking Strength (lb)	Percent Loss (%)
A. Radiation Flux 85 cal/cm^2/sec					
0 (control)	7492*	-	0 (Control)	7000*	-
6.7	5580	25.5	16.0	5560	20.5
8.4	4880	34.8	20.0	3480	50.2
10.0	3900	47.9	24.0	4460	36.2
11.8	3470	53.6	28.0	880	87.4
13.4	3520	53.0	32.0	1020	85.4
B. Radiation Flux 42 cal/cm^2/sec					
7.8	6600	11.9	15.0	4020	42.5
9.8	4780	36.1	18.8	6560	6.2
11.7	4070	45.6	22.5	4800	31.4
13.6	4050	45.9	26.2	3930	43.8
15.6	3280	56.2	30.0	2840	59.4
C. Radiation Flux 20 cal/cm^2/sec					
12.0	4740	36.7	24.0	6800	2.8
15.0	5440	27.3	30.0	7060	+0.8
18.0	3420	54.3	36.0	6170	11.8
21.0	3310	55.8	42.0	3370	51.8
24.0	3410	54.4	48.0	3180	54.5

*Average of five specimens; all other values are individual readings.

posure was terminated.

10.2.4 Conclusions

1. For both nylon and Dacron, at constant energy exposure (cal/cm^2), the lower the flux (cal/cm^2/sec) the less the strength loss.

2. At constant energy exposure (cal/cm^2) and constant flux (cal/cm^2/sec) the nylon sustains a greater strength loss than does the Dacron. This could be attributed to the color difference of the webbings.

10.2.5 References

Sections 10.3 and WADD TR 60-584, pp. 2 to 8,333 to 338; WADC TR 55-264, pp. 105 to 156.

10.3 The Effect of Thermal Radiation on Nylon Parachute Webbings, Lines, and Seams

Approved for Public Release

Contrails

A study of the effect of thermal radiation on the breaking strength of nylon tubular webbing, lines, and cloth seams, all containing manufacturer's marking threads, was conducted by WADC Materials Laboratory. Results are reported in WCLT T-58-87, December 1958.

10.3.1 Materials Tested

Nylon parachute cloth, MIL-C-7020, Type I and II, sewn into seam test samples according to Specification CCC-T-191b, Methods 5100 and 5110.

Nylon suspension line, MIL-C-5040, Type III.

Nylon tubular webbings, MIL-W-5625, one inch.

10.3.2 Test Procedures

All samples were subjected to a sufficient dosage of thermal radiation to cause the first signs of deterioration. Exposure was continued until the marker threads were completely deteriorated. The specimens were then tested for breaking strength. The tubular webbings, during radiation, were directly exposed or covered with one or two layers of nylon parachute cloth MIL-C-7020, Type II.

10.3.3 Test Results

See Table 70.

10.3.4 Conclusions and Recommendations

The amounts of radiation required to cause initial evidence of deterioration were insufficient to produce significant losses in strength or seam efficiency. At radiation dosages sufficient to completely deteriorate the marker threads, seam efficiencies and percent strength retentions were less as the color of the marker threads became darker. Thus the red and light green colors were superior to the dark blue and black colors.

The nylon parachute cloth offered protection to the tubular webbing as measured by an increased webbing strength retention.

It is recommended that all marker threads be removed from textile materials which might be subjected to thermal radiation.

10.3.5 References

Sections 10.1, and 10.2; WADD TR 60-584, pp. 2 to 8, 333 to 338; WADC TR 55-264, pp. 105 to 154.

10.4 Effect of Thermonuclear Radiation on Parachute Textile Components

Selected parachutes which were exposed to thermonuclear radiation were then returned to WADD where textile components were tested for air permeability, breaking strength and elongation. The parachutes, manufactured by Pioneer Parachute Company were originally identified by serial numbers. In several instances, however, the serial numbers and panel numbers were "burned"

Approved for Public Release

Contrails

Table 70. Properties of Thermally Radiated Samples

Fabric Seam Efficiencies

Marker Threads	Amount of Radiation (cal/cm²)	Seam Efficiency Before Radiation (%)	Seam Efficiency After Radiation (%)
None*	33	89.6	50.9
None*	44	68.3	41.3
1 red-1 green*	33	91.4	47.6
1 red-1 green*	44	80.9	43.0
2 blue*	33	56.6	46.8
2 blue*	44	72.0	31.1
None**	33	93.5	49.5
None**	44	91.4	46.4

Suspension Lines

Marker Threads	Amount of Radiation (cal/cm²)	Strength Retention After Radiation (%)
None	44	65.5
None	55	44.9
Blue and black	44	75.4
Blue and black	55	36.4

Tubular Webbings

Number of MIL-C-7020-II Fabric Layers Covering Webbing During Radiation	Amount of Radiation (cal/cm²)	Strength Retention After Radiation
None	27	50.1
None	31.5	41.3
1 layer	27.0	42.2
1 layer	39.0	43.1
2 layers	28.5	41.6
2 layers	42.0	40.1

*MIL-C-7020, Type II.
**MIL-C-7020, Type I.

out and not identifiable. Information concerning the actual parachute drops was not available. The test program was conducted by J. McGrath, and is reported in WCRT T55-61, November 1955.

10.4.1 Test Procedure

After thermonuclear exposure, sections of parachute fabric, ribbon and suspension lines were tested according to the following specifications:

Nylon Fabric: Specification MIL-C-7020, Type I. Tested for air permeability, breaking strength and elongation.

Nylon Ribbon: From Fist Ribbon Parachute, Specification MIL-T-5608, tested for breaking strength.

Approved for Public Release

Contrails

Nylon Suspension Line: Specification MIL-C-5040, Type III, tested for breaking strength and elongation.

10.4.2 Test Results

Tables 71 and 72 list properties of the various components in comparison with original specifications.

Table 71. Properties of Nylon Fabric Specification MIL-C-7020, Type I After Exposure to Thermonuclear Radiation

	Specification	Range of Test Results
Breaking Strength		
Warp (lb/in.)	40 (min)	36.1-42.3(a)
Filling (lb/in.)	40 (min)	27.0-40.6(b)
Elongation		
Warp (%)	22 (min)	20.7-29.6(c)
Filling (%)	22 (min)	25.7-34.3(d)
Air Permeability $ft^3/min/ft^2$	80-120	89-124(e)

(a) Of 90 test specimens, 60 were below the 40-lb warp minimum, i.e., they fell between 36.1 and 39.9. Thirty specimens were above the 40-lb minimum.
(b) Of 90 test specimens, 87 were below the 40-lb filling minimum.
(c) Of 90 test specimens, all but 8 exceeded the 22%-warp minimum.
(d) Of 90 test specimens, all exceeded the 22%-filling minimum.
(e) Of 65 test specimens, 2 specimens exceeded the upper limit of 120 $ft^3/min/ft^2$. All others fell within the specification limits.

Table 72. Breaking Strength of Nylon Ribbon, Specification MIL-T-5608

Specification	Range
300 lb	192-273

Of 16 specimens tested, all failed to meet the minimum specification of 300 lb.

Breaking Strength and Elongation of Suspension Time
Specification MIL-C-5040, Type III

Breaking Strength (lb)	Elongation (%)
452	23.6
427	28.0
200	20.6

All samples failed to meet the 550-lb and 30% minimum strength and elongation.

Approved for Public Release

Contrails

10.4.3 Conclusions

Very few breaking strength results meet the requirements of Specification MIL-C-7020, Type I for either the warp or filling. However, breaking strengths of fabric from the damaged parachutes were as high as for those from undamaged parachutes. The air permeability of the parachute fabric apparently was not affected by the drop tests. Only two sections from all the parachutes tested failed to meet specification requirements. Breaking strengths of ribbons and suspension lines failed to meet specification requirements in all cases.

10.4.4 References

Sections 10.1, 10.2, and 10.3.

Approved for Public Release

Contrails

Section XI

AERODYNAMIC HEATING

11.1 Aerodynamic Heating-Rate Calculations for Nylon Parachute Ribbons

The construction of a deceleration device to function at high Mach numbers in the region of approximately 100,000 ft poses some very stringent material requirements. The material used to construct such a device not only must be able to withstand the severe shock of deployment at high speeds but also must be able to endure the temperatures that result from aerodynamic heating (the conversion of the relative kinetic energy of the air into thermal energy). The mechanical requirements could be met quite easily with existing materials and parachute configurations. The opening of a high speed parachute under the aforementioned conditions does not pose serious difficulty. After opening, however, the thermal problem comes into play.

The temperatures to which the parachute is exposed can be calculated from thermodynamic relations:

$$T_o = T_1 \left[1 + \left(\frac{\gamma - 1}{2}\right) M^2\right] \qquad (1)$$

where T_o is the stagnation temperature (temperature due to aerodynamic compression); T_1 is the ambient temperature; γ is the ratio of specific heats and M is the Mach number (ratio of the speed to the local speed of sound).

The results of such a calculation are presented in Figure 49 as a plot of stagnation temperature vs. Mach number for 100,000 ft pressure altitude on an NACA standard day. As can be seen, the stagnation temperature at Mach 5 and 100,000 ft is 2060°F. This value is above the softening point of most commercially available metals and vastly greater than the softening points of almost all textile materials. In fact, the only materials capable of enduring such a temperature are some of the refractory metals and ceramics. At present, the technology of metallic and ceramic fibers has not advanced to the stage where they are available to the parachute builder. This means that the parachute material must be protected from its thermal environment to remain below its softening temperature. In the case of nylon this means it must be kept below 350°F.

Methods for keeping nylon parachute components at functional temperatures have been examined by A. L. Ruoff, S. W. Lin and F. Frank. They prepared comprehensive calculations of heat transfer rates to nylon parachute ribbons and webbings, and then considered the theoretically potential utilization of water, selected hydrated inorganic salts and selected organic and inorganic compounds which, via evaporation or sublimation, would maintain the nylon at a functional temperature.

This analysis was conducted by Ruoff and co-workers, Cornell University, and is reported in WADC TR 57-157, December 1957.

11.1.1 Materials Investigated

Nylon parachute ribbons and webbings.

Approved for Public Release

Contrails

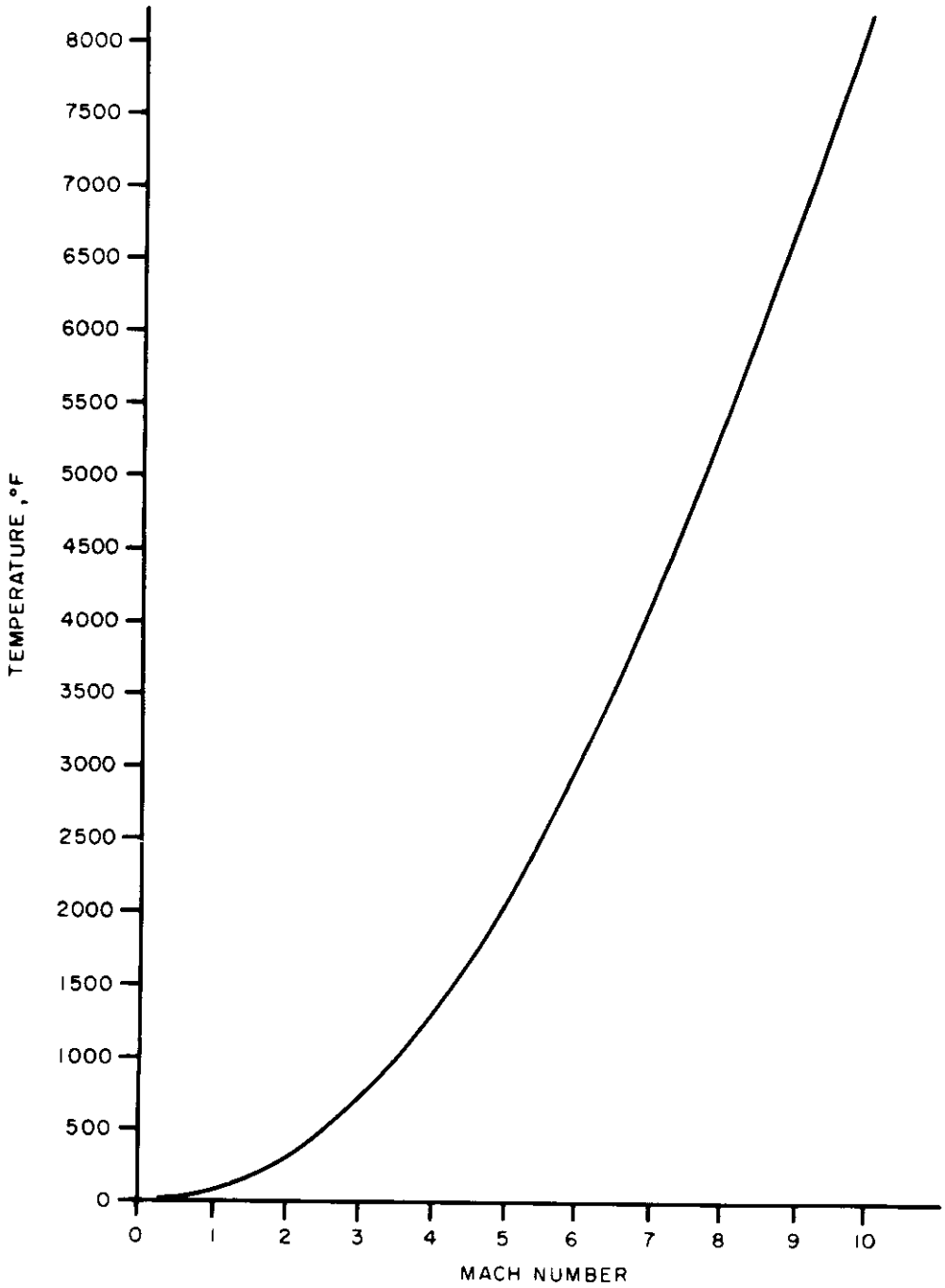

Figure 49 Stagnation Temperature in Degrees Fahrenheit vs. Mach number at 100,000 ft

Approved for Public Release

Contrails

Many organic and inorganic compounds of selected melting and boiling points.

Many hydrated inorganic salts (with high waters of crystallization).

11.1.2 Theoretical Analysis

The first part of the study is concerned primarily with the calculation of heat transfer rates to the parachute ribbons and webbings. Specific calculations were made for velocities at 5 Mach and 100,000 ft altitude. Under these conditions, calculations of the heating rate at the forward stagnation point of a ribbon with a semi-circular leading edge gave a value of 67.8 $Btu/ft^2/sec$ for a 1/16-in. thick ribbon. For a 1/4-in. thick webbing the value is half the above.

When a parachute, considered to be a hemispherical shell of very small permeability P, is subjected to supersonic stream flow at 5 Mach and 100,000 ft, the maximum heat input is calculated as (2.68 + 793P) $Btu/ft^2/min$ where P = $ft^3/ft^2/sec$ airflow at a given pressure difference. This equation holds only as P approaches zero, because it is only under these conditions that turbulence is insured, and one can expect the gas particles to leave the parachute at essentially the surface temperature of the cloth. As the permeability P increases there will be a tendency for streamlines to be set up in the vicinity of the cloth and so the above equation greatly overestimates the heat transfer rate. As the geometrical porosity increases, a critical value is reached (other conditions being kept constant) after which the shock over the entire front opening of the shell can no longer be maintained; then the flow in the shell becomes supersonic. The critical permeability in the case considered is calculated to be 43.9 $ft^3/ft^2/sec$. On the basis of data available this type of shock would not be present for MIL-C-8020, Type II, at 5 Mach and 100,000 ft in a hemispherical parachute. When the flow through the cloth becomes supersonic the flat plate model should apply but with the restrictions that we must use the throat condition in our calculations. In the case of the high permeabilities such as occur in practice it is reasonable to assume that a laminar flow pattern occurs in the vicinity of the cloth; this means that in the roof of the parachute (in the case of a ribbon parachute) a region of stagnant air would exist over the faces of the ribbons which are nearly perpendicular to the flow. Since the thermal conductivity of air is low, the heating over the face of these particular webbings would not be critical. The critical heating would occur at the edges in the roof webbings. Calculations using the flat plate (with the flow now along the thin edge of the webbing and normal to the large area) with the proper throat conditions should give a very valid estimate here. The complete calculations of heating rates and possible coatings rest on the availability of velocity-time data for a given parachute. Calculations suggest that continued flight at 5 Mach and 100,000 ft for 60 sec gives difficult but not insurmountable heating problems.

11.1.3 Consideration of Utilization of Coatings

Calculations using the flat plate theory show the average rate of heat input for a webbing located at the leading edge. To protect this webbing (one-half strength or more at end of 60 sec) it would be necessary to have a permanent coating, with the same diffusivity as the webbing, as thick as

Approved for Public Release

Contrails

the nylon webbing itself on each side of the flat plate. The surface of this permanent coating would reach about 1000°F. A more rigorous calculation of this leading webbing would take into account the finite thickness of the leading edge using the theory of the forward stagnation point. It is to be pointed out here that the heating will be more critical in the case of the thin ribbons and less critical in the case of thicker webbings, both with respect to the forward stagnation point and the averaged value for the flat plate.

Mass transfer calculations are based on the greatly simplified model in which we ignore air-vapor interaction. Since the rate of evaporation would have to be high so that the nylon remains below 350°F a complete analysis even in the case of the flat plate would not allow the usual approximation of constant pressure and would also include thermal diffusion. Under these conditions we have a set of non-linear linked simultaneous equations. The theoretical analysis becomes extremely involved except in a few simplifying cases. Therefore experimental analysis should be initiated to ascertain the effectiveness of coatings.

11.1.4 Consideration of Types of Coatings

Permanent Coatings: A suitable material should have a low conductivity, high temperature resistance and a low modulus of elasticity. In addition, it should not become tacky and should adhere to fabric.

A material that satisfies the thermal properties is Dow Silicone Foam R-7002 which is manufactured by the Dow Chemical Corporation, Midland, Michigan. This material is, however, rigid. The diffusivity of the Silicone Foam is actually about one-third that of the nylon; hence, if a material possessing similar properties were used for a coating, the protection given would be much better than calculated.

Non-Permanent Coatings: Coatings may be of a non-permanent solid or liquid type which will vaporize or evaporate in use, thus carrying off heat. Since, in this analysis, no laboratory work was conducted, one can only opine on the most promising compounds. Over 250 organic and inorganic compounds are listed (in the original report) which because of their boiling points, melting points, water of hydration, and heats of vaporization might be effective for nylon. Table 73 lists those compounds that appear most promising in terms of melting range and heat of vaporization.

Calculations show that a layer of water 0.06-in. thick applied to each side of a parachute would protect it for 60 sec at 5 Mach. At the high velocities encountered it is doubtful whether any water at all could be retained on the surface. However, a coating of absorbent foam capable of holding the water is suggested for an experimental try.

Highly conducting metal films, for example Woods' metal (50% Bi, 27% Pb, 13% Sn, 10% Cd) might also be effective.

11.1.5 Conclusions

Theoretical calculations indicate that the heat deterioration of nylon due to aerodynamic heating may be prevented by using water, volatile

Approved for Public Release

Contrails

Table 73. Listing of Compounds Falling in the Allowable Melting Range Which Meet the Vapor Pressure Requirements

Name of Compound	Melting Point (°C)	Boiling Point (°C)	Heat of Vaporization* (Btu/lb)
Anthracene	216.18	339.77	99
Benzoic acid	122.3	250	283
Borneol	208.6	subl	177
Hexachlorethane	186	subl	94
Methyl fumarate	102	193.25	147
Naphthalene	80.27	217.96	155
Nitrophenol (p)	113.4	subl	174
Octane (2233 tetramethylbutane)	100.7	106.3	141
Ortho-hydroxbenzoic acid	158.3	-----	246 (200°C)
Phenanthrene	100.5	-----	161 (230°C)
Quinol	172.3	-----	414 (160°C)
Succinic acid	182	-----	257 (40°C)

*Heat of vaporization at 100°C except when noted.

solids, volatile liquids or metallic coatings. It is proposed that experimental work be initiated to determine the efficacy of selected coatings.

11.1.6 References

Section 11.2 and WADD TR 60-584, pp. 333 to 338; WADC TR 55-264, pp. 154 to 156.

11.2 Mass Transfer Cooling of Parachute Ribbons

Continuing the work discussed in Section 11.1 above, experiments were conducted to evaluate the ability of selected organic compound non-permanent type coatings to melt and sublime, thus absorbing heat and preventing the nylon parachute materials from reaching fusion or deterioration temperatures. The work was carried out by R. H. Cornish and co-workers at Cornell University and is reported in WADC TR 58-684, September 1957.

11.2.1 Materials Tested

Thirty-nine organic coating compounds were originally considered, and of these, for reasons of commercial availability, experimental efforts were confined to the following: hexachloroethane, methyl anthraquinone, chloroanthraquinone, hydroxy anthraquinone, and camphene.

Nylon ribbon Specification MIL-T-5608E, Type II.

11.2.2 Test Procedures

Ribbon specimens were coated with the various candidate compounds

Approved for Public Release

Contrails

and were then subjected to a Mach 5 air stream at a pressure equivalent to an altitude of 100,000 ft and stagnation temperatures of 750-900°F. This work was carried out using the E-2 wind tunnel at Arnold Engineering Development Center, Tullahoma, Tennessee.

Coating Techniques: Several coating techniques were tried; no one method was successful for all compound applications. The methods used were:

1. Solution Coating: The compound was dissolved in a suitable solvent, the nylon ribbon immersed, and the solvent evaporated. Any desired thickness was obtained by successive dippings. This method was used to apply hexachloroethane in hot carbon tetrachloride.

2. Direct Melting and Application: The compound was melted and the nylon dipped in the melt. The method was successful for the application of camphene in spite of large losses due to vaporization.

3. Vapor Coating: Hexachloroethane and chloroanthraquinone were applied by exposing the nylon to heavy clouds of vapor.

The nylon specimens were weighed before and after coating to determine the percent weight pickup. Those specimens with coatings which were easily sublimable at room temperature were stored and shipped while packed in dry ice.

Instrumentation: Each test specimen had five copper-constantan thermocouples inserted so that they ran from front to back at the center of the specimen, the distance between thermocouples being 3/8 in. To measure as closely as possible the temperature of the nylon itself, the thermocouples were inserted into the ribbons before coating.

The specimens were inserted into a clamp or jig which, in turn, was installed in the wind tunnel. In this way each specimen was oriented so that its flat surface was parallel to the direction of air flow. The thermocouple leads were connected to a recorder which indicated temperatures at the five points on the specimen, the record being a plot of temperature vs. time. A high speed movie camera was employed to observe when ribbon melting occurred. The times of initial melting, one-third, two-thirds, and total failure were determined. Failure was defined as that time when any part of the ribbon receded to the indicated point, i.e., two-thirds of failure is that time when the lead edge of the ribbon has receded to a position two-thirds of the distance from the leading edge to the trailing edge. Graphs of time in seconds vs. extent of failure were plotted.

11.2.3 Test Results

Tables 74 and 75 list the effect of the various organic compounds on heating rates and on times to cause progressive ribbon failures. Obviously the lower the heating rate, and the longer the time required to cause failure, the more effective the coating. Table 76 tabulates lifetime augmentations.

11.2.4 Conclusions

Approved for Public Release

Contrails

Table 74. Initial Heating Rates vs. Thermocouple Positions Nylon Ribbon*

Coating	Coating Weight (oz/yd)	Leading Edge	Heating Rate (°F/sec) Thermocouple Position 1	3	5	Trailing Edge
Bare nylon	0	1325	1250	775	450	325
Hexachloroethane	6.46	190	160	75	60	60
Hexachloroethane	2.53	30	30	40	40	40
Chloroanthraquinone	.270	1075	1050	900	825	800
Chloroanthraquinone	.305	350	325	190	100	60
Chloroanthraquinone	.57	50	50	40	30	30
Methyl anthraquinone	.335	660	625	390	220	190
Methyl anthraquinone	.863	125	110	60	50	50

*Data taken from illustrations in original report, WADC TR 58-684.

Table 75. Time to Cause Progressive Failure*

Coating	Coating Weight	Time (sec) Initial Melting	1/3 Failure	2/3 Failure	Total Failure
Bare nylon	0	0.5	1.0	1.7	2.1
Hexachloroethane	0.15	0.7	1.3	2.0	2.6
Hexachloroethane	1.18	0.6	1.2	2.0	2.3
Hexachloroethane	2.62	1.9	4.6	6.1	7.9
Chloroanthraquinone	0.33	0.7	1.8	3.0	4.0
Chloroanthraquinone	0.65	0.7	2.4	3.5	5.0
Chloroanthraquinone	1.18	0.5	5.0	7.2	9.3
Methyl anthraquinone	0.29	0.8	1.3	2.5	3.0
Methyl anthraquinone	0.48	0.8	3.2	5.2	7.0
Methyl anthraquinone	1.30	0.5	1.7	3.6	4.8
Hydroxy anthraquinone	0.80	0.7	1.2	2.4	3.7
Hydroxy anthraquinone	0.20	0.3	0.9	1.5	2.0
Camphene	2.65	0.7	3.0	5.0	6.6

*Data taken from illustrations in original report, WADC TR 58-684.

Subliming compounds can give substantial thermal protection to the base materials. Lifetime increases of up to 500-600% at stagnation temperatures of 750-900°F were observed. Therefore such compounds seem to provide an excellent solution to the problem of "aerodynamic heating" except that the coating weight required is at least twice the weight of the base material. Test results show that the total ribbon weight must be doubled to achieve a lifetime increase of 3 sec at 750°F, and 2 sec at 900°F. It is reasonable to assume that at 2000°F the lifetime increase resulting from doubling the ribbon weight would be substantially less than

Approved for Public Release

Contrails

Table 76. Lifetime Augmentation of Nylon Ribbons Resulting From Use of Coatings*

Coating	Coating Weight (oz/yd)	Life Augmentation (sec/oz/yd) Stagnation Temperature 1210°R	1360°R
Hexachloroethane	0.15	3.5	---
Hexachloroethane	1.20	2.5	0.9
Hexachloroethane	2.60	2.2	1.5
Chloroanthraquinone	0.35	5.8	---
Chloroanthraquinone	0.69	4.7	2.7
Chloroanthraquinone	1.18	6.2	---
Methyl anthraquinone	0.29	3.2	---
Methyl anthraquinone	0.48	10.5	2.8
Methyl anthraquinone	0.57	18.0	---
Methyl anthraquinone	0.70	2.2	---
Methyl anthraquinone	1.10	2.2	---
Hydroxy anthraquinone	0.20	0.2	---
Hydroxy anthraquinone	0.80	2.5	---
Camphene	0.80	--	3.8
Camphene	2.60	1.5	1.3

*Time (in sec) per unit coating weight (oz/yd). Data taken from illustrations in original report, WADC TR 58-684.

2 sec. Thus doubling the ribbon thickness gives as effective results as applying any of the coatings.

It was noted that the flutter of the ribbons during testing was sufficient to break the bond between the coating and the nylon. Once this bond is weakened, the coating is removed by mechanical rather than thermal means, and cannot result in increased life due to sublimation. Therefore development of flexible properly adhering coatings would be advantageous.

The thickness of the leading edge, as predicted by Ruoff (Section 11.1) has a great effect on heat transfer and on total life. Whenever the leading edge was folded back or thickened by any means, the lifetime was greatly enhanced.

11.2.5 Recommendations

It is opined that a ribbon with a lead edge four times the thickness of the present leading edge could at least double the life of the ribbon. Addition of a thin subliming coating of the proper flexibility and adhesion to the ribbon, and the covering of the lead edge with a conductive foil could produce a life of 10-15 sec at Mach 5 and 100,000 ft.

11.2.6 References

Section 11.1, and WADD TR 60-584, pp. 333 to 338; WADC TR 55-264, pp. 154 to 156.

Approved for Public Release

Contrails

BIBLIOGRAPHY

Air Force Cambridge Research Center, Effect of Low Temperature on Elongation Characteristics of Nylon Braid, Evaluation Report WCLT T58-23, April 1958 (Aeronautical Systems Division).

Chu, C. C., Kaswell, E. R., and Doull, D. J., Development of High Tenacity-Heat Stable Dacron Parachute Items, WADC Technical Report 57-765, May 1958 (Fabric Research Laboratories, Inc.).

Chu, C. C., Kaswell, E. R., and Doull, D. J., Development of Improved Nylon Webbings, WADC Technical Report 58-509, April 1959 (Fabric Research Laboratories, Inc.).

Cornish, R. H., Ahimaz, F. J., Beadle C. W., and Foster, K., Mass Transfer Cooling of Parachute Materials, WADC Technical Report 58-684, September 1959 (Cornell University).

Corry, W. A., Some Principles of Parachute Fabric Construction, WADC Technical Note WCRT 54-181, November 1954 (Aeronautical Systems Division).

Holmes, C. F., Jr., Evaluation of Nylon "6" Cords, Ribbons, and Tapes, WADC Technical Note 59-14, January 1959 (Aeronautical Systems Division).

Klein, W. G., Lermond, C. A., and Platt, M. M., Research Program for the Development of a Design Procedure to Engineer Parachute Fabrics, WADC Technical Report 58-65, May 1958 (Fabric Research Laboratories, Inc.)

Klein, W. G., Lermond, C. A., and Platt, M. M., Development of Design Data on the Mechanics of Air Flow Through Parachute Fabrics, WADC Technical Report 56-576, September 1957 (Fabric Research Laboratories, Inc.).

Krizik, J. G., Victory, E., Cheatham, J. F., and Backer, S., Design Data on Biaxial Forces Developed in Parachute Fabrics, WADC Technical Report 57-443, December 1957 (Massachusetts Institute of Technology).

Landis, M. B. and F. W. Fraim III, Development of Coreless Type Braids for use in Personnel Parachute Suspension Lines, WADC Technical Report 58-410, December 1958 (Essex Mills, Inc.).

Little, C. O., Jr., Amount of Deterioration Present in Parachutes Manufactured Over 15 Years Ago, WADC Technical Note 59-30, February 1959 (Aeronautical Systems Division).

Materials Laboratory, Effect of Duco Lacquer, 3661 Thinner, on Nylon, Test Report WCRT T-57-14, February 1957 (Aeronautical Systems Division).

Materials Laboratory, Status Report on Project 61550, WADC Technical Memorandum TM-56-9, March 1956 (Aeronautical Systems Division).

Approved for Public Release

Contrails

Materials Laboratory, Thermal Radiation of Nylon and Dacron Webbings, Test Report WCRT T56-20, April 1956 (Aeronautical Systems Division).

McGrath, J. C., Evaluation of Nylon Cloth Finished with Silicone Type Oils (For Use in Parachutes), WADC Technical Note 59-10, January 1959 (Aeronautical Systems Division).

McGrath, J. C., Evaluation of F-100 Brake Parachutes, WADC Technical Note 58-20, January 1958 (Aeronautical Systems Division).

McGrath, J. C., Evaluation of B-47 Deceleration Parachutes, WADC Technical Note 57-326, November 1957 (Aeronautical Systems Division).

Neff, R. J., Development and Evaluation of Webbing Made from Nylon "6," WADC Technical Report 57-538, March 1958 (Phoenix Trimming Company).

Palko, F. L., Aerodynamic Heating Tests at Mach Number 5 of Nylon Parachute Material Protected with Various Subliming Compounds, AEDC-TN-59-41, May 1959 (Arnold Engineering Development Center).

Parachute Branch (WCLEH-4) Aeronautical Accessories Laboratory, Strength Retention of Radiated Nylon, WCLT T58-87, December 1958 (Aeronautical Systems Division).

Parachute Branch (WCLEH-4) Aeronautical Accessories Laboratory, Effect of Environmental Conditions on the Breaking Strength of Textile Materials Used in Parachute Systems, Evaluation Report, WCLT T-58-4, January 1958 (Aeronautical Systems Division).

Parachute Branch (WCLEH-4) Aeronautical Accessories Laboratory, Ribbon Test Samples, Test Report WCLT T57-71, August 1957 (Aeronautical Systems Division).

Parachute Branch (WCLEH-4) Aeronautical Accessories Laboratory, Cannister Project, Test Report WCRT T55-61, No ember 1955 (Aeronautical Systems Division).

Ruoff, A. L., Liu, S. W., and Frank, F., Aerodynamic Heating of Parachutes, WADC Technical Report 57-157, December 1957 (Cornell University).

Waite, J. V., Drop Tests of Nylon Parachute Canopies (Chemstrand), AFFTC TN 58-17, September 1958 (Aeronautical Systems Division).

Wilkinson, R. A., The Effect of Solar Radiation on the Breaking Strength of Outdoor Exposed Webbings, WADC Technical Report 58-201, November 1958 (Aeronautical Systems Division).

Approved for Public Release